THE SYNTHESIS OF MACROCYCLIC MOLECULES RELATED TO TELOMESTATIN

by

Wafa Saeed S. Aldarini

A thesis submitted in partial fulfillment
of the requirements for the degree of
Master of Science (MSc) in Chemical Sciences

The Faculty of Graduate Studies
Laurentian University
Sudbury, Ontario, Canada

THESIS DEFENCE COMMITTEE/COMITÉ DE SOUTENANCE DE THÈSE
Laurentian Université/Université Laurentienne
Faculty of Graduate Studies/Faculté des études supérieures

Title of Thesis Titre de la thèse	The Synthesis of Macrocyclic Molecules Related to Telomestatin	
Name of Candidate Nom du candidat	Aldarini, Wafa Saeed S.	
Degree Diplôme	Master of Science	
Department/Program Département/Programme	Chemical Sciences	Date of Defence Date de la soutenance January 13, 2017

APPROVED/APPROUVÉ

Thesis Examiners/Examinateurs de thèse:

N/A
(Supervisor/Directeur(trice) de thèse)

Dr. Hélène Joly
(Committee member/Membre du comité)

Dr. Stephan Siemann
(Committee member/Membre du comité)

Dr. William Ogilvie
(External Examiner/Examinateur externe)

Approved for the Faculty of Graduate Studies
Approuvé pour la Faculté des études supérieures
Dr. Shelley Watson
Madame Shelley Watson
Acting Dean, Faculty of Graduate Studies
Doyenne intérimaire, Faculté des études supérieures

ACCESSIBILITY CLAUSE AND PERMISSION TO USE

I, **Wafa Saeed S. Aldarini**, hereby grant to Laurentian University and/or its agents the non-exclusive license to archive and make accessible my thesis, dissertation, or project report in whole or in part in all forms of media, now or for the duration of my copyright ownership. I retain all other ownership rights to the copyright of the thesis, dissertation or project report. I also reserve the right to use in future works (such as articles or books) all or part of this thesis, dissertation, or project report. I further agree that permission for copying of this thesis in any manner, in whole or in part, for scholarly purposes may be granted by the professor or professors who supervised my thesis work or, in their absence, by the Head of the Department in which my thesis work was done. It is understood that any copying or publication or use of this thesis or parts thereof for financial gain shall not be allowed without my written permission. It is also understood that this copy is being made available in this form by the authority of the copyright owner solely for the purpose of private study and research and may not be copied or reproduced except as permitted by the copyright laws without written authority from the copyright owner.

Abstract

G-quadruplex DNA represents an attractive target for the development of anti-cancer therapeutic agents as it plays important roles in transcriptional regulation and the maintenance of telomeric length. Oxazole-containing macrocycles such as telomestatin are considered to be a promissing new class of G-quadruplex binding ligands. In this work, poly-oxazole building blocks were synthesized to prepare a tetraoxazole peptide macrocycle in good yield. The macrocycle was obtained by employing standard peptide coupling conditions using a convergent solution phase approach. The synthetic unit of the oxazole amino acid containing compound was prepared by cyclodehydration/oxidation of protected serine and phenylalanine. Two-cycle coupling of the unit gave a linear tetraoxazole amide. The final macrocyclization was accomplished by using O-[(1-cyano-2-ethoxy-2-oxoethylidene)amino]-oxytri(pyrrolidin-1-yl) phosphonium hexafluorophosphate (PyOxP) and the product (45% yield) was characterized by ^{1}H NMR. Finally, the Cu (II) coordination chemistry of the tetraoxazole macrocycle was investigated by spectrophotometric titration.

Keywords

G-quadruplexes, telomestatin, poly-oxazole macrocycles, macrocyclization, dinuclear copper (II) complex.

Acknowledgements

I would like to thank my supervisor, Professor Gerardo Ulibarri, whose scholarly advice, help and constant encouragement have significantly contributed to the completion of this thesis work. I would like to thank my committee members Professors Hélène Joly and Stefan Siemann for their critical input and suggestions for my thesis work. I wish to thank my external thesis committee member for his/her critical input for my work. I also wish to thank my fellow labmates Catrina and Azizah Al Rathwan for their invaluable input and for being a great source of support to me during my study. I also would like to acknowledge the generous financial support provided by the Ministry of Higher Education in the Kingdom of Saudi Arabia. Finally, I would like to thank my sisters Nohaiah Aldarini, Mai Ahajlan and Mesheal Aldarini for being there for me throughout the entire Master program.

Dedication

I dedicate this work to my Father Seed Aldarini and Mother Sareeia Mubark who surrounded me with their endless support, encouragement, love and prayers. They have been a great source of motivation and inspiration.

Table of Contents

List of Figures

List of Schemes

List of Appendix

List of Abbreviations

6OTDs	Macrocyclic hexaoxazole-type telomestatin derivatives
7OTDs	Macrocyclic heptaoxazole-type telomestatin derivatives
Boc	*Tert*-butyloxycarbonyl
BOP	(Benzotriazol-1-yloxy)tris(dimethylamino)phosphonium hexafluorophosphate
$BrCCl_3$	Bromotrichloromethane
Bu	Butyl
Cbz	Carboxybenzyl
CH_3CN	Acetonitrile
$Cu(OAc)_2$	Copper(II) acetate
DAST	Diethylaminosulfur trifluoride
DBU	1,8-diazabicyclo[S.4.0]undec-7-ene
DCE	1,2-dichloroethane
DCM	Dichloromethane

DIC	*N,N′*-Diisopropylcarbodiimide
DIPEA	*N*,*N*-Diisopropylethylamine, or Hünig's base
DMA	*N*,*N*-Dimethylaniline
DMAP	4-dimethylaminopyridine
DMF	*N, N*-dimethylformamide
DMSO	Dimethylsulfoxide
DNA	Deoxyribonucleic acid
EDC	1-Ethyl-3-(3-dimethylaminopropyl) carbodiimide
Equiv	Equivalent
EtOAc	Ethyl acetate
FMOC	9-Fluorenylmethoxycarbonyl
G4	G-quadruplexes
H_4pat[1]	Macrocycles patellamide A
HATU	2-(1H-7-azabenzotriazol-1-yl)-1,1,3,3-tetramethyluronium hexafluorophosphate
HMPA	Hexamethylphosphoramide

HMPB	(4-hydroxymethyl-3-methoxyphenoxy)butanoic acid
HOAt	Hydroxyazatriazole
HOBt	Hydroxybenzotriazole
HPLC	High Performance Liquid Chromatography
hTERT	Telomerase Reverse Transcriptase
hTR	Human telomerase RNA
HXDV	Hexaoxazole-divaline
HXPV-4	Hexaoxazole- propenyl valine
iPrOH	Isopropyl alcohol
L2H2-6OTD-HXDL	Diaminobuty(lysyl)hexaoxazole
mp	Melting point
mRNA	Messenger RNA
NBS	*N*-bromosuccinimide
NMR	Nuclear magnetic resonance
NMP	N-Methyl-2-pyrrolidone

PEG	Polyethylene glycol
PEG-PS	Polyethylene glycol–polystyrene
Pbf	2,2,4,6,7-Pentamethyldihydrobenzofuran-5-sulfonyl chloride
PG	Protecting group
Phe	Phenylalanine
PLP	Protected linear pentapeptide
PyBOP	(Benzotriazol-1-yloxy)tripyrrolidinophosphonium hexafluorophosphate
PyOxim	(Ethyl cyano(hydroxyimino)acetato)-tri-(1-pyrrolidinyl)-phosphonium hexafluorophosphate
PyOxP	O-[(1-cyano-2-ethoxy-2-oxoethylidene)amino]-oxytri(pyrrolidin-1-yl) phosphonium hexafluorophosphate
RP-HPLC	Reverse phase high performance liquid chromatography
Ser	Serine
SPPS	Solid-Phase Peptide Synthesis
SPPS-CC	Solid phase peptide synthesis and cyclization cleavage
TBSCl	*Tert*-butyldimethylsilyl chloride

1. Introduction

1.1. General Review of Telomeres

Telomeres are the deoxyribonucleic acid (DNA) sequences at the end of linear chromosomes. They play a vital role in preserving genetic integrity within the nucleus by protecting the ends of the chromosomal DNA from degradation or fusion, and in segregating the chromosomes during cell division. Telomeres are comprised of specific sequences of certain repetitive patterns that depend on the organism. For example, in humans, there are several thousands of TTAGGG repetitive sequences at the ends of the chromosomes.[1] This repetitive hexanucleotide is present on the 5'-3' strand. During the replication of chromosomes, the lagging strand replicates these G-rich repetitive sequences. Due to the discontinuous replication pattern in the lagging strand, there is a 3' single–stranded overhang varying in length from 24 to 360 nucleotides.[2] Studies have shown that the 3' single-stranded telomeric overhang forms a 't'-loop structure that interacts with the internal TTAGGG repeats of the telomere. Moreover, the telomeric DNA does not form nucleosomes as a result of the lack of typical nucleoproteins, which are required to arrange nuclear DNA into nucleosomes.[3] Rather, the interaction of specific types of proteins, which are Telomeric Repeat Factor 1 (TRF1) and Telomeric Repeat Factor 2 (TRF2), stabilize the DNA at the telomeres by forming specific nucleoprotein complexes. These nucleoprotein complexes also maintain the structural and functional integrity of telomeres.[3] Telomeres resolve the replication problem at the end of linear chromosomes, by involving a specialized enzyme called telomerase. After each round of DNA replication, all telomeric repeats are lost and the DNA risks losing coding sequences with subsequent rounds. Therefore, a telomerase attaches to the end of a chromosome and adds the complementary RNA bases to the 3' end of the DNA. Telomerase enables the mammalian cells to

differentiate between the normal chromosomal ends and the double–stranded DNA breaks, which in turn prevents the initiation of DNA damage repair or apoptotic pathways.[3, 4] Therefore, a telomere forms a physical cap over the end of linear chromosomes which is entirely vital for maintaining the genetic repository in eukaryotic cells.

1.1.1. Biological Background of G-quadruplex Stabilizing Agents

The secondary structure of DNA is a standard right-handed double helical conformation (B-DNA). However, biophysical techniques such as X-ray crystallography and circular dichroism have shown that DNA can assume secondary structures other than the standard B-form. These include cruciforms, ZDNA (a left-handed double helical conformation) and G–quadruplexes, depending upon the specific DNA sequence motifs and the interaction of DNA with various proteins.[5, 6] The G-quadruplex structures or G-quartets (G4) were first observed in 1910 by Bang,[7] who noted that when a concentrated solution of guanylic acid is cooled down, it forms a transparent gel in an aqueous solution, suggesting that guanine-rich DNA sequences can form stable higher-order structures. The absolute structure and arrangement of these G-quadruplexes was determined in 1962 when Gellert and Davies found that tetrameric guanine bases form a novel structure by internal hydrogen bonding (called the Hoogsteen bonds).[8] Recent evidence shows that G-quadruplex structures play significant roles in the regulation of various steps of gene expression including the initiation of transcription, the alternate splicing of mRNA, the modulation of translation, and the synthesis of microRNAs.[9] The *in vivo* role of G-quadruplex structures was first elucidated by studying the transcriptional regulation of a myelocytomatosis viral oncogene (v-myc) of the avian myelocytomatosis virus.[9] The transcription of this oncogene is tightly controlled by a set of four promoters (P1-P4), nuclease hypersensitivity elements, and various transcription start sites.[10] One of

the nuclease hypersensitivity elements, NHE III1, located upstream of the P1 promoter, contributes largely to the transcription regulation. This region contains five consecutive sets of G-rich sequences (G/A)G(G/A)AGGGGT, which are thought to arrange and stabilize the G-quadruplex structure, and possibly inhibit the transcription of this gene.[10, 11]

1.1.2. G-quadruplex DNA

The G-quadruplex (G4) structures are formed in genomic regions that are rich in guanine nucleotides. These G-rich sequences are mostly present in telomeres, near transcriptional start sites, and at double-stranded break sites for mitosis and meiosis. Telomeres consist of a square planar arrangement of four-guanine molecules attached to each other through Hoogsteen hydrogen bonding. These G-quadruplexes stack over each other just like the nucleotide bases stack over each other in double-stranded DNA, forming a three-dimensional complex termed G4 structure, (Figure 1).[12] Between the stacked G-quadruplexes, there may be intervening sequences that are not involved in G4 structure formation, and thereby persist as small single-stranded loops varying from one to seven nucleotides in length.[12] The stability of the G4 structure is achieved by the presence of monovalent cations, particularly K^+ (and less frequently NH_4^+ and Na^+), between the stacked G-quadruplexes. The monovalent cation helps to decrease the electrostatic repulsion between the guanine and carbonyl oxygen atoms in the adjacent layers.[13, 14]

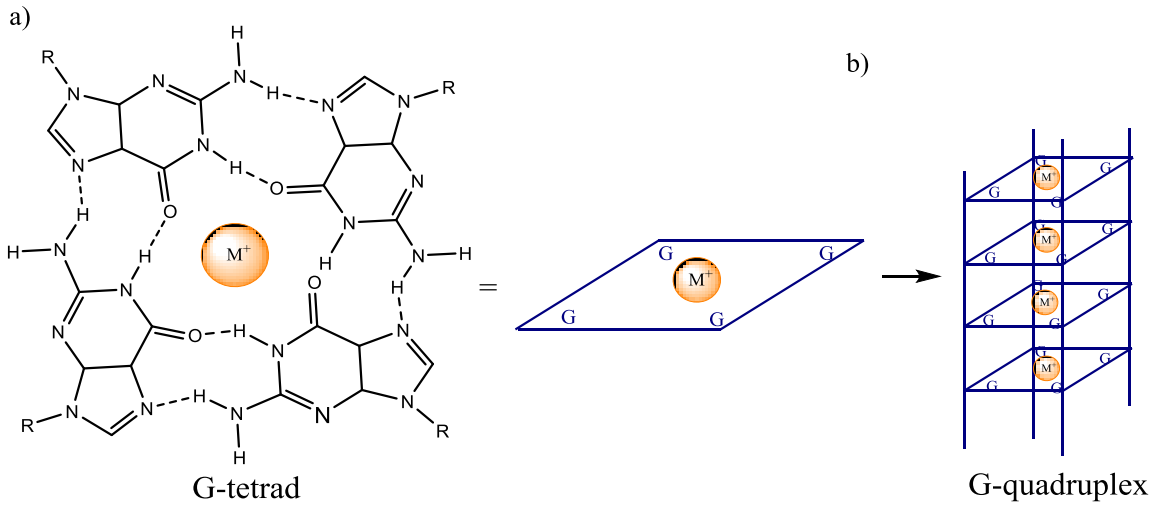

Figure 1: (A) Formation of a G-quartet in a square planar arrangement after hydrogen bonding among guanine molecules, and (B) Stacking of G-quartets to form a G4 structure.[6]

1.1.3. Telomere and Telomerase in Cancer

Telomeres are the DNA sequences that are found at the end of linear chromosomes. In the late 1980s it was found that the biology of telomeres was altered in the process of tumorigenesis. [15] Subsequent studies have shown that the telomerase enzyme is actively present in human malignant hematopoietic cells and in human ovarian carcinoma.[16, 17] The PCR-based technique, Telomeric Repeat Addition Protocol (TRAP), enabled the amplification and detection of the telomerase-elongated 3'-overhang of the leading strand. Using this technique, it was found that 82%–95% of breast cancers and 80% - 85% of other human tumors show telomerase activity.[30] Telomerase in cancer cells was found to be actively involved in the maintenance of the short length of telomeres,

thus, providing genetic stability and saving the cell from apoptosis.[19] Histological studies of malignant cells of various human tissues show that telomerase activity is due to the over-expression of the hTERT domain. Cancer cells attain replicative immortality by being able to maintain the length of telomeres by the over-expression of hTERT.[20] As a result of the association of telomerase with human cancers, telomerase has been tested in hundreds of studies as a potential sensitive biomarker for screening, early detection, prognosis, and the monitoring of the pathophysiology of the residual disease.[21]

1.1.4. G-quadruplex Binding Ligands as Potential Telomerase Inhibitors

Telomeric G-quadruplex stabilizers (ligands) have been recognized as a potential new approach for anticancer therapeutic agents for their inhibition of telomerase activity.[22] This recognition has led to an interest in G-quadruplex structures as a potential anticancer drug target that hinges on the ability to design and develop a large number of small molecules that selectively bind and stabilize the telomeric G-quadruplexes, thus blocking the action of the telomerase or deactivating G-quadruplex–related gene expression.[23, 24] The common features shared by many of the G-quadruplex ligands are a flat or planar aromatic ring structure and, in most cases, cationic side chains with sizes corresponding to G-quadruplexes.[25, 26] The ligand model interacts mainly with the terminal G-quadruplexes through a potential π-π stacking at the end of G-quadruplexes and electrostatic interactions (or hydrogen bonding with G-quadruplexes).[27, 28] The most famous and potent compound discovered so far is the metabolite telomestatin,[27, 29] a macrocyclic polyoxazole

natural compound that has proven to be a highly selective G-quadruplex stabilizer. The compound was identified as a particularly useful probe of the telomerase function as a result of its valuable biological properties.

In the 1990s, many natural products containing oxazole and thiazole were isolated from marine organisms [30, 31] that had attractive biological activities toward G-quadruplex stabilization. Although a diverse array of G–quadruplex-interactive ligands have been prepared using various synthetic processes; most researchers have screened natural products in order to identify new G–quadruplex stabilizers. Of the G–quadruplex interactive agents identified to date, many have significant selectively in terms of G–quadruplex structures with telomerase inhibition. This selectivity has led some researchers to search for natural products that inhibit telomerase activity. Among these, telomestatin, a 24-member macrocycle consisting of the linkage of two methyloxazoles, five oxazoles, and one thiazoline ring (Figure 2), has been identified and characterized by Shin-Ya and co-workers.[32] Telomestatin was isolated from *Streptomyces anulatus* 3533-SV4 and is one of the most potent inhibitory agents with low nanomolar activity reported against telomerase (IC_{50} = 5 nM).[33, 34, 35] Hurlely and co-workers experimentally proved that telomestatin resembles G-tetrads, which selectively facilitate the formation or stabilization of intramolcular G-quadruplexes produced from 3' telomeric overhangs of human chromosomes.[27] Studies have indicated that the proposed mode of action of telomestatin which contains planar aromatic rings,[36, 37] involves the interaction of telomestatin with human telomeric G-quadruplex by stacking on the terminal G-tetrads.[28] The stabilization of telomeric G-quadruplex structures with telomestatin as a ligand has reportedly inhibited the telomerase activity that elongates the telomere sequences.[38] Telomestatin is involved in various biological activities. For instance, it induces prompt cell death selectively, killing cancer cells but not

killing cells in normal fibroblasts. It was reported that telomestatin does not cause a significant weakening of the telomere in either cancer or noncancerous cells under short time conditions, and it induces the loss of single–-stranded telomeric 3' overhangs.[39, 40, 41] In addition, the telomere shortens with the G–quadruplex formation, and telomestatin induces the dissociation of TRF2, which is the telomere–binding protein that is responsible for telomere stabilization[42] and induce the expression of ribonuclease PO1 from telomere in cancer cells. Therefore, telomestatin induces apoptosis.

The reasons behind these biological activities are due to the high affinity of telomestatin for intramolecular G-quadruplexes over the intermolecular G-quadruplex structures. Interestingly, telomestatin was found to have a > 70 fold selectivity for intramolecular G-quadruplex structures over duplex DNA.[43] The selectivity of telomestatin between different G-quadruplex sequences and the binding affinity toward G-quadruplexes are rationalized by size and shape that are comparable with G-tetrads of G4 DNA.[44, 27] However, the shape of telomestatin is not ideal because of the presence of a single thiazoline unit (sp^3 carbon).[45] Despite its superior properties and selectively, telomestatin is not available in great quantity. [25] Moreover, telomestatin has one major drawback: it is difficult to obtain.[26, 44] The most effective method of obtaining telomestatin is by isolation from *Streptomyces anulatus.* Although telomestatin can be produced by bacterial fermentation, the yield is quite low because of the inefficient fermentation.[46, 47] Several synthetic approaches have been unsuccessful,[31, 48, 49, 50] a total synthesis of telomestatin has been described only in one patent,[51] (with the stereocenter of a thiazoline ring in an R configuration).[52, 53] However, the synthetic route of (R)-telomestatin is incompatible with industrial–scale production[26] and even with the production of derivatives. Recently, the total synthesis of the (S)-isomer of telomestatin[54] (Figure 2) was reported by the Takahashi group. It was found to be more potent and a stronger inhibitor than that

isolated from *Streptomyces anulatus*. Synthetic (S)-telomestatin was four times more active against telomerase. More significantly, since it has no hydrophilic functional groups, thus explaining the poor solubility in water.[26] The poor solubility of telomestatin can seriously hinder its bioavailability, an important consideration when dealing with medical drug candidates.

Despite the low availability of telomestatin, its noteworthy biological activities have motivated and inspired some researchers to synthesize and design telomestatin analogues that have improved features over telomestatin.[44, 55] Telomestatin is difficult to synthesize and hard to formulate because it lacks water-solubilizing groups, such as hydroxyl or amine groups. Recently, several telomestatin derivatives have been reported as G-quadruplex stabilizers or binders.

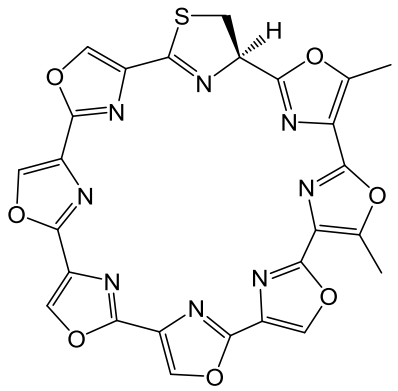

Telomestatin (R)-1

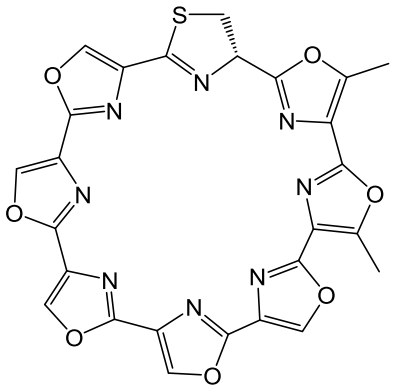

Telomestatin (S)-1

Figure 2:Structures of telomestatin (R)-1 and its enantiomer (S)-1.[54]

1.2. An Alternative Approach to Prepare Synthetic Analogues of Telomestatin

1.2.1. Structure and Evaluation of Poly-oxazole Macrocycles as G-Quadruplex Stabilizers

Many research groups have undertaken the design of G-quadruplex ligands with the aim to stabilize telomeric G-quadruplexes. A series of macrocyclic hexaoxazole-type (6OTDs) and heptaoxazole-type (7OTDs) telomestatin derivatives containing various functional groups have been synthesized and evaluated. These novel telomestatin derivatives possess a characteristic planar aromatic core structure with a size corresponding to the G-tetrad to promote an end π-stacking with the G-quadruplex structure.[56] Many of these G-quadruplex ligands contain cationic moieties (basic side chains) to cause an attractive interaction with the anionic backbone (phosphate backbone) and the grooves of the telomeric G4.[57] All of these compounds exhibit a high degree of specificity towards the interaction with G-quadruplex structures,[58] and inhibit both human telomerase activities and telomeric DNA-binding proteins by preventing their access to the telomere.[59,60]

1.2.2. Macrocyclic Hexaoxazoles (6OTDs)

The first derivative of macrocyclic hexaoxazoles was hexaoxazole HXDV, **2**, a 24-membered macrocycle containing 6 oxazole and 2 valine side chain (Figure 3). Rice and co-workers[61] determined that HXDV binds and thermally stabilizes the telomeric G-quadruplexes in the presence of K^+ ions, but has no ability to stabilize the duplex or triplex form of DNA. The high selectivity of HXDV towards G-quadruplexes appears to be related to its structure which is suited

for binding to G-quadruplexes. Its scaffold is derived from a particular telomestatin-like concave shape, which has 2-planar trioxazole moieties linked by a valine residue on the same face of the cycle.[45] Thus, its structure facilitates π-stacking interactions with quartets. Current studies have indicated that the binding mode of this molecule to G-quadruplexes is via a "terminal capping" interaction with a stoichiometry of 2:1 between HXDV and $[d\ (T_2AG_3)]_4$ repeats.[62,55] Unlike HXDV, macrocycle **3,** containing four oxazole rings with alternative tetra-isopropyl substitutions (Figure 3), did not stabilize G-quadruplex DNA and was not cytotoxic. HXDV has a moderate level of cytotoxicity towards human lymphoblastomas and murine leukemias with an IC_{50} value of 0.4 μM. Since HXDV is not very soluble in aqueous solution, the side chain of HXDV has been modified in an attempt to prepare derivatives with improved solubility.

A related derivative, **4**, was synthesized using a ring-closing metathesis approach. This involved replacing one of the valine linkages in HXDV with a propenyl group.[63] The compound **4** displayed a high cytotoxic potency against five different tumor cell lines, having an IC_{50} of 25 μM. It also exhibited a preference for G-quadruplex structures over any other form of DNA, indicating that the amide bonds are not important for enhancing the activity in these structures. Bistrioxazole acetate (**5)** was synthesized and its biological activity has been tested.[64] It exhibits telomerase inhibitory activity with an IC_{50} of 2 μM. The asymmetric centers in the macrocyclic bisamide-related telomestatin derivatives are thought to play an important role in their interaction with G-quartets.

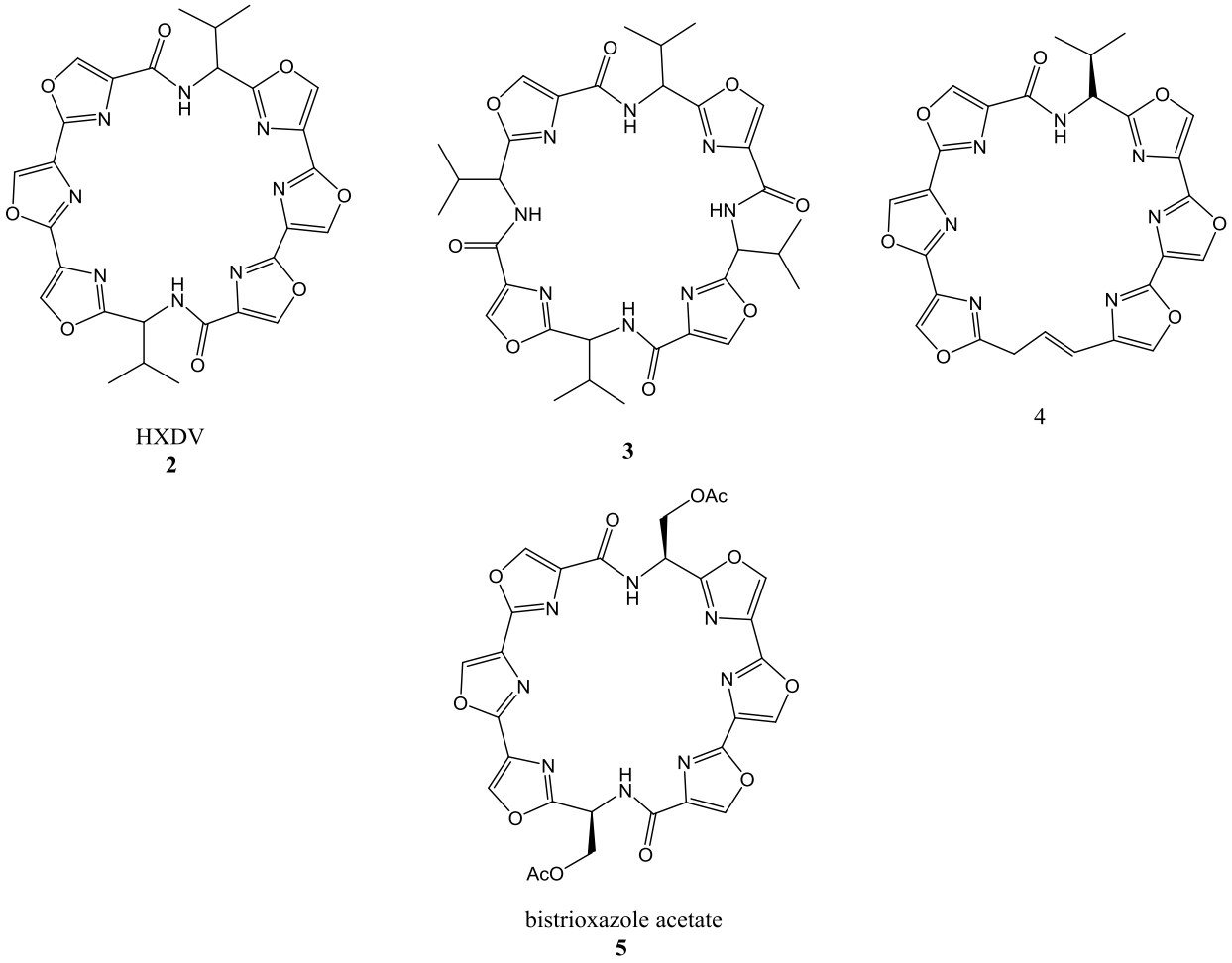

Figure 3: Structures of HXDV and related uncharged telomestatin derivatives.[25]

Nagaswa and co-workers [65] reported the synthesis of a set of telomestatin derivatives, L2H2-6OTD dimers (Figure 4), which have macrocyclic hexaoxazole structures. The dimers **6**, **7** and **8** were connected by linkers of 3 different lengths (9-11). The ability of these compounds to interact with telomeric DNA was compared to that of corresponding hexaoxazole monomers. The optimum interaction with the telomeric G4 was obtained with dimer **7** because its scaffold is able to span the thickness of the G-quadruplex DNA. Thus, dimer **7** had a ten-fold higher selectivity for interaction

with telomeric DNA when compared to the corresponding monomer. Unexpectedly, **7** has a lower affinity compared to the corresponding monomer. Therefore, **7** exhibits potent G-quadruplex stabilizing activity. Since it interacts with the telomeric G-quadruplex DNA forming a 1:1 complex (Figure 5), the two macrocyclic moieties in **7** are expected to interact as terminal caps of outer G-tetrads on the same quadruplex, whereas the ratio of the corresponding monomer is 2:1 similar to that found for telomestatin and HXDV.[65]

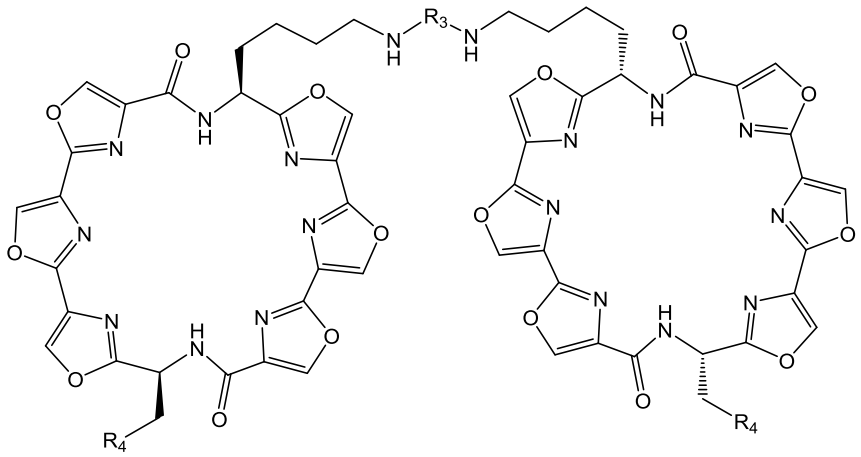

(6) R_3 = C(O)
R_4 =OAc
(7) R_3 = C(O)$(CH_2)_4$C(O)
R_4 =OAc
(8) R_3 = C(O)$(CH_2)_{12}$CO)
R_4 =OAc

Figure 4: Structure of hexaoxazole macrocyclic L2H2-(6OTD) dimers.[65]

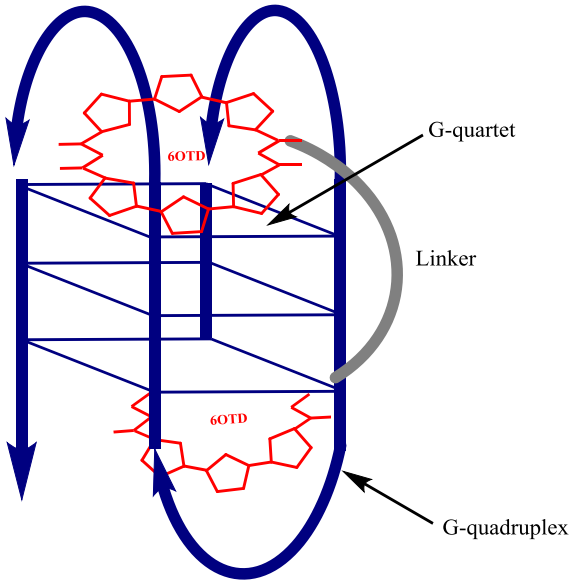

Figure 5: The binding mode of the 6OTD dimers.[57]

Although telomestatin-like molecules that consist of the macrocyclic oxazole scaffold interact and stabilize the G-quadruplex structure, they exhibit limited aqueous solubility. It was suggested that the replacement of one or both isopropyl groups of HXDV (**2**) with cationic side chains would help improve the aqueous solubility of the compounds, and enhance the affinity and selectivity for specific G-quadruplex sequences, especially because these derivatives have a planar core. This strategy would be expected to provide strong, selective G4 binders with the cationic functional groups that would directly bind to G-quadruplex grooves by forming salt bridges with the phosphate backbone.

A series of the symmetrical macrocyclic hexaoxazole analogues of HXDV **2** with cationic side chain appendages was synthesized and evaluated (Figure 6). Rice and co-workers investigated the ability of L2H2-6OTD-HXDL, diaminobuty(lysyl)hexaoxazole **9**, to stabilize telomeric DNA, and they found that **9** is the most promising; it provides the greatest ability to stabilize the G-quadruplex structure as compared to HXDV **2** and related analogues that contain only one amino group.[44] Compound **9** was found to form an anti-parallel-type G4 structure when it interacted with telo 24 or longer telomeric DNA (i.e., telo 48, 72, and 96) in an end-stacking mode using two molecules of HXDL.[66] The reason behind the high solubility of HXDV **2** is that it has water-soluble functional groups on both of the terminal amino acid groups, which makes it charged at physiological pH. Apart from π-stacking (planarity of trioxazole) and electrostatic interactions (hydrogen bonds with phosphate backbone), such functionality may also impart HXDL **9** the efficiency of enhancing the binding to G-quadruplex-DNA.

Compound **10** is a G-quadruplex binder which has a guanidine-containing side chain hexaoxazole macrocycle (6OTDs).[58] Compound **10**, reported by Nagasawa and co-workers,[56] exhibited a superior ability to inhibit telomerase activity, and a preference toward anti-parallel telomeric G4 structures over the parallel one, while L2A2-6OTD (*N*-acetylaminopropyl) **11** did not. Both HXDL (**9**) and L2G2-6OTD (**10**), which contain positively charged functional groups, showed significant induction of the intramolecular quadruplex structure in the absence of metal ions.[57] Rice and co-workers have studied the variation of side chains in a series of hexaoxazole macrocycle ligands. Ligand **12**, [(dimethyl)amino]ethyl-isopropylhexaoxazole, displayed a high degree of specificity towards G-quadruplex stabilization, as observed from the UV melting profiles. The cytotoxic activity of **12** was greater than that of HXDV, with the IC_{50} range between 0.025 and 3.5

μM. Ligand **12** was evaluated *in vivo* as a potential antitumor agent against human tumor xenografts in mice.[67]

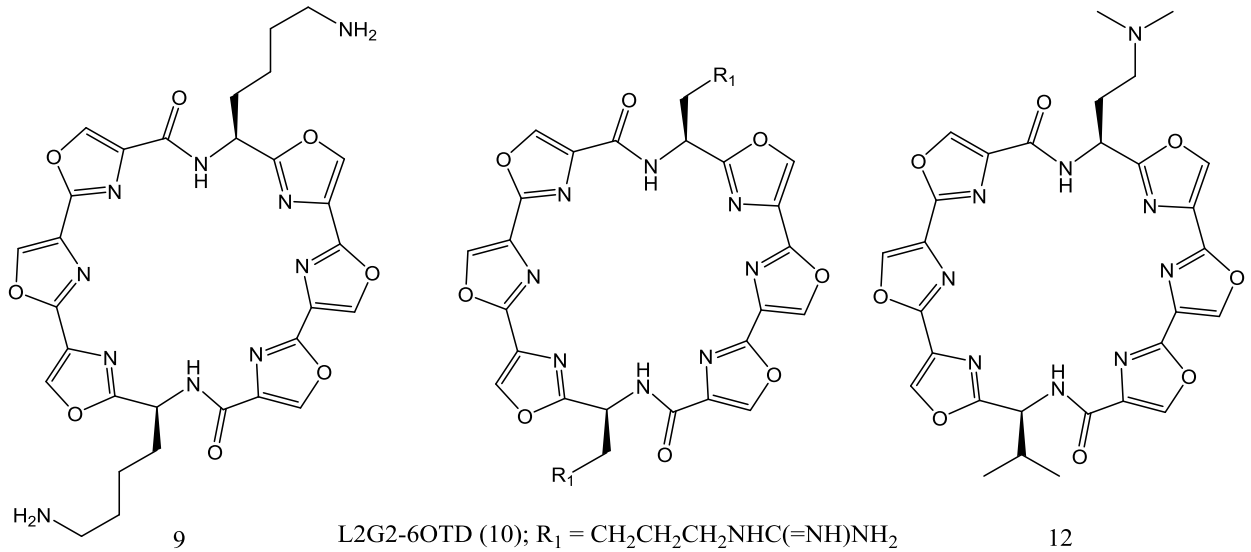

Figure 6: Structures of hexaoxazole macrocyclic amine-based G-quadruplex ligands with cationic side chains. [44,58,67]

The hexaoxazole-based macrocycle-containing methyl oxazoles, L2A2-6M(2)OTD **13** and L2A2-6M(4)OTD **14**, were recently reported by Nagasawa and co-workers (Figure 7). They found **14** to be a more effective stabilizer than **13**. Thus, it was revealed that the ligand-induced stabilization of G-quadruplex DNA increased by an incremental number of "methyl oxazole" moieties in the macrocyclic hexaoxazole.[68] Y2H2-6OTD **15**, a macrocyclic hexaoxazole with a L-tyrosyl side chain, exhibited a significant improvement in stabilizing telo 24. This might be due to the presence of OH groups, which interact with the phosphate backbone.[56]

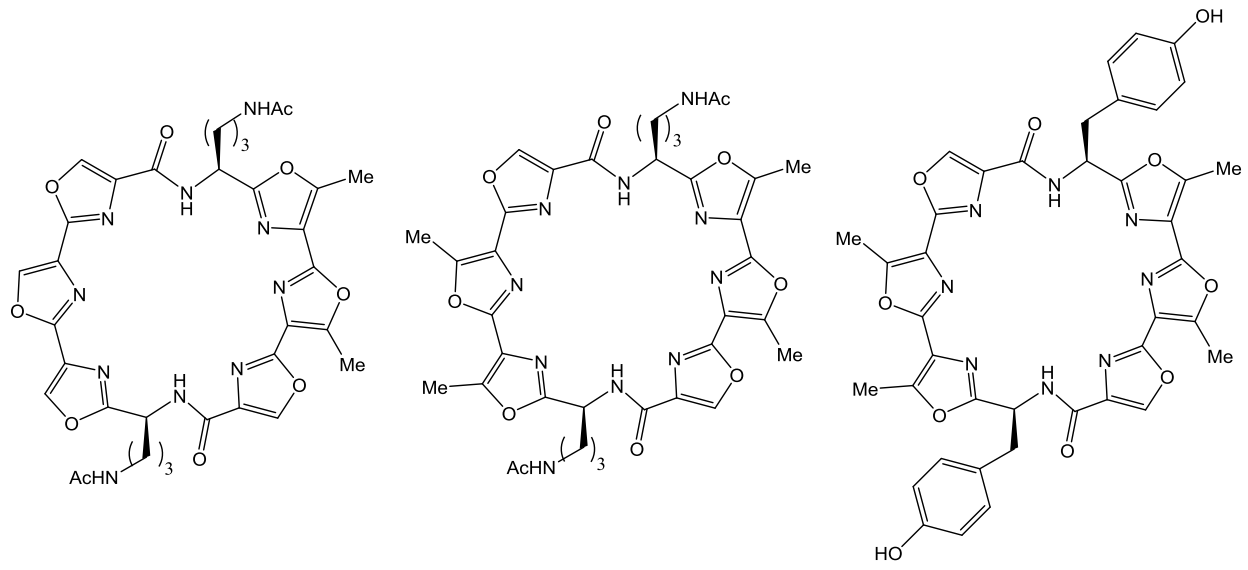

L2A2-6M(2)OTD (13) L2A2-6M(4)OTD (14) Y2H2-6OTD (15)

Figure 7: Structures of substituted hexaoxazole macrocyclic G-quadruplex ligands.[68]

1.2.3. Macrocyclic Heptaoxazoles (7OTDs)

Recently, Takayuki and co-workers have designed a series of heptaoxazole macrocycles that have planar skeletons resembling telomestatin. They anticipated that adding one more oxazole moiety into the corresponding hexaoxazole scaffold would increase the planarity of the macrocyclic structure. Thus, it was expected that the heptaoxazole macrocycles interact strongly and more efficiently with telomeric G-quadruplex DNA through π–π stacking interactions, regardless of the functional group of the side chain. The planar amine-linked heptaoxazole analogues (L1H1-7OTD) **16** (Figure 8), with positively charged side chains, were found to be more favorable G-quadruplex binders than the corresponding hexaoxazole. Compound **16** appears to be a powerful scaffold for stabilizing telomeric antiparallel G-quadruplexes. The

amino group in the heptaoxazole scaffold has a significant role in stabilizing telomeric G-quadruplexes due to the protonation of this group under physiological conditions. Compound **16** exhibited potent telomerase-inhibitory activity.[69]

The novel fluorescently-labeled G-quadruplex ligand L1BOD-7OTD **17** has been developed by attaching a BODIPY (4,4-difluoro-4-bora-3a, 4a-diaza-s-indacene) moiety to the side chain. This was used to visualize the G-quadruplex structure in cells. Moreover, it can selectively induce the formation of intramolecular G-quadruplex from some G-quadruplex-forming oligonucleotides (GFOs).[70]

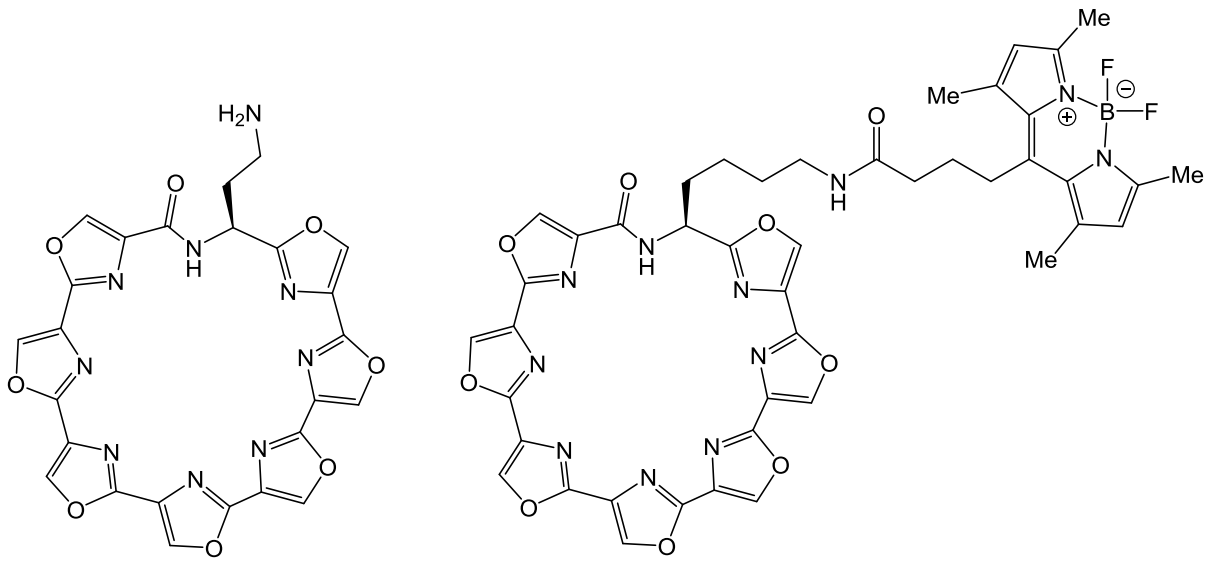

16

L1BOD-7OTD (17)

Figure 8: Structures of telomestatin–related heptaoxazole macrocycles.[69]

Takayuki and his co-workers studied the effects of side chain variation in (R)-heptaoxazole macrocyclic analogues of telomestatin, and have evaluated the telomerase-inhibitory activity. They synthesized three different methyloxazoles moieties (R) **18a-c** and one with a bromooxazole moiety **19** (Figure 9).[53] They found that substitution of the oxazole rings in heptaoxazole macrocycles, such as a methyl group or a bromine atom, have no significant effect on telomerase inhibitory activity or on the interaction with the G-quadruplex backbone, although it was reported that the induction and stabilization of G-quadruplexes increased with an incremental number of methyl oxazole moieties in the hexaoxazole.[68] Based on their observations, the planarity of heptaoxazole macrocycles could allow the ligands to interact whit the telomeric G-quadruplex structure by π–π stacking interactions regardless of the character of side-chain groups. Furthermore, the various aromatic rings introduced in **20a–f** on the oxazole rings had no effect on the telomerase inhibitory activity suggesting that the side chain do not interact with the telomeric G-quadruplex. In addition, the authors synthesized three amine-linked heptaoxazole macrocyclic analogues **21a–c** (Figure10) and examined their activity against telomerase. The amine-linked heptaoxazole macrocycle **21a** proved to be as potent as telomestatin, while **21b–c** were slightly less potent. Side-chain length was found to enhance the potencies of the ligands. It is worth noting that the positively charged amine-linker favors electrostatic interactions. Such functionality could reach the phosphate groups of quadruplex grooves to stabilize the G-quadruplex DNA structure.

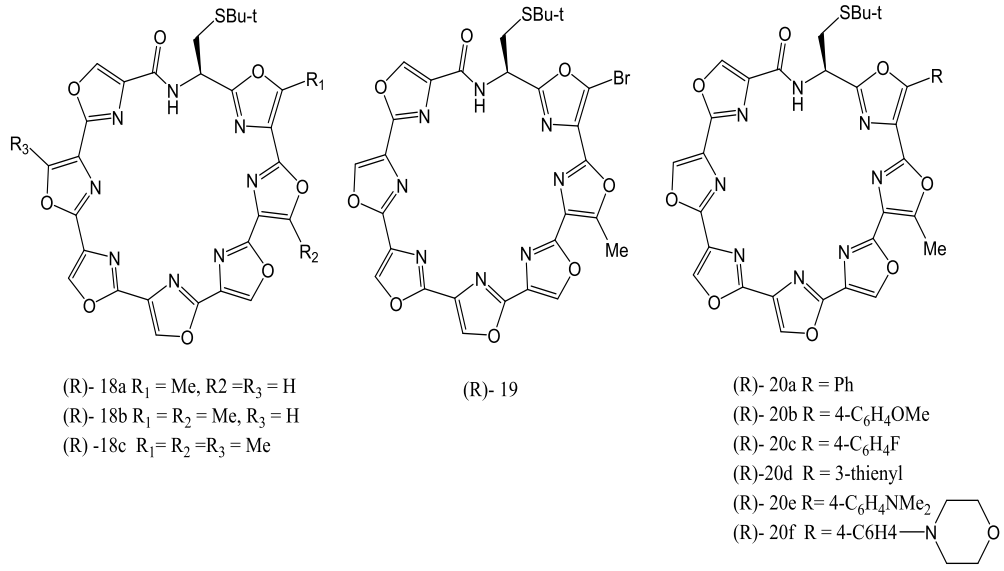

Figure 9: Structures of substituted heptaoxazole macrocyclic G-quadruplex ligands.[53]

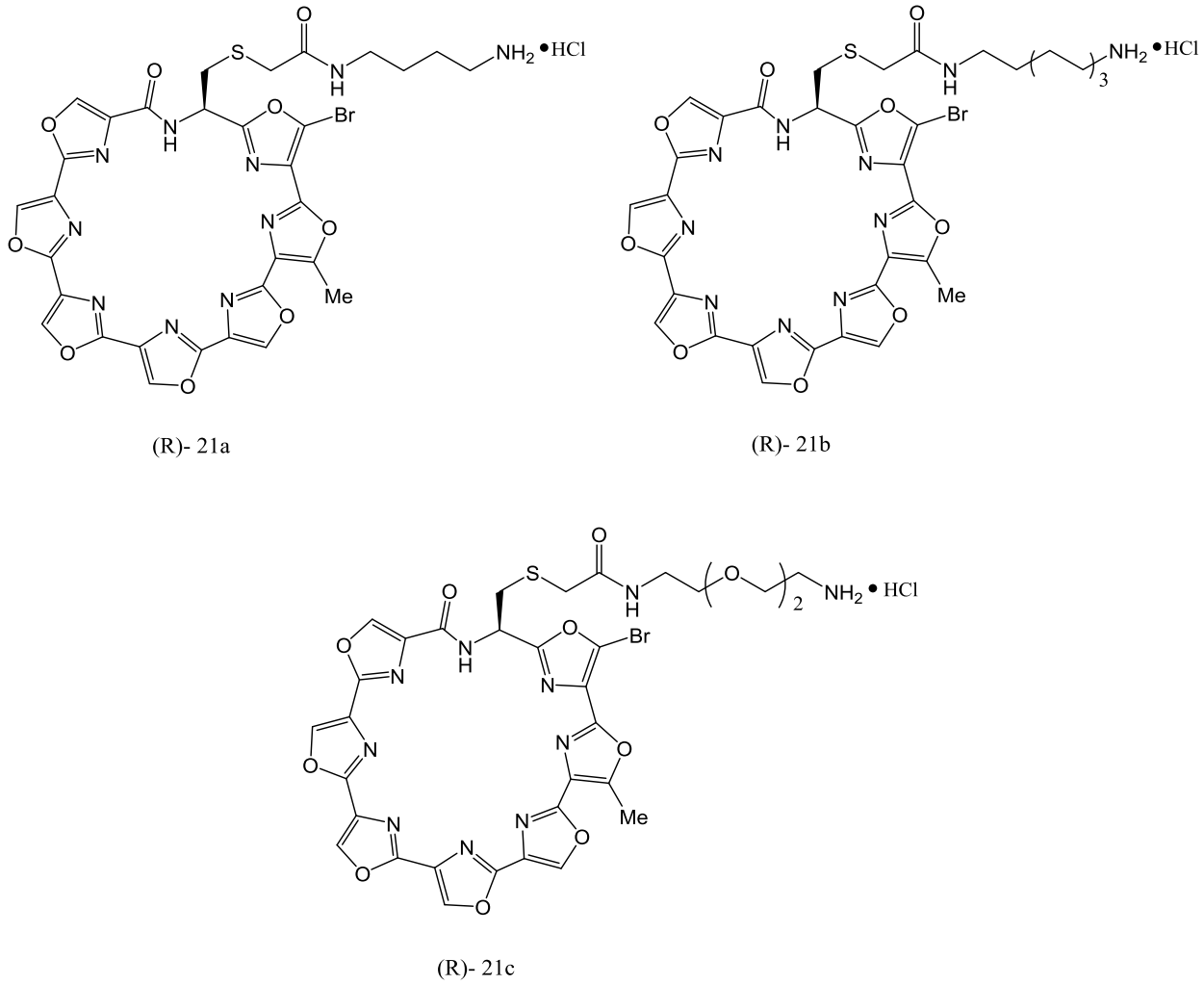

Figure 10: Structures of amine-linked heptaoxazole macrocyclic based G-quadruplex ligands.[53]

1.2.4. Synthesis of Macrocyclic Hexaoxazole Ligands (6OTD)

The synthesis of telomestatin-related hexaoxazoles was achieved by Shin-ya and co-workers[64] using a convergent synthesis. The compound was built from two segments of trioxazole **25**

(Scheme 1), which was the key synthetic intermediate in the synthesis for macrocyclic hexaoxazoles. The synthesis of the **25** began by coupling L-serine methylester bearing different protecting groups. The coupling was done using 1-[3-(diethylamino)propyl]-3-ethylcarbodiimide hydrochloride (EDCl). The resulting dipeptide **22** (Scheme 1) was subjected to a 2-step reaction with the fluorinating agent diethylaminosulfur trifluoride (DAST) to give an oxazoline, followed by an oxidation using bromotrichloromethane $BrCCl_3$ /DBU to yield the oxazole **23**. The resulting compound **23** was deprotected and dimerised to give **24**. Compound **25**, was generated by a cyclodehydration reaction of **24** with DAST followed by oxazole formation with DBU/$BrCCl_3$ to give trioxazole, which represents half of the target compound. Macrocyclic bisamide **27** was synthesized by dimerization of trioxazole **25**, giving the linear hexaoxazole **26** (Scheme 2), followed by deprotection of **26** and a macrocyclization performed under dilute conditions (1 mM) using *N*,*N*-bis(2-oxo-3-oxazolidinyl)phophinic chloride(BOPCl) and diisopropylethylamine in DCM-DMF. A final deprotection step allowed for the installation of various functional groups on the side chain, e.g., an acetyl group (OAc), to obtain compound **27**. Rice and co-workers [61] synthesized HXDV **2** (Figure 3) by following a similar strategy. Shin-ya developed the 6OTD that has an amine-containing side chain instead of alcohols. [58]

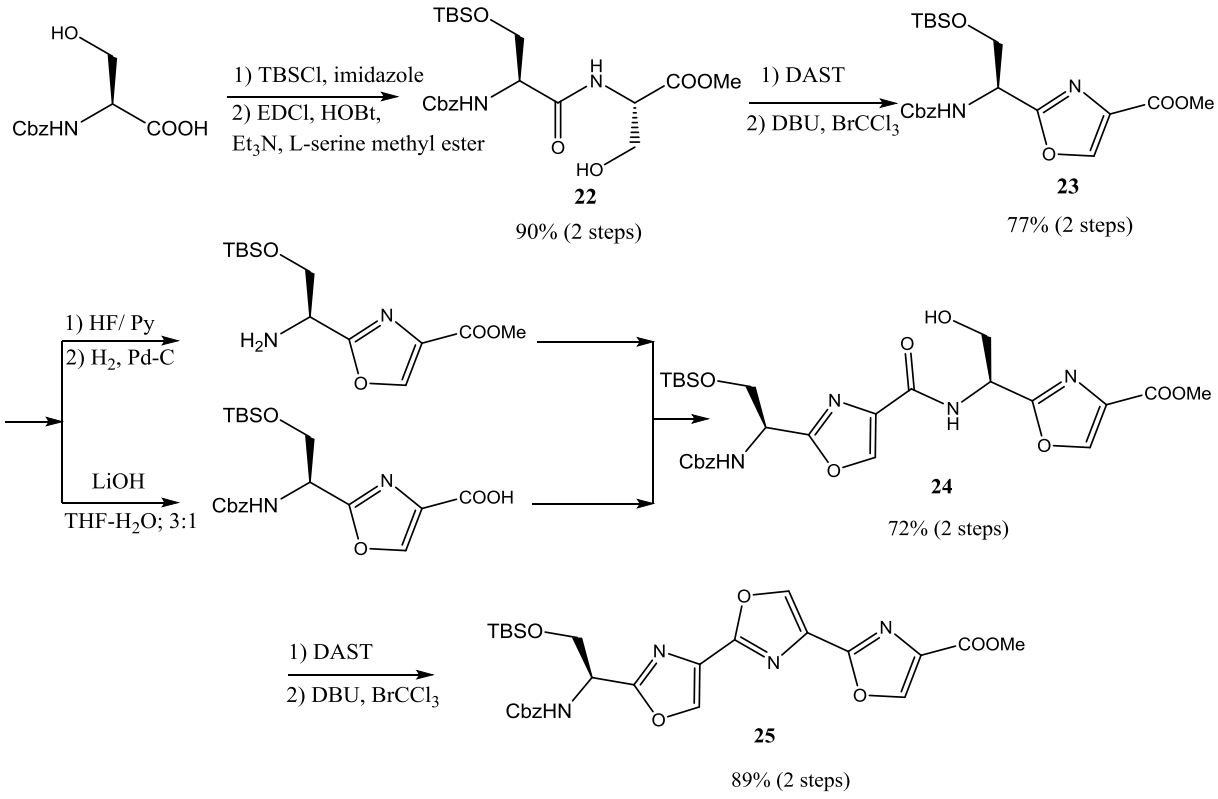

Scheme 1: Synthesis of the trioxazole (**25**).[64]

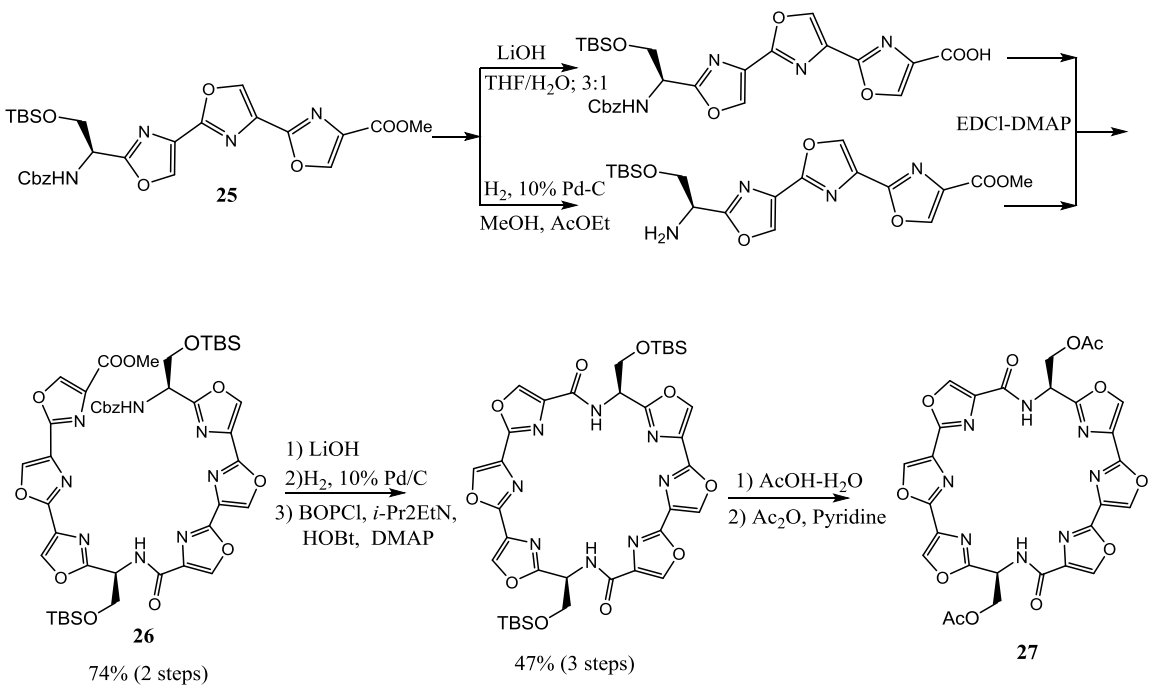

Scheme 2: Synthesis of hexaoxazoles (**27**).[64]

1.2.5. Synthesis of Macrocyclic Heptaoxazole ligands (7OTD)

Shin and co-workers proceeded to synthesize 7OTDs after the synthesis of telomestatin and related hexaoxazoles.[69] The total synthesis of heptaoxazoles (Scheme 3) is similar to that used for hexaoxazoles. The only difference between them is the use of two different trioxazoles that afforded a macrocycle with orthogonally protected side chains. The trioxazole **28** was prepared as previously reported.[64, 58] Briefly, coupling of the two of trioxazoles **28**, which was prepared in 6 steps, yielded the macrocyclic bisamide **29**. Compound **29** has two orthogonally protected side chains, of which TBS was deprotected to furnish the alcohol, and then converted into the enamide **30** by mesylation

and DBU treatment. By reacting with *N*-bromosuccinimide (NBS) and Cs_2CO_3 in acetonitrile at a high temperature **(**65 °C), **30** was transformed into **31**. This unconventional method was likely chosen due to the problem encountered when using the typical reagent DAST. Compound **30** was problematic because of the strained structure of the β-hydroxyamide moiety.[44, 61, 62, 71, 52]

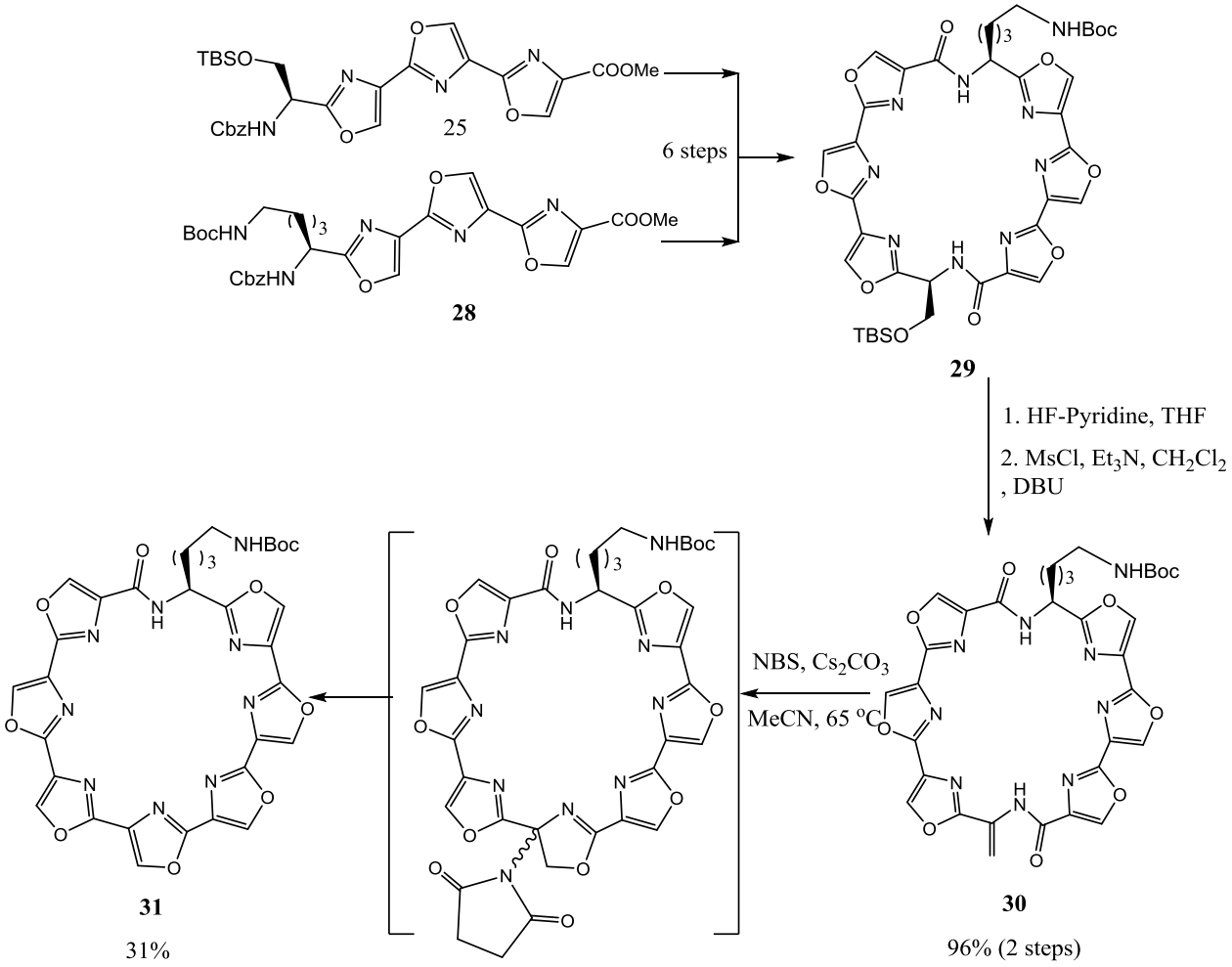

Scheme 3: Synthesis of heptaoxazoles (**31**).[69]

1.3. Development of a Synthetic Methodology for Poly-oxazole Macrocycles

Cyclic peptides that are derived from natural products are present in every living cell, and carry out a variety of biological activities. They work as hormones, enzymes, receptors, as well as antibacterial, antiviral, immunosuppressor, and anticancer agents.[72,73] The isolation of these naturally occurring cyclic peptides required long incubation times (fermentation or degradation), with such methods often providing low quantities of related analogues.[74,75] Despite the difficulties of scaling up these products, scientists have been synthesizing them in laboratories in great quantities, as they are needed for the study of their biological activities.

1.3.1. Common Methods of Oxazole Synthesis

Hantzsch discovered oxazoles in 1887.[76, 77] Oxazoles are widespread, occurring in many natural products and their heterocyclic oxazole derivatives have been synthesized and have been reviewed extensively.[78, 79, 80] Because these compounds are known to display a wide range of biological activities, a number of methods have been developed for their efficient construction. By far the most common type of oxazole found in natural products are the 2,4-disubstituted oxazoles. There are two general pathways to generate the 2,4-disubstituted oxazoles from hydroxyamides: (A) by dehydrative cyclization affording an oxazoline followed by oxidation to obtain the corresponding, oxazole, or (B) by oxidation to a 1,4-dicarbonyl species followed by cyclodehydration to give the oxazole (Scheme 4).

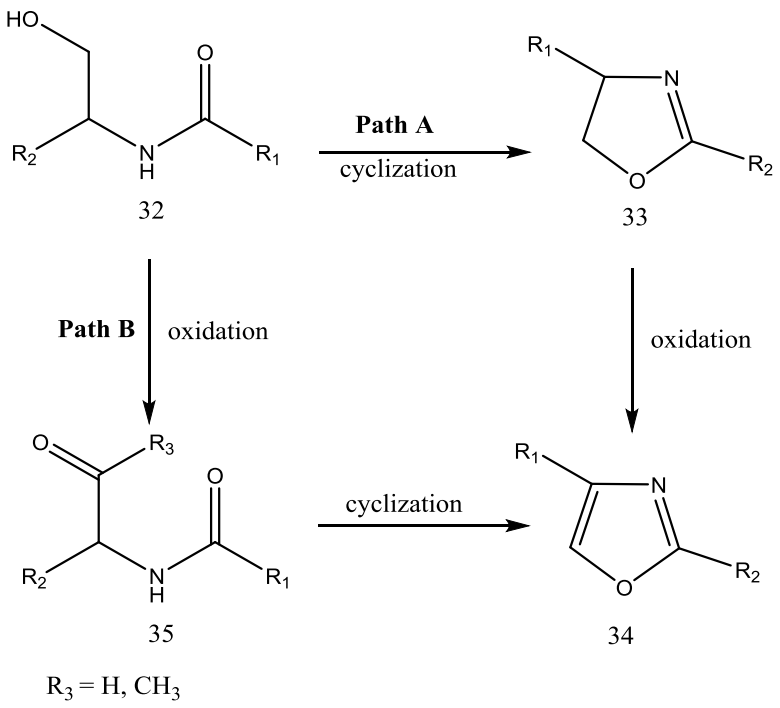

Scheme 4: Possible routes in the synthesis of 2,4-disubstituted oxazoles from hydroxyamides.

Researchers have therefore sought to develop an efficient synthesis based on these types of reactions. Initially, the formation of oxazoline could only be achieved by the activation of the hydroxyamide function in a manner that would induce the cyclization without any racemization at the chiral centers. There are many ways to activate the hydroxyamide prior to cyclization such as the Mitsunobu reaction,[81,82] using triphenylphosphine, carbontetrachloride (tetrachloromethane) and DIPEA,[83] or the more commonly encountered Burgess regent,[85] and DAST.[85, 86, 87] The most commonly used route toward oxazole synthesis is the cyclization–oxidation pathway. This approach is utilized in this work, and discussed in the following sections.

Wipf and co-workers introduced methyl *N*-(triethylammoniumsulfonyl)carbamate, also known as Burgess reagent **36**, in the preparation of natural products containing oxazoles.[88] The Burgess reagent acts as a mild and selective dehydrating agent, which is often used for the cyclodehydration of hydroxyl amides to afford the corresponding 5–membered heterocycles. The mechanism is outlined in Scheme 5. The hydroxyl group attacks the sulfonyl group of the Burgess reagent to form a sulfonyl ester, which can be easily transformed into oxazoline by the inversion of the configuration at the carbon (β–position) bearing the sulfamate as the leaving group or intramolecular cyclization (S_N2 substitution). According to the literature, the Burgess reagent allows the successful suppression of the epimerization at the α-carbon compared to other cyclization methods.[89]

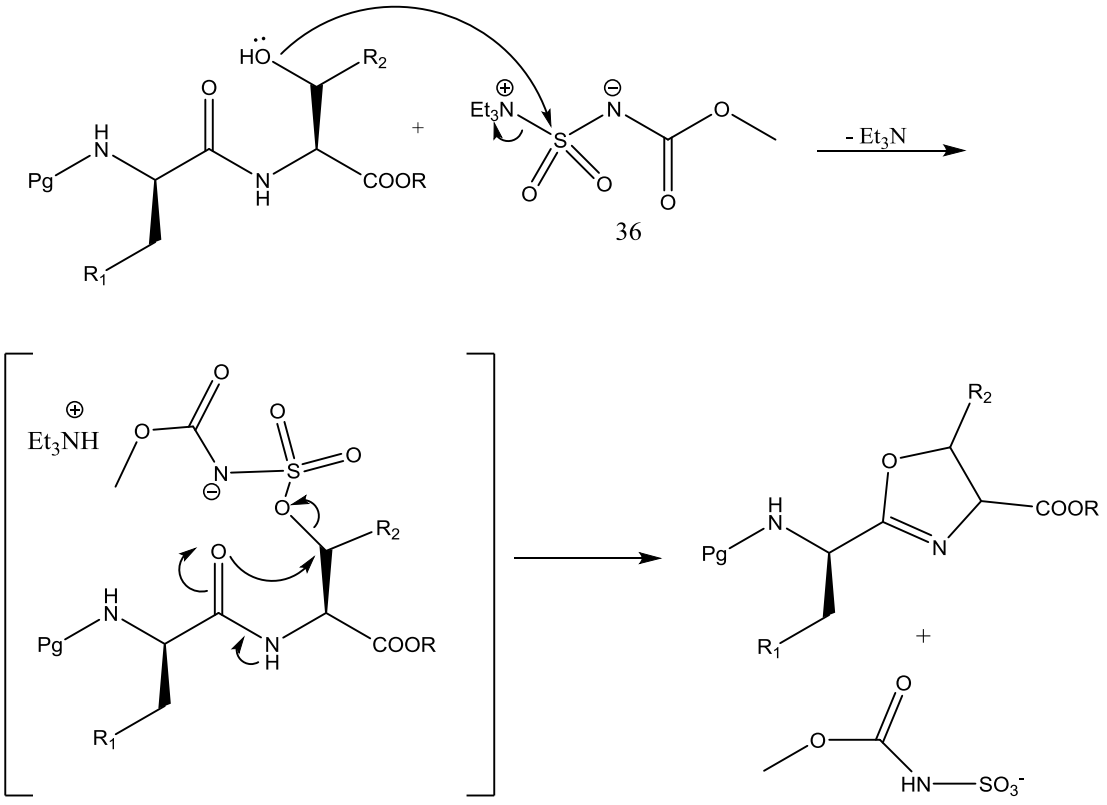

Scheme 5: The proposed mechanism of oxazoline formation with Burgess reagent.

In a typical Burgess-mediated cyclization, the starting material in dry THF reacts with 1 equiv. of the Burgess reagent and is refluxed under a nitrogen atmosphere at 70^{o} C. The use of the Burgess reagent has been demonstrated by Pattanden and Freeman's in the total synthesis of **38** as the final step for cyclodehydration (Figure 11).[90]

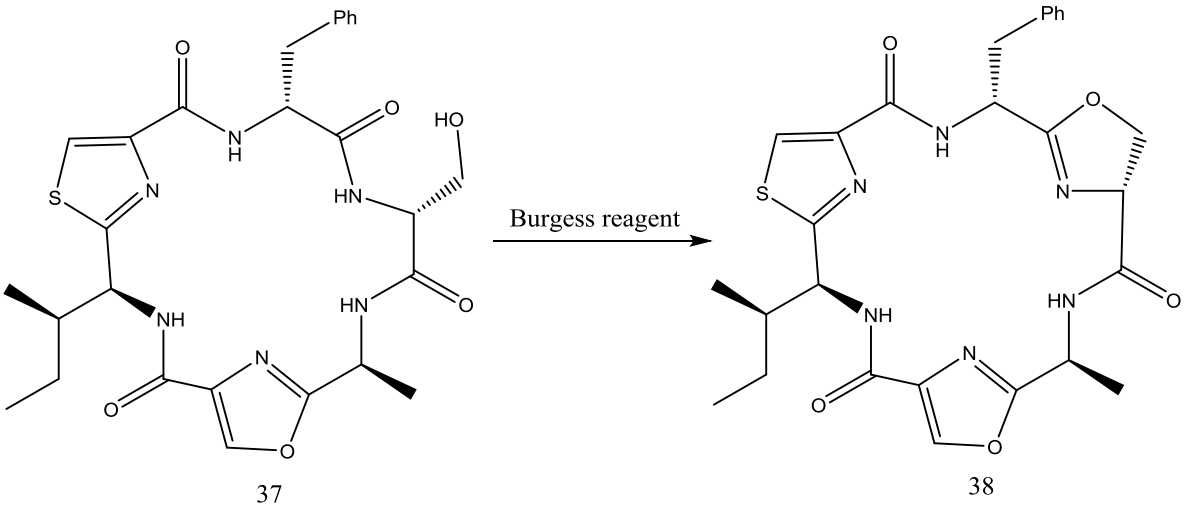

Figure 11: Conversion of β-hydroxyamide into oxazoline by Burgess reagent.[90]

Alternatively, the conversion of β-hydroxyamide into the corresponding oxazoline proceeds more efficiently when DAST (diethylaminosulfur trifluoride) was employed in the cyclodehydration step.[87] DAST (**39**) is a nucleophilic fluorinating agent used for the conversion of alcohol to the corresponding alkyl fluorides. The oxazoline formation involves the nucleophilic displacement of fluoride from highly electrophilic sulfur atoms in DAST. The alcohol oxygen atom of the β-hydroxyamide is converted into an activated species with a higher leaving group capacity.[91, 92] The carbonyl group or amide oxygen atom is a good nucleophile that causes the intramolecular attack of the activated hydroxyl group (inversion of configuration) which is faster than the substitution by the fluoride, thereby producing the corresponding oxazoline (Scheme 6).

An important safety consideration associated with the use of DAST in the laboratory is the shock and thermal instability of pure DAST.[93] Therefore, the oxazoline formation with DAST must proceed at -78°C to avoid local overheating and the risk of an explosion.

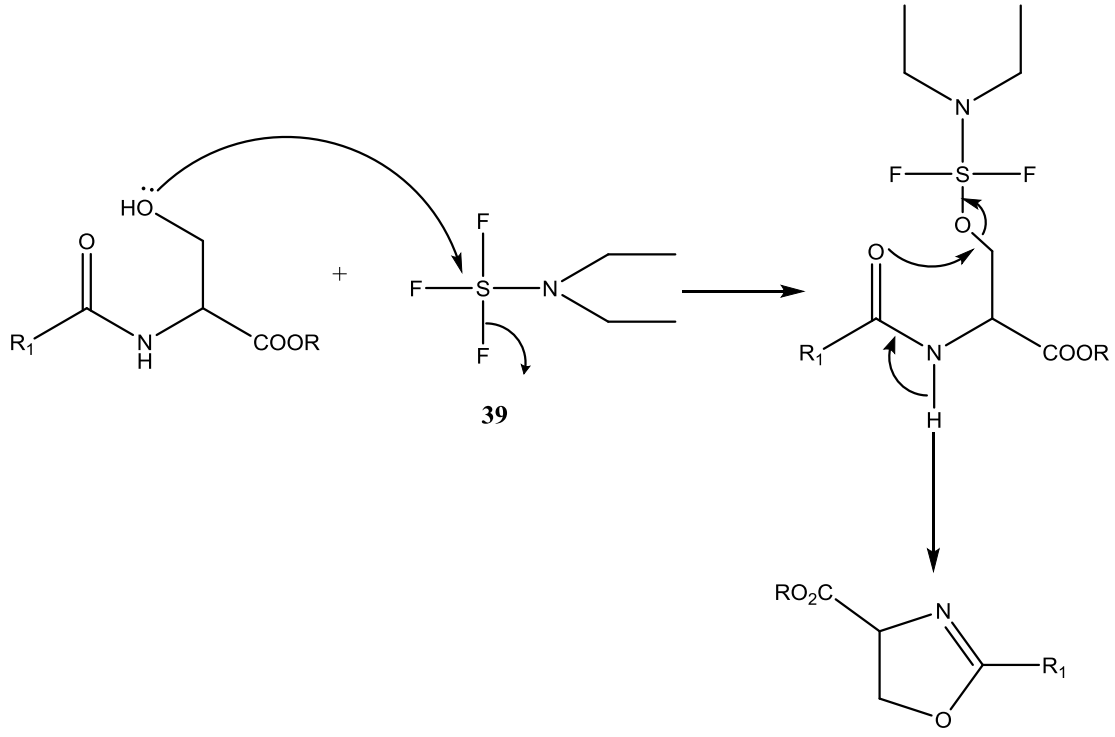

Scheme 6: Mechanism of the DAST-mediated cyclodehydration of β-hydroxyamide into oxazoline.

The oxidation of oxazoline has been developed extensively to proceed by either an addition–elimination sequence or a radical pathway. In either case, the transformation requires the need for an enolizable group at the 4–position to obtain the oxazole with a good yield. Many methods have been reported for the oxidation of oxazoline to oxazoles, including (1) nickel peroxide in refluxing benzene,[94] (2) NBS with either benzyl peroxide or light,[95] (3) the Kharasch–Sosnovsky reaction,[96, 97] and (4) bromotrichloromethane and 1,8-diazabicycloundec-7-ene (DBU).[98] The disadvantage of the first and second methods is that the yield of oxidized products rarely exceeds 40-50%,[94] and that α-bromination side products are formed when using NBS, with either benzyl peroxide or light.[95] Both of the two remaining methods have been investigated for the synthesis of 2-substituted-4-

carbomethoxy oxazole and thiazole.[96, 97, 98] The Kharasch–Sosnovsky reaction was the first chosen to be optimal for the oxidation to take place.[96, 97]

A cocktail of copper (II) acetate, copper (I) bromide, and *tert*-butyl perbenzoate was successfully applied to the oxidation of oxazoline and thiazoline. Scheme 7 shows the proposed mechanism of the copper-ion catalyzed radical reaction. The proposed process involves either of two mechanisms. In both there is the generation of a radical at the oxazoline by the peroxyester radical, catalyzed by Cu^{+}, followed by the oxidation of the radical to a carbocation by Cu^{2+} at the 4 or 5 position of the oxazoline ring. In the mechanistic pathway A, the resulting radical intermediate at the α-carbon is oxidized to form the intermediate cation **40a**. This carbocation is rapidly neutralized by a rapid elimination of a proton to provide the oxazole. On the other hand, in path B, the radical is oxidized to the intermediate **40b,** which provides the oxazole after elimination of a proton at the β-carbon to neutralize the positive charge.[95]

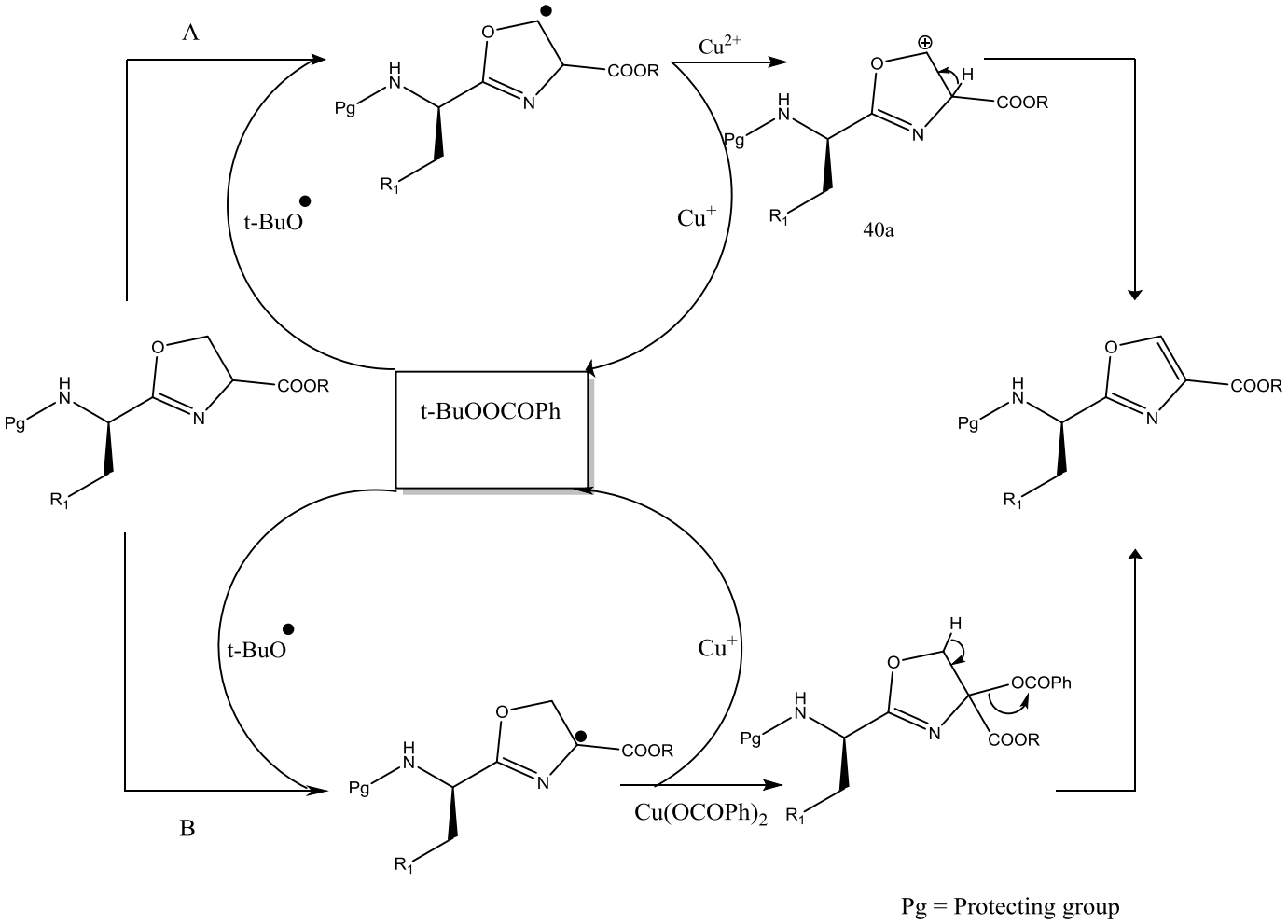

Scheme 7: The proposed mechanism for the oxidation of oxazoline to oxazole.

The addition-elimination of the bromotrichloromethane-DBU oxidation reagent is used for the selective oxidation of the oxazoline into an oxazole.[98] This oxidation using $BrCCl_3$–DBU proceeds through a C_4-bromooxazoline intermediate which readily eliminates HBr to afford the oxazole (Scheme 8).[86, 87, 99]

Hennoxazole A **46** was isolated from the chloroform extracts of the marine sponge, polyfibrospongia sp. and it is found to exhibit potent antiviral activity against herpes simplex virus (HSV-1). William successfully applied the cyclodehydration-oxidation protocol to the synthesis of 2,4–disubstituted bisoxazole **45** in his total synthesis of hennoxazole A **46** using DAST and the DBU–$BrCCl_3$ regent.[100] The total synthesis of **46** involved the treatment of **41** with DAST at -78 °C that first led to oxazoline **42**, followed by mild oxidation with the $BrCCl_3$–DBU reagent to allow the rapid dehydration and formation of the oxazole **43** in good yield. The ester was saponified to give the corresponding acid precursor, which was then coupled with serine methylester to obtain an amide **44**. The latter was subjected again to the cyclodehydration-oxidation strategy and yielded the bis-oxazole core **45** of hennoxazole A **46** (Scheme 9).

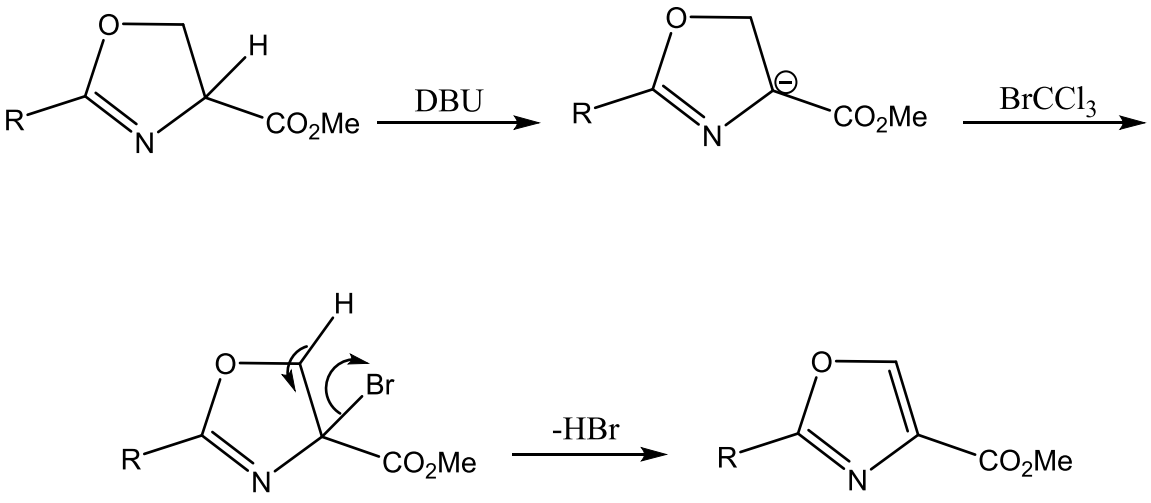

Scheme 8: The addition–elimination mechanism of the oxidation of oxazoline to oxazole by DBU-$BrCCl_3$.

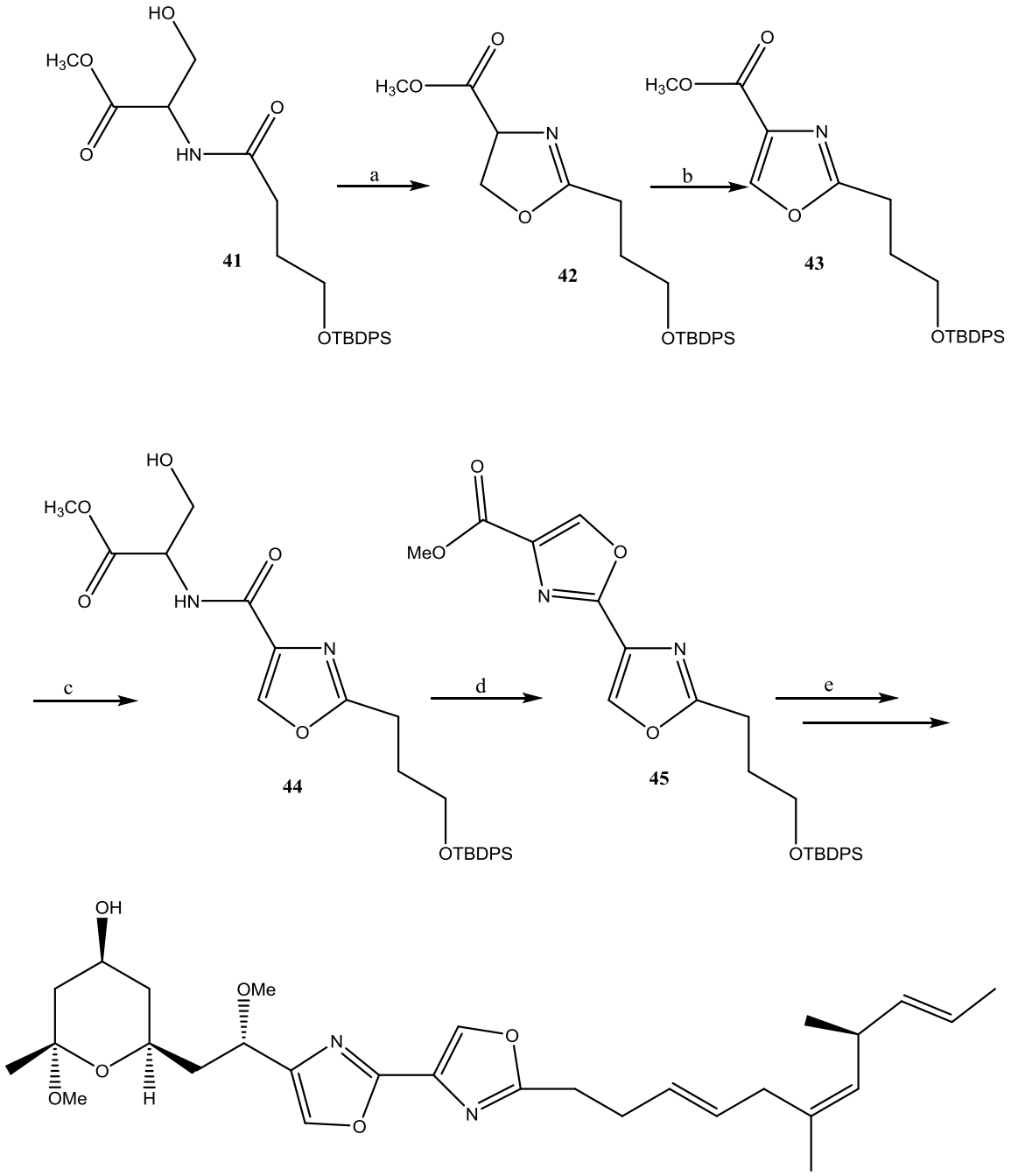

Scheme 9: Total synthesis of hennoxazole A using cyclodehydration-oxidation protocol.[100] Reagent: (a) DAST (1eq), DCM, -78°C, 1h; (b) K_2CO_3, -78°C- 0°C; (c) $BrCCl_3$, DBU; (d) LiOH, THF, H_2O; (e) iBuOCOCl, Et_3N, serine methylester.HCl, DCM, -20°C.

1.3.2. Macrocyclization Strategies for Cyclic Peptides

Cyclic peptides have several advantages as therapeutic agents, such as high resistance to degradation and elimination, and an increased affinity towards a molecular target.[101] The macrocyclization is one key step in the synthesis of cyclic peptides and is a useful strategy to reduce their flexibility. In general, there are four ways to constrain a peptide into a macrocycle: head-to-tail (C-terminus to N-terminus), head-to-side chain, side chain-to-tail, or side chain-to-side chain (Figure 12). Researchers have used all of these methods to form a variety of macrocycles.[102]

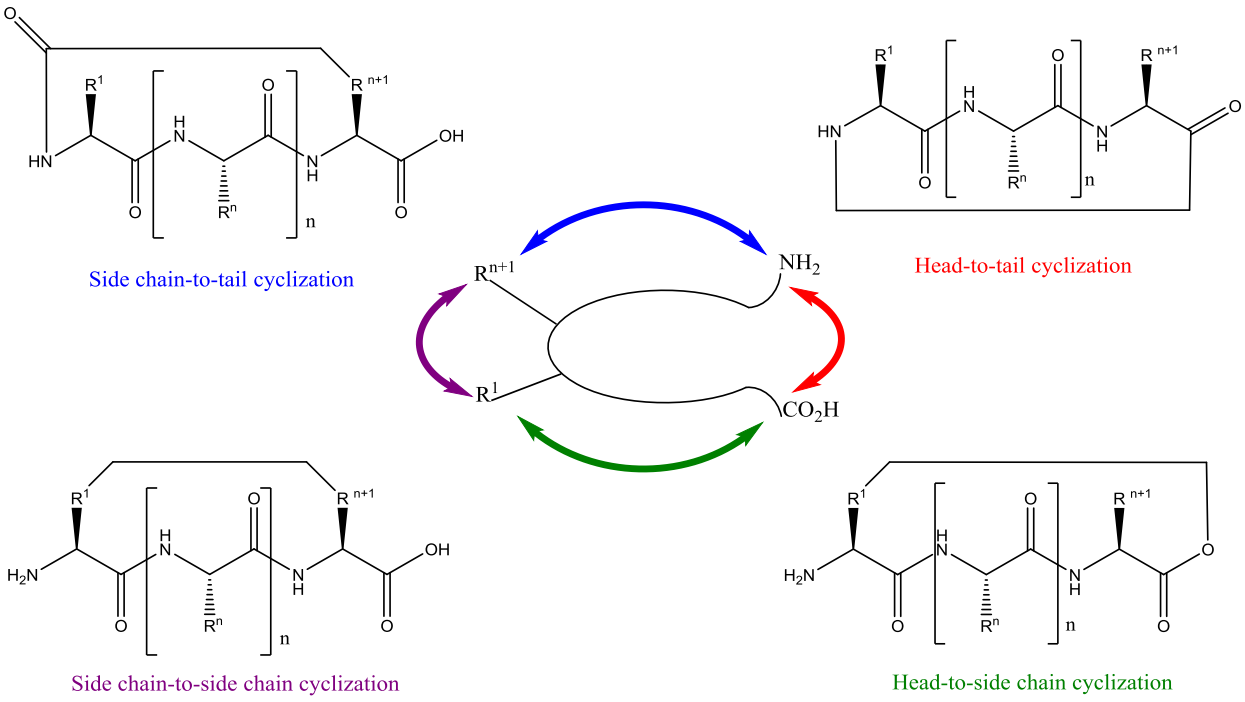

Figure 12: The four different ways of peptide cyclization.[102]

An example of the side chain-to-side chain macrocyclization is the synthesis of a cyclic peptide that interrupts the Tat-RNA interaction for the inhibition of HIV-gene expression.[103] To cyclize a peptide via this strategy, the linear precursor was anchored to a solid support and the peptide bond (amide bond) was formed between the side chains of L-glutamic acid and L-lysine (Figure 13).

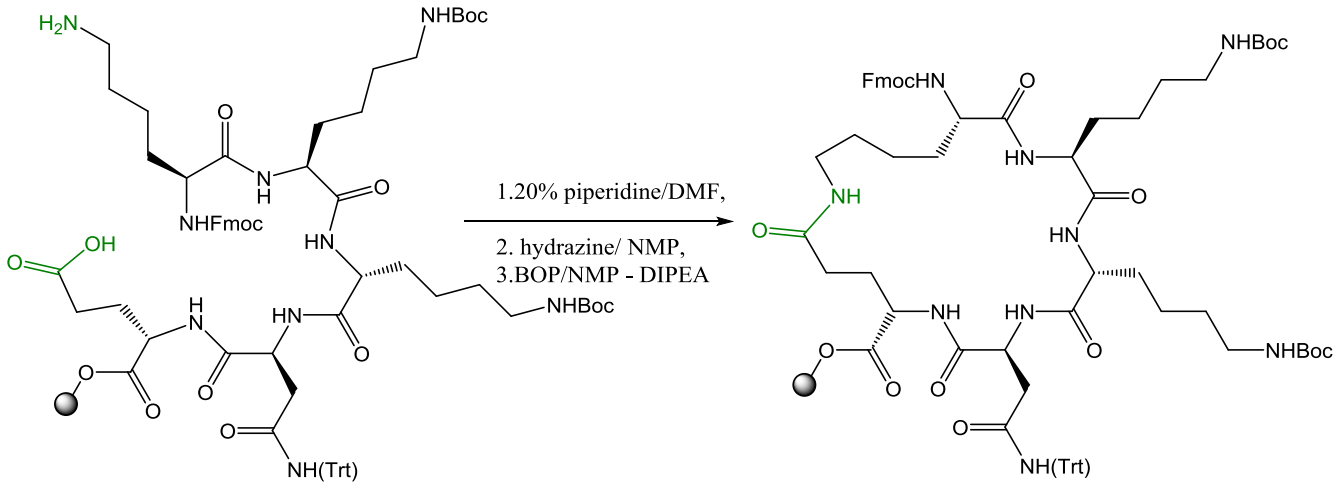

Figure 13: Synthesis of a cyclic peptide via side chain-to-side chain cyclization.[103]

Aldrich and co-workers[104] synthesized dynorphin A analogs using the head-to-side chain cyclization. Dyn A is an endogenous opioid peptide that is produced in many parts of the brain, and plays a role in the modulation of pain responses. The Dyn A analog was synthesized through the

formation of a lactam bond in which the *N*-terminus was attached to the glutamic acid side chain (Figure 14).[105]

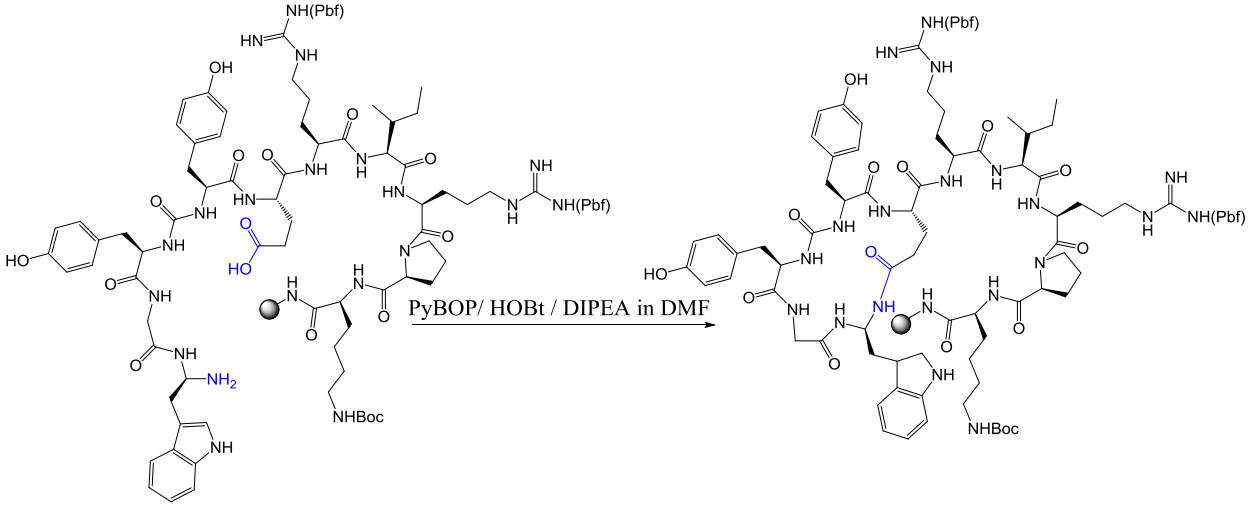

Figure 14: Side chain-to-tail cyclization of cyclic dynorphin A.[105]

Williams and co-workers[106] used the head-to-side chain macrocyclization strategy in synthesizing a class of thiolactone cyclic pentapeptides that are responsible for inhibiting staphylococcal virulence. The cyclization to generate the staphylococcal virulence inhibitor peptide involved a thiolactone linkage formation via a condensation of the cysteine side chain to the C-terminal carboxylic acid (Figure 15).

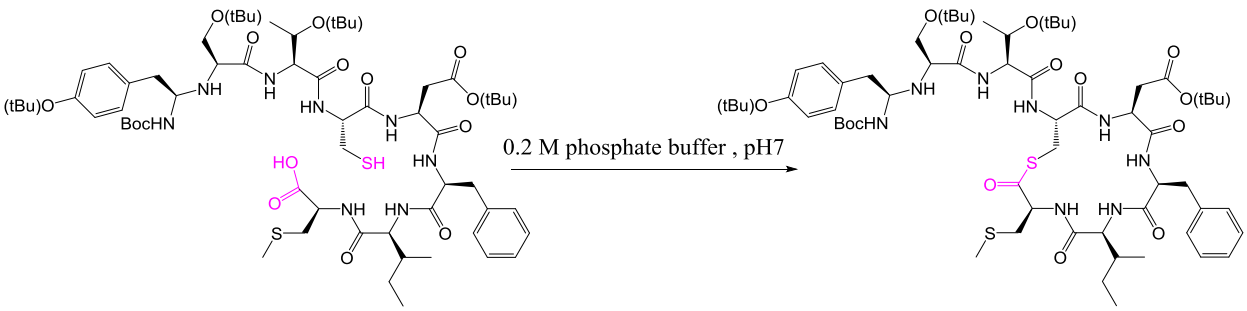

Figure 15: Head-to-side chain cyclization to generate the thiolactone linkage in a staphylococcal virulence inhibitor.[106]

Head-to-tail macrocyclization is a convenient and efficient methodology for cyclizing a peptide in solution. This method has been successfully applied in synthesizing long peptides (up to 20 residues), although the factor that governs the success or failure of a head-to-tail peptide macrocyclization is the conformation of the linear peptide precursor in the solution. One of the notable examples of the use of head-to-tail macrocyclization is the synthesis of the cyclic depsipeptide Halipeptin A [107]. Halipeptin A has been isolated from the marine sponge *Haliclona* sp., and exhibits promising anti-inflammatory activity *in vivo*.[108] The cyclization of Halipeptin A was done by the Hamada group, where the macrocyclization was achieved through peptide coupling at the N-MeOH-IIe/ Ala site (Figure 16).

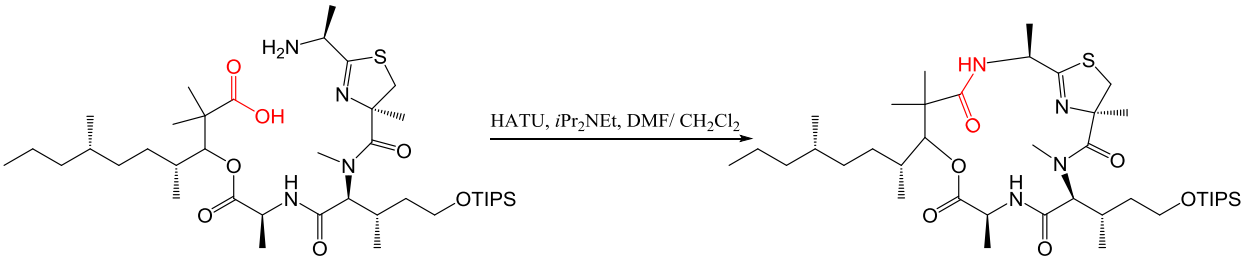

Figure 16: Head-to-tail cyclization in the synthesis of halipeptin A.[107]

1.3.3. Conformational Elements to Assist the Cyclization

The success of macrocyclization depends on the ability of the linear precursor to prearrange its two reactive ends in close proximity to each other.[102] Such prearrangement provides an efficient macrocyclization with fewer by-products from intermolecular processes. Helping to bring the two reactive ends of a peptide into close spatial proximity involves examining the secondary protein structure, and introducing turns into the peptide sequences.

The incorporation of L- and D-stereochemistry affects the orientation of linear peptides because these variations are suited to induce β-turns. When a peptide sequence consists of only all L- or D-amino acids, the cyclization is usually difficult or impossible because the β-turns are not present.[102] Kessler and co-workers have documented that *N*-methylamine acids and prolines play a role as β-turn-inducing elements to position the linear peptide in an orientation that facilitates the cyclization.[109]

1.4. Structural Features of Pseudo Cyclic Peptides

Studies on the configuration of azole-based marine cyclic peptides, both in solution and in the solid state, have provided insight into the factors that may affect the reactivities and the biological function of these unique secondary metabolites. The structure of westiellamide and its analogues has been investigated using X-ray diffraction and DFT- based molecular modeling. The structure of cyclic pseudo-peptides and their analogues depends on the configuration (R* vs S*) of the amino acid residues that connect to the macrocycles. The flexibility of macrocycles depends on the azole moieties. The structure of the macrocycles becomes relatively rigid due to the presence of the macrocyclic ring which fixes the position of the five ring atoms of the azole moieties, a feature which reduces the number of possible conformers.[110]

Usually, all peptide NH protons are located in the interior of the ring structure, and the carbonyl groups point towards the outside of the macrocycles. In case of westiellamide (Figure 17), the functional groups (L-valine side chain) face the same side of the molecule, and adopt pseudo-axial positions. The heterocyclic rings of oxazole- or oxazoline-based pseudo cyclic peptides are almost coplanar, whereas the incorporation of thiazole and imidazole lead to a cone-like structure.[111]

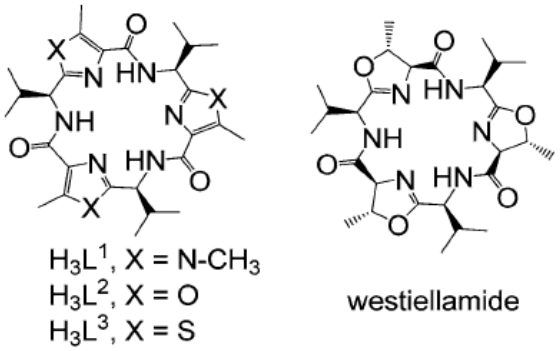

Figure 17: The chemical structures of the natural cyclic pseudo hexapeptide westiellamide and the cyclic pseudo hexapeptide $H_3L^{1\text{-}3}$.[110]

Haberhauer and co-workers used DFT to determine the structure of the cyclic peptides. The dihedral angle, χ [N_{amide}-$C\alpha$-C_{azole}-X], can be used to express the extent of deviations from planarity (χ = 180° in case of planarity) (Figure 18). The authors showed that χ depends on the azole system, and on the size of the amino acid side chains.[110]

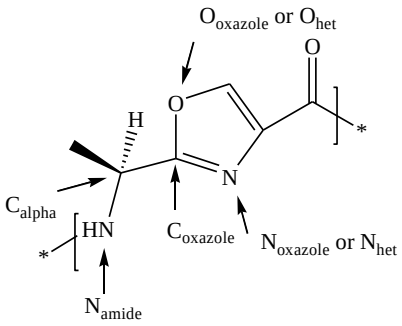

Figure 18: Nomenclature of heterocyclic building blocks of macrocycles.

They calculated the change in relative energy of reference systems with a chiral amino acid coupled to an azole moiety induced by a change of χ by using density functional theory (DFT). The obtained energy profiles of the imidazole and oxazole reference systems with a small methyl side chain (Figure 19, left) exhibit two minima between 0°and 200°. The minima of the imidazole system are at 90° and 150°, and those of the oxazole system are at 60° and 170°. However, the thiazole reference system with a small side chain has three energetically similar minima at 30°, 80° and 160°. From these observations, Haberhauer and co-workers suggested that thiazole-containing macrocycles are more flexible. The energy profiles change significantly when replacing the methyl group by the sterically more demanding *tert*-butyl group (Figure 19, right). As a consequence, the larger side groups increase the activation barrier for rotation around χ. The energy profile changes remarkably which leads to shifts in the minima in the profile especially between χ= 120°- 200°, which are caused by electronic and steric effects. Each energy profile has only one minimum in the 100° to 150° range. The distinctive minima are at 149°, 129°, 104° for oxazole, thiazole, and imidazole *tert*-butyl reference system, respectively. The reason for this behavior is mainly of electronic nature (Natural Bond Orbital (NBO) analysis): the π (C_{azole}-N_{het})-orbital of an imidazole ring is of high energy and, accordingly, the π-bond prefers to interact with the σ* (C_{α}-N_{amide})- orbital. The optimum interaction between these two orbitals is at an angle of 90°, where the σ* (C_{σ}-N_{amide})-orbital is oriented parallel to the π (C_{azole}-N_{het})-orbital. In contrast, in the oxazole system, the π* (C_{azole}-N_{het})-orbital is of low energy and therefore preferably interacts with the high energy σ(Cα-Cβ)- and σ(Cα-Hα)-orbitals. This interaction has its optimum at an angle χ of 180°.[110,112]

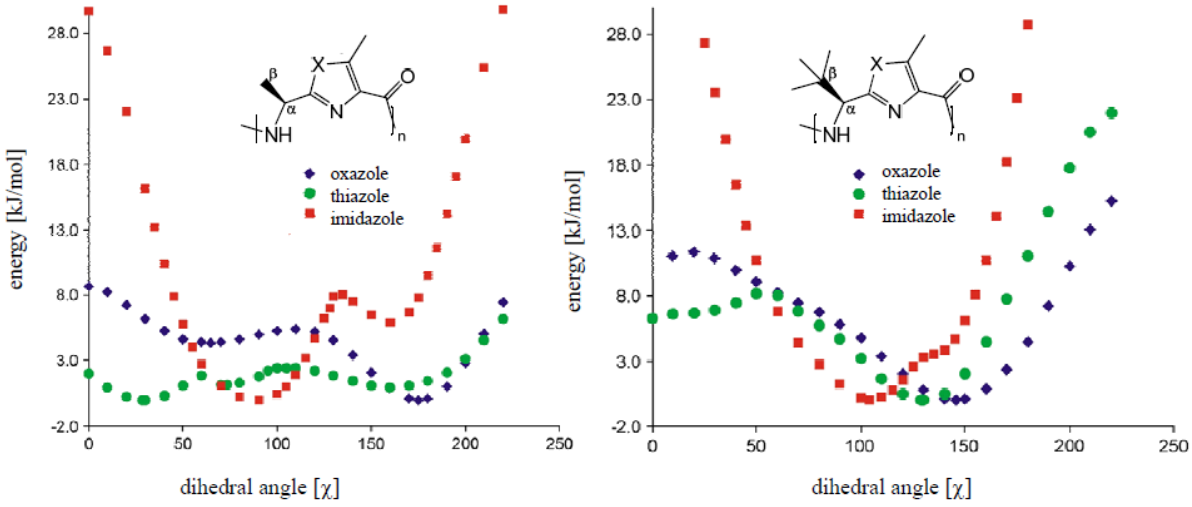

Figure 19: DFT-calculated energy profiles of the oxazole-, imidazole-, and thiazole- reference systems, in relation to the dihedral angel χ.[110]

In the case of cyclic pseudo octapeptides, the conformation is dependent on the configuration of the connecting amino acids and the system's symmetry.[113, 114] The symmetrical peptides, such as C_2-symmetric ascidiacyclamide, adapts a "square or saddle-shaped" conformation (Figure 20, left), in which all nitrogen atoms point towards the interior of the macrocycle with alternating oxazoline and thiazole moieties located at each corner of the macrocycle.[115, 114] On the other hand, patellamide D, takes on a "figure-of-eight" conformation (Figure 20, right), which is stabilized by two intramolecular hydrogen bonds, and by π-stacking of its thiazole rings [116, 113] hence, leading to a rotation of the oxazoline rings such that the nitrogen atoms face the outside of the macrocycle.

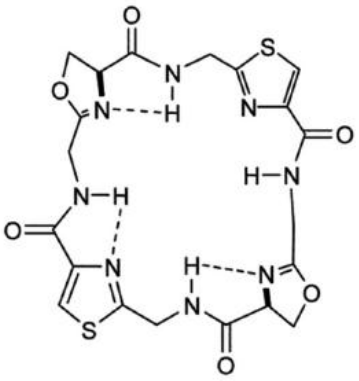

Square or saddle shaped

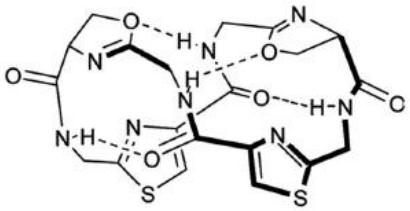

Figure of eight

Figure 20: Conformation of the backbones of the cyclic octapeptides ascidiacyclamide (left) and patellamide (right) in solution.[113, 114]

1.5. Copper (II) Coordination of Cyclic Pseudo Peptide

The described macrocycle conformations make the cyclic pseudo-peptides well suited for the binding of metal ions.[117, 118] The 24-azacrown-8 (pseudooctapeptide) macrocycle of ascidiacyclamide, patellamides, and some of their synthetic analogues have been shown to be able to coordinate divalent metal ions such as Zn^{2+} and Cu^{2+}.[119, 117 b, 120] The circular dichroism spectra of the mono- and dinuclear copper (II) complexes of patellamide D have been reported.[121, 122] In addition, the potentially biologically relevant ability of the dinuclear copper (II) complex of ascidiacyclamide to form carbonato-bridged complexes, where the copper (II) ions are bridged by a carbonate anion and embedded into the saddle-shaped conformation, has been reported.[119] As shown in Figure 21, the copper (II) ions are coordinated to three nitrogen atoms (donors), from two heterocycles and a deprotonated amide, and its coordination sphere is

completed by two water molecules. [120, 122] These metal peptide conjugates could be involved in activation and transport of CO_2 *in vivo*.

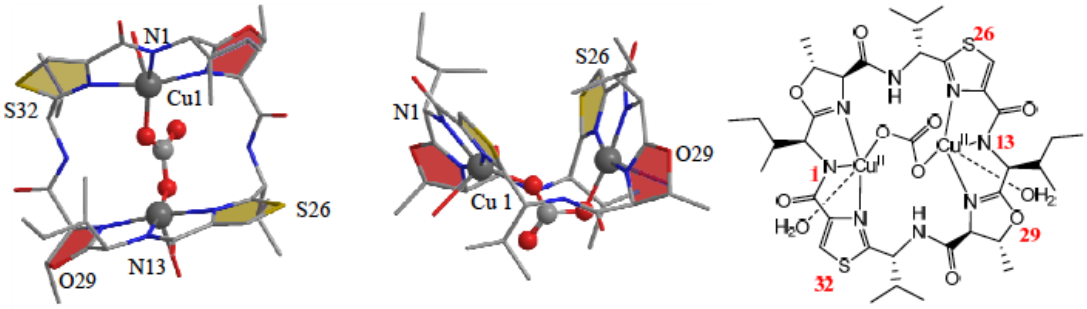

Figure 21: X-ray structure of the carbonato-bridged dinuclear copper(II) complex of ascidiacyclamide. Top view (left), side view (middle) and chemical structure (right). (Color code: carbon = grey, sulfur = yellow, nitrogen = blue, oxygen = red).[119]

Wipf and co-workers[123, 124] were the first to describe the synthesis and X-ray structure of an Ag_4 cluster of the C_3-symmetric cyclic peptide westiellamide, which provided clear evidence of binding of the westiellamide to metal ions. In addition, the authors observed weak interactions between westiellamide and other metal ions such as sodium (I), copper (I), iron (II), iron (III), mercury (II), gold (II), and zinc (II),[124] and found evidence for a strong interaction of copper (II) with the westiellamide macrocycles.[125] Comba and co-workers have revealed that after the addition of base to copper (II) westiellamide and its synthetic analogues, the cyclic pseudo hexapeptides readily from stable dinuclear copper (II) complexes.[126]

In the complexes, each copper (II) is coordinated by three nitrogen atoms of the macrocycle, and its coordination sphere is completed by one or two solvent molecules. In

mononuclear and dinuclear copper (II) complexes, the Cu (II) is coordinated with two of the coordinating nitrogen atoms originating from the heterocycles (azole rings) and one nitrogen atom from a deprotonated amide group, thus forming a N_{het}-N_{amide}-N_{het} binding motif. In order to complex copper (II), the nitrogen atoms of the binding site need to be deprotonated. The deprotonation is metal ion-assisted, hence acidifying the solution due to the protons being released upon the coordination of copper (II) and thus, the addition of a base is mandatory to achieve complete complexation.[125]

H_4pat^1, a C_4-symmetric macrocycle that has four identical methyl imidazole units connected via *L*-valine linkers, is a simple model system for natural cyclic pseudo peptides (Figure 22). The formation of a carbonato-bridged dinuclear Cu^{2+} complex, which has been demonstrated with patellamide D and ascidicyclamide, could not be observed experimentally in the H_4pat^1 because the combination of imidazole heterocycles with an alternating R^* and S^* configuration. The imidazole rings induce a rigidity in the system and the alternating configuration induces steric strain that seems to hamper the reaction with CO_2 imidazole heterocycle.[127] Copper (II) complexation of patellamide D was observed based on the electronic, CD and EPR spectral titrations. The sequence of the complexation reactions with Cu^{2+} was similar to that observed with the dicopper (II) complex with ascidicyclamide.[119, 128]

A general scheme of solution equilibria has been proposed after extensive studies with a series of the synthetic analogues H_4pat^1- H_4pat^5 (Scheme 10). It is interesting note that the Cu^{2+} in H_4pat^3 is not coordinated to the usual N_{het}-N_{amid}-N_{het} binding motif but to the outside of the

macrocyclic system by oxygen atoms of the amide bond. In addition, the outside coordination has a higher stability than the mono- or dinuclear complexes at low base concentrations. However, high concentrations of base enable the coordination of copper (II) in the " normal" N_{het}-N_{amid}-N_{het} binding motif, indicating that the addition of base increases the deprotonation the amide nitrogens. The mono-hydroxo-dicopper (II) complexes have two isomers, one with a terminal and one with a bridging hydroxide. Upon addition of excess base and the exposure to air to the carbonato-bridged and diaqua complexes, there is one more species in equilibrium (referred to as the "pink species") which has not been fully characterized yet. These species have been observed with H_4pat^3 and H_4pat^2, but not for H_4pat^1 and H_4pat^{ascA}.

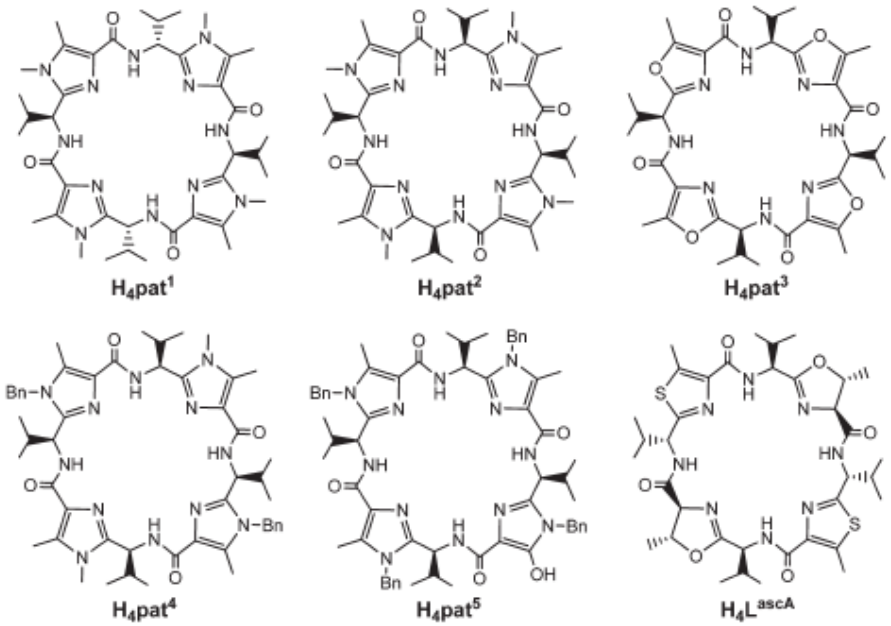

Figure 22: Structures of the patellamide model systems H_4pat^1 to H_4pat^5, and the ascidiacyclamide analogue H_4L^{ascA}

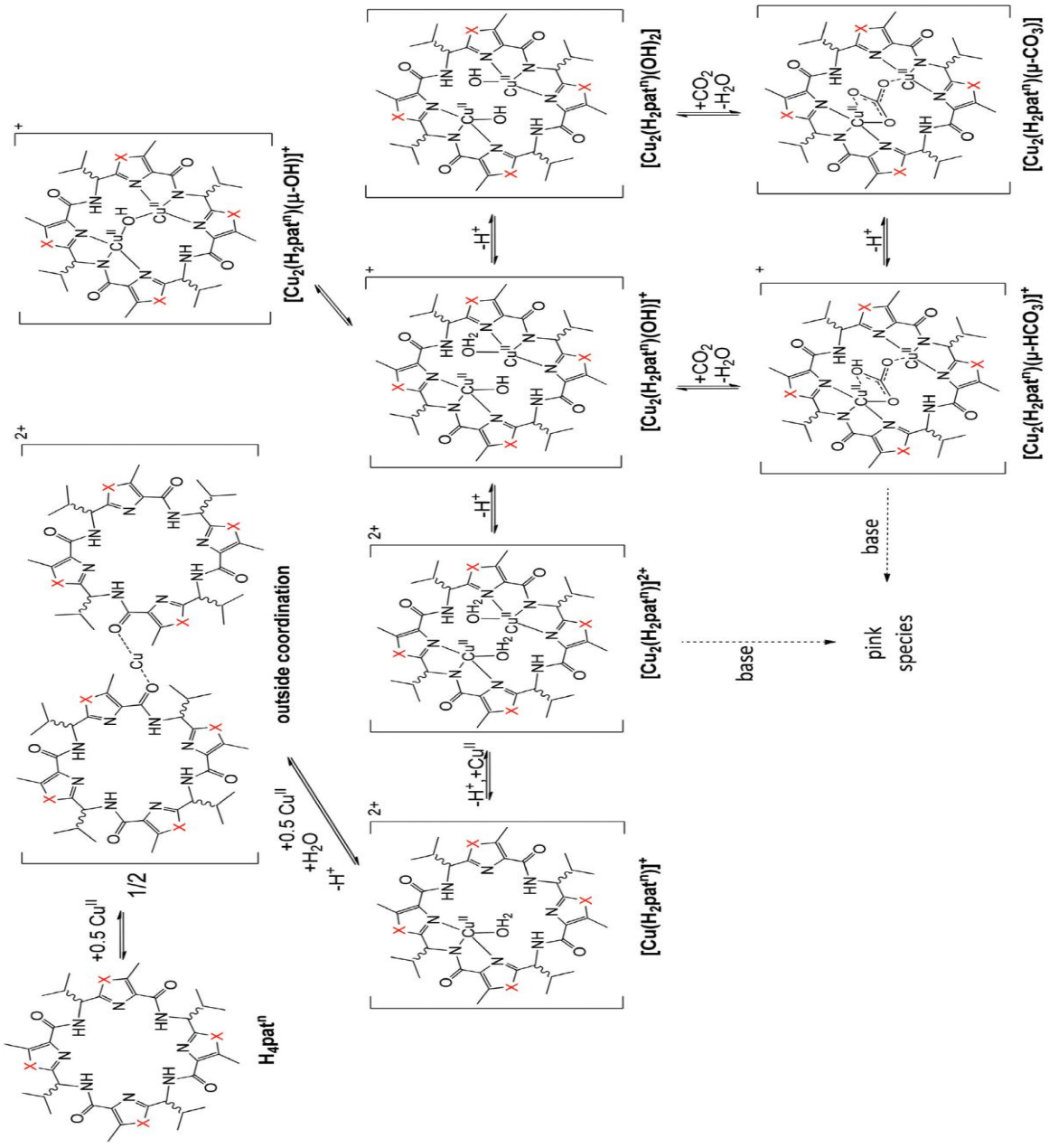

Scheme 10: Assumed copper (II) complexation equilibria of H_4pat^n[1-5].[129]

1.6. Objectives

The objectives of the thesis are two-fold:

1) To prepare the tetraoxazole-containing macrocyclic compound, **55**.

2) To determine the ability of the macrocycle to complex Cu(II) ions.

Boc- solution and solid phase chemistry will be investigated as means to accomplish the formation of the oxazole ring and macrocyclization in a one-step process. The two approaches proposed to achieve this goal are:

1) the cyclodehydration-oxidation of the hydroxyamide, and

2) the use of an oxime resin to facilitate the cyclitive-cleavage strategy.

The ability of **55** to complex Cu(II) will be tested using the procedure developed by Comba and co-workers for the H_4pat^1 macrocycle.[126]

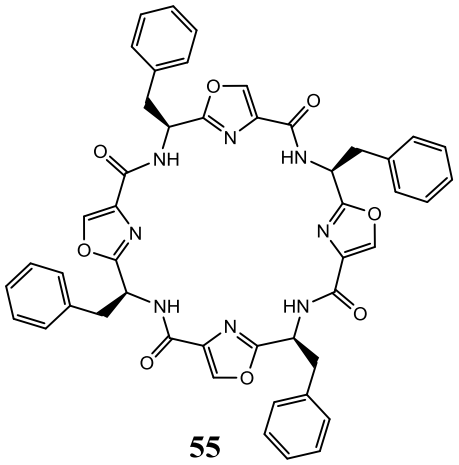

55

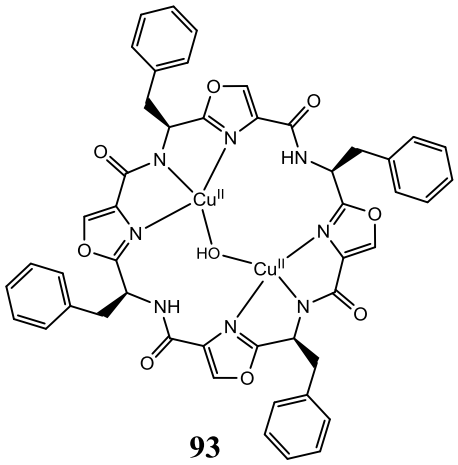

93

Figure 23: Structures of tetraoxazole macrocycle (**55**) and copper(II)-tetraoxazole macrocycle complex (**93**)

2. Results and Discussion

2.1. Solid Phase Peptide Synthesis

2.1.1. Synthesis of Cyclic Octaserine-OtBu (47)

Our initial efforts focused on the synthesis of 24-membered cyclopeptides via solid phase peptide synthesis using microwave energy. Figure 23 shows a retrosynthetic scheme of the desired macrocyclic peptide **47**, which outlines macrocyclization via the head-to-tail peptide coupling of the linear octapeptide precursor **48**. This linear octapeptide precursor, **48**, was generated via a step-wise assembly onto a preloaded Wang resin. Commercially available Wang resin preloaded with Fmoc-Ser-OtBu (**49**) (0.8 mmol/g, 0.125 g) was swollen in DMF for 20 min with the aid of a CEM Liberty Automated Microwave Peptide Synthesizer (Scheme 11). Next, the resin-bound amino acid was deprotected by treating the materials with 20% piperidine in DMF at room temperature for 3 s followed by raising the temperature to 75°C and allowing the reaction to proceed for 3 min. The liquid was removed and the resin was washed with DMF. The first coupling reaction was performed by adding 3 equivalents of HOBT, 3 equivalents of HBTU, and 6 equivalents of DIPEA to 0.5 mmol of resin-bound Fmoc-Ser-OtBu-OH and agitating the mixture for 5 min at 75°C. These reaction cycles were repeated until the desired linear octapeptide, **52**,was obtained. The final peptide product was released from the resin by treatment with 25% TFA in DCM for 20 min followed by deprotection of the Fmoc protecting group using 20% piperidine in DMF. We anticipated that we could obtain the fully protected octapeptide, **53**, if the peptidyl resin was treated with 25% TFA in DCM. Unfortunately, all our attempts to isolate the linear protected octapeptide failed, and only decomposition products were detected. A major drawback to the success of this

synthetic route was due to the fact that the orthogonal protecting group, *tert*-butyl ether, is acid labile. To remedy this problem, the synthesis of the macrocyclic peptide was attempted via a cyclitive-cleavage approach using oxime resin.

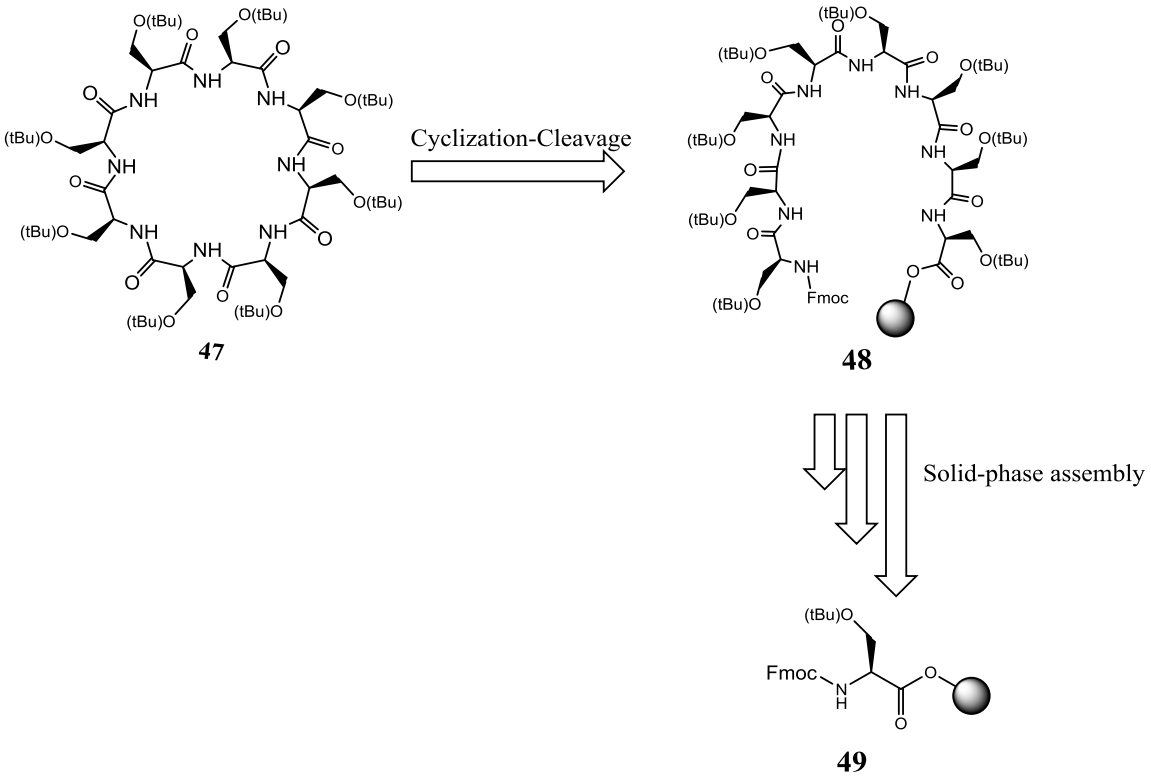

Figure 24: Retrosynthetic approach for the synthesis of **47**, an octaserine macrocycle

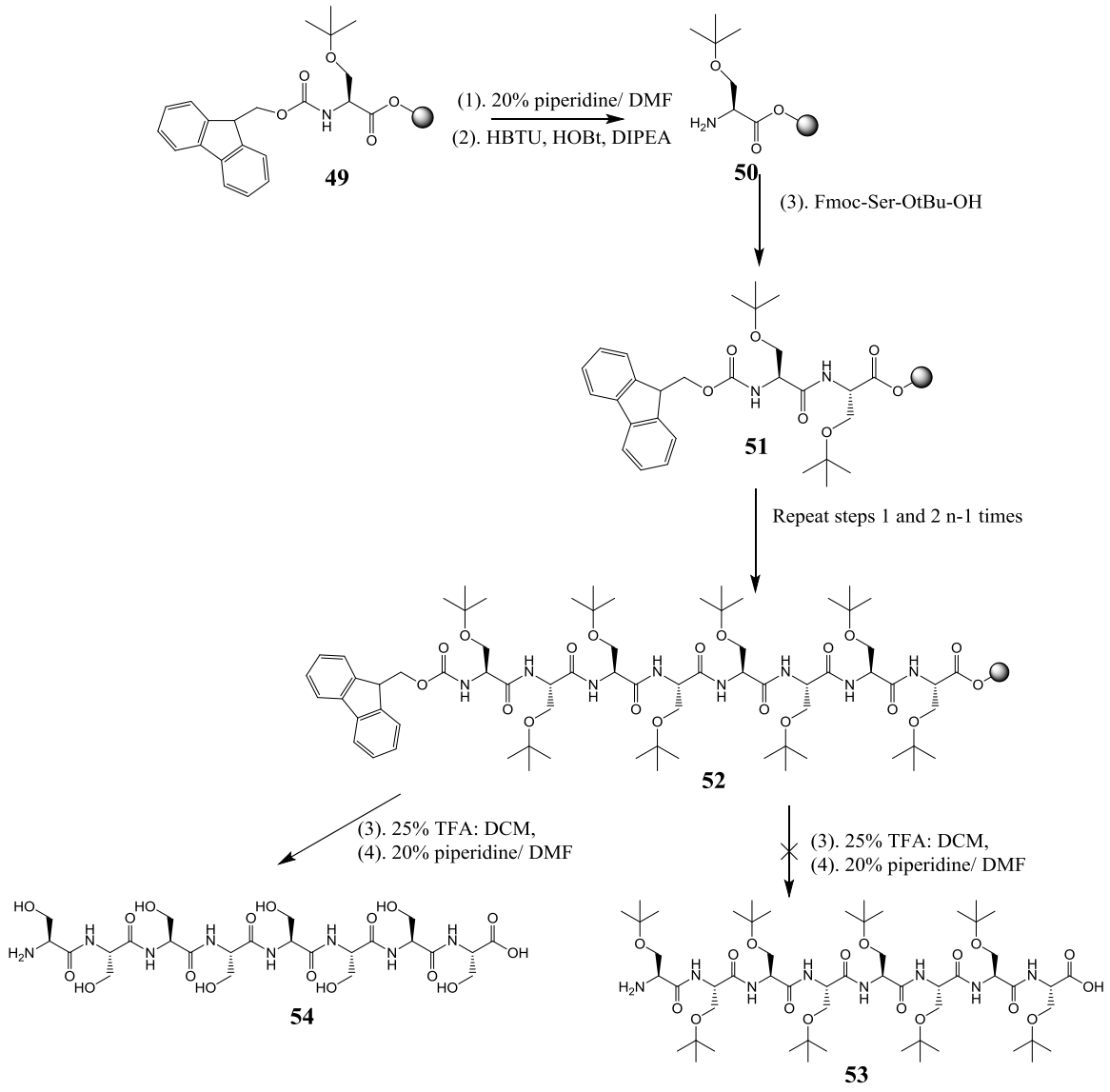

Scheme 11: Reaction of Wang resin preloaded with Fmoc-Ser-OtBu results in the formation of **51**, **52**, and **54**. **53** is not formed because the *tert*-butyl ether groups are cleaved when the resin is treated with weak acid.

2.1.2. Synthesis of the Heterocyclic Ring (Oxazole)

Our next task was to develop a convenient procedure to prepare the 5-membered heterocyclic ring (oxazole) directly on a solid support from readily available resin-bound protected Fmoc-α-amino acids. These building blocks would enable the total synthesis of tetraoxazole macrocycle **55** (Figure 24). Prior to preparing the macrocycle, our intention was to obtain the oxazole-based peptide from a serine residue that could be readily converted into oxazole.

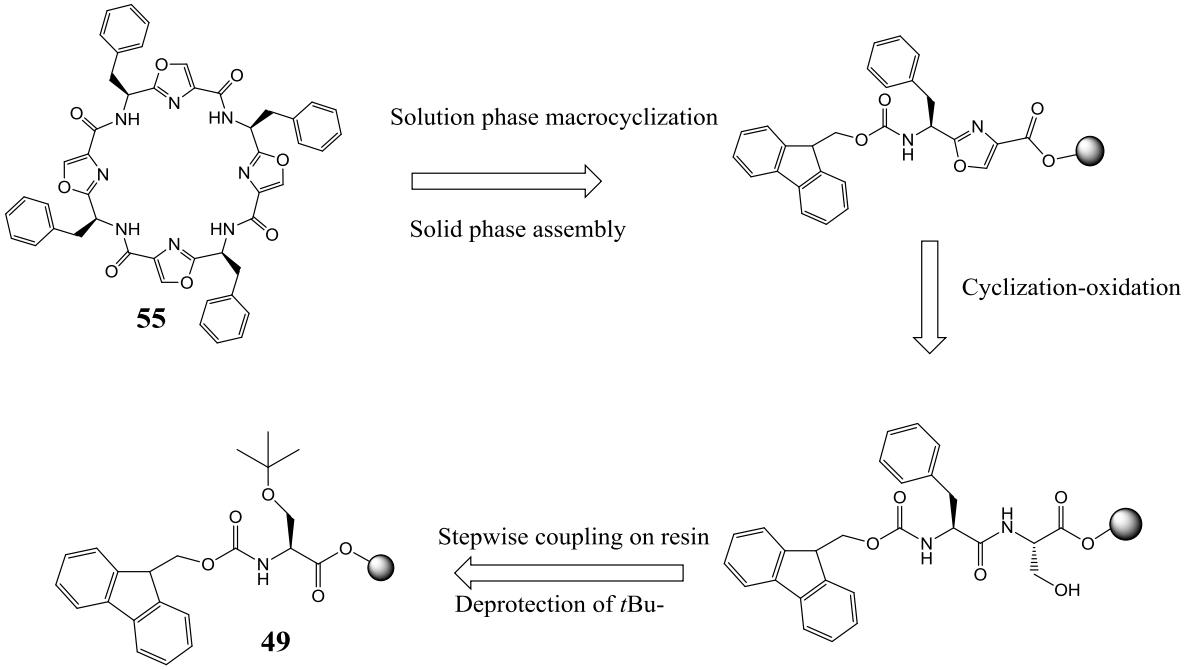

Figure 25: Potential retrosynthetic analysis of tetraoxazole macrocycle **55** via a solid phase peptide synthesis approach using Wang resin.

As shown in Scheme 12, we selected *N*-Fmoc-Ser-OtBu-Wang resin, **49**, as a starting material, and the dipeptide was synthesized by using a CEM Liberty Automated Microwave Peptide Synthesizer. In order to investigate the efficient preparation of oxazole, we decided to reduce the number of amino acids assembled onto the solid support to avoid complication from aggregation or steric hindrance due to the peptide sequences. The resin-bound amino acid, **49**, was swollen in DMF for 20 min, and a 20% piperidine solution in DMF was used to remove the N^{α} -Fmoc protecting group. The resin was washed several times after being coupled to Fmoc-Phe-OH using HOBT/HBTU in the presence of DIPEA. After coupling, we attempted to selectively remove the *t*-Bu group using hydrated $CeCl_3$ / NaI in CH_3CN at 70°C.[130] The resin was washed with DCM (2x), DMF (3x) and MeOH (1x), and then dried under vacuum. The dried resin, bound to dipeptide **57,** was subjected to cyclodehydration with TPP, I_2 and imidazole[131] in DCM for 15 min at room temperature. The resulting oxazoline was treated with NBS/ K_2CO_3[132] in an attempt to prepare the oxazole-containing dipeptide **58**. Subsequently, adding 25% TFA/DCM gave **59** rather than the desired **60**.

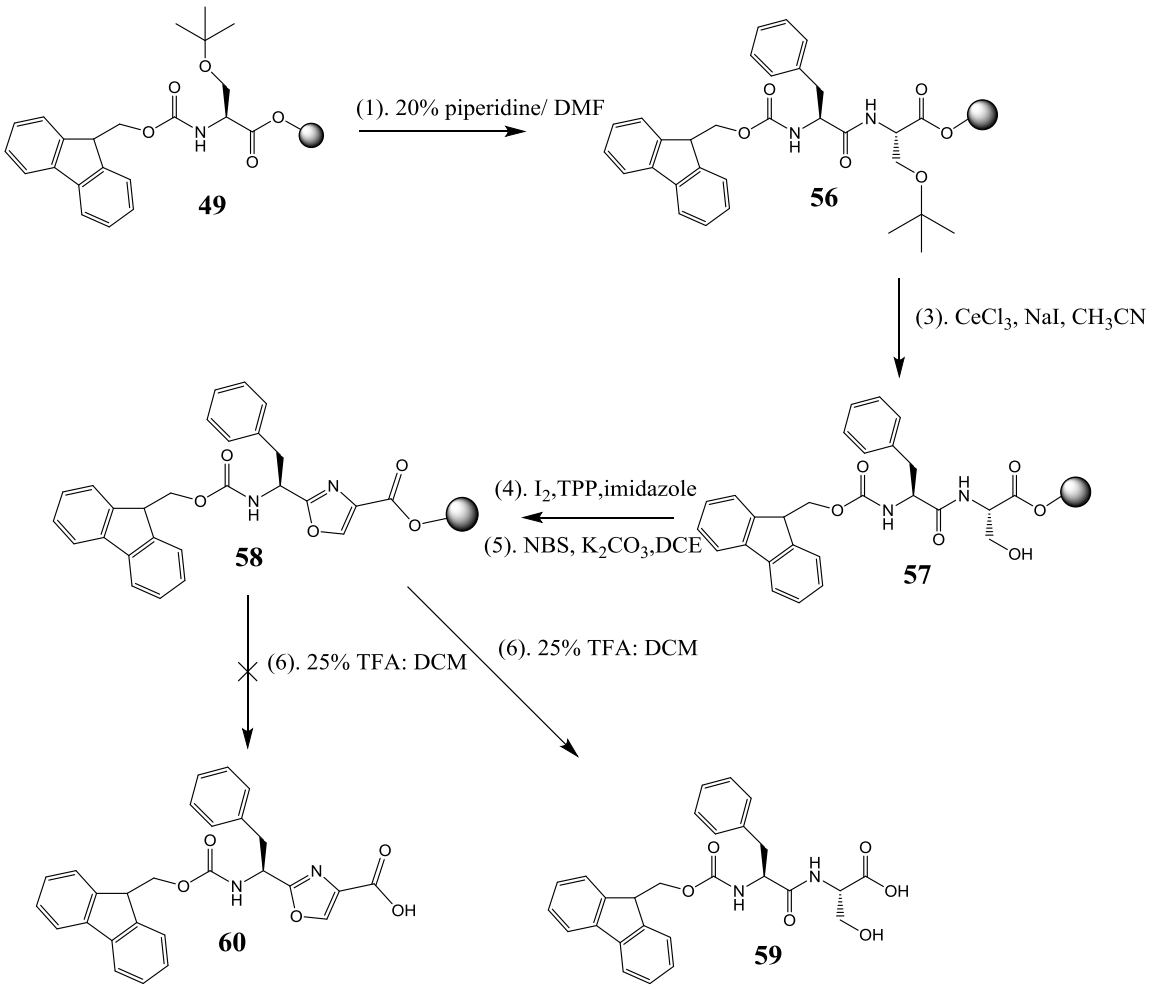

Scheme 12: Failed attempt to remove the *t*Bu-protecting group and to prepare oxazole- containing dipeptide using a one-pot synthesis.

In a second attempt, we anticipated that the treatment of **58** with the $CeCl_3$ / NaI system, would cleave the OtBu protective group selectively. However, it was difficult to judge whether this treatment was efficient or not. In other words, using a solid support makes it difficult to confirm that this reaction goes to completion, and it would be challenging to identify the compound before

cleaving it from the resin. The difficulty in purifying the dipeptide is likely because treatment with TFA/ DCM removes both the resin and the *t*Bu group. Because the amino acid is attached to the resin all along the reaction process, it is difficult to determine if the deprotection of the *t*Bu ether occurs upon treatment with $CeCl_3$ / NaI (Scheme 12).

The failure to remove the *t*-Bu group needed for oxazole formation led us to shift our effort from solid support synthesis to a solution phase synthesis.

2.2. Solution Phase Peptide Synthesis (Fmoc-chemistry)

2.2.1. Retrosynthetic Approach: Synthetic Studies towards the Preparation of a Tetraoxazole Macrocycle

It was our initial intention to develop a convenient procedure to form an oxazole moiety on a solid support, but all attempts met with failure. Furthermore, we were also interested in obtaining a strategy for directing macrocyclization from a linear precursor attached to a solid resin bead.

In this section, we provide the procedure for the cyclization of the β-hydroxyamide from a serine residue into a substituted oxazole, which is based on work by Wipf and co-workers,[113] to optimize the conditions needed for the cyclization of a linear precursor. For the preparation of tetraoxazole macrocycle **55**, we envisioned the use of the *N*-Fmoc- protected amino acids.

The retrosynthetic analysis for the tetraoxazole macrocycle, **55**, is shown in Figure 25. It involves cyclizing **61** which consists of alternating oxazoles and amino acid residues. Compound **61** was prepared via a convergent solution phase synthetic approach, using commercially available fluorenylmethyloxycarbonate (Fmoc) and methyl ester (OMe) protected amino acids. The preferred coupling reagents were HBTU and Hünig's base (*N*, *N*- diisopropylethylamine, DIPEA). The macrocyclization was achieved from the condensation of the free carboxylic acid and the free amine of double deprotected linear tetraoxazole amide **61**. Compound **61** was obtained by the peptide coupling of **64**, and, **63** followed by the removal of the Fmoc protecting group and hydrolysis of the ester functionality. The dioxazole intermediates were synthesized via condensation of an oxazole-4-carboxylic acid **66** and a 2-(α-amino) oxazole (**67**) derived from serine and phenylalanine. The oxazole moiety was formed via a cyclodehydration/dehydrogenation of the serine residue. The

mono-oxazole, **68**, was generated by coupling the commercially available Fmoc and methyl ester amino acids **71** and **70**.

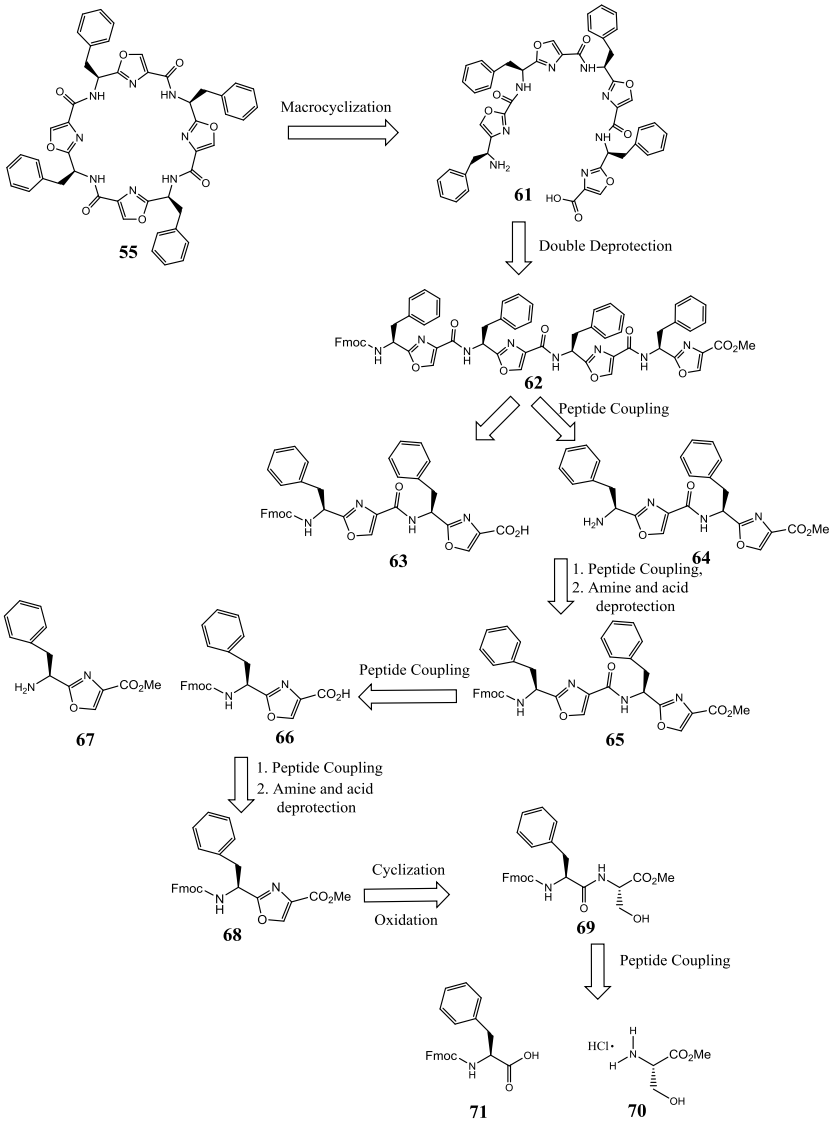

Figure 26: Retrosynthesis scheme of the tetraoxazole macrocycle,**55**, in solution-phase, using Fmoc-chemistry.

2.2.1.1. Synthesis of *N*-Fmoc-L-Phe-L-Ser-OMe (69)

The proposed synthesis of tetraoxazole macrocycle **55** requires that the protected dipeptide, **69**, be prepared by a standard peptide coupling reaction. Addition of Fmoc-protected phenylalanine, *N*-Fmoc-L-Phe-OH (**71**), to serine methyl ester, HCl•H-L-Ser-OMe (**70**), under standard peptide-coupling conditions gave **69** in 85% yield after recrystallization with hexane (Scheme 13).[30, 133, 134] Its purity and structure were confirmed via ^{1}H and ^{13}C NMR spectroscopy.

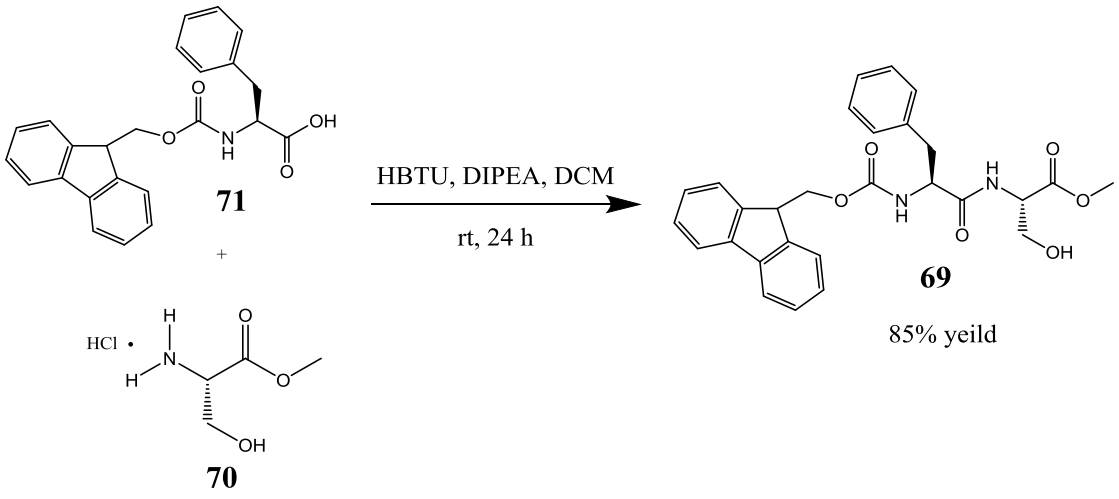

Scheme 13: Chemical reaction for the formation of *N*-Fmoc-L-Phe-L-Ser-OMe (**69**).

2.2.1.2. Oxazole Ring Formation

2.2.1.2.1. Cyclodehydration Reaction

Treatment of **69** with Burgess reagent (Scheme 14) promoted cyclization of the β-hydroxyamide of serine to the corresponding oxazoline. First, **69** was dissolved in anhydrous THF. Next, Burgess Reagent was added and the reaction mixture was refluxed for 2.5 h.[30, 88, 135] The reaction's progress was monitored for the disappearance of starting material by TLC. The crude reaction mixture was purified by flash column chromatography. Pure *N*-Fmoc-L-Phe-L-Oxazoline-OMe (**72**)**,** eluted with 30:80 ethyl acetate/ hexane, was produced in 45% yield. Its structure and purity were verified via ^{1}H and ^{13}C NMR spectroscopy.

Yonetaint and co-worker[136] reported that the pure oxazoline is unstable when exposed to air and it decomposed during column chromatography. Apparently, the oxazoline ring re-opens to form the corresponding dipeptide.

The low yield of this reaction was likely due to the decomposition of the oxazoline during purification by column chromatography.[137] Therefore, when 'Dry Column Vacuum Chromatography' was used to purify our oxazoline the yield increased to 71%. The yield of the oxazoline would therefore depend on the amount of the open chain dehydration product formed in the competing reaction.[97]

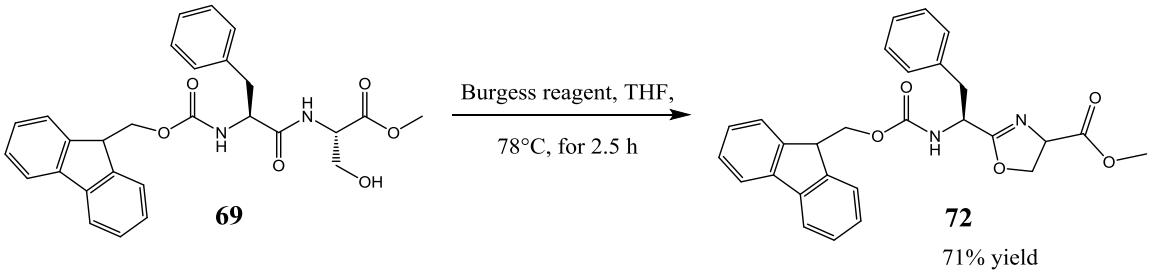

Scheme 14: Synthesis of the oxazoline-containing dipeptide (**72**).

2.2.1.2.2. Oxidation of Oxazoline

The next step was to oxidize the oxazoline to oxazole under basic conditions using 1,8-diazabicyclo[5.4.0]undec-7-ene (DBU) and bromotrichloromethane ($BrCCl_3$). DBU and $BrCCl_3$ were added to *N*-Fmoc-D-Phe-Oxazoline-OMe (**72**) dissolved in cold anhydrous DCM. The reaction mixture was stirred overnight slowly attaining room temperature. The crude oxazole was subjected to base-acid extraction and eluted from a silica gel-containing chromatography column with ethyl acetate/ hexane as a gradient system.

This method was successfully used in oxidizing the oxazoline to the oxazole, **73**. Disappointingly, the Fmoc-protecting group was lost (Scheme 15). Typically, the DBU/$BrCCl_3$ oxidation system would be incompatible with the use of Fmoc protecting groups, possibly because the Fmoc group is cleaved in the presence of 20% DBU.[138, 139, 140]

Next, attention was directed towards finding a way to oxidize the oxazoline while maintaining the Fmoc protecting group. The alternative approach was to attempt to oxidize the oxazoline-containing dipeptide, **72**, using the Kharasch-Sosnovsky reaction. [30, 141]

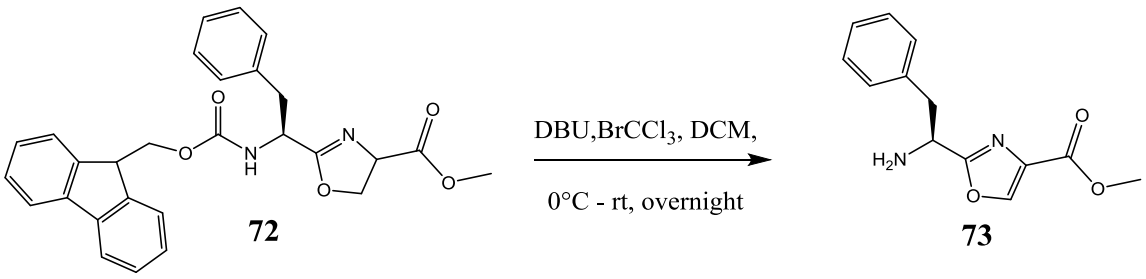

72 **73**

Scheme 15: Oxidation of the oxazoline-containing dipeptide, **72**, using DBU-$BrCCl_3$.

The Kharasch-Sosnovsky reaction involves a cocktail of CuBr, $Cu(OAc)_2$, and *t*-butylperbenzoate. The oxazoline was oxidized by refluxing **72**, CuBr, $Cu(OAc)_2$, and *t*-butylperbenzoate in benzene (Scheme 16). After 8 h, the reaction mixture was cooled to room temperature and washed with base to remove the excess copper. The crude product was purified using flash column chromatography yielding pure *N*-Fmoc-L-Phe-L-Oxazole-OMe (**68**) in 68% yield. The structure and purity of **68** were confirmed via ^{1}H, and ^{13}C NMR spectroscopy.

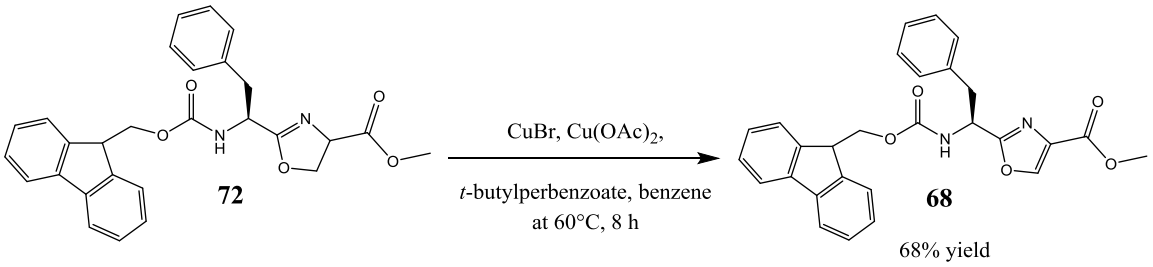

Scheme 16: Synthesis of oxazole-containing dipeptide, **68**, using Kharasch-Sosnovsky reaction conditions.

2.2.1.3. Acid Deprotection

Both the Fmoc and methylester protecting groups are base labile. The selective cleavage of the methyl ester using an aluminium chloride ($AlCl_3$) and *N*,*N*-dimethylaniline (DMA) reagent system is dependent on the molar ratio of $AlCl_3$ to DMA.[142, 143] Thus, the chemoselective removal of the methyl ester protecting group was obtained with a 9:14 molar ratio of $AlCl_3$/DMA.

The reaction mixture containing **68** and $AlCl_3$/DMA (9:14) dissolved in anhydrous DCM was refluxed for 8 h (Scheme 17). The reaction was monitored via TLC for the disappearance of starting material. We found this reaction produced a mixture of products (many spots on the TLC plate). The reaction mixture was first treated with acid and the crude product was purified by flash column chromatography. Despite the longer reaction time only 10% of pure *N*-Fmoc-D-Phe-Oxazole-OH (**66**) was obtained. ^{1}H NMR spectra indicated that a trace of DMA remained trapped

with **66**. The disappearance of the proton signal at δ = 3.94 ppm due to the loss of OCH_3 confirmed that the methyl ester was cleaved.

It was thought that the reaction would lead to selective cleavage of the OMe group. However, analysis of the by-products showed that some of the Fmoc protecting group was lost during purification of the dipeptide via flash column chromatography.

In order to increase the yield of this reaction, selective cleavage of the OMe group in **68** was attempted by using $CaCl_2$, *i*PrOH/ H_2O and NaOH.[144] This procedure also afforded a disappointing yield of **66** in that no improvement in yield was obtained by carrying out the reaction with $CaCl_2$, *i*PrOH/ H_2O and NaOH. Our failure to deprotect OMe selectively led us to use another *N*-terminal protecting group that is cleaved by acid, i.e., *t*-butyloxycarbonyl, (Boc).

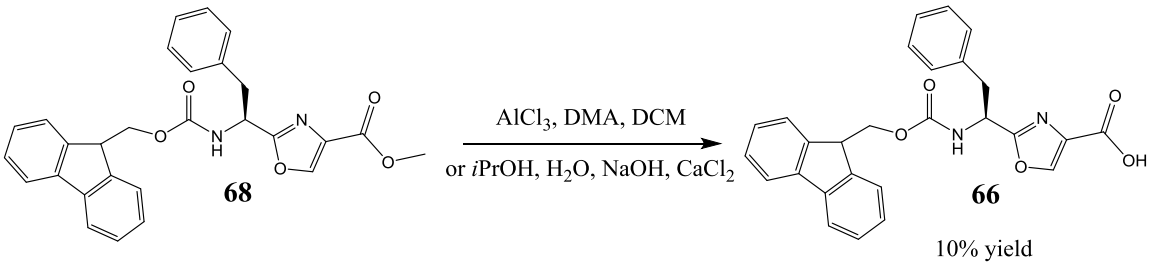

Scheme 17: Selective deprotection of the methyl ester protecting group in **68**.

2.2.2. Retrosynthetic Approach: Solution Phase Peptide Synthesis of the Tetraoxazole Macrocycle (Boc-chemistry)

This section describes the results obtained when *t*-butyloxycarbonyl (Boc) was used as a protecting group for *N*-terminal amino acids. By using Boc instead of Fmoc it was anticipated that the methyl ester functionality could be selectively hydrolyzed under basic condition.

The retrosynthesis analysis for tetraoxazole macrocycle **55**, shown in Figure 26, involves preparing peptides with alternating oxazoles and amino acid residues prior to macrocyclization. The synthesis of macrocyclic tetraoxazole precursors were carried out via a convergent solution phase synthesis approach using commercially available Boc- and methyl ester (OMe)- protected amino acids, coupling reagents (HBTU) and Hünig's base (*N, N*- diisopropylethylamine, DIPEA). The desired macrocycle, **55**, results upon the condensation of the free acid and free amine of linear tetraoxazole amide, **74**. The double deprotection of **75** yields **74**. The coupling of the Boc- protected dioxazole precursor, **76**, with the carboxy-protected dioxazole precursor, **77**, gives **75**. The dioxazole precursors, **76** and **77**, are obtained by the selective deprotection of *N*-Boc, CO_2-Me protected dioxazole, **78**. Condensation of the oxazole-4-carboxylic acid, **79,** and a 2-(α-amino) oxazole, **80**, derived from serine and phenylalanine gives **78**. The oxazole moiety was formed via the cyclodehydration/dehydrogenation of the serine residue. The mono-oxazole, **81**, was generated by coupling the commercially available amino acid building blocks, (**83** and **84)** followed by cyclodehydration oxidation.

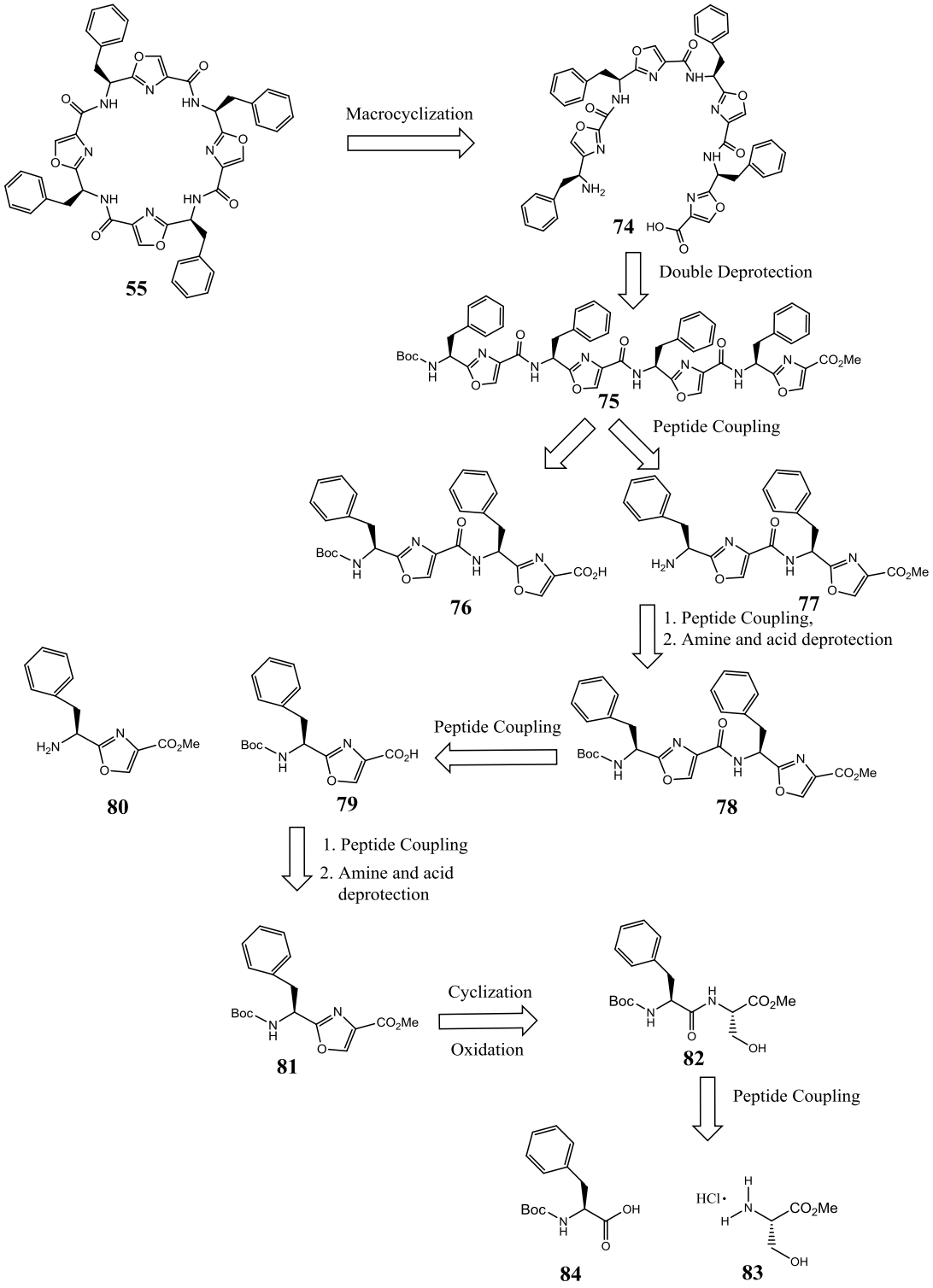

Figure 27: Retrosynthetic approach towards the tetraoxazole macrocycle using solution-phase peptide synthesis and Boc-chemistry.

2.2.2.1. Synthesis of Protected Dipeptide *N*-Boc-L-Phe-L-Ser-OMe (82)

The protected dipeptide, *N*-Boc-L-Phe-L-Ser-OMe (**82**), was prepared using *N*-Boc-L-Phe-OH (**84**) and HCl•H-Ser-OMe (**83)** as both were commercially available, Scheme 18. Condensation of **84** and **83** was carried out using the coupling reagent O-(benzotriazol-1-yl)-*N*,*N*,*N*',*N*'-tetramethyluronium tetrafluoroborate (HBTU) and Hünig's base (DIPEA) in dry DCM. The reaction mixture was subjected to an acid-base extraction to remove the excess coupling agent (HBTU) as well as any by-products. Purification of the crude mixture by flash column chromatography afforded the protected dipeptide, *N*-Boc-L-Phe-L-Ser-OMe (**82**), in 67% yield. Analysis of ^{1}H NMR and ^{13}C NMR spectra of the pure compound was consistent with that expected for **82**. It should however be noted that the ^{1}H NMR and ^{13}C NMR chemical shifts of a mixture of **84** and **83** are almost identical to those of **82**. The identity and purity of **82** were therefore confirmed by melting point analysis.

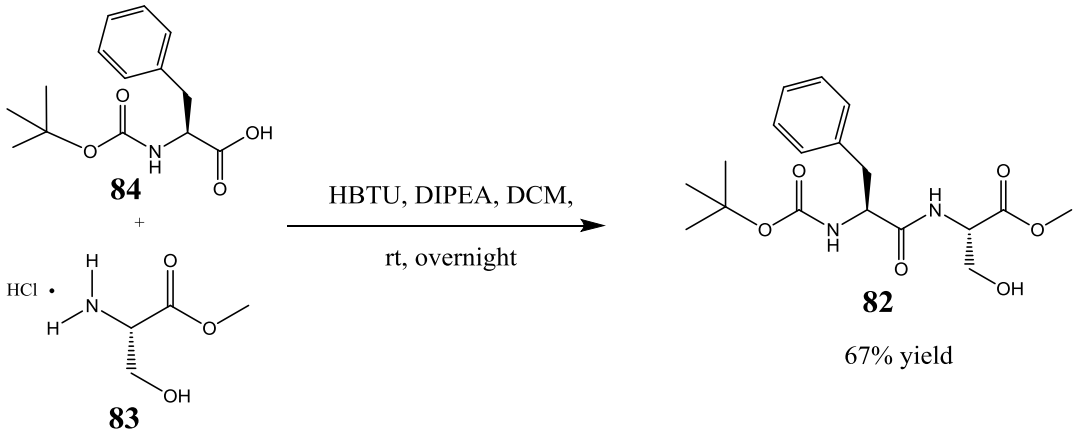

Scheme 18: Synthesis of the *N*-Boc protected dipeptide, **82**.

2.2.2.2. Oxazole Ring Formation

2.2.2.2.1. Cyclodehydration Reaction

The oxazoline ring was prepared in two different ways. The first method involved the treatment of *N*-Boc-L-Phe-L-Ser-OMe (**82**), dissolved in THF, with Burgess reagent (Scheme 19) yielding **85**. The intramolecular cyclization was achieved with inversion of configuration at the serine β-carbon.[145, 146] The reaction was monitored, via TLC, for the disappearance of starting material. The crude product was purified via "Dry Column Vacuum Chromatography" with natural silica gel and ethyl acetate- hexane as a gradient system giving *N*-Boc-L-Phe-Oxazoline-OMe (**85**) in 84% yield.

The two spots visible on the TLC plate were thought to arise because of the formation of diastereoisomers of the oxazoline. ^{1}H NMR confirmed the oxazoline structure by the absence of the resonances of the serine hydroxyl group and adjacent amide protons. The multiplet signals at 4.73 ppm (2H) and 4.60 ppm (1H) were assigned to the protons attached to the oxazoline ring.

Alternatively, the cyclodehydration of the protected dipeptide, *N*-Boc-L-Phe-L-Ser-OMe (**82**), was carried out using diethylaminosulfur trifluoride (DAST) (Scheme 19).[87, 147, 148] *N*-Boc-L-Phe-L-Ser-OMe (**82**) was dissolved in anhydrous DCM and cooled to -78°C. DAST was then added to the solution and stirred at the same temperature for 1 h. Addition of K_2CO_3 to the reaction mixture with stirring for 1 h resulted in the intramolecular cyclization of **82** yielding the oxazoline intermediate. The reaction was monitored by TLC until the starting material could no longer be detected. The crude reaction mixture was subjected to an acidic workup. The product was purified

by flash column chromatography yielding pure *N*-Boc-L-Phe-Oxazoline-OMe (**85**) (88% yield). The structure and purity were verified using ^{1}H NMR and ^{13}C NMR spectroscopy.

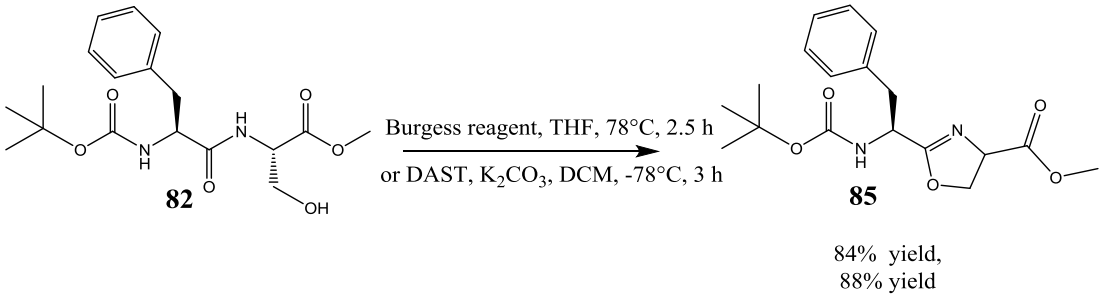

Scheme 19: Cyclization of the *N*-Boc protected dipeptide (**82**) yielding the oxazoline (85). Cyclization was accomplished using either the Burgess reagent or with DAST/K_2CO_3.

2.2.2.2.2. Oxidation of Oxazoline

The resulting oxazoline intermediate was subjected to oxidation using a 1,8-diazabicycloundec-7-ene (DBU) - bromotrichloromethane system (Scheme 20).[133, 149, 98] *N*-Boc-L-Phe-Oxazoline-OMe (**85**) was dissolved in anhydrous DCM and cooled to 0°C. The base, DBU, was then added to the reaction mixture followed by the addition of $BrCCl_3$. The reaction was allowed to stir overnight while warming up to room temperature. TLC analysis revealed the absence of oxazoline and the presence of the product along with some impurities. Upon completion, the reaction mixture was neutralized and the product purified by flash column chromatography. The

mono-oxazole dipeptide amide, *N*-Boc-L-Phe-Oxazole-OMe (**81**), was produced in 91% yield. Its structure and purity were confirmed by ^{1}H NMR and^{13}C NMR spectroscopy. In particular, the distinctive singlet appearing at δ= 8.23 ppm (s, 1H; OC<u>H</u>=C(oxaz)) in the ^{1}H NMR spectrum is characteristic of the presence of the oxazole ring.

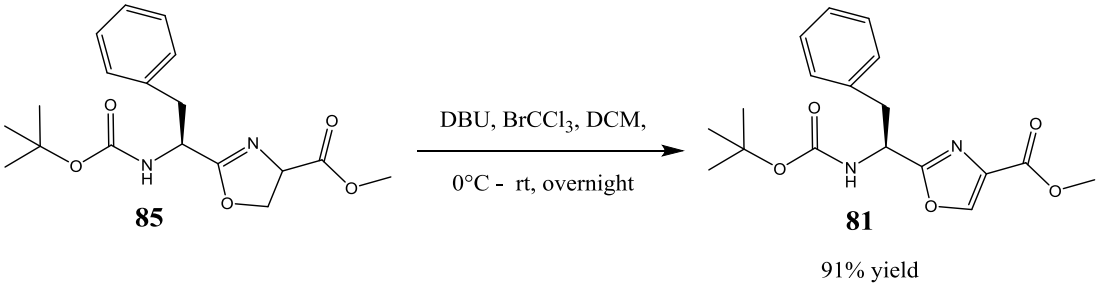

Scheme 20: Synthesis of *N*-Boc-Phe-Oxa-OMe (**81**) by oxazoline oxidation.

2.2.2.3. Amine Deprotection: Synthesis of Dipeptide HCl•H_2N-L-Phe-Oxazole-OMe (80)

In order to generate the linear precursor, the pure mono-oxazole dipeptide amide, **81,** was divided into two portions. The amine functionality of one portion of **81** was deprotected to yield **80** (Scheme 21).[54, 71, 150] while the ester functionality of the remaining portion was hydrolyzed to give **79** (Scheme 22). More specifically, **80** was formed when the dipeptide, **81**, dissolved in THF, was treated with a 4 M HCl-dioxane solution cooled to 0°C. After 4 h, the starting material could no longer be detected by TLC, indicating that the reaction went to completion. The solution was washed with dry diethyl ether. Concentration of the diethyl ether phase *in vacuo* gave HCl•H_2N-L-

Phe-Oxazole-OMe (**80**). The disappearance of the *N*-Boc protecting group was confirmed by NMR spectroscopy. The NMR data of **80** were similar to that of **81** with the exception of the disappearance of the proton signal at δ = 1.43 ppm (s, J = 7.8 Hz, 9H) and the ^{13}C signal at 28.24 ppm due to the *N*-Boc group. The product was used without further purification.

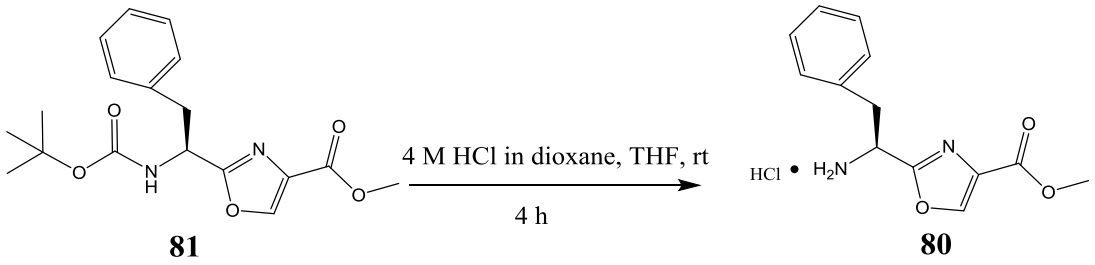

81 **80**

Scheme 21: Synthesis of the hydrochloride salt of H_2N-L-Phe-Oxazole-OMe (80).

2.2.2.4. Acid Deprotection: Synthesis of *N*-Boc-Phe-Oxazole-OH (79)

The remaining mono-oxazole dipeptide amide, **81**, was treated with LiOH in THF/H_2O (1:1) to hydrolyze the methyl ester group (Scheme 22).[151, 152, 153] After the reaction had gone to completion (3 h), the reaction mixture was concentrated to half of the original volume. The resulting aqueous mixture was neutralized and concentrated in *vacuo* to afford *N*-Boc-L-Phe-Oxa-OH (**79**). ^1H and ^{13}C NMR spectroscopy were used to confirm the identity and the purity of the product. ^1H and ^{13}C NMR analysis confirmed the absence of methyl ester signals at 3.82 ppm (s,

3H) and 52.46 ppm, respectively. The product was used in coupling reaction described below without further purification.

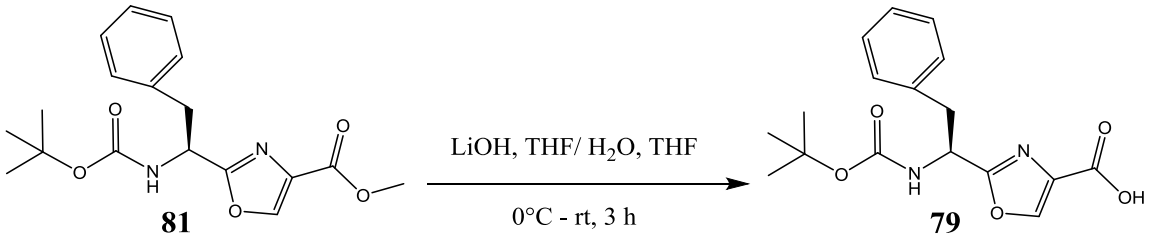

Scheme 22: Synthesis of *N*-Boc-L-Phe-Oxazole-OH (**79**).

2.2.2.5. Synthesis of *N*-Boc-L-Phe-L-Oxazole-L-Phe-Oxazole-OMe (78)

The protected linear dioxazole amide, **78**, was assembled by coupling the free acid, *N*-Boc-L-Phe-Oxa-OH (**79**), with the free amine, HCl•NH_2-L-Phe-OMe (**80**), using HBTU and Hünig's base (DIPEA) in anhydrous DCM (Scheme 23). The reaction was allowed to proceed under nitrogen atmosphere at room temperature and its progress was monitored via TLC. After washing the reaction mixture with acid followed by base, the crude product was purified using flash column chromatography. Pure **78** (73% yield) was eluted with 30:80 ethyl acetate/ hexane. ^{1}H and ^{13}C NMR spectroscopy were used to confirm its structure and purity. Characteristic peptide resonances in the ^{1}H NMR spectrum of **78** included broad singlets at δ = 8.13 and 8.08 ppm attributable to the

oxazole protons, and doublets of doublets between 7.49 and 5.16 ppm corresponding to amide NH protons.

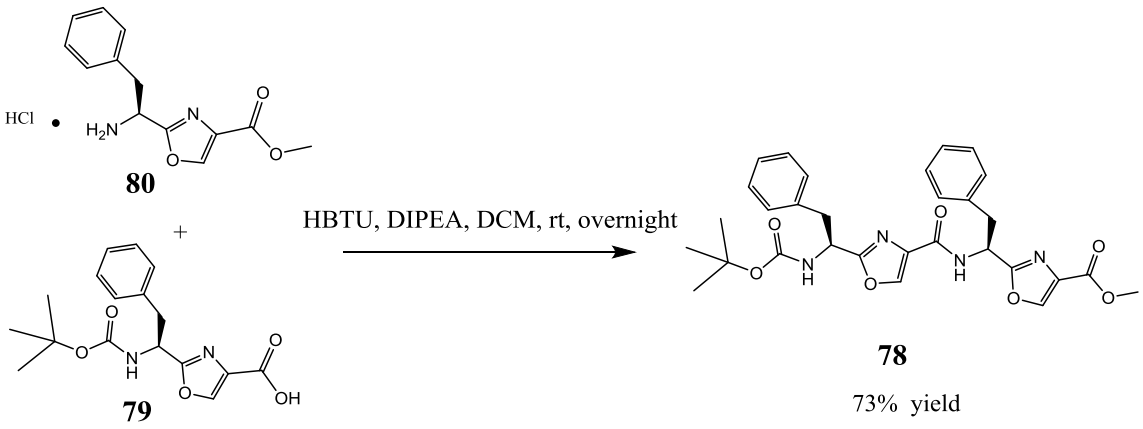

Scheme 23: Synthesis of *N*-Boc-L-Phe-L-Oxazole-L-Phe-Oxazole-OMe (**78**).

2.2.2.6. Synthesis of Protected Linear Tetraoxazole Amide (75)

Prior to synthesizing the protected linear tetraoxazole amide, **75**, the protected linear dioxazole amide, **78**, was divided into two portions. The Boc group in one portion of **78** was removed (Scheme 24) using an HCl/dioxane mixture in THF. The amine deprotection was monitored via TLC and was complete in 4 h. The residue was washed with dry diethyl ether which was subsequently concentrated *in vacuo* to furnish HCl•NH_2-L-Phe-Oxazole-L-Phe-Oxazole-OMe (**77**). Its structure and purity were confirmed via ^{1}H NMR and ^{13}C NMR spectroscopy. The NMR data of the deprotected product, **77**, was almost identical to that of protected **78** except for the

absence of the signals for the Boc group at δ = 1.45 ppm (s, 9H) in the ^{1}H NMR spectrum and 28.29 ppm in the ^{13}C NMR spectrum.

The remaining portion of **78** was treated with LiOH in THF/H_2O (1:1) to hydrolyze the methyl ester-protecting group. The reaction was completed in 4 h as confirmed by TLC. When complete, the crude was concentrated to one-half volume. The resulting aqueous mixture was purified via an acidic wash and concentrated *in vacuo.* This provided the required acid *N*-Boc-L-Phe-Oxa-Phe-Oxa-Phe-OH (**76**). The ^{1}H and ^{13}C NMR spectroscopy were used to verify the product and its purity. The methyl ester signals at 3.93 ppm (s, 3H) and 48.32 ppm were no longer visible in ^{1}H and ^{13}C NMR spectra, respectively. Compound **76** was used in the subsequent coupling reaction without any further purification.

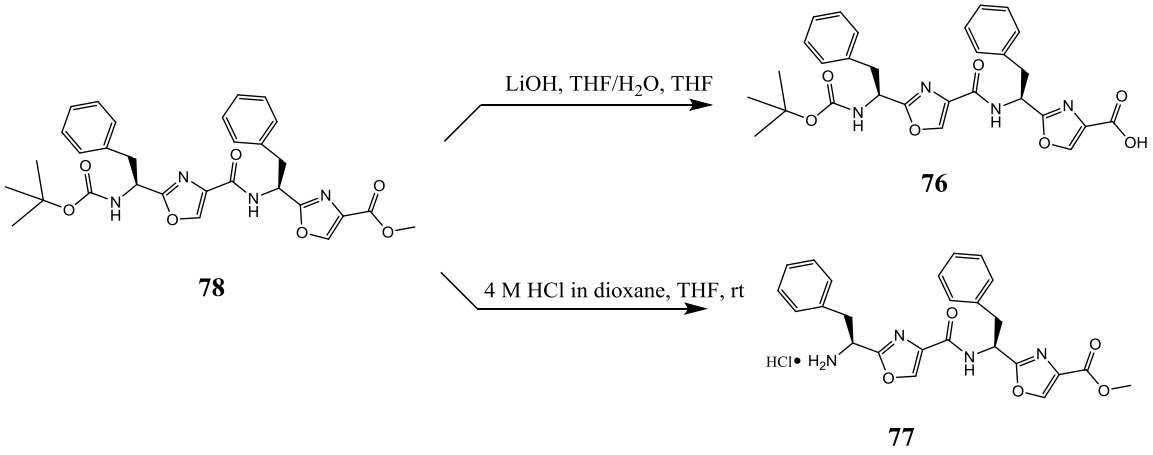

Scheme 24: Removal of the methyl ester and *t*-butyloxycarbonyl protecting groups from protected linear dioxazole amide

The next phase of the synthesis required coupling compounds **76** and **77** with the aid of

HBTU and DIPEA in anhydrous DCM. The reaction mixture was stirred at room temperature under a nitrogen atmosphere for 24 h. The yield of *N*-Boc-L-Phe-Oxazole-L-Phe-Oxazole-L-Phe-Oxazole-L-Phe-Oxazole-OMe (**75**) was 57%. Trace amounts of *N*, *N*'-diisopropylurea were detected in the ^{1}H and ^{13}C NMR spectra of **75**. We believe that the solvent system used for the flash column chromatography allowed the elution of both **75** and *N*, *N*'-diisopropylurea. Therefore, an alternative coupling procedure that involved the water-soluble coupling agent 1-ethyl-3-(3-dimethylaminopropyl)carbodiimide (EDC) was used since the urea by-product could be readily removed by aqueous extraction.[154, 155] Using this coupling system proved to be more successful and the overall yield was 10% better than that obtained using HBTU (Scheme 25). The ^{1}H and ^{13}C NMR spectra were consistent with what one would expect for **75**. Characteristic peptide resonances in the ^{1}H NMR spectrum of **75** included doublets of doublets at 7.52 ppm (1H), 7.28 ppm (1H), and 7.02 ppm (2H), corresponding to four amide protons. In addition, broad singlets at 8.12 ppm (3H) and 8.08 ppm (1H), attributable to four oxazole protons were observed. The ^{1}H and ^{13}C NMR data obtained for 75 were identical to those reported in the literature.[153b]

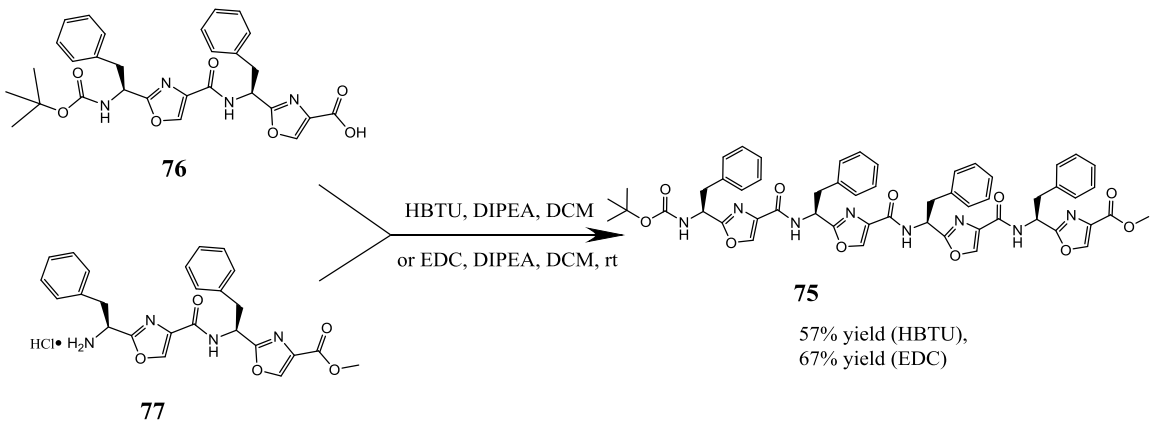

Scheme 25: Synthesis of the protected linear tetraoxazole amide, **75**.

2.2.2.7. Double Deprotection of the Linear Precursor to Form 74

A stepwise approach was employed to generate the double deprotected linear tetraoxazole amide, **74** (Scheme 26). By adding 2N LiOH in THF/H_2O the methyl ester was converted to the carboxylic acid functionality after 4 h. The reaction progress was monitored by observing the appearance of the free acid and the disappearance of starting material via TLC. After standard work up, the Boc protecting group was removed from the crude product using an HCl/dioxane mixture (4M) in anhydrous THF. The reaction was allowed to proceed to completion at room temperature, and verified via TLC by observing for the presence of the free amine and the disappearance of starting material. The resulting amine was washed with dry diethyl ether and collected by filtration to furnish the double deprotected linear precursor, **74**. This product was used in the macrocyclization step without any further purification.

The NMR data of the deprotected product **74** were almost identical to that of the starting material with the exception of the disappearance of the signals for the tertiary butyl group at δ = 1.42 ppm (s, 3H) and the methylester group at δ = 3.90 ppm (s, 9H) in the ^{1}H NMR spectrum and at δ = 28.26 and 39.97 ppm in the ^{13}C NMR spectrum.

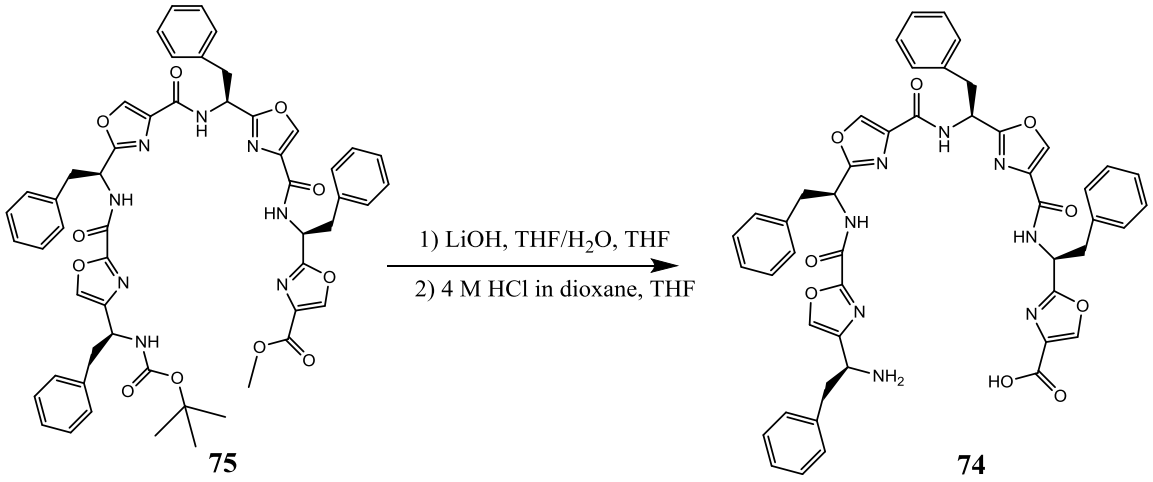

Scheme 26: Stepwise double deprotection strategy for the formation of the linear tetraoxazole amide, **74**.

2.2.2.8. Macrocyclization of the Linear Tetraoxazole-Containing Peptide to Form Tetraoxazole Macrocycle

Typically, the macrocyclization reaction was carried out under highly diluted conditions (<0.001M) to disfavor the unwanted intermolecular reaction of the peptide[156, 102, 157]. In order to achieve the cyclization of linear deprotected peptide **74** and maximize the yield of cyclization, the coupling reagent *O*-[(1-cyano-2-ethoxy-2-oxoethylidene)amino]-oxytri(pyrrolidin-1-yl) phosphonium hexafluorophosphate (PyOxP) and DIPEA were used to push the reaction to completion. PyOxP is a novel coupling reagent of the oxyma-based family of phosphonium salts. This phosphonium salt gives high coupling efficiency not only in peptide coupling but also in cyclic peptide synthesis because of its higher propensity to reduce racemization. In contrast to HBTU,

PyOxP gives an active ester that is extremely reactive due to the low hindrance and acidity, which results in an excellent leaving group.[158a] To generate the tetraoxazole macrocycle, **55**, PyOxP and DIPEA (Scheme 27) were added to a solution of **74** in DMF (0.001M). The reaction mixture was stirred at room temperature under a nitrogen atmosphere and the progression of the reaction was monitored by TLC. After 3 days there was no evidence of the presence of the starting material. The crude product was concentrated *in vacuo* to a quarter of its volume. The crude product was washed with dilute acid followed by dilute base. Then, DCM was used to extract the product from the aqueous phase. After the removal of DCM *in vacuo*, the by-product was removed by trituration with hot hexane twice to afford **55** in 45% yield. This was confirmed by ^{1}H NMR spectroscopy. The four amide protons resonate between 7.16 – 7.11 ppm while the protons of the oxazole rings are found at 8.13 ppm. This is consistent with the spectroscopic data of **55** reported in a patent.[158b]

The success of using the orthogonal protecting group (Boc) to synthesize the tetraoxazole macrocycle led us to investigate the compatibility of Boc with an oxime resin so that the macrocycle could be produced in higher yield by a cyclitive-cleavage strategy.

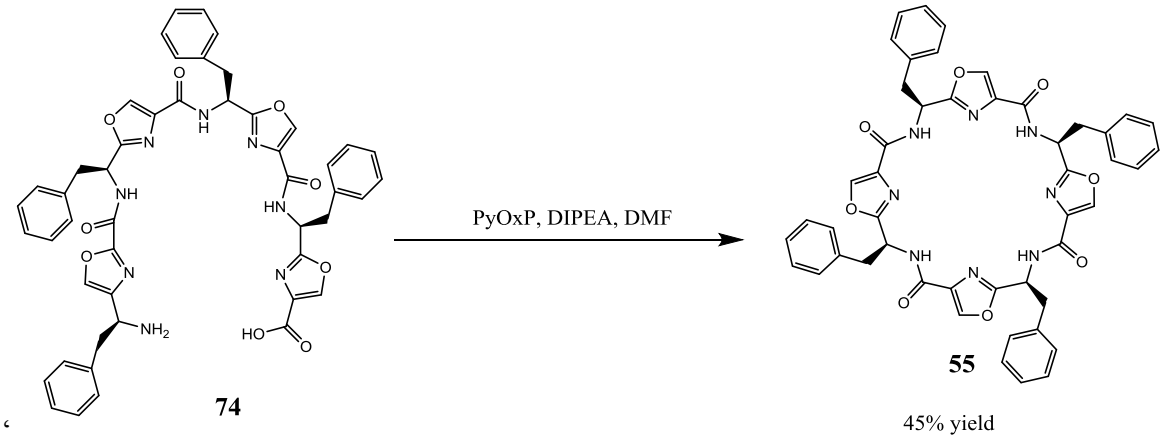

Scheme 27: Macrocyclization of **74**.

2.2.3. Retrosynthetic Approach: Solid Phase Peptide Synthesis

The tetraoxazole macrocycle, **55**, can be efficiently synthesized by exploiting elongation-cyclization-cleavage sequential reactions on a Kaiser-oxime resin,[159, 160] which incorporates a combination of solution and solid phase synthesis (Figure 27). The tetraoxazole-containing precursor (**86**) was assembled by solid phase synthesis. This involved the coupling of **79** to an oxime resin by a standard method followed by the stepwise addition of three more molecules of **79**. The fragment **79** was afforded by coupling the commercially available *t*-butyloxycarbonyl (Boc) and methyl ester protected amino acids **84** and **83** and subjecting the product to cyclodehydration followed by oxidation.

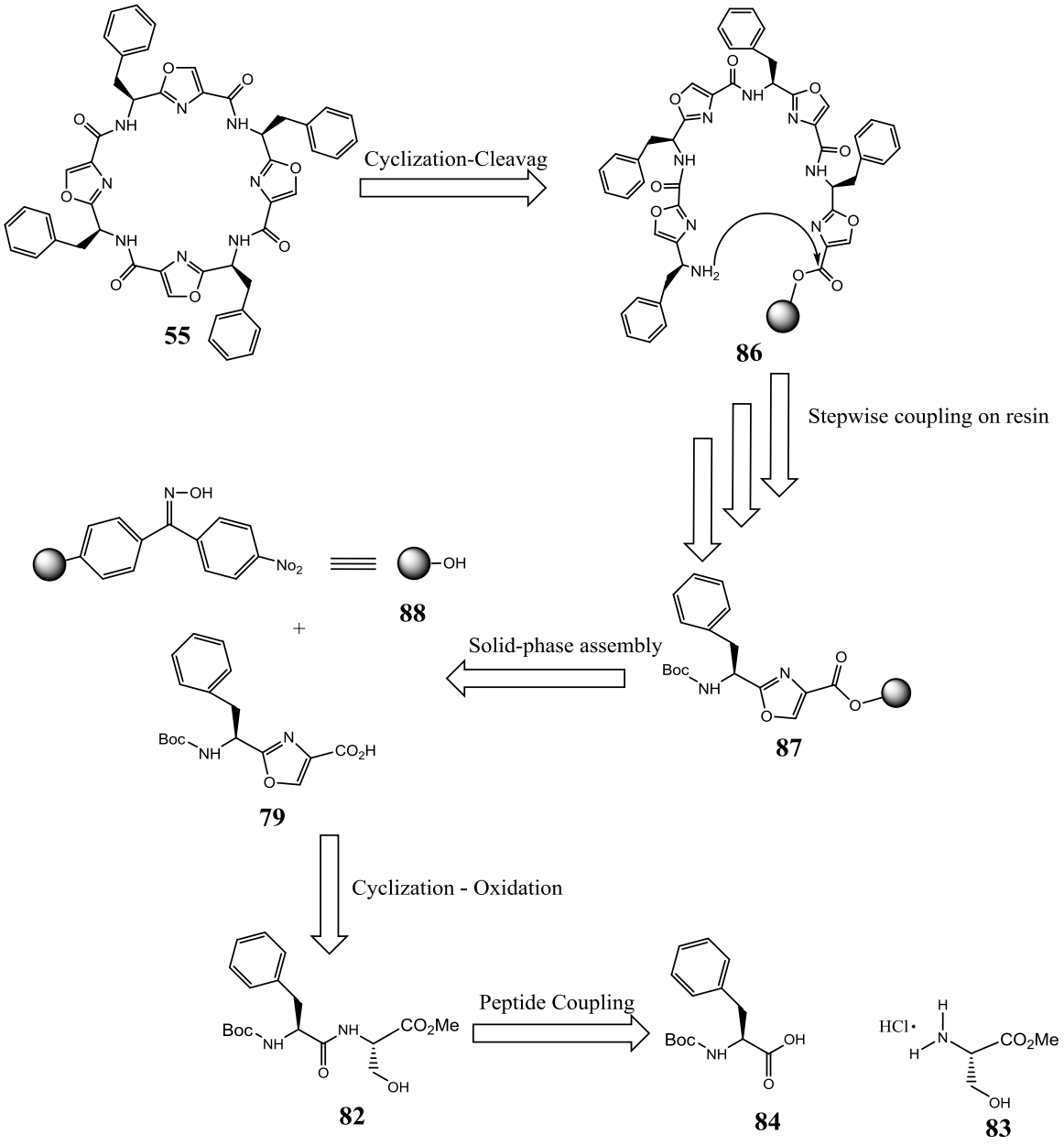

Figure 28: Retrosynthetic strategy for the formation of the tetraoxazole macrocycle, **55**, via solid phase peptide synthesis and cyclization cleavage (SPPS-CC) from an oxime resin.

2.2.3.1. Solution Phase Synthesis of *N*-Boc-L-Phe-L-Oxazole-OH (79)

The synthesis of **79** was carried out by first coupling the free acid **84** and free amine **83** to give the corresponding dipeptide, *N*-Boc-L-Phe-L-Ser-OMe (**82**) (Scheme 28). Subsequently, subjecting **82** to cyclodehydration-oxidation followed by acid conversion resulted in the formation of **79**. Firstly, the free acid, **84**, and the free amine, **83**, were coupled using HBTU and DIPEA in anhydrous DCM to give *N*-Boc-L-Phe-L-Ser-OMe (**82**) in 85% yield. The structure and purity of the compound were verified by ^{1}H and ^{13}C NMR spectroscopy. Next, heating **82** to reflux with Burgess reagent in anhydrous THF for 2 h gave *N*-Boc-L-Phe-L-Oxazoline-OMe (**85**) in 84% yield after purification of the crude product using dry column chromatography. The ^{1}H and ^{13}C NMR spectral data obtained were consistent with that expected for **85**. Oxidation of oxazoline **85** with DBU-$BrCCl_3$ in DCM gave *N*-Boc-L-Phe-L-Oxa-OMe (**81)** in 91% yield after purification. The ^{1}H and ^{13}C NMR spectra of **81** were recorded and are what is expected based on the structure of **81**. Finally, the carboxylic acid moiety of **81** was deprotected using LiOH in THF/H_2O (1:1). The reaction went to completion, and resulted in the formation of *N*-Boc-L-Phe-L-Oxa-OH (**79**).

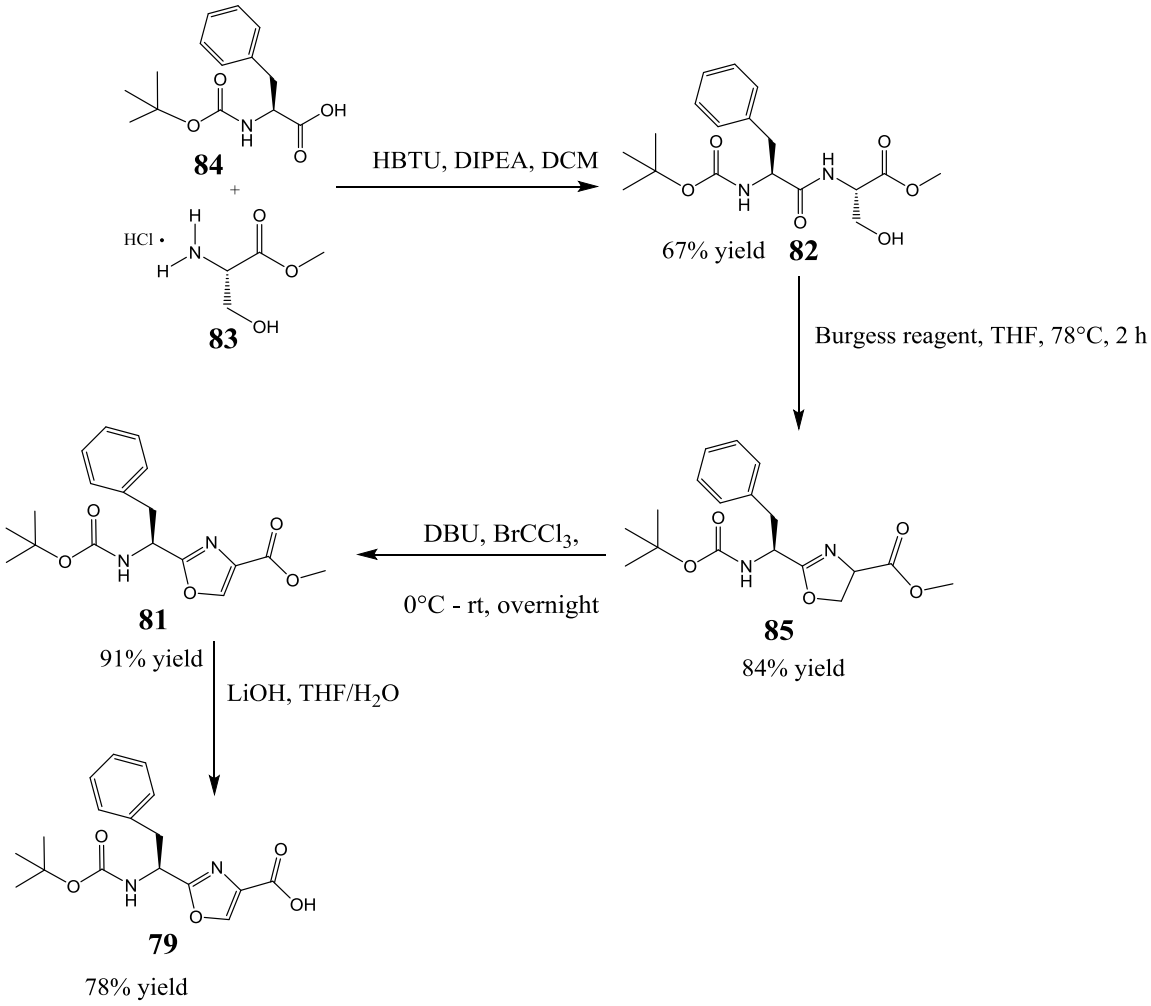

Scheme 28: Synthesis of *N*-Boc-L-Phe-L-Oxa-OH (**79**).

2.2.3.2. Synthesis of Tetraoxazole-containing Macrocycle 55 Using Solid Phase Peptide Synthesis

A stepwise strategy was used to generate the linear heterocycle-containing peptide bound to resin (Scheme 29) needed for the solid phase synthesis of **55**. The intermediates on the resin were not structurally characterized. However, since the final compound **55** was isolated and characterized by NMR, it is assumed that the intermediates on the resin (**87**, **90**, **91**, **92**, **86**) were successfully prepared. First, **79** was loaded onto the commercially available *p*-nitrobenzophenone oxime resin (**88**). This involved adding a solution containing **79** in DMF and HBTU to **88** followed by the addition of DIEPA. A Kaiser test was conducted to monitor the progress of the reaction. The Kaiser test is a quantitative ninhydrin test used in the detection of primary and secondary amines. The solution turns from blue to yellow when the coupling reaction is complete. This occurred after the solution had been agitated for 12 h. The resin was collected by filtration and washed with DMF (5x), DCM (5x), and DMF (1x). Next, acetylation of the oxime functionality on the resin using 50/50 (v/v) acetic anhydride/DMF with DIPEA[161] gave *N*-Boc-L-Phe-Oxa-resin (**87**). The *t*-Boc group in **87** was removed using 25% TFA/DCM followed by DIPEA treatment to generate the free amino group.[162] A solution containing **79**, HBTU, and HOBt in DMF resulted in formation of the activated ester **89**. Adding **89** to the preloaded resin, **90**, in the presence of DIPEA in DMF yielded *N*-Boc-L-Phe-Oxa-L-Phe-Oxa-resin (**91**) after 3 h of stirring. Then, **91** was subjected to a subsequent amine deprotection step using 25% TFA/DCM. Two more molecules of **79** were coupled to the resin, using the procedure described above, giving *N*-Boc-L-Phe-Oxa-L-Phe-Oxa-L-Phe-Oxa-L-Phe-Oxa-resin (**92**). Each coupling was monitored by the Kaiser test to confirm completion of the reaction. Once the peptide sequences were completed, **92** was treated with 25%

TFA/DCM followed by DIPEA to give **86**. Compound **86** was treated with 6% acetic acid and agitated for 3 days to complete the cyclization-cleavage reaction. Acetic acid is used as a catalyst for the cyclization cleavage reaction being able to activate the oxime ester linkage bond for nucleophilic attack by free amine.[160, 163] Finally, the resin was washed with DCM and the filtered solution was concentrated *in vacuo* to give **55** in 20% yield.

The tetraoxazole macrocycle, **55**, was successfully prepared in both of the macrocyclization protocols. However, the yield of **55** obtained by convergent solution phase peptide synthesis is much higher than that obtained by the cyclitive cleavage strategy (SPS-CC). The low yield of **55** using SPS-CC was not expected because simultaneous cyclization and cleavage is allowing the cyclic product to be isolated in high yield and purity. Although, the reason for low yield of **55** using the SPS-CC strategy is not known, it is possible that the oxime resin is labile to nucleophiles thus leading to the loss of some peptide from the resin upon neutralization with base after the removal of t-Boc under acidic condition.[164]

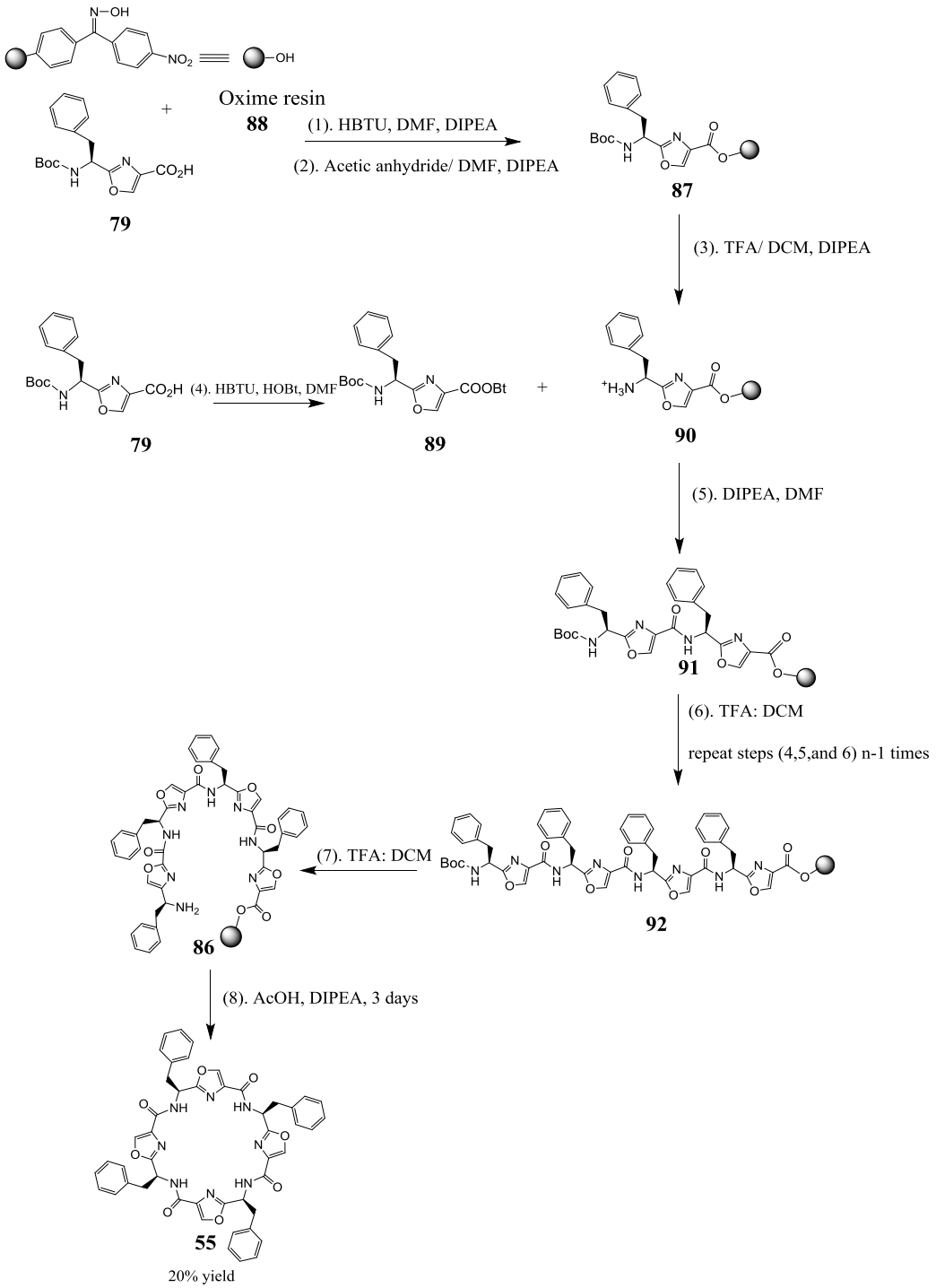

Scheme 29: Synthesis of *N*-Boc Protected Peptidyl-bond oxime resin and the head to tail cyclization with concomitant cleavage from resin.

2.3. UV-Vis Spectrophotometric Titration of Tetraoxazole Macrocycle with Cu(II)

Having prepared **55**, the next objective was to test its ability to complex metal ions. Comba and co-workers[127] studied the Cu(II) coordination chemistry of the cyclic pseudo peptide H_4pat^1, a dimethylimidazole analogue of the naturally occurring cyclic peptides, patellamide A-F and ascidiacyclamide. Because of the similarities between H_4pat^1 and **55**, it was decided to use the protocol developed by Comba and co-workers[127] to study the interaction of Cu(II) with **55**.

The first part of the experiment involved recording the UV spectra of a solution of the tetraoxazole after the stepwise addition of 0.25 equivalents of Cu(II) until a tetraoxazole to Cu(II) ratio of 1:4 was attained (Figure 29). The absorption band at 840 nm ($\varepsilon = 28\ M^{-1}\ cm^{-1}$) is presumably due to the d-d transition of Cu(II). Interestingly, the relationship between the absorbance at 840 nm and the amount of Cu(II) added to the macrocycle was linear beyond the addition of 2 equivalents of the metal ion (see inset of Figure 29).

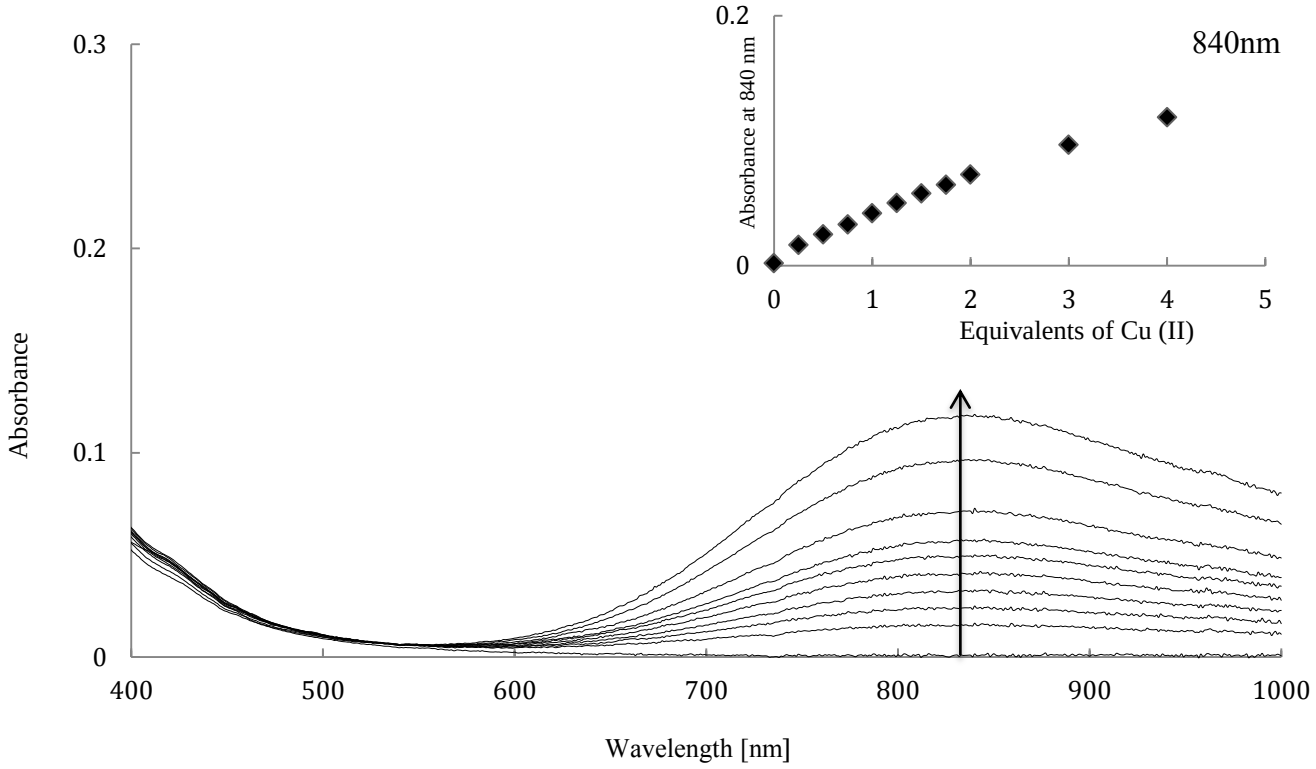

Figure 29: UV-Vis spectra of the titration of the tetraoxazole macrocycle (1.5 mM) with Cu(II) in methanol. The titration was performed with 0-4 equivalents of Cu(II), in 0.25 eq steps.

In another set of experiments, an incremental amount of base (tetrabutylammonium ethoxide) was added to a solution of the tetraoxazole macrocycle supplemented with 2 equivalents of Cu(II). The addition of base resulted in a shift of the d-d transition from 840 nm to 634 nm (ε = 174 $M^{-1}cm^{-1}$), Figure 30 a. Upon the addition of > 2 equivalents of base, a shoulder at 537 nm emerged (Figure 30 b). The intensity of the absorption bands at 634 nm and 537 nm increased dramatically following an increase in the amount of base from 2.0 to 2.25 equivalents. The intensity remained constant when more than 2.25 equivalents of base were added.

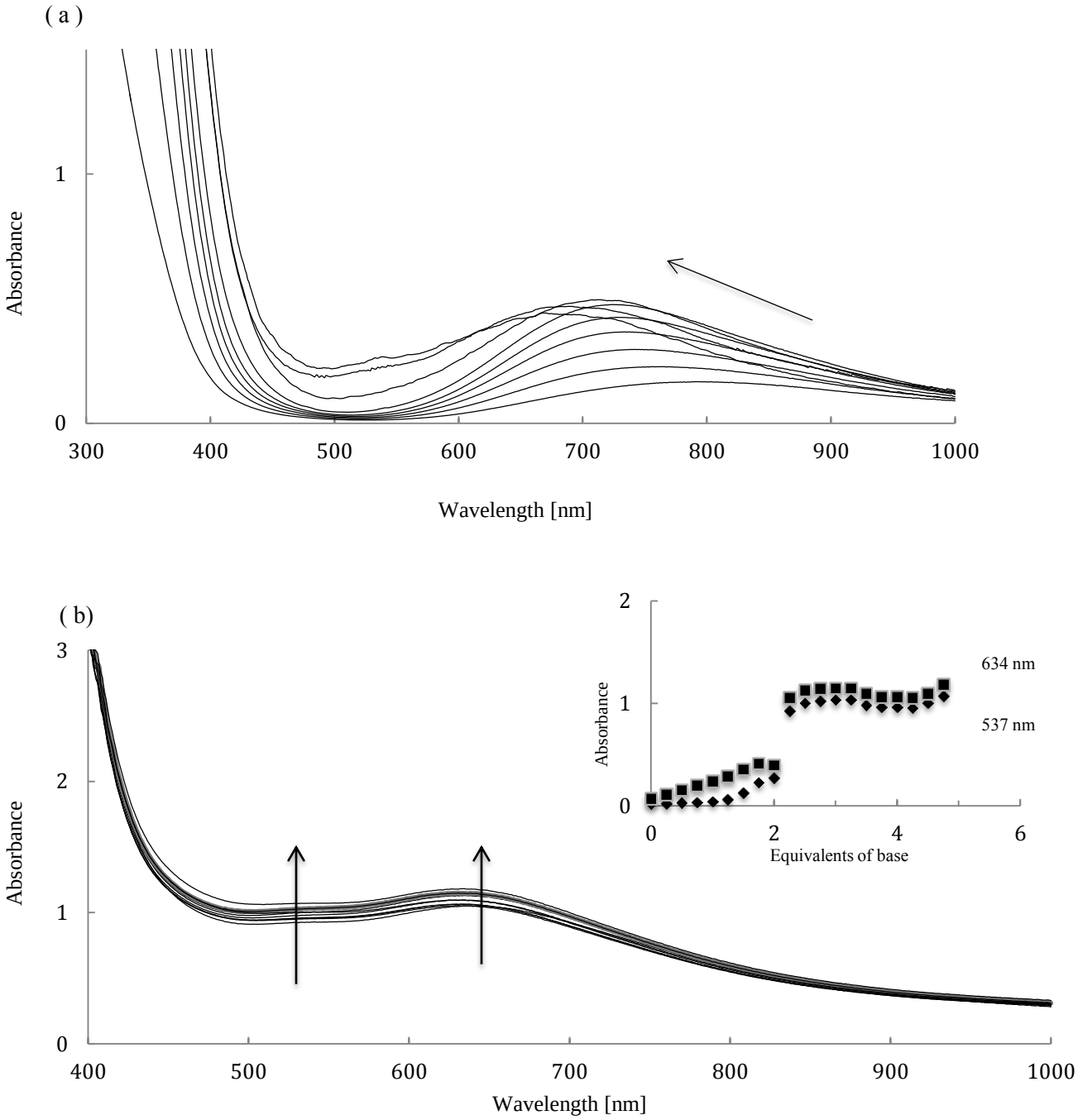

Figure 30: UV-Vis spectra of macrocycle-copper complex (1:2) titrated with tetrabutylammonium ethoxide. (a) 0-2 equivalents of base. (b) 2-5 equivalents of base. The inset shows a plot of the absorbance at λ_{max}= 634 nm (squares) and λ_{max}= 537 nm (diamonds) as a function of base concentration.

Similarly, Comba and co-workers, found that the addition of copper (II) to a H_4pat^1 caused the emergence of a d-d band at λ_{max} = 714 nm (see Figure 31 a).[127] Addition of the base, (n-Bu_4N)(OMe), to the H_4pat^1-Cu(II) solution resulted in an increase in the absorbance and the formation of a new band at 685 nm (Figure 31 b). Upon addition of up to 2-3 equivalents of base a shoulder at 550 nm emerged (Figure 31 c). The authors observed that the intensities of the absorption bands at 685 and 550 nm have an inflection point after the addition of two equivalents of base (Figure 31 c).[127] The intensity of the absorption band at 685 nm increased upon addition of up to three equivalents of base, a result similar to that recorded for the absorption band at 550 nm (Figure 31 d). Comba and co-workers suggested that the absorption maximum at 685 nm correlates with the dinuclear copper(II) complex $[Cu_2^{II}\ H_2pat^1\ (OH_2)]^{2+}$, which is converted into the hydroxo species upon deprotonation $[Cu_2^{II}H_2pat^1(OH)]^+$ (Figure 32). The intensity of the spectra marginally decreased during the addition of 4-5 equivalents of base. This decrease was thought to be caused by the formation of a bluish precipitate (most likely Cu(II) methoxide or hydroxide formed under highly basic conditions), resulting in the removal of copper(II) from the solution.

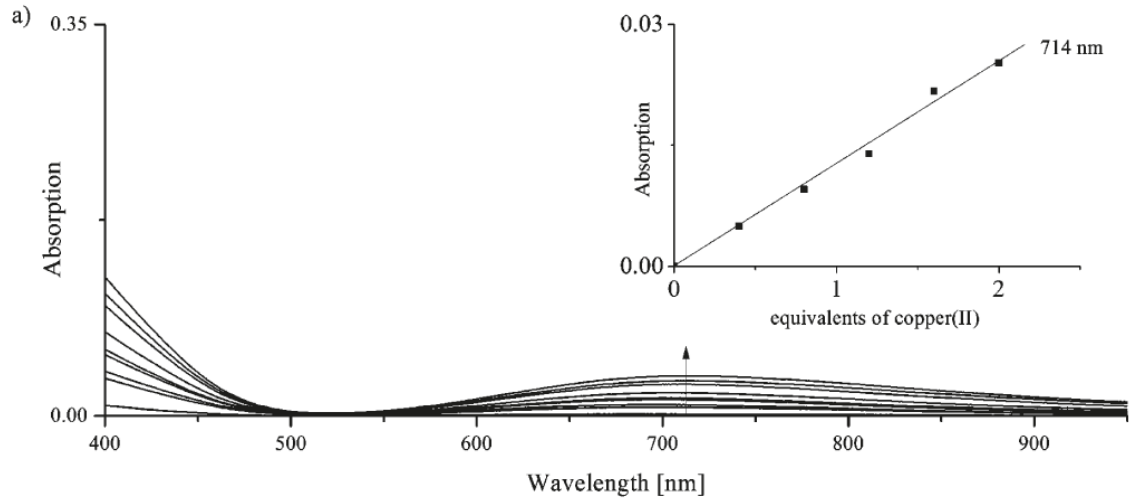
a)
0.35
0.00
Absorption
400
500
600
700
800
900
Wavelength [nm]
0.03
0.00
Absorption
0
1
2
equivalents of copper(II)
714 nm

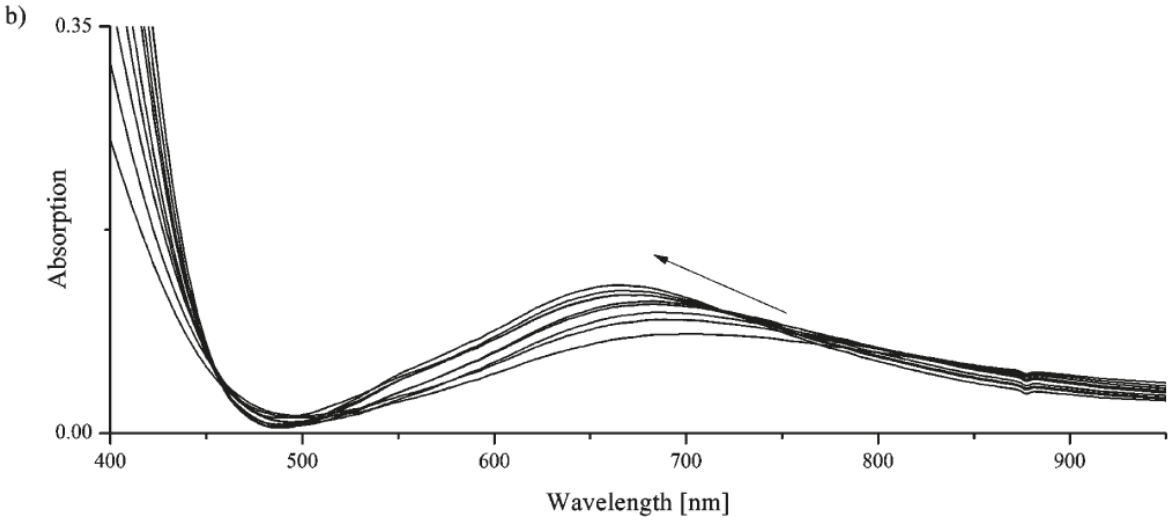
b)
0.35
0.00
Absorption
400
500
600
700
800
900
Wavelength [nm]

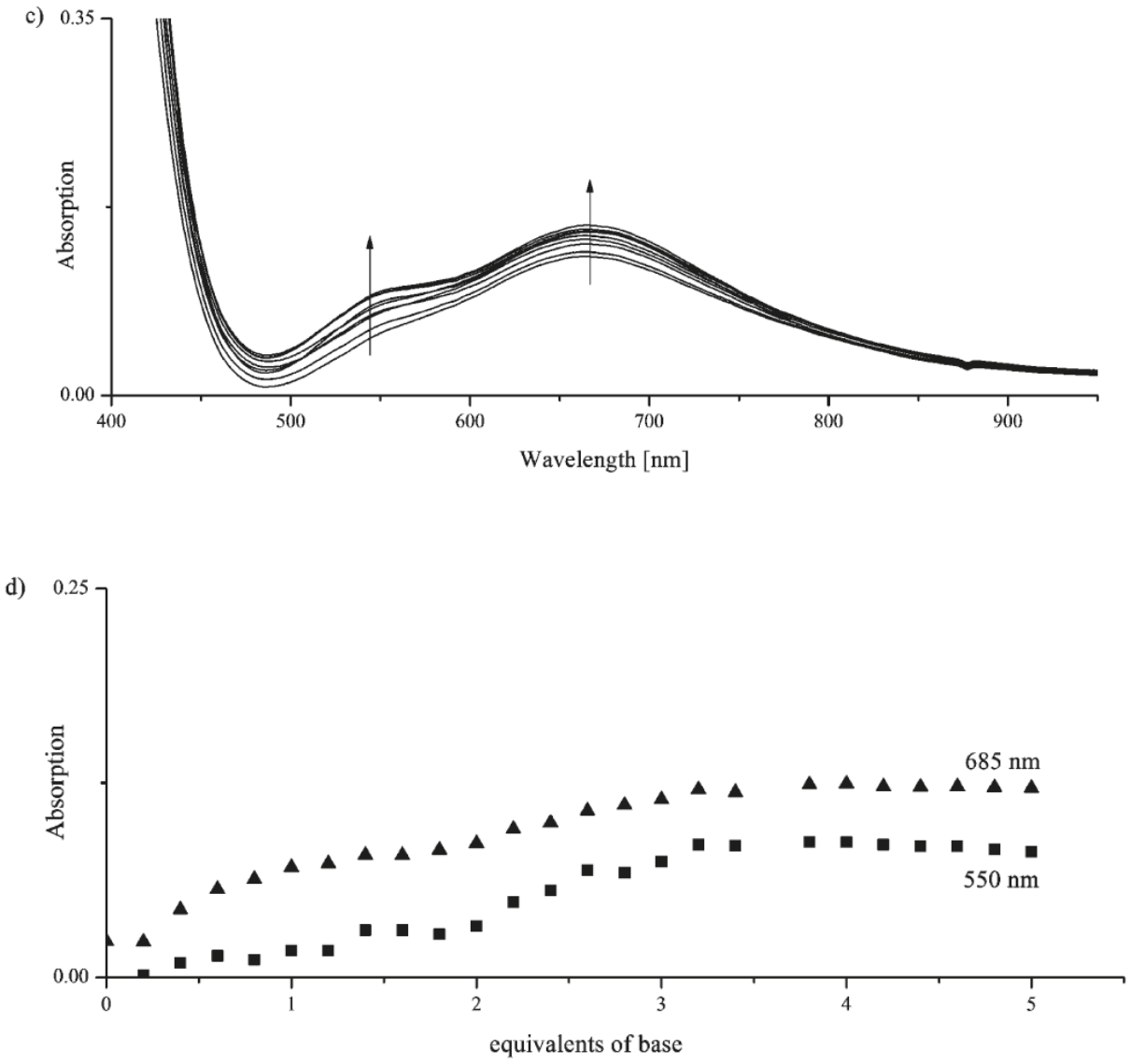

Figure 31: UV-Vis spectra of the titration of H_4pat^1 (1.25 mM) with Cu(II) in methanol. (a) titration of H_4pat^1 with 0-2 equivalents of Cu(II) in 0.2 eq steps, (b) titration of H_4pat^1/copper (II) (1:2) with 0–2 equivalents of (n-Bu_4N)(OMe) in 0.2 eq steps, (c) titration of H_4pat^1/copper (II) (1:2) with 2-5 equivalents of base in 0.2 eq steps, (d) absorbance of the bands at λ = 685 and 550 nm as a function of equivalents of base.[127]

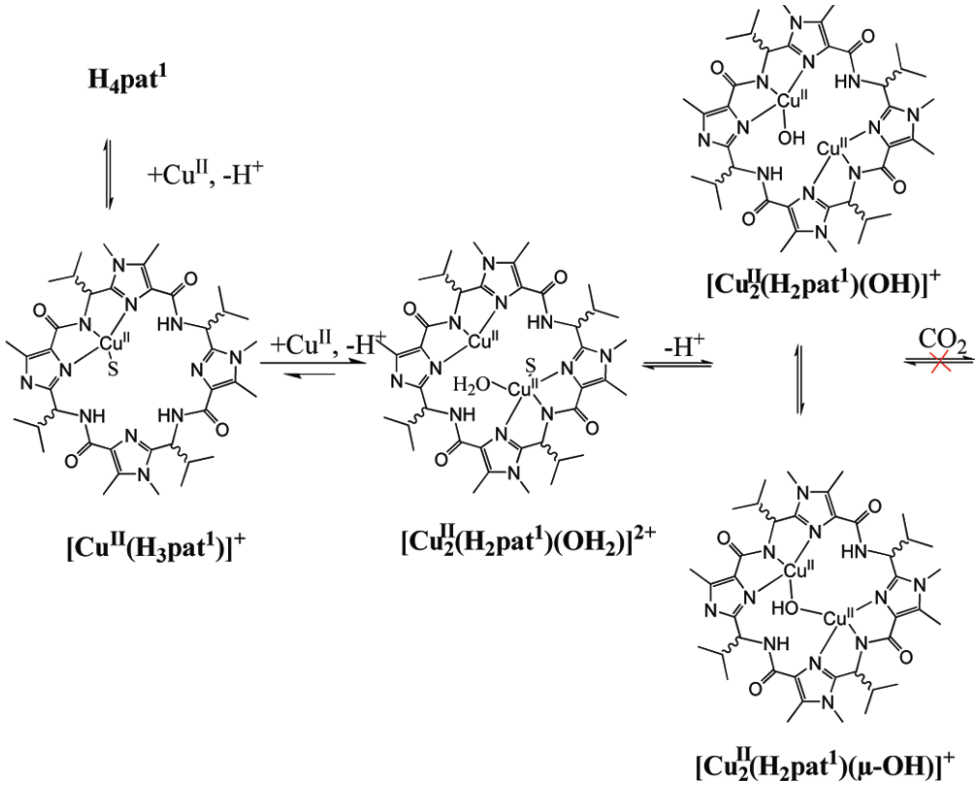

Figure 32: Proposed copper(II) complexation equilibria of H_4pat^1 (S = methanol).[127]

It is therefore tempting to assign the species responsible for the absorption at 634 nm in the Cu(II)- **55** system to the dinuclear Cu(II) compound, **93**, as it behaved in a similar manner to that reported for $[Cu_2^{II}H_2pat^1(OH)]^+$. [127]

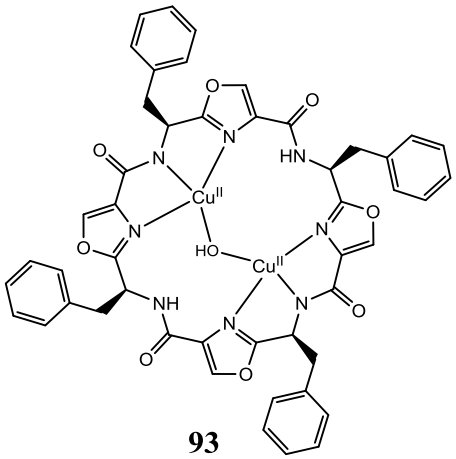

93

Figure 33: Structure of copper(II)- tetraoxazole macrocycle (**55**) complex

However, a solution containing only copper(II) and tetrabutylammonium ethoxide gave a UV-Vis spectrum identical to that found for the solution of the tetraoxazole macrocycle supplemented with 2 equivalents Cu (II) at high base concentration (compare Figures 34 and 30 b). Based on this observation we are unable to conclude that the dinuclear Cu(II)-tetraoxazole macrocycle was formed. This also brings into question the interpretation of the results reported by Comba and co-workers.[127] In order to confirm the species formed in the Cu(II)-tetraoxazole macrocycle system over a range of base concentrations another technique such as ESI-MS would have to be utilized.

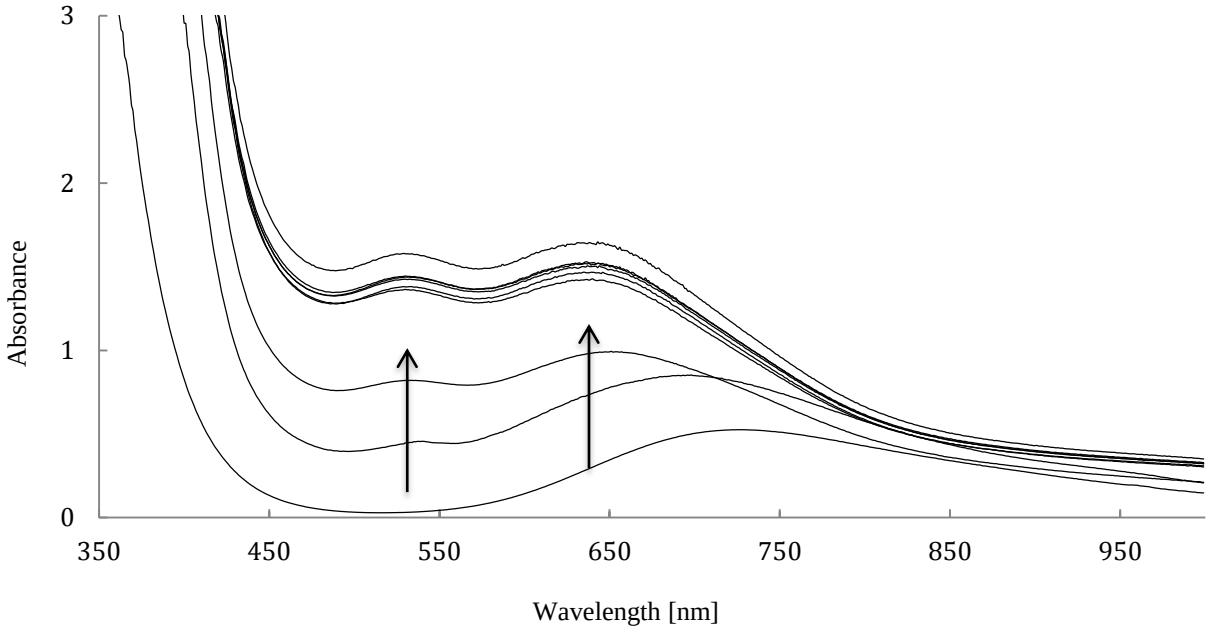

Figure 34: UV-Vis spectra of the titration of copper(II) (6 mM) in methanol with (tetrabutylammonium ethoxide). The titration of (0-5 equivalents) of base was performed in 0.5 eq steps.

2.4. Conclusion and Future Direction

We have shown how the tetraoxazole macrocycle, **55**, can be synthesized using a convergent solution phase peptide synthetic strategy from the readily available starting materials, namely, *N*-Boc-L-Phe-OH and HCl•NH_2-L-Ser-OMe. The key to this synthetic strategy was the stepwise coupling of peptides to produce di-, tetra- and octa- peptides. The treatment of the β-hydroxyamide functionalities with the Burgess reagent or DAST followed by DBU/$BrCCl_3$ resulted in cyclodehydration-dehydrogenation giving the desired oxazole moiety. The convergent synthesis generated the precursor **75**. Cyclization of **74** to form **55** proved to be challenging but with PyOxP as the coupling agent, **55** was formed in 45% yield.

The solid phase peptide synthesis (SPS-CC) method with oxime resin also provided a highly efficient strategy to synthesize the desired macrocycle **55** in 20% yield. It was concluded that the treatment of the peptidyl resin with acetic acid led to the concomitant cleavage of oxime resin to obtain the macrocycle.

We attempted to investigate the ability of **55** to complex copper(II) ions using UV-Vis spectroscopy. Although the UV-Vis spectrum of a Cu(II)-**55** solution changed as a function of a hydroxide concentration, the change was identical to that observed for a solution not containing **55**. Unfortunately, the results were not conclusive.

Future work will be focused on crystallizing the macrocycle to obtain its X-ray structure. EPR and NMR spectroscopies as well as electrospray ionization mass spectrometry (ESI-MS) could be used to characterize the copper(II) complexes formed in solution. In addition, a better understanding of the coordination chemistry could be gained by determining the X-ray structures of the metal-free macrocycle and the dinuclear copper(II) complex of tetraoxazole macrocycle. Molecular modeling could be performed to gain better insight into the molecular structure of the tetraoxazole macrocycle and its complex, and to understand and predict the behaviour of molecular systems.

3. Experimental Section

3.1. Experimental Methods

3.1.1. General Remarks

Solvents were purchased from Sigma-Aldrich or Fisher Scientific and used without further purification. They include hexane, tetrahydrofuran (THF), benzene, ethyl acetate (EtOAc), methanol (MeOH) and dichloromethane (DCM). Diethyl ether was dried over metallic sodium and freshly distilled prior to use. All protected D-amino acids, purchased from Chem-Impex, were of the highest purity available. *O*-benzotriazole-*N,N,N',N'*-tetramethyluroniumhexafluorophosphate (HBTU), hydroxybenzotriazole (HOBt), *N,N*-diisopropylethylamine (DIPEA), 1-ethyl-3-(3-dimethylaminopropyl)carbodiimide (EDC), and trifluoroacetic acid (TFA), were purchased from Chem-Impex. Oxime resin with a substitution level around 0.61 mmol/g was purchased from Chem-Impex. Aluminum-backed thin layer chromatography (TLC) plates, with a 254 nm fluorescence indicator, were purchased from Silicycle and used to monitor all the reactions. Silica gel (Silicaflash P60, 230-400, 40-63 μm particle size) was obtained from Silicycle. Nuclear magnetic resonance spectra (^{1}H NMR and ^{13}C NMR) were recorded at room temperature on a Bruker Avance 500 MHz NMR spectrometer. Chemical shifts were relative to TMS or the deuterated solvents $CDCl_3$ (δ_H = 7.26 ppm and δ_C = 77.2 ppm), DMSO (δ_H= 2.50 ppm and δ_C= 93.5 ppm), or CD_3OD (δ_H = 3.31 ppm, δ_H = 7.74 ppm, and δ_C = 49.2 ppm).

3.2. General Experimental Procedures

3.2.1. Solution Phase Peptide Coupling Procedures

The di-, tetra-, and octa- peptide-coupling reactions were carried out under nitrogen in dichloromethane (DCM) or tetrahydrofuran (THF). The free carboxylic acid (1equiv.), HBTU (1.3 equiv.), DIEPA (3.5 equiv.), and the free amine (1 equiv.) were added to anhydrous DCM or THF at 0°C to generate a 0.1 M solution. The mixture was stirred at room temperature for 24 h and the reaction progress was monitored by TLC. The organic solution was washed with 0.5 N $NaHSO_4$, H_2O, saturated (aqueous) $NaHCO_3$ and brine, dried over $MgSO_4$ and filtered. The filtrate was concentrated *in vacuo*. The residue was purified by column chromatography on silica gel.

3.2.2. Boc-Removal Reaction (Amine Deprotection)

The Boc-protected compound (0.2 mmol) was dissolved in THF (0.1 M) and the solution was cooled to 0°C under N_2 gas. A solution of HCl/ dioxane (4 M, 4 mL) was added in one portion. The ice bath was removed after 30 min, and stirring continued at room temperature for 4 h. The mixture was concentrated *in vacuo*. The residue was then washed with dry diethyl ether and collected by filtration to provide the hydrochloride, which was used in the next step without further purification.

3.2.3. Methyl Ester Hydrolysis (Acid Deprotection)

Acids were deprotected by slowly adding LiOH (2 M, 2.3 mmol) to a stirred solution of oxazole ester in THF/H_2O (1:1) at 0°C. The reaction mixture was stirred at 0°C for 1.5 h. The mixture was allowed to warm to room temperature over a period of 2 h. Stirring continued until TLC analysis showed the consumption of starting material. The solution was concentrated to one-half the volume. The resulting aqueous mixture was acidified with 1 M HCl to a pH~2 at 0°C. The product was extracted from the aqueous phase using 2 x 10 mL portions of EtOAc; the organic layers were combined, washed with brine, dried over $MgSO_4$, and filtered. The filtrate was concentrated *in vacuo*. The crude product was used in the next step without further purification.

3.2.4. Oxazole Formation

3.2.4.1. Oxazoline Generation with Burgess Reagent

Burgess reagent (2.6 g, 11 mmol) was added to 3.7 g of peptidyl-phenylserine (1 mmol) in about 100 mL of THF and the mixture was refluxed for 2 h. The solvent was removed *in vacuo* to give the crude product which was subsequently purified by flash chromatography.

3.2.4.2. Oxazoline Oxidation with DBU

Oxazoline (2.27 g, 6.5 mmol) was dissolved in 65 mL of anhydrous DCM and the solution cooled to 0 °C in an ice bath. DBU (1.95 mL, 13 mmol) was added dropwise followed by $BrCCl_3$ (1.28 mL, 13 mmol). The mixture gradually attained room temperature as it was left to stir

overnight. The mixture was washed with saturated aqueous NH_4Cl, and the product was extracted from the aqueous phase with 30 mL portions of EtOAc. The combined organic phases were washed with brine, dried with $MgSO_4$, and concentrated *in vacuo*. The residue was purified by flash chromatography.

3.2.5. Macrocyclization

The linear octa-peptide (0.1 mmol) was cyclized by treatment with 0.11 mmol of PyOxP and 0.44 mmol of DIPEA in DMF. After being stirred for 3 days, the mixture was washed with saturated aqueous $NaHSO_4$, H_2O and brine, dried over ($MgSO_4$) and concentrated *in vacuo*.

3.3. Preparation of Tetraoxazole Macrocycle (55)

3.3.1. Synthesis *N*-Fmoc-L-Phe-L-Ser-OMe (69)

The dipeptide, **69**, was synthesized using the following solution phase peptide coupling procedure. To a round bottom flask charged with a magnetic stirrer were added *N*-Fmoc-Phe-OH (**71**) (8.52 g, 22 mmol), HCl•H-L-Ser-OMe (**70**) (3.1 g, 20 mmol), *O*-benzotriazole-*N*,*N*,*N'*,*N'*-tetramethyluroniumhexafluorophosphate (HBTU) (9.8 g, 26 mmol), and anhydrous DCM (220 mL) at room temperature and the mixture was cooled to 0 ^{0}C. *N*,*N*-diisopropylethylamine (17.4 mL, 100 mmol), was added to the mixture at 0 ^{0}C under a nitrogen atmosphere and stirred at room temperature for 24 h. The mixture was quenched with 1 M HCl, subsequently treated with saturated $NaHCO_3$, and brine. The organic layer was collected and dried over magnesium sulfate, and the

solution filtered and concentrated *in vacuo*. The residue was purified by flash column chromatography on silica gel with 20% ethyl acetate in hexane as eluent to afford **69**, a white solid (85% yield). m. p. 188 ^{0}C, ^{1}H NMR (500 MHz, DMSO-d_6) δ 8.47 (d, *J* = 7.6 Hz, 1H; NH), 7.88 (d, *J* = 7.6 Hz, 2H; 2x H_{Ar}), 7.73 – 7.58 (m, 3H; 3x H_{Ar}), 7.47 – 7.08 (m, 8H; 8x H_{Ar}), 5.14 (t, *J* = 5.3 Hz, 1H; NH), 4.50 – 4.32 (m, 2H; CHCH$_2$O, CHCH$_2$Phe), 4.22 – 4.00 (m, 3H; CHCH$_2$OFMOC, CHCH$_2$OH SERINE), 3.77 (dt, *J* = 11.3, 5.4 Hz, 1H; CHCH$_2$OH), 3.64 (s, 4H; CHCH$_2$OH, OCH$_3$), 3.14 – 2.97 (m, 1H; CH$_2$Phe), 2.77 (t, *J* = 12.3 Hz, 1H; CH$_2$Phe). ^{13}C NMR (126 MHz, DMSO-d6) δ 172.45; (CO)OCH$_3$, 171.45; CONH, 156.25; OCONH , 144.22-144.18; CH_{Ar} , 141.11-141.09; CH_{Ar} , 138.65; CH_{Ar}, 129.77; CH_{Ar}, 128.45; CH_{Ar} , 128.08; CH_{Ar} , 127.51; CH_{Ar} , 126.66; CH_{Ar} , 125.82-125.73; CH_{Ar} , 120.54; CH_{Ar} , 66.10; CHCH$_2$O, 61.68; CHCH$_2$OH , 56.31; CHCH$_2$OH , 55.19; OCH$_3$, 52.37; CHCH$_2$Phe , 46.99; CHCH$_2$O , 37.91; CHCH$_2$Phe .

3.3.2. Synthesis of *N*-Fmoc-L-Phe-L-Oxazoline-OMe (72)

To a solution of compound **69** (1.95 g, 4 mmol) in THF (40 mL) was added 1.04 g (4.4 mmol) of Burgess reagent. The mixture was refluxed for 2.5 h. The solvent was removed in *vacuo*. The residue was purified using "Dry Column" Flash Chromatography or Dry Column Vacuum Chromatography. The compound was eluted through neutral silica gel with 30% and 40% diethyl ether in hexane, respectively, to afford compound *N*-Fmoc-L-Phe-L-Oxazoline-OMe (**72**) (1.33 g, 2.8 mmol, 71%) as a white solid. ^{1}H NMR (500 MHz, Chloroform-*d*) δ 7.80 (d, *J* = 7.4 Hz, 2H; 2x H_{Ar}), 7.60 (q, *J* = 7.6, 6.0 Hz, 2H; 2x H_{Ar}), 7.43 (q, *J* = 6.7, 6.1 Hz, 2H; 2x H_{Ar}), 7.38 – 7.18 (m, 5H; 5x H_{Ar}), 7.12 (d, *J* = 7.2 Hz, 2H; 2x H_{Ar}), 5.46 (d, *J* = 8.7 Hz, 1H; NH), 4.82 (q, *J* = 7.2, 6.6 Hz, 1H; CH$_2$-oxazoline), 4.79 – 4.70 (m, 1H; CH$_2$-oxazoline), 4.68 – 4.58 (m, 1H; CH-oxazoline), 4.50 (td,

J = 11.0, 10.4, 7.0 Hz, 2H; OC$\underline{H}_2$CH), 4.35 (dd, *J* = 10.8, 7.1 Hz, 1H; C$\underline{H}$CH$_2$Phe), 4.23 (t, *J* = 7.3 Hz, 1H; OCH$_2$C$\underline{H}$), 3.78 (d, *J* = 5.4 Hz, 3H; OC$\underline{H}_3$), 3.19 (dd, *J* = 13.8, 5.9 Hz, 1H; C$\underline{H}_2$Phe), 3.12 (dd, *J* = 13.9, 5.9 Hz, 1H; C$\underline{H}_2$Phe). ^{13}C NMR (126 MHz, $CDCl_3$) δ 170.83; ($\underline{C}$O)OCH$_3$, 168.95; O$\underline{C}$=N , 155.47; O$\underline{C}$ONH , 143.76; $\underline{C}H_{Ar}$, 141.33; $\underline{C}H_{Ar}$, 135.49; $\underline{C}H_{Ar}$, 129.65; $\underline{C}H_{Ar}$, 128.41; $\underline{C}H_{Ar}$, 127.71; $\underline{C}H_{Ar}$, 127.07; $\underline{C}H_{Ar}$, 125.10; $\underline{C}H_{Ar}$,119.98; $\underline{C}H_{Ar}$, 70.14; O$\underline{C}$H$_2$CH , 67.77;OCH$_2\underline{C}$H , 66.88; CH$\underline{C}$H$_2$O , 52.74; O$\underline{C}$H$_3$, 50.12; $\underline{C}$HCH$_2$Phe, 47.19 ; $\underline{C}$HCH$_2$O, 38.70; CH$\underline{C}$H$_2$Phe .

3.3.3. Synthesis of *N*-Fmoc-L-Phe-L-Oxazole-OMe (68)

To the oxazoline, **72**, (3.3 g, 7.07 mmol) in a 100 mL round-bottomed flask, were added CuBr (1.104 g, 1.10 mmol) and $Cu(OAc)_2$ (1.39 g, 1.10 mmol). The flask was evacuated and then filled with argon. The evacuation/argon addition was repeated twice. Benzene (44.1 mL) was added to the flask with a syringe and stirring initiated. The reaction mixture was heated to 60°C and *tert*-butyl perbenzoate (1.5 ml, 1.50 mmol) was added gradually over 15 min. The reaction mixture was then refluxed for 8.5 h. After cooling to room temperature, ethyl acetate (50 mL) was added and the mixture was washed with 10% NH_4OH solution to remove all the copper salts. The aqueous layer was extracted with 3 x 50 mL portions of ethyl acetate. The combined organic extracts were dried over $MgSO_4$ and the crude product, obtained after concentration under vacuum, was subjected to flash column chromatography on SiO_2 [hexane /ethyl acetate; (60:40)]. This produced 2.22 g (68% yield) of **68**, a white solid with a m. p. of 146^{0}C. ^{1}H NMR (500 MHz, Chloroform-*d*) δ 8.16 (s, 1H; OC$\underline{H}$=C), 7.79 (d, *J* = 7.6 Hz, 2H; 2x $\underline{H}_{Ar}$), 7.58 (dd, *J* = 10.5, 7.6 Hz, 2H; 2x $\underline{H}_{Ar}$), 7.43 (t, *J* = 7.5 Hz, 2H; 2x $\underline{H}_{Ar}$), 7.39 – 7.30 (m, 3H; 3x $\underline{H}_{Ar}$), 7.30 – 7.22 (m, 2H; 2x $\underline{H}_{Ar}$), 7.08 – 6.99 (m, 2H; 2x

$\underline{H}_{Ar}$), 5.56 (d, *J* = 8.8 Hz, 1H; N$\underline{H}$), 5.30 (q, *J* = 7.3 Hz, 1H; C$\underline{H}$CH_2Phe), 4.45 (td, *J* = 10.8, 7.0 Hz, 1H; C$\underline{H}_2$), 4.36 (dd, *J* = 10.7, 6.9 Hz, 1H; C$\underline{H}_2$), 4.21 (t, *J* = 7.1 Hz, 1H; C$\underline{H}$), 3.94 (s, 3H; OC$\underline{H}_3$), 3.33 – 3.23 (m, 2H; CHC$\underline{H}_2$Phe). ^{13}C NMR (126 MHz, Chloroform-*d*) δ 164.27; (C$\underline{O}$)OCH_3, 161.41; O$\underline{C}$=N, 155.47; O$\underline{C}$ONH , 144.02; $\underline{C}H_{Ar}$, 143.70; O$\underline{C}$H=C , 141.31; $\underline{C}H_{Ar}$, 135.26; $\underline{C}H_{Ar}$, 133.32; N$\underline{C}$(CO), 129.24; $\underline{C}H_{Ar}$, 128.71; $\underline{C}H_{Ar}$, 127.74; $\underline{C}H_{Ar}$, 127.26; $\underline{C}H_{Ar}$, 127.08; $\underline{C}H_{Ar}$, 125.08; $\underline{C}H_{Ar}$, 67.13; $\underline{C}HCH_2O$, 52.34; O$\underline{C}H_3$, 50.60; $\underline{C}HCH_2$Phe , 47.11; CH$\underline{C}H_2O$, 40.18; CH$\underline{C}H_2$Phe.

3.3.4. Synthesis of HO-Oxazole-L-Phe- NHFmoc (66)

The reagent system, $AlCl_3$ (0.350 g, 9 mmol)/*N*,*N*-dimethylaniline (15 mmol), was added to a suspension of **68** (0.3068 g, 0.3 mmol) in dry DCM (3 mL). The resulting mixture was refluxed for 6 h. The conversion of **68** was monitored by TLC (DCM/methanol, 90:10). HCl (1 N) was then added to acidify the solution (pH~2). The product was extracted with DCM (4 x 10 mL). The combined organic layers were washed with brine, then dried over $MgSO_4$ and evaporated to dryness to give a crude reaction product that was purified by column chromatography on SiO_2 (DCM/methanol; 95:5) to obtain the pure compound, **66**, as a white solid (10% yield). ^{1}H NMR (500 MHz, DMSO-d_6) δ 8.70 (s, 1H; OC$\underline{H}$=C), 8.20 (d, J = 8.4 Hz, 1H; $\underline{H}_{Ar}$), 7.88 (d, J = 7.7 Hz, 2H; 2x $\underline{H}_{Ar}$), 7.62 (d, J = 6.3 Hz, 2H; 2x $\underline{H}_{Ar}$), 7.41 (t, J = 7.5 Hz, 3H; 3x $\underline{H}_{Ar}$), 7.35 – 7.28 (m, 3H; 3x $\underline{H}_{Ar}$), 7.27 (d, J = 4.7 Hz, 4H; 4x$\underline{H}_{Ar}$), 6.72 (d, J = 8.2 Hz, 2H, 2x$\underline{H}_{Ar}$), 6.64 (t, J = 7.2 Hz, 1H; N$\underline{H}$), 4.95 (d, J = 7.6 Hz, 1H; C$\underline{H}$CH_2Phe), 3.27 (dd, J = 13.7, 5.7 Hz, 2H; CHC$\underline{H}_2$Phe).

3.3.5. Synthesis of *N*-Boc-L-Phe-L-Ser-OMe (82)

To a solution of *N*-Boc-L-Phe-OH (**84**) (7.9 g, 30 mmol) in DCM (0.1 M, 300 mL) was added HCl•H-Ser-OMe (**83**) (4.6 g, 30 mmol), and HBTU (13.6 g, 36 mmol) at room temperature. The mixture was cooled to 0°C before adding DIEPA (16.6 mL, 96 mmol). The mixture was then stirred at room temperature under an atmosphere of nitrogen for 16 h. The mixture was then diluted with DCM and poured into 0.5 N $NaHSO_4$. The aqueous layer was extracted twice with DCM. The organic layer was washed with saturated aqueous $NaHCO_3$, H_2O, and brine, dried over $MgSO_4$ and filtered. The filtrate was concentrated *in vacuo*. The product was purified by column chromatography on flash silica gel with 50% ethyl acetate in hexane as eluent to afford compound **82** in 67% yield. (m. p. 85 ^{0}C). ^{1}H NMR (500 MHz, Chloroform-*d*) δ 7.36 – 7.24 (m, 4H; 4x $\underline{H}_{Ar}$), 7.23 (m, 1H; 1x $\underline{H}_{Ar}$), 6.87 (d, *J* = 7.3 Hz, 1H; N$\underline{H}$-Ser), 5.09 (s, 1H; N$\underline{H}$-Phe), 4.61 (d, *J* = 6.2 Hz, 1H; C$\underline{H}$CH$_2$Phe), 4.36 (q, *J* = 7.2 Hz, 1H; C$\underline{H}$CH$_2$OH), 3.97 (d, *J* = 11.9 Hz, 1H; CHC$\underline{H}_2$OH), 3.91 (d, *J* = 11.4 Hz, 1H; CHC$\underline{H}_2$OH), 3.78 (s, 3H; OC$\underline{H}_3$), 3.11 (qd, *J* = 14.0, 6.9 Hz, 2H; CHC$\underline{H}_2$Phe), 2.69(s, 1H; CHCH$_2$O$\underline{H}$), 1.42 (s, 9H; C(C$\underline{H}_3$)$_3$OCO). ^{13}C NMR (126 MHz, $CDCl_3$) δ 171.64; ($\underline{C}$O)OCH$_3$, 170.49; $\underline{C}$ONH, 155.7; C(CH$_3$)$_3$O$\underline{C}$O, 136.45; $\underline{C}H_{Ar}$, 129.30; $\underline{C}H_{Ar}$, 128.66; $\underline{C}H_{Ar}$, 127.01; $\underline{C}H_{Ar}$, 80.57; $\underline{C}$(CH$_3$)$_3$OCO,[77.28, 77.02, 76.77], 62.76; CH$\underline{C}$H$_2$OH, 56.0; $\underline{C}$HCH$_2$OH, 54.94; $\underline{C}$HCH$_2$Phe, 52.70; O$\underline{C}$H$_3$, 38.04;CH$\underline{C}$H$_2$Phe, 28.23; C($\underline{C}$H$_3$)$_3$OCO.

3.3.6. Synthesis of *N*-Boc-L-Phe-Oxazoline-OMe (85)

Method (A):

To a solution of 3.7 g compound **82** (10 mmol) in 101 mL of THF was added 2.6 g of Burgess reagent (11.1 mmol). The mixture was refluxed for 2.5 h at which point the solvent was removed *in vacuo*. The residue was filtered through a dry column of natural silica gel, and the compounds was eluted first with 30% and then with 40% ethyl acetate in hexane to afford 2.9 g of **85** (84%) as a yellow syrup. ^{1}H NMR (500 MHz, Chloroform-*d*) δ 7.27 (q, *J* = 10.5, 8.6 Hz, 3H; 3x$\underline{H}_{Ar}$), 7.13 (d, *J* = 7.3 Hz, 2H; 2x $\underline{H}_{Ar}$), 5.17 (d, *J* = 8.4 Hz, 1H; N$\underline{H}$-Phe), 4.73 (t, *J* = 8.9 Hz, 2H; OC$\underline{H}_2$CH-oxaz), 4.60 (t, *J* = 8.3 Hz, 1H; $OCH_2C\underline{H}$-oxaz), 4.46 (dd, *J* = 10.6, 8.6 Hz, 1H; C$\underline{H}CH_2$Phe), 3.76 (s, 3H; OC$\underline{H}_3$), 3.16 (dd, *J* = 14.0, 5.8 Hz, 1H; CHC$\underline{H}_2$Phe), 3.06 (dd, *J* = 13.9, 5.6 Hz, 1H; CHC$\underline{H}_2$Phe), 1.42 (s, 9H; C(C$\underline{H}_3$)$_3$OCO). ^{13}C NMR (126 MHz, $CDCl_3$) δ 170.88; ($\underline{C}$O)OCH_3, 169.28; O$\underline{C}$=N, 154.85; O$\underline{C}$ONH, 135.79; $\underline{C}H_{Ar}$, 129.61; $\underline{C}H_{Ar}$, 129.45; $\underline{C}H_{Ar}$, 128.29; $\underline{C}H_{Ar}$, 126.81;$\underline{C}H_{Ar}$, 79.75;$\underline{C}(CH_3)_3OCO$, [77.30, 77.25, 77.04, 76.79], 69.99; $OCH_2\underline{C}H$, 67.81; O$\underline{C}H_2$CH, 52.25; O$\underline{C}H_3$, 49.65; $\underline{C}HCH_2$Phe, 38.87; $CH\underline{C}H_2$Phe, 28.29; C($\underline{C}H_3$)$_3$OCO.

Method (B):

A solution of 1.95 g of **82** (4 mmol) in 40 mL DCM was cooled to -78 ^{0}C. DAST (0.50 mL, 5.2 mmol) was added under a nitrogen atmosphere at a rate of 0.1 mL/ min. After being stirred for 1.5 h, anhydrous K_2CO_3 (1.1 g. 8 mmol) was added and the reaction mixture was stirred at -78 ^{0}C for 1 h. Then, the reaction mixture was stirred for an additional 1.5 h at room temperature. The organic solution was poured into saturated aqueous sodium bicarbonate and extracted twice with DCM. The organic layers were combined, dried over magnesium sulfate, filtered, and concentrated *in vacuo*. The product was purified by column chromatography on flash silica gel with 70% ethyl acetate in hexane as an eluent to give the oxazoline, **85** (88%) as an oil.

3.3.7. Synthesis of *N*-Boc-L-Phe-Oxazole-OMe (81)

A solution of oxazoline (**85**) (2.2 g, 6.5 mmol) dissolved in 65 mL of DCM was cooled in an ice bath. DBU (1.95 mL, 13 mmol) was added dropwise under a nitrogen atmosphere. $BrCCl_3$ (1.28 mL, 13 mmol) was slowly added to the mixture so as to maintain the temperature at 0 ^{0}C. The reaction mixture attained room temperature as it was left to stir overnight. The mixture was poured into aqueous saturated $NHCl_4$. The product was extracted with EtOAc. The combined organic phases were washed with brine, dried over $MgSO_4$ and taken to dryness. The residue was purified by column chromatography on flash silica gel with 30% ethyl acetate in hexane as an eluent yielding 2.1 g (91% yield) of **81** as a white powder (m. p. 109 ^{0}C). ^{1}H NMR (500 MHz, Chloroform-*d*) δ 8.15 (d, *J* = 8.8 Hz, 1H; OC<u>H</u>=C(oxaz)), 7.43 – 7.19 (m, 3H; 3x $\underline{H}_{Ar}$), 7.06 (s, 2H; 2x $\underline{H}_{Ar}$), 5.39 – 5.18 (m, 2H; C<u>H</u>CH_2Phe, N<u>H</u>-Phe), 3.93 (s, *J* = 3.5 Hz, 3H; OCH_3), 3.26 (d, *J* = 15.6 Hz, 2H; CHC<u>H</u>$_2$Phe), 1.43 (s, *J* = 7.8 Hz, 9H; C(C<u>H</u>$_3$)$_3$OCO). ^{13}C NMR (126 MHz, $CDCl_3$) δ 164.75; (<u>C</u>O)OCH_3, 161.47; <u>C</u>=N,154.84; O(<u>C</u>O)NH, 143.86;O<u>C</u>H=C, 135.58;<u>C</u>H-Ar, 133.27; OCH=<u>C</u>, 129.23; $\underline{C}H_{Ar}$, 128.59; $\underline{C}H_{Ar}$, 127.07; $\underline{C}H_{Ar}$, 80.20; <u>C</u>$(CH_3)_3OCO$, 52.23; O<u>C</u>H_3, 50.14; <u>C</u>HCH_2Phe, 40.37; CH<u>C</u>H$_2$Phe, 28.24; C(<u>C</u>H$_3$)$_3$OCO.

3.3.8. Synthesis of HCl•H_2N-L-Phe-Oxazole-OMe (80)

Compound **81** (2.9 g, 8.3 mmol) was dissolved in 83 mL of THF. The solution was added in one portion to 4 mL of a 4 M HCl/dioxane solution cooled to 0 ^{0}C and kept under a nitrogen atmosphere. The ice bath was removed after 30 min and stirring continued at room temperature for 4 h. The mixture was concentrated *in vacuo*. The residue was washed with dry diethyl ether and

collected by filtration to provide **80** (1.4 g), a pale yellow solid used in the next step without further purification (m. p. 205 ^{0}C). ^{1}H NMR (500 MHz, DMSO-d_6) δ 9.17 (s, 2H; N$\underline{H}_2$-Phe), 8.93 (s, 1H; OC$\underline{H}$=C(oxaz)), 7.26 (dd, *J* = 14.3, 7.0 Hz, 3H; 3x$\underline{H}_{Ar}$), 7.12 (d, *J* = 7.1 Hz, 2H; 2x $\underline{H}_{Ar}$), 4.88 (dd, *J* = 9.7, 5.2 Hz, 1H; C$\underline{H}$CH$_2$Phe), 3.82 (s, 3H; OC$\underline{H}_3$), 3.44 (dd, *J* = 13.5, 5.1 Hz, 1H; CHC$\underline{H}_2$Phe), 3.24 (dd, *J* = 13.5, 9.7 Hz, 1H; CHC$\underline{H}_2$Phe). ^{13}C NMR (126 MHz, DMSO) δ 161.12; ($\underline{C}$O)OCH$_3$, 160.93; $\underline{C}$=N, 146.80; O$\underline{C}$H=C, 135.00; OCH=$\underline{C}$, 132.9; $\underline{C}H_{Ar}$, 129.59; $\underline{C}H_{Ar}$, 129.08; $\underline{C}H_{Ar}$, 127.74; $\underline{C}H_{Ar}$, 66.82; 52.46; O$\underline{C}$H$_3$, 49.38; $\underline{C}$HCH$_2$Phe, 37.91; CH$\underline{C}$H$_2$Phe.

3.3.9. Synthesis of *N*-Boc-Phe-Oxazole-OH (79)

A solution of LiOH•H$_2$O (2M, 31 mL) was added dropwise over a 10 min period to a solution of 2.1 g of **81** (6.2 mmol) in 62 mL of THF/H$_2$O (1:1) and the mixture was stirred at 0°C for 1.5 h under a nitrogen atmosphere. The mixture was allowed to warm to room temperature and to stir for an additional 2 h. The solution was concentrated to half its volume. The resulting aqueous phase was acidified with 1 M HCl to pH~2 at 0 °C. The aqueous phase was repeatedly extracted with EtOAc; the organic layers were combined, washed with brine, dried over MgSO$_4$, and filtered. The filtrate was concentrated *in vacuo*. The crude product (1.63 g, m. p. 120 ^{0}C) was used in the next step without further purification. ^{1}H NMR (500 MHz, Chloroform-*d*) δ 8.23 (s, 1H; OC$\underline{H}$=C(oxaz)), 7.28 (d, *J* = 7.5 Hz, 3H; 3x$\underline{H}_{Ar}$), 7.10 (s, 2H; 2x$\underline{H}_{Ar}$), 5.86 (s, 1H; N$\underline{H}$-Phe), 5.27 (s, 1H; C$\underline{H}$CH$_2$Phe), 3.26 (d, *J* = 6.9 Hz, 2H; CHC$\underline{H}_2$Phe), 1.41 (s, 9H; C(C$\underline{H}_3$)$_3$OCO). ^{13}C NMR (126 MHz, CDCl$_3$) δ 165.75; ($\underline{C}$O)OH, 163.86; $\underline{C}$=N, 155.10; O($\underline{C}$O)NH , 144.73; O$\underline{C}$H=C, 135.55; $\underline{C}H_{Ar}$, 132.86; OCH=$\underline{C}$, 129.22; $\underline{C}H_{Ar}$, 128.64; $\underline{C}H_{Ar}$, 127.13; $\underline{C}H_{Ar}$, 80.27;$\underline{C}$(CH$_3$)$_3$OCO, [77.26, 77.01, 76.75] , 50.29; $\underline{C}$HCH$_2$Phe, 40.35; CH$\underline{C}$H$_2$Phe, 28.25; C($\underline{C}$H$_3$)$_3$OCO.

3.3.10. Synthesis of N-Boc-L-Phe-Oxazole-L-Phe-Oxazole-OMe (78)

To a solution of 1.06 g of **79** (3.9 mmol) in 39 mL of DCM was added 0.66 g of **80** (3.9 mmol), and 1.77 g of HBTU (4.6 mmol). Once cooled to 0°C, 22.1 mL of DIEPA (12.4 mmol) was added to the reaction mixture which was subsequently stirred at room temperature under a nitrogen atmosphere. The following day the reaction mixture was diluted with DCM and poured into 0.5 N $NaHSO_4$. The aqueous layer was extracted twice with DCM. The organic layer was washed with saturated aqueous $NaHCO_3$, H_2O, and brine, dried over $MgSO_4$ and filtered. The filtrate was concentrated *in vacuo*. The product was purified by column chromatography on flash silica gel with 50% ethyl acetate in hexane furnishing **78** in 75% yield (m. p. 155 ^{0}C) ^{1}H NMR (500 MHz, Chloroform-*d*) δ 8.13 (s, 1H;OC<u>H</u>=C(oxaz)), 8.08 (s, 1H;OC<u>H</u>=C(oxaz)), 7.49 (d, *J* = 8.8 Hz, 1H; N<u>H</u>-Phe), 7.27 (d, *J* = 16.8 Hz, 6H; 6x<u>H</u>$_{Ar}$), 7.11 (d, *J* = 6.8 Hz, 2H; 2x<u>H</u>$_{Ar}$), 7.04 (d, *J* = 7.0 Hz, 2H; 2x<u>H</u>$_{Ar}$), 5.67 (q, *J* = 7.5 Hz, 1H; N<u>H</u>-Phe), 5.16 (d, *J* = 22.0 Hz, 2H; C<u>H</u>CH$_2$Phe, C<u>H</u>CH$_2$Phe), 3.93 (s, 3H; OC<u>H</u>$_3$), 3.38 (dd, *J* = 7.1, 3.7 Hz, 2H; CHC<u>H</u>$_2$Phe), 3.26 – 3.14 (m, 2H; CHC<u>H</u>$_2$Phe), 1.45 (s, 9H; C(C<u>H</u>$_3$)$_3$OCO). ^{13}C NMR (126 MHz, $CDCl_3$) δ 164.75; (<u>C</u>O)OCH$_3$, 163.52;<u>C</u>=N, 161.39;C=N, 159.84; <u>C</u>ONH, 154.79; O(<u>C</u>O)NH, 143.88; O<u>C</u>H=C, 141.38; O<u>C</u>H=C,135.62; <u>C</u>H$_{Ar}$, 135.37; <u>C</u>H$_{Ar}$, 133.44; 2x OCH=<u>C</u>, 129.23; 2x<u>C</u>H$_{Ar}$, 128.55; 2x<u>C</u>H$_{Ar}$, 127.22;2x <u>C</u>H$_{Ar}$, 80.31; <u>C</u>(CH$_3$)$_3$OCO, 52.23; O<u>C</u>H$_3$, 49.91; <u>C</u>HCH$_2$Phe, 48.32; <u>C</u>HCH$_2$Phe, 40.07; CH<u>C</u>H$_2$Phe, 38.80; CH<u>C</u>H$_2$Phe, 28.29; C(C<u>H</u>$_3$)$_3$OCO.

3.3.11. Synthesis of *N*-Boc-L-Phe-Oxazole-L-Phe-Oxazole-Phe-OH (76)

A solution of methyl ester, **78** (0.97 g, 1.7 mmol), in 8.5mL of THF/H_2O (1:1) was added dropwise to 17 mL of a 2 M LiOH•H_2O solution over a 10 min period at 0°C under a nitrogen atmosphere. The mixture was stirred at 0 °C for 1.5 h. At this point, the mixture was allowed to warm to room temperature and was stirred for additional 2 h. TLC was used to monitor the reaction until the starting material had been consumed. The solution was concentrated to one-half volume. The resulting aqueous phase was acidified with 1 M HCl to a pH~2 at 0°C. The aqueous phase was extracted with several portions of ethyl acetate; the organic layers were combined, washed with brine, dried over $MgSO_4$, and filtered. The filtrate was concentrated *in vacuo* resulting in 1.32 g of crude **76** (m. p. 191 ^{0}C). ^{1}H NMR (500 MHz, DMSO-d_6) δ 8.79 (d, *J* = 8.6 Hz, 1H;N<u>H</u>-Phe), 8.70 (s, 1H; OC<u>H</u>=C (oxaz)), 8.54 (s, 1H; OC<u>H</u>=C (oxaz)), 7.61 (d, *J* = 8.4 Hz, 1H; N<u>H</u>-Phe), 7.26 (d, *J* = 4.1 Hz, 10H; 10xH_{Ar}), 5.45 (s, 1H; C<u>H</u>CH_2Phe), 4.90 (s, 1H; C<u>H</u>CH_2Phe), 3.41 (d, *J* = 5.2 Hz, 2H; CHC<u>H_2</u>Phe), 3.24 (m, 1H; CHC<u>H_2</u>Phe), 3.08 (d, *J* = 13.1 Hz, 1H; CHC<u>H_2</u>Phe), 1.30 (s, 9H; C(C<u>H_3</u>)$_3$OCO). ^{13}C NMR (126 MHz, DMSO) δ 164.37; (<u>C</u>O)OH, <u>C</u>=N, 163.52; <u>C</u>=N, 160.16; <u>C</u>ONH, 155.41; O(<u>C</u>O)NH, 142.74; 2x O<u>C</u>H=C, 137.72; 2x <u>C</u>H_{Ar}, 135.65; 2x OCH=<u>C</u>, 129.60; 2x<u>C</u>H_{Ar}, 128.68; 2x <u>C</u>H_{Ar}, 126.99; 2x <u>C</u>H_{Ar}, 78.84; <u>C</u>$(CH_3)_3$OCO, 50.44; <u>C</u>HCH_2Phe, 48.41; <u>C</u>HCH_2Phe, 31.42; 2x CH<u>C</u>H_2Phe, 28.56; C(<u>C</u>H_3)$_3$OCO.

3.3.12. Synthesis of HCl•NH_2-L-Phe-Oxazole-L-Phe-Oxazole-OMe (77)

The Boc-protected compound, **78**, (0.965 mmol) was dissolved in 9.7 mL of THF and added in one portion to 4 mL of a 4M HCl/dioxane solution cooled to 0°C under a N_2 atmosphere. The ice bath was removed after 30 min and stirring continued at room temperature. The TLC analysis indicated that the reaction was complete after 4 h. The mixture was concentrated *in vacuo*. The residue was washed with dry diethyl ether and collected by filtration to provide 0.6920 g of **77** as a pale yellow solid (m. p. 120 ^{0}C) that was used in the next step without further purification. ^{1}H NMR (500 MHz, DMSO-d_6) δ 8.87 – 8.80 (m, 2H; NH_2-Phe), 8.69 (s, 3H; 2x OCH=C(oxaz),1x NH-Phe), 7.44 – 7.04 (m, 10H, ; 10x H_{Ar}), 5.45 (s,1H; C<u>H</u>CH_2Phe), 4.78 (s, 1H; C<u>H</u>CH_2Phe), 3.82 (s, 3H; OC<u>H</u>$_3$), 3.39 (s, 2H; CHC<u>H</u>$_2$Phe), 3.29 (s, 2H; CHC<u>H</u>$_2$Phe). ^{13}C NMR (126 MHz, DMSO) δ164.11; (<u>C</u>O)OCH_3, 163.52; <u>C</u>=N, 160.16; <u>C</u>=N, <u>C</u>ONH, 145.41; O<u>C</u>H=C, 142.74; O<u>C</u>H=C, 137.72; 2x <u>C</u>H_{Ar}, 135.65; 2x OCH=<u>C</u>, 129.66; 2x <u>C</u>H_{Ar}, 129.70; 2x <u>C</u>H_{Ar}, 128.70; 2x <u>C</u>H_{Ar}, 127.74; 2x <u>C</u>H_{Ar}, 52.46; O<u>C</u>H_3. 52.31; 2x <u>C</u>HCH_2Phe, 39.50; 2x CH<u>C</u>H_2Phe.

3.3.13. Synthesis of *N*-Boc-L-Phe-Oxazole-L-Phe-Oxazole-L-Phe-Oxazole-L-Phe-Oxazole-OMe (75)

A solution of 696 mg of **76** (1.5 mmol) in DCM was added to 375 mg of **77** (1.5 mmol), 340 mg of HOBt (1.8 mmol), and 275 mg of EDC (1.5 mmol) at room temperature. Once cooled to 0°C, 0.65 mL of DIEPA (1.8 mmol) was added under a nitrogen atmosphere and the mixture was stirred

for 24 h. The reaction mixture was diluted twice with DCM and poured into 0.5 N $NaHSO_4$. The aqueous layer was extracted with DCM. The organic layer was washed sequentially with saturated aqueous $NaHCO_3$, H_2O, and brine, dried over $MgSO_4$, and filtered. The filtrate was concentered *in vacuo*. The product was purified by column chromatography on flash silica gel with 50% ethyl acetate in hexane giving 986 mg of **75** (67% yield) as a white solid (m. p. 160 ^{0}C). ^{1}H NMR (500 MHz, Chloroform-*d*) δ 8.12 (d, *J* = 7.4 Hz, 3H; 3x OC<u>H</u>=C(oxaz)), 8.08 (s, 1H; OC<u>H</u>=C(oxaz)), 7.52 (s, 1H; N<u>H</u>-Phe), 7.28 (s, 15H; 15x <u>H</u>$_{Ar}$), 7.12 (d, *J* = 8.6 Hz, 5H; 5x<u>H</u>$_{Ar}$), 7.02 (s, 2H; 2x N<u>H</u>-Phe), 5.65 (s, 2H; C<u>H</u>CH$_2$Phe), 5.18 (s, 1H; C<u>H</u>CH$_2$Phe), 5.06 (s, 1H; N<u>H</u>-Phe), 3.90 (s, 3H; OC<u>H</u>$_3$), 3.45 – 3.16 (m, 8H; 4x CHC<u>H</u>$_2$Phe), 1.42 (s, 9H; C(C<u>H</u>$_3$)$_3$OCO). ^{13}C NMR (126 MHz, $CDCl_3$) δ 164.02; (<u>C</u>O)OCH$_3$, 163.52-162.67; 2x <u>C</u>=N, 162.61; <u>C</u>=N, 161.39; <u>C</u>=N, 159.79; 3x<u>C</u>ONH, 159.76; O(<u>C</u>O)NH, 143.92;O<u>C</u>H=C, 141.71; O<u>C</u>H=C, 141.60; O<u>C</u>H=C, 141.53; O<u>C</u>H=C, 135.52; OCH=<u>C</u>, 135.47; OCH=<u>C</u>, 135.42; OCH=<u>C</u>, 135.37, OCH=<u>C</u>, 133.40; 2x <u>C</u>H$_{Ar}$, 129.26; 2x <u>C</u>H$_{Ar}$, 129.24; 2x <u>C</u>H$_{Ar}$, 129.21; 2x <u>C</u>H$_{Ar}$, 128.70; 2x <u>C</u>H$_{Ar}$, 128.66; 2x <u>C</u>H$_{Ar}$, 128.59; 2x <u>C</u>H$_{Ar}$, 127.24; 2x <u>C</u>H$_{Ar}$, 127.14; 2x <u>C</u>H$_{Ar}$, 80.42; <u>C</u>(CH$_3$)$_3$OCO, 52.22; O<u>C</u>H$_3$, 48.34, 2x <u>C</u>HCH$_2$Phe, 48.11; 2x <u>C</u>HCH$_2$Phe, 39.63; CH<u>C</u>H$_2$Phe, 39.52; CH<u>C</u>H$_2$Phe, 31.58; CH<u>C</u>H$_2$Phe, 30.92; CH<u>C</u>H$_2$Phe, 28.26; C(<u>C</u>H$_3$)$_3$OCO.

3.3.14. Synthesis of HO-Oxazole-L-Phe-Oxazole-L-Phe-Oxazole-L-Phe Oxazole-L-Phe-NH_2 (74)

10 mL of LiOH•H_2O (2 M) was added dropwise, over a 10 min period, to solution of 986 mg of **75** (0.996 mmol) in 10 mL of THF/H_2O (1:1). The mixture was stirred at 0°C for 1.5 h under N_2.

The mixture was allowed to warm to room temperature and stirred for an additional 2 h. The solution was concentrated to one-half volume. The resulting aqueous phase was acidified to pH~ 2 with 1 M HCl at 0°C. The aqueous phase was repeatedly extracted with ethyl acetate; the organic layers were combined, washed with brine, dried over $MgSO_4$, and filtered. The filtrate was concentrated *in vacuo*. The crude acid was dissolved in 9 mL of THF. A 4 M HCl/dioxane (4 mL) solution, cooled to 0°C, was added in one portion under a nitrogen atmosphere. The ice bath was removed after 30 min and stirring continued at room temperature for 4 h. The mixture was concentrated *in vacuo*. The residue was then washed with dry diethyl ether and collected by filtration to provide 724 mg of **74** as a yellow solid (m. p. 170 ^{0}C) used without further purification. ^{1}H NMR (500 MHz, Methanol-d_4) δ 8.42 (d, *J* = 6.2 Hz, 2H; 2x OC<u>H</u>=C(oxaz)), 8.33 (d, *J* = 12.6 Hz, 2H; 2x OC<u>H</u>=C(oxaz)), 7.28 (dd, *J* = 23.5, 6.8 Hz, 12H; 12x<u>H</u>$_{Ar}$), 7.22 (s, 8H; 8x<u>H</u>$_{Ar}$), 5.57 (d, *J* = 7.8 Hz, 3H; 3x C<u>H</u>CH$_2$Phe),4.94 (s, 1H; C<u>H</u>CH$_2$Phe), 3.47 (s, 4H; CHC<u>H</u>$_2$Phe), 3.38 (s, 4H; 4x CHC<u>H</u>$_2$Phe).^{13}C NMR (126 MHz, CDCl3) δ 163.33; <u>C</u>ONH, 160.74; <u>C</u>=N, 159.59; <u>C</u>ONH, 144.33; <u>C</u>=N, 143.14; 2xO<u>C</u>H=C, 142.16; <u>C</u>H$_{Ar}$, 136.2; 2xO<u>C</u>H=C, 135.35; 4xOCH=<u>C</u>, 133.78; <u>C</u>=N , 128.93; 2x<u>C</u>H$_{Ar}$, 128.92; 2x <u>C</u>H$_{Ar}$, 128.70; 2x <u>C</u>H$_{Ar}$, 128.18; 2x <u>C</u>H$_{Ar}$, 127.53; 5x <u>C</u>H$_{Ar}$, 126.64; <u>C</u>=N, 49.75; 2x <u>C</u>HCH$_2$Phe, 48.62; 2x <u>C</u>HCH$_2$Phe, 38.23; CH<u>C</u>H$_2$Phe, 38.06; 3x CH<u>C</u>H$_2$Phe.

3.3.15. Synthesis of Macrocycle Oxazole-L-Phe-Oxazole-L-Phe-Oxazole-L-Phe-Oxazole-L-Phe (55)

A solution of 458 mg of PyOxP (0.86 mmol) and 0.60 mL of DIPEA (3.47 mmol) in 794 mL of DMF was added dropwise at room temperature, under a nitrogen atmosphere, to 724 mg of **74** (0.794 mmol). After being stirred for 3 days, DMF was removed under reduced pressure. The mixture was diluted with DCM and was poured into 1 N $NaHSO_4$. The aqueous layer was extracted

twice with DCM. The organic layers were washed with saturated aqueous $NaHCO_3$ and brine, dried over $MgSO_4$, and filtered. The filtrate was concentrated *in vacuo*. The crude product was precipitated with diethyl ether. The residue was purified by trituration with hot hexane resulting in 400 mg of macrocycle, **55** (45% yield, m. p. 140 ^{0}C). ^{1}H NMR (500 MHz, Chloroform-d) δ 8.13 (s, 4H; 4x OCH=C(oxaz)), 7.35 – 7.27 (m, 16H; 4xNH-Phe, 12xH_{Ar}), 7.16 – 7.11 (m, 4H; 4xH_{Ar}), 5.75 (q, J = 6.6 Hz, 4H; 4xCHCH_2Phe), 3.45 – 3.32 (m, 8H; 4x CHCH_2Phe). ^{13}C NMR (126 MHz, CDCl3) δ 163.03; 4xCONH, 159.33; 4x N=CO, 141.87; 4x OCH=C, 153.6; 4x CH_{Ar}, 135.53; 4x OCH=C, 129.32; 4x CH_{Ar}, 128.69; 4x CH_{Ar}, 127.36; 4x CH_{Ar}, , 47.50; 4x CHCH_2Phe, 40.28; 4x CHCH_2Phe.

3.3.16. SPPS of Macrocycle Oxazole-L-Phe-Oxazole-L-Phe-Oxazole-L-Phe-Oxazole-L-Phe (55)

3.3.16.1. Loading *N*-Boc-L-Phe-Oxa-OH (79) onto the Oxime resin

The Oxime resin (100-200 mesh, 0.61 mmol/g, 164 mg) was initially washed with DMF (5x 3 mL) and DCM (5x 3 mL). Next it was allowed to swell in DCM for 0.5 h and then with DMF for 1 h. After the solvent was decanted from the resin, *N*-Boc-L-Phe- Oxa-OH (**79**) (0.265 g, 0.24 mmol), HBTU (0.303 g, 0.24 mmol), and DIPEA (0.209 mL, 0.36 mmol) dissolved in 3 mL of DMF was added and the mixture was shaken for 12 h. After 12 h, the solution was drained and the resin was washed exhaustively with DMF (5x 5mL), DCM (5x 5mL), and DMF (1x 5 mL).

3.3.16.2. Acetylation of the *N*-Boc-L-Phe-Oxa-OH-loaded resin

Acetylation was carried out by adding 0.64 mL of acetic anhydride (7 mmol) and 0.5 mL of DIPEA (3.9 mmol) in 1.5 mL of DMF to the *N*-Boc-L-Phe- Oxa-OH-loaded resin. After shaking the mixture for 1 h, the resin was rinsed with DMF (5x 5 mL), DCM (5x, 5 mL), and DMF (1x 5 mL).

3.3.16.3. Deprotection of *N*-Boc group of acetylated *N*-Boc-L-Phe-Oxa-OH-loaded resin

The *N*-Boc group was removed by adding 3 mL of a 25% TFA/DCM solution to the resin. After agitating the mixture for 1 min, the liquid was decanted and an additional 3 mL of TFA/DCM solution was added to the resin. After 0.5 h of agitation, the liquid was decanted and the resin was treated with 3 mL of 5% DIPEA in DMF to remove excess TFA.

3.3.16.4. Procedure used to couple amino acids to the NH_2-L-Phe-Oxa-Oxime resin (90)

The second coupling reaction was performed using fragment **89** (0.18 g, 0.12 mmol) in the presence of HBTU (0.037 g, 0.12 mmol), HOBt (0.13 g, 0.12 mmol), and DIPEA (0.025 mL, 0.18 mmol) in 3 mL of DMF. After agitating the reaction mixture for 3 h, a Kaiser ninhydrin test indicated the coupling was complete. The liquid was decanted and the resin was washed with DMF (5x 5mL), DCM (5x 5mL), and DMF (1x, 5 mL).

The *N*-Boc group was removed with a solution of TFA in DCM using the procedure outlined above. The symmetric anhydride of *N*-Boc-L-Phe-Oxa-OH (**79**) in DMF was subsequently coupled to the resin in the presence of DIPEA (0.05 mL, 0.18 mmol). After 3 h, the product was recovered and the *N*-Boc group removed as outlined above. This was repeated until the desired number of oxazole units was obtained.

3.3.16.5. Cyclization-Cleavage

The cyclization-cleavage reactions were carried out by shaking the peptidyl resin, **86**, in DCM (10 mL) in the presence of 6% acetic acid at room temperature for 3 days. The resin was filtered from the solution containing the cyclic peptide. The resin was washed with DCM (3X 5mL). The filtrate was combined with the cyclic peptide containing solution above and was concentrated *in vacuo.* The residue was washed with ice cold water, 0.1 N HCl, 5% $NaHCO_3$, and brine. The organic layer was evaporated and the crude product, **55**, was purified by reverse phase HPLC. This procedure gave a 20% yield of **55**.

3.4. Method Used to Study the Copper(II)-Macrocyclic Tetraoxazole (55) Complexation

Preparation of the stock solutions:

A stock solution of **55** (6 mM) was prepared by adding methanol to 23 mg of **55** in a 10

mL volumetric flask. To prepare a 37.5 mM stock solution of copper(II) triflate, 138 mg of the compound were added to a 10 mL volumetric flask, and diluted with methanol to the mark. A 75 mM stock solution of tetrabutylammonium ethoxide was prepared by diluting 300 μL of the compound (20% w/v) in a 10 mL volumetric flask with methanol.

UV-Vis titration of the tetraoxazole macrocycle (55) with Cu(II):

Spectrophotometric titrations were performed in methanol at 25 °C in a 1 cm^3 quartz cuvette. The spectrophotometer (Cary 60, Agilent) was set to 0.0 absorbance from 300 to 1000 nm using methanol as a blank. A volume of 250 μL of **55** (6 mM) was diluted with 750 μL methanol to make a final concentration of 1.5 mM, and the absorbance of the sample between 300 nm and 1000 nm was recorded. The Cu(II)-containing samples were prepared in the same manner, except for the inclusion of copper(II) triflate (ranging from 0.25 molar eq to 4 molar eq). All samples were incubated for 2-3 min prior to measurement of the UV–Vis spectra.

UV-Vis titration of the Cu^{2+}-tetraoxazole macrocycle (55) complex with tetrabutylammonium ethoxide

In a final volume of 1 mL, 250 μL of **55** (6 mM) were mixed with 200 μL of the copper(II) triflate stock solution (37.5 mM) and 550 μL methanol to prepare the copper complex (2:1 metal:macrocycle ratio). The mixture was incubated for 5 min, transferred to a cuvette, and the UV-Vis spectrum was recorded as outlined above. Samples containing various concentrations of tetrabutylammonium ethoxide (using a 75 mM stock solution) were prepared following the protocol described above, except for the inclusion of the base. Each sample (final volume of 1

mL) was incubated in the presence of the base for 2-3 min before UV-Vis spectra were recorded at room temperature.

4. References

(1) Wright, W. E.; Tesmer, V. M.; Huffman, K. E.; Levene, S. D.; Shay, J. W. *Genes Dev.* **1997**, *11*, 2801.

(2) Cimino, R. G.; Pascale, E.; Battiloro, E.; Starace, G.; Verna, R.; D'Ambrosio, E. *Nucleic Acids Res.* **2001**, *29*, E35.

(3) Mondello, C.; Scovassi, A. I. *Biochem. Cell Biol.* **2004**, *82*, 498.

(4) d'Adda di Fagagna, F.; Reaper, P. M.; Clay, F. L.; Fiegler, H.; Carr, P.; Von, Z. T.; Saretzki, G.; Carter, N. P.; Jackson, S. P. *Nature* **2003**, *426*, 194.

(5) Kypr, J.; Kejnovska, I.; Renciuk, D.; Vorlickova, M. *Nucleic Acids Res.* **2009**, *37*, 1713.

(6) Bochman, M. L.; Paeschke, K.; Zakian, V. A. *Nat. Rev. Genet.* **2012**, *13*, 770.

(7) Bang, I. *Biochem. Z.* **1910**, *6*, 293.

(8) Gellert, M.; Lipsett, M. N.; Davies, D. R. *Proc. Natl. Acad. Sci. U.S.A.* **1962**, *48*, 2013.

(9) Maizels, N. *Ann. N.Y. Acad. Sci.* **2012**, *1267*, 53.

(10) Gonzalez, V.; Hurley, L. H. *Annu. Rev. Pharmacol. Toxicol.* **2010**, *50*, 111.

(11) Bidzinska. J.; Cimino-Reale. G.; Zaffaroni, N.; Folini, M. *Molecules* **2013**, *18*, 12368.

(12) Huppert, J. L. *FEBS J.* **2010**, 277, 3452.

(13) Williamson, J. R.; Raghuraman, M. K.; Cech, T. R. *Cell* **1989**, *59*, 871.

(14) Huppert, J. L. *Biochimie* **2008**, *90*, 1140.

(15) Greider, C. W.; Blackburn, E. H. *Cell* **1987**, *51*, 887.

(16) Counter, C. M.; Hirte, H. W.; Bacchetti, S.; Harley, C. B. *Proc. Natl. Acad. Sci. U.S.A.* **1994**, *91*, 2900.

(17) Nilsson, P.; Mehle, C.; Remes, K.; Roos, G. *Oncogene* **1994**, *9*, 3043.

(18) Masutomi, K.; Possemato, R.; Wong, J. M.; Currier, J. L.; Tothova, Z.; Manola, J. B.; Ganesan, S.; Lansdorp, P. M.; Collins, K.; Hahn, W. C. *Proc. Natl. Acad. Sci. U.S.A.* **2005**, *102*, 8222.

(19) DePinho, R. A.; Polyak, K. *Nat. Genet*. **2004**, *36*, 932.

(20) Meyerson, M. *J. Clin. Oncol*. **2000**, *18*, 2626.

(21) Shay, J. W.; Zou; Y.; Hiyama, E.; Wright, W. E. *Hum. Mol. Genet*. **2001**, *10*, 677.

(22) Neidle, S. *FEBS J*. **2010**, *277*, 1118.

(23) Oganesian, L.; Karlseder, J. *J. Cell Sci*. **2009**, *122*, 4013.

(24) De Cian, A.; Lacroix, L.; Douarre, C.; Temime-Smaali, N.; Trentesaux, C.; Riou, J.-F.; Mergny, J.-L. *Biochimie* **2008**, *90*, 131.

(25) Nielsen, M. C.; Ulven, T. *Curr. Med. Chem*. **2010**, *17*, 3438.

(26) Chung, W. J.; Heddi, B.; Tera, M.; Iida, K.; Nagasawa, K.; Phan, A. T. *J. Am. Chem. Soc*. **2013**, *135*, 13495.

(27) Kim, M. Y.; Vankayalapati, H.; Shin-Ya, K.; Wierzba, K.; Hurley, L. H. *J. Am. Chem. Soc*. **2002**, *124*, 2098.

(28) Monchaud, D.; Teulade-Fichou, M. P. *Org. Biomol. Chem.* **2008**, *6*, 627.

(29) Osawa, T.; Namiki, M. *Tetrahedron Lett*. **1983**, *24*, 4719.

(30) You, S. L.; Kelly, J. W. *Tetrahedron* **2005**, *61*, 241.

(31) Chattopadhyay, S. K.; Biswas, S.; Ghosh, S. K. *Synthesis*. **2008**, *7*, 1029.

(32) Shin-Ya, K.; Wierzba, K.; Matsuo, K.; Ohtani, T.; Yamada, Y.; Furihata, K.; Hayakawa, Y.; Seto, H. *J. Am. Chem. Soc.* **2001**, *123*, 1262.

(33) Rosu, F.; Gabelica, V.; Shin-Ya, K.; De Pauw, E. *Chem. Commun.* **2003**, 2702.

(34) Rezler, E. M.; Seenisamy, J.; Bashyam, S.; Kim, M. Y.; White, E.; Wilson, W. D.; Hurley, L. H. *J. Am. Chem. Soc.* **2005**, *127*, 9439.

(35) Shirude, P. S.; Gillies, E. R.; Ladame, S.; Godde, F.; Shin-Ya, K.; Huc, I.; Balasubramanian, S. *J. Am. Chem. Soc*, **2007**, *129*, 11890.

(36) Tsai, Y. C.; Qi, H.; Lin, C. P.; Lin, R. K.; Kerrigan, J. E.; Rzuczek, S. G.; LaVoie, E. J.; Rice, J. E.; Pilch, D. S.; Lyu, Y. L.; Liu, L. F. *J. Biol. Chem.* **2009**, *284*, 22535.

(37) Linder, J.; Garner, T. P.; Williams, H. E.; Searle, M. S.; Moody, C. J. *J. Am. Chem. Soc.* **2011**, *133*, 1044.

(38) Zahler, A. M.; James R. W.; Thomas, R. C.; David, M. P. *Nature* **1991**, *350*, 718.

(39) Tauchi, T.; Shin-Ya, K.; Sashida, G.; Sumi, M.; Okabe, S.; Ohyashiki, J. H.; Ohyashiki, K. *Oncogene* **2006**, *25*, 5719.

(40) Tahara, H.; Shin-Ya, K.; Seimiya, H.; Yamada, H.; Tsuruo, T.; Ide, T. *Oncogene* **2005**, *25*, 1955.

(41) Nakajima, A.; Tauchi, T.; Sashida, G.; Sumi, M.; Abe, K.; Yamamoto, K.; Ohyashiki, J. H.; Ohyashiki, K. *Leukemia* **2003**, *17*, 560.

(42) Smogorzewska, A.; Van Steensel, B.; Bianchi, A.; Oelmann, S.; Schaefer, M. R.; Schnapp, G.; de Lange, T. *Mol. Cell. Biol.* **2000**, *20*, 1659.

(43) Mu-Yong, K.; Gleason-Guzman, M.; Izbicka, H.; Nishioka, D.; Hurley, H. L. *Cancer Res.* **2003**, *63*, 3247.

(44) Rzuczek, S. G.; Pilch, D. S.; LaVoie, E. J.; Rice, J. E. *Bioorg. Med. Chem. Lett.* **2008**, *18*, 913.

(45) Monchaud, D.; Granzhan, A.; Saettel, N.; Guédin A, Mergny JL, Teulade-Fichou MP.. *J. Nucleic Acids*. **2010**, *2010*, 19.

(46) Seto, H.; Shin-Ya, K.; Wierzba, K. Substance gm-95, process for producing the same and utilization thereof. Patent WO2000024747 A1, May 4, **2000**.

(47) Boyer, S.; Dumas, J.; Phillips, B.; Scott, W. J.; Smith, R. A.; Chen, J.; James, B.; Wang, G. 2-oxo-1,3,5-perhydrotriazapine derivatives useful in the treatment of hyper-proliferative, angiogenesis, and inflammatrory disorders. Patent WO 2004078746 A3, Sept. 16, **2004**.

(48) Marson, C. M.; Saadi, M. *Org. Biomol. Chem*. **2006**, *4*, 3892.

(49) Chattopadhyay, S. K.; Biswas, S.; Pal, B. K. *Synthesis*. **2006**, 1289.

(50) Araki, H.; Katoh, T.; Inoue, M. *Tetrahedron Lett*. **2007**, *48*, 3713.

(51) Shozo, Y.; Kazuhiko, S.; Shigeo, O.; Tetsuji, A. Method of preparing a substance gm-95 Patent . WO2002048153 A1, Dec 12, **2000**.

(52) Doi, T.; Yoshida, M.; Shin-Ya, K.; Takahashi, T. *Org. Lett.* **2006**, *8*, 4165.

(53) Shibata, K.; Yoshida, M.; Takahashi, T.; Takagi, M.; Shin-Ya, K.; Doi, T. *Bull. Chem. Soc. Jpn.* **2013**, *86*, 1453.

(54) Doi, T.; Kazuaki, S.; Masahito, Y.; Motoki, T.; Masayuki, T.; Kazuo, N.; Shin-Ya, K.; Takashi, T. *Org. Biomol. Chem.* **2011**, *9*, 387.

(55) Pilch, D. S.; Barbieri, C. M.; Rzuczek, S. G.; Lavoie, E. J.; Rice, J. E. *Biochimie* **2008**, *90*, 1233.

(56) Iida, K.; Nagasawa, K. *Chem. Rec*. **2013**, *13*, 539.

(57) Iida, K.; Tera, M.; Hirokawa, T.; Shin-ya, K.; Nagasawa, K. J. *Nucleic Acids* **2010**Minhas, G. S.

(58) Tera, M.; Ishizuka, H.; Takagi, M.; Suganuma, M.; Shin-Ya, K.; Kazuo, N. *Angew. Chem., Int. Ed.* **2008**, *47*, 5557.

(59) Han, H.; Hurley, L. H. *Trends Pharmacol. Sci*. **2000**, *21*, 136.

(60) Helder, M. N.; Wisman, G. B.; Van der Zee, G. J. *Cancer Invest*. **2002**, *20*, 82.

(61) Minhas, G. S.; Pilch, D. S.; Kerrigan, J. E.; LaVoie, E. J.; Rice, J. E. *Bioorg. Med. Chem. Lett.* **2006**, *16*, 3891.

(62) Barbieri, C. M.; Srinivasan, A. R.; Rzuczek, S. G.; Rice, J. E.; LaVoie, E. J.; Pilch, D. S. *Nucleic Acids Res*. **2007**, *35*, 3272.

(63) Satyanarayana, M.; Rzuczek, S. G.; LaVoie, E. J.; Pilch, D. S.; Liu, A.; Liu, L. F.; Rice, J. E. *Bioorg. Med. Chem. Lett.* **2008**, *18*, 3802.

(64) Tera, M.; Sohtome, Y.; Ishizuka, H.; Doi, T.; Takagi, M.; Shin-Ya, K.; Nagasawa, K. *Heterocycles* **2006**, *69*,505.

(65) Iida, K.; Tera, M.; Hirokawa, T.; Shin-Ya, K.; Nagasawa, K. *Chem. Commun.* **2009**, *42*, 6481.

(66) Iida, K.; Majima, S.; Nakamura, T.; Seimiya, H.; Nagasawa, K. *Molecules* **2013**, *18*, 4328.

(67) Satyanarayana, M.; Kim. Y. A.; Rzuczek, S.G.; Pilch, D. S.; Liu, A. A.; Liu, L. F.; Rice, J. E.; LaVoie, E. J. *Bioorg. Med. Chem. Lett.* **2010**, *20*, 3150.

(68) Majima, S.; Tera, M.; Iida, K,; Shin-Ya, K.; Nagasawa, K. *Heterocycles* **2010**, *82*, 1345.

(69) Tera, M.; Iida, K.; Ishizuka, H.; Takagi, M.; Suganuma, M.; Doi, T.; Shin-Ya, K.; Nagasawa, K. *ChemBioChem*. **2009**, *10*, 431.

(70) Tera, M.; Iida, K.; Ikebukuro, K.; Seimiya, H.; Shin-Ya, K.; Nagasawa, K. *Org. Biomol. Chem.* **2010**, *8*, 2749.

(71) Deeley, J.; Bertram, A.; Pattenden, G. *Org. Biomol. Chem.* **2008**, *6*, 1994.

(72) Lewis, J. R. *Nat. Prod. Rep.* **1993**, *10*, 29.

(73) Lewis, J. R. *Nat. Prod. Rep*. **2000**, *17*, 57.

(74) Smith, M. *Annu. Rev. Genet.* **1985**, *19*, 423.

(75) Carter, P. *Biochem. J.* **1986**, *237*, 1.

(76) Fittig, R.; Hantzsch, A. *Ber. Dtsch. Chem. Ges.* **1888**, 21, 3189.

(77) Metzger, J. V. *The Chemistry of Heterocyclic Compounds, Thiazole and Its Derivatives;* John Wiley and Sons: Toronto, **2009**; p. 34.

(78) Turchi, I. J. Oxazoles. In *Chemistry of Heterocyclic Compounds: Oxazoles*; Turchi, I. J. , Ed.; John Wiley and Sons: Toronto, **1986**; Vol. 45, p. 1.

(79) Turchi, I. J. *Ind. Eng. Chem. Res. Dev.* **1981**, *20*, 32.

(80) Turchi, I. J.; Dewar, M.J.S. *Chem. Rev.* **1975**, *75*, 389.

(81) Vorbrüggen, H.; Krolikiewicz K. *Tetrahedron* **1993**, *49*, 9353.

(82) Galéotti, N.; Montagne, C; Poncet, J.; Jouin, P. *Tetrahedron Lett*. **1992**, *33*, 2807.

(83) Misra, R. N.; Brown, B. R.; Sher, P. M.; Patel, M. M.; Hall, S. E.; Han, W. C.; Barrish, J. C.; Kocy, O.; Harris, D. N.; Goldenberg, H. J.; Michel, I. M.; Schumacher,W. A.; Webb, M. L.; Monshizadegan, H.; Ogletree, M. L. *J. Med. Chem.* **1993**, *36*, 1401.

(84) Atkins, G. M, Jr.; Burgess, E. M. *J. Am. Chem. Soc*. **1968**, *90*, 4744.

(85) Lafargue, P.; Guenot, P.; Lellouche, J.-P. *Synlett.* **1995**, *2*, 171.

(86) Lafargue, P.; Guenot, P.; Lellouche, J.-P. *Heterocycles* **1995**, *41*, 947.

(87) Phillips, A. J.; Uto, Y.; Wipf, P.; Reno, M. J.,Williams, D.R. *Org. Lett.* **2000**, *2*, 1165.

(88) Wipf, P.; Miller, C. P. *Tetrahedron Lett*. **1992**Meyers, A. I..

(89) Khapli, S.; Dey, S.; Mal, D. *J. Indian Institute Sci*. **2001**, *81*, 461.

(90) Freeman, D. J.; Pattenden, G. *Tetrahedron Lett*. **1998**, *39*, 3251.

(91) Pankiewicz, K. W.; Watanabe, K. A. *J. Fluorine. Chem.* **1993**, *64*, 15.

(92) Baptista, L.; Bauerfeldt, G. F.; Arbilla, G.; Silva, E. C. *J. Mol. Struct.: THEOCHEM* **2006**, 761, 73.

(93) Furuya, T.; Kuttruff, C. A.; Ritter, T. *Curr. Opin. Drug Discovery Dev.* **2008**, *11*, 803.

(94) Evans, D. L.; Minster, D. K.; Jordis, U.; Hecht, S. M.; Mazzu, A. L., Jr.; Meyers, A. I. *J. Org. Chem.* **1979**, *44*, 497.

(95) Meyers, A. I.; Tavares, F. *Tetrahedron Lett.* **1994**, *35*, 2481.

(96) Mink, D.; Mecozzi, S.; Rebek, J., Jr. *Tetrahedron Lett.* **1998**, *39*, 5709.

(97) Meyers, A. I.; Tavares, F. X. *J Org Chem.* **1996**, *61*, 8207.

(98) Williams, D. R.; Lowder,P. D.; Gu, Y.-G.; Brooks, D. A. *Tetrahedron Lett.* **1997**, *38*, 331.

(99) Wipf, P.; Uto, Y. *Tetrahedron Lett.* **1999**, *40*, 5165.

(100) Williams, D. R.; Brooks, D. A.; Berliner, M. A. *J. Am. Chem. Soc.* **1999**, *121*, 4924.

(101) Liskamp, R. M. J.; Rijkers, D. T. S.; Bakker, S. E. Bioactive Macrocyclic Peptide Mimics. In *Modern Supramolecular Chemistry: Strategies for Macrocycle Synthesis;* Diederich, F., Stang, P. J., Tykwinski, R. R., Eds.; Wiley-VCH: Weinheim; Germany. **2008**; p 1- 27.

(102) White, C. J.; Yudin, A. K. *Nat. Chem.* **2011**, *3*, 509.

(103) Tamilarasu, N.; Huq, I.; Rana, T. M. *Bioorg. Med. Chem. Lett*. **2000**, *10*, 971.

(104) Vig, B. S.; Murray, T. F.; Aldrich, J. V. *Biopolymers* **2003**, *71*, 620.

(105) Vig, B. S.; Murray, T. F.; Aldrich, J. V. *J. Med. Chem.* **2003**, *46*, 1279.

(106) Chan, W. C.; Coyle, B. J.; Williams, P. *J. Med. Chem*. **2004**, *47*, 4633.

(107) Yu, S.; Pan, X.; Lin, X.; Ma, D. *Angew. Chem., Int. Ed.* **2005**, *44*, 135.

(108) Hara, S.; Makino, K.; Hamada, Y. *Tetrahedron Lett*. **2006**, *47*, 1081.

(109) Demmer, O.; Frank, A. O.; Kessler, H. Design of Cyclic Peptides. In *Peptide and Protein Design for Biopharmaceutical Applications;* Jensen, K., Ed.; .; Wiley-VCH: New York. **2009**; p 133- 135.

(110) Haberhauer, G.; Drosdow, E.; Oeser, T.; Rominger, F.; *Tetrahedron* **2008**, *64*, 1853.

(111) Pintér, A.; Haberhauer, G. *Tetrahedron* **2009**, *65*, 2217.

(112) Haberhauer, G.; Pintér, A.; Oeser, T.; Rominger, F. *Eur. J. Org. Chem.* **2007**, 1779.

(113) Ishida, T.; In, Y.; Shinozaki, F.; Doi, M.; Yamamoto, D.; Hamada, Y.; Shioiri, T.; Kamigauchi, M.; Sugiura, M. *J. Org. Chem*. **1995**, *60*, 3944.

(114) Ishida, T.; Tanaka, M.; Nabae, M.; Inoue, M.; Kato, S.; Hamada, Y. Shioiri, T. *J. Org. Chem*. **1988**, *53*, 107.

(115) (a) Ishida, T.; In, Y.; Doi, M.; Inoue, M.; Hamada, Y.; Shioiri, T. *Biopolymers* **1992**, *32*, 131; (b) In, Y.; Doi, M.; Inoue, M.; Ishida, T. *Acta Crystallogr., Sect. C: Cryst. Struct. Comm*. **1994**, *C50*, 2015; (c) Ishida, T.; Inoue, M.; Hamada, Y.; Kato, S.; Shioiri, T. *J. Chem. Soc., Chem. Commun*. **1987**, 370; (d) Shinozaki, F.; In, Y.; Doi, M.; Yamamoto, D.; Kamigauchi, M.; Sugiura, M.; Ishida, T.; Hamada, Y.; Shioiri, T. *Pept. Chem*. **1996**, *60* 405.

(116) (a) In, Y.; Doi, M.; Inoue, M.; Ishida, T.; Hamada, Y.; Shioiri, T. *Chem. Pharm. Bull*. **1993**, *41*, 1686; (b) In, Y.; Doi, M.; Inoue, M.; Ishida, T.; Hamada, Y.; Shioiri, T. *Acta Crystallogr., Sec. C: Cryst. Struct. Comm*. **1994**, C50, 432.

(117) (a) Bernhardt, P. V.; Comba, P.; Fairlie, D. P.; Gahan, L. R.; Hanson, G. R.; Lötzbeyer, L. *Chem. - Eur. J*. **2002**, *8*, 1527; (b) Van den Brenk, A. L.; Tyndall, J. D. A.; Cusack, R. M.; Jones, A.; Fairlie, D. P.; Gahan, L. R.; Hanson, G. R. *J. Inorg. Biochem*. **2004**, *98*, 1857; (c) Comba, P.; Gahan, L. R.; Haberhauer, G.; Hanson, G. R.; Noble, C. J.; Seibold, B.; van den Brenk, A. L. *Chem. - Eur. J*. **2008**, *14*, 4393.

(118) Cusack, R. M.; Grøndahl, L.; Abbenante, G.; Fairlie, D. P.; Gahan, L. R.; Hanson, G. R.; Hambley, T. W. *J. Chem. Soc., Perkin Trans*. 2 **2000**, 323.

(119) Van den Brenk, A. L.; Byriel, K. A.; Fairlie, D. P.; Gahan, L. R.; Hanson, G. R.; Hawkins, C. J.; Jones, A.; Kennard, C. H. L.; Moubaraki, B.; Murray, K. S. *Inorg. Chem*. **1994**, *33*, 3549.

(120) Hawkins, C.J. *Pure Appl. Chem*. **1988**, *60*, 1267.

(121) Van den Brenk, A. L.; Hanson, G. R.; Hawkins, C. J. *J. Inorg. Biochem.* **1989**, *36*, 165.

(122) Van den Brenk, A. L.; Fairlie, D. P.; Hanson, G. R.; Gahan, L. R.; Hawkins, C. J.; Jones, A. *Inorg. Chem*. **1994**, *33*, 2280.

(123) Wipf, P.; Miller, C. P. *J. Am. Chem. Soc*. **1992**, *114*, 10975.

(124) Wipf, P.; Venkatraman, S.; Miller, C.P.; Geib, S.J. *Angew. Chem. Int. Ed*. **1994**, 33, 1516

(125) Van den Brenk, A. L. An investigation into the metal complexes of cyclic peptides isolated from the ascidians, *Lissoclinum bistratum* and *Lissoclinum patella*. Ph.D. Thesis, University of Queensland, Australia, **1994**.

(126) Comba, P.; Gahan, L.R.; Haberhauer, G.; Hanson, G.R.; Noble, C.J.; Seibold, B.; van den Brenk, A.L. *Chem. - Eur. J*. **2008**, *14*, 4393.

(127) Comba, P.; Dovalil, N.; Hanson, G. R.; Linti, G. *Inorg. Chem*. **2011**, *50*, 5165.

(128) Morris, L. A.; Milne, B. F.; Thompson, G. S.; Jaspars, M. *J. Chem. Soc., Perkin Trans.* 2 **2002**, 1072.

(129) Comba, P.; Dovalil, N.; Gahan, L. R.; Haberhauer, G.; Hanson, G. R.; Noble, C.J.; Seibold, B.; Vadivelu, P. *Chem. - Eur. J*. **2012**, 18, 2578.

(130) Bartoli, G.; Bosco, M.; Carlone, A.; Locatelli, M.; Marcantoni, E.; Melchirre, P.; Samnria. *Adv. Synth. Catal*. **2006**, *348*, 905.

(131) Benito, J. M.; Christensen, C. A.; Meldal, M. *Org. Lett.* **2005**, *7*, 581.

(132) Xu, S.; Zou, W.; Wu, G.; Song, H.; He, Z. *org. lett.* **2010**, *12*, 3556.

(133) Davis, M. R.; Singh, E. K.; Wahyudi, H.; Alexander, L. D.; Kunicki, J. B.; Nazarova, L. A.; Fairweather, K. A.; Giltrap, A. M.; Jolliffe, K. A.; McAlpine, S. R. *Tetrahedron.* **2012**, *68*, 1029.

(134) Butler, S. J.; Jolliffe, K. A. *Org. Biomol. Chem.* **2011**, *9*, 3471.

(135) Wipf, P.; Miller, C. P. *Tetrahedron Lett.* **1992**, *33*, 6267.

(136) Yonetani, K.; Hirotsu, Y.; Shiba, T. *Bull Chem Soc Jpn.* **1975**, *48*, 3302.

(137) Miller, J. J.; Rajaram, S.; Pfaffenroth, C.; Sigman, M. S. *Tetrahedron.* **2009**, *65*, 3110.

(138) Biron, E.; Chatterjee, J.; Kessler, H. *Org Lett.* **2006**, *8*, 2417.

(139) Fields, G. B. Methods in Molecular. In *Peptide Synthesis Protocols.* Pennington, M. W.; Dunn, B. M., Eds.; Humana Press: Totowa, NJ, **1995**; 35, p 17.

(140) Peña, S.; Scarone, L.; Manta, E.; Stewart, L.; Yardley, V.; Croft, S.; Serra, G. *Bioorg. Med. Chem. Lett.* **2012**, 22, 4994.

(141) Downing, S. V.; Aguilar, E.; Meyers, A. I. *J Org Chem.* **1999**, *64*, 826.

(142) Di Gioia, M. L.; Leggio, A.; Le Pera, A.; Liguori, A.; Perri, F.; Siciliano, C. Eur. J. Org. Chem. 2004, 2004, 4437.

(143) Di Gioia, M. L.; Leggio, A.; Le Pera, A.; Siciliano,C.; Sindona, G. *J Pept Res.* **2004**, *63*, 383.

(144) Pascal, R.; Sola, R. *Tetrahedron Lett.* **1998**, *39*, 5031.

(145) Wipf, P.; Miller, C. P.; Grant, C. M. *Tetrahedron.* **2000**, *56*, 9143.

(146) Wipf, P. *Chem Rev.* **1995**, *95*, 2115.

(147) Somogyi, L.; Haberhauer, G.; Rebek, J. *Tetrahedron.* **2001**, *57*, 1699

(148) Hernández, D.; Vilar, G.; Riego, E.; Canedo, L. M.; Cuevas, C.; Albericio, F.; & Álvarez, M. *Org Lett.* **2007**, *9*, 809.

(149) Chattopadhyay, S. K.; Biswas, S.; Ghosh, S. K. *Synthesis.* **2008**, *7*, 1029.

(150) Han,G.; Tamaki, M. ; Hruby, V. J. *J Pept Res.* **2001**, *58*, 338.

(151) Hernández, D.; Riego, E.; Albericio, F.; Álvarez, M.. *Eur. J. Org. Chem.* **2008**, *2008*, 3389.

(152) Bertram, A.,; Maulucci, N.; New, O. M.; Nor, S. M. M.; Pattenden, G. *Org. Biomol. Chem.* **2007**, *5*, 1541.

(153) (a) Endoh, N., Tsuboi, K., & Kim, R.; Yonezawa,Y.; Shin, C. Heterocycles. **2003**, *60*, 1567, (b) Zhang, Z.; Yuan, G. *Arkivoc.* **2011**, *10*, 360.

(154) Bertram, A.; Pattenden, G. *Heterocycles.* **2002**, *58*, 521.

(155) Xia, Z.; Smith, C. D. *J. Org. Chem.* **2001**, *66*, 3459.

(156) Moasson, G.; Neuville, L.; Bughin, C. Topic in Herterocyclic chemistry. In *Synthesis of heterocycles via multicomponent reactions II*. Romano V. A. Orru; Ruijter, E., Eds.; Springer: Heidelberg, **2010**, *25*, p 2-7.

(157) Hamada, Y.; Shioiri, T. *Chem. Rev.* **2005**, *105*, 4441.

(158) (a) Subirós-Funosas, R.; El-Faham, A.; Albericio, F. *Org. Biomol. Chem.* **2010**, *8*, 3665,

(b) Balasubramanian, S.; Jantos, K.; Ladame, S. Heteroaromatic-based peptide macrocycles as g-quadruplex ligands Patent WO2008009942 A1, Jan 24, **2008**.

(159) Mihara, H.; Yamabe, S.; Niidome, T.; Aoyagi, H.; Kumagai, H. *Tetrahedron Lett.* **1995**, *36*, 4837.

(160) DeGrado, W. F.; Kaiser, E. T. *J. Org. Chem.* **1980**, *45*, 1295.

(161) Paulitz, C.; Steglich, W. *J. Org. Chem.* **1997**, *62*, 8474.

(162) Tao, H.; Peng, L.; Zhang, Q. *ACS Comb. Sci.* **2013**, *15*, 447.

(163) Gisin, B. F.; Merrifield, R. B. *J. Am. Chem. Soc.* **1972**, *94*, 3102.

(164) Lloyd-Williams, P.; Albericio, F.; iralt, E. *Tetrahedron*. **1993**, *49*, 11065.

Appendix -Supporting Spectra for Chapter 2

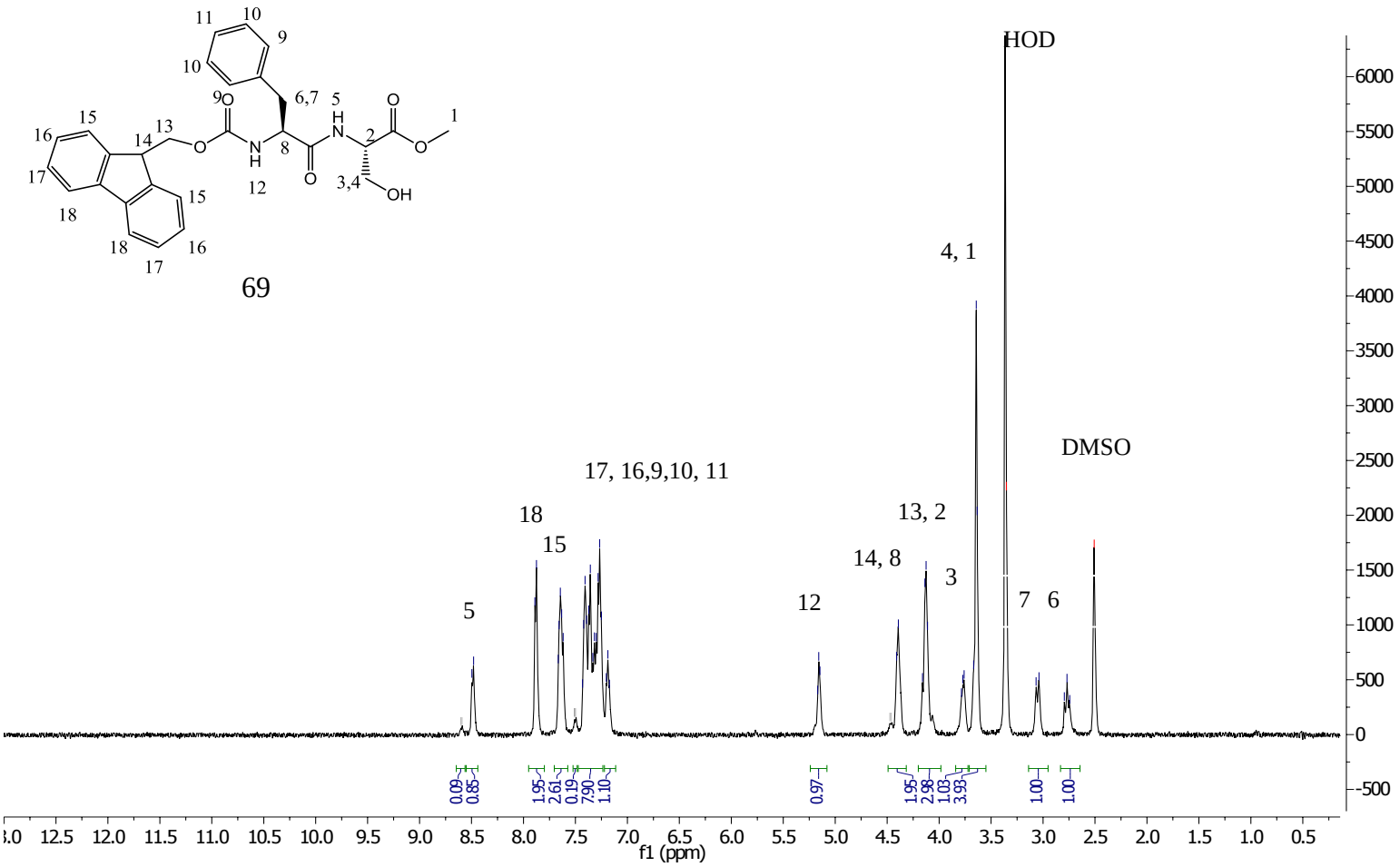

Appendix S 1: ^{1}H NMR Spectrum of *N*-Fmoc-L-Phe-L-Ser-OMe (**69**) in DMSO-d_6

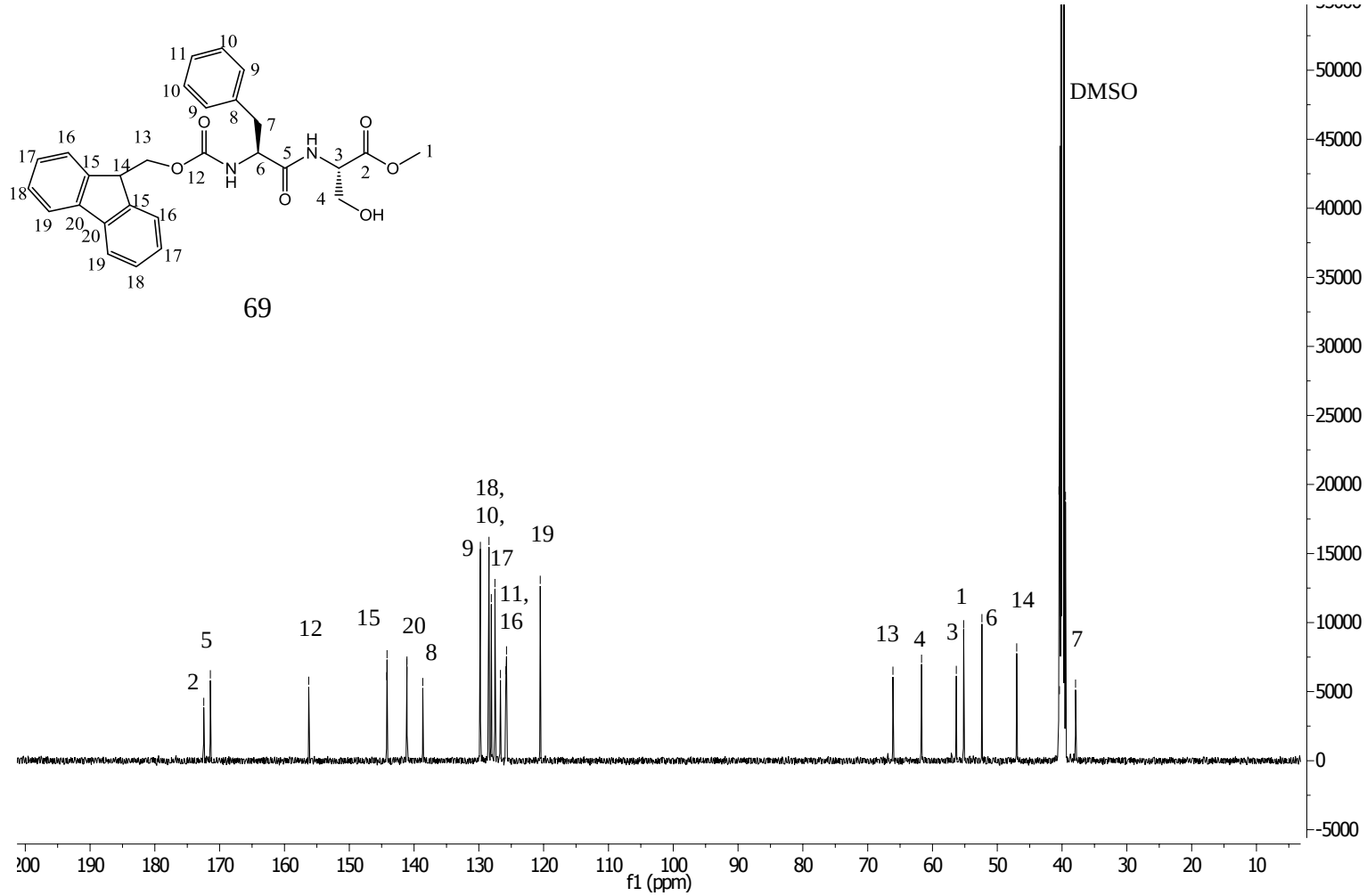

Appendix S 2: ^{13}C NMR Spectrum of *N*-Fmoc-L-Phe-L-Ser-OMe (**69**) in DMSO-d_6 for an enlargement of the 110-160 ppm range see next page)

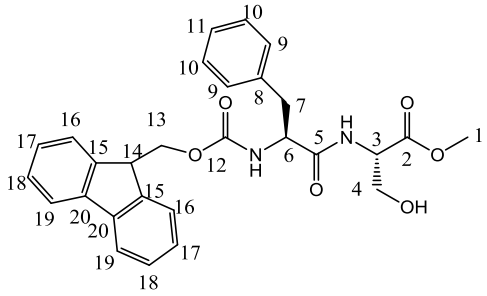

69

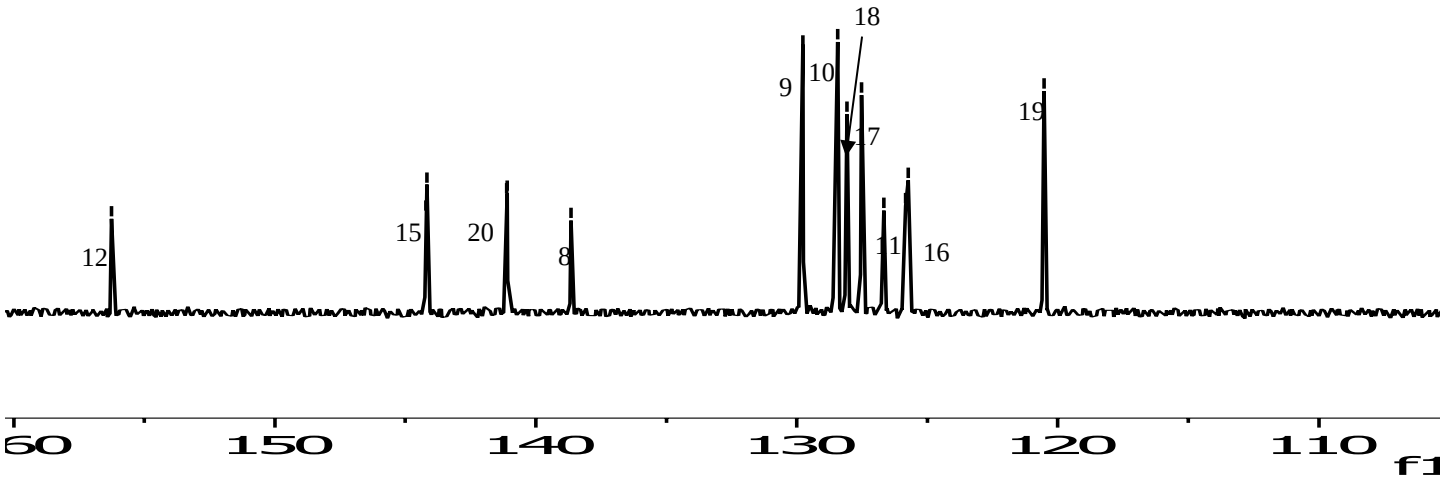

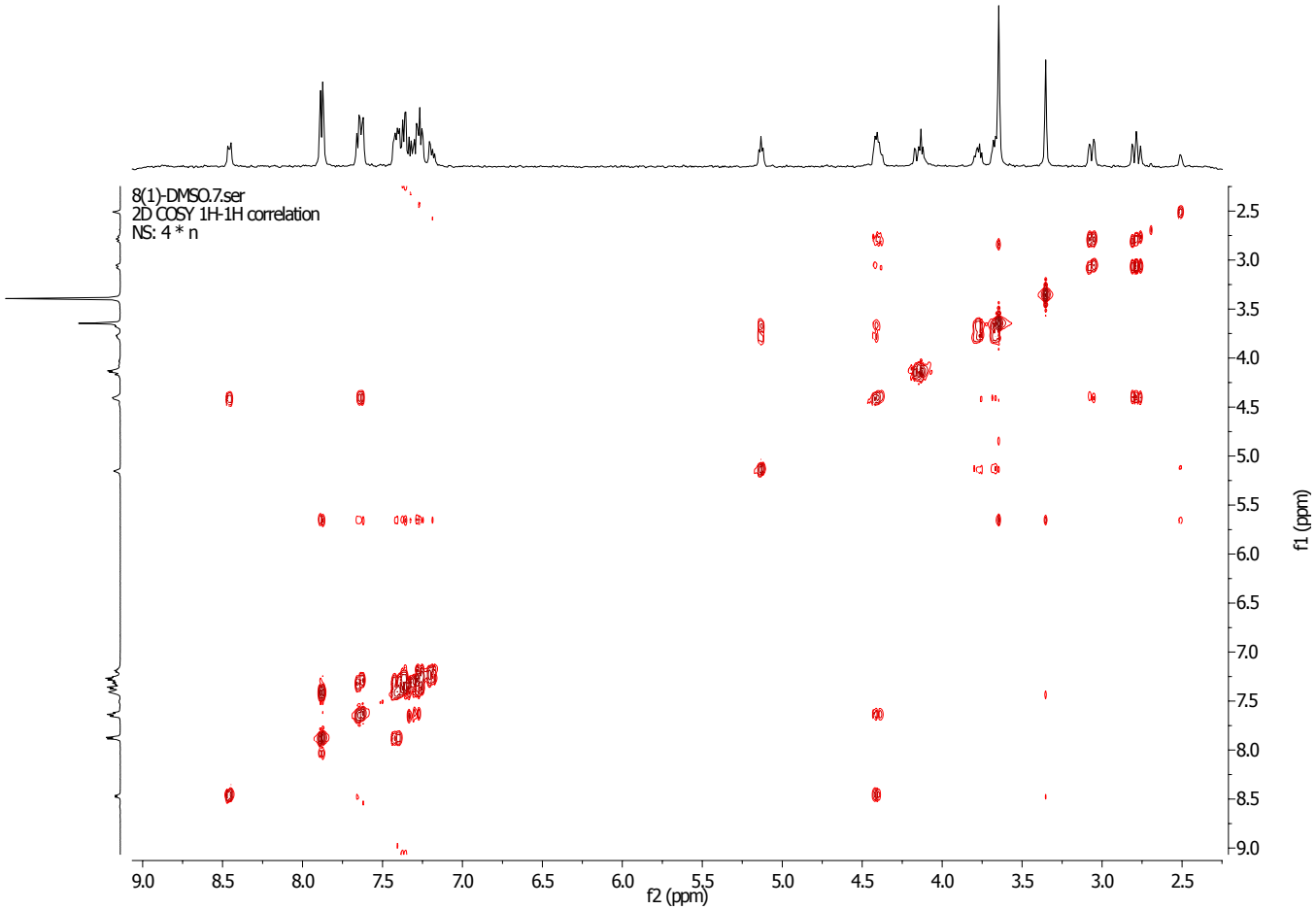

Appendix S 3: COSY NMR Spectrum of *N*-Fmoc-L-Phe-L-Ser-OMe (**69**) in DMSO-d_6

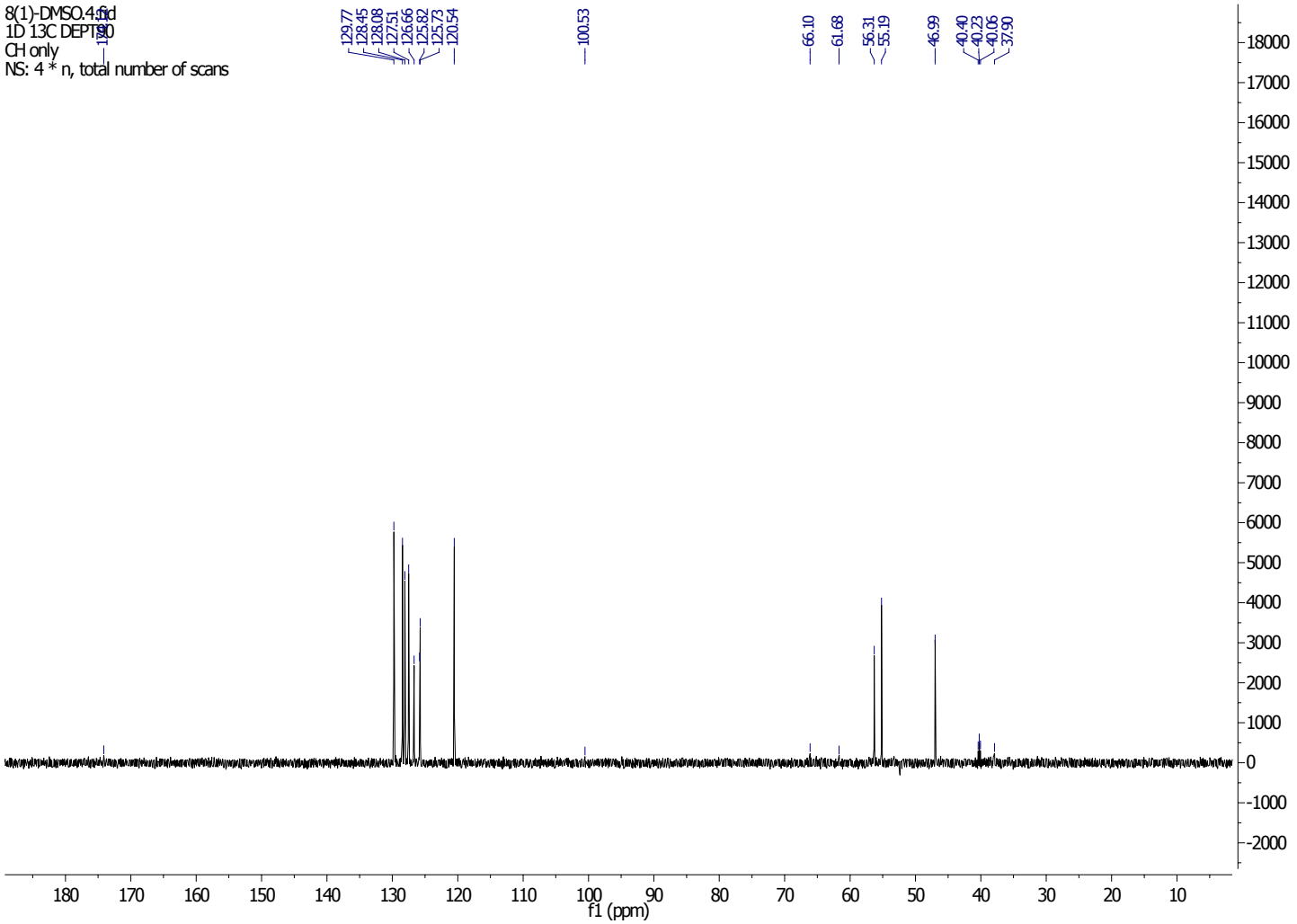

Appendix S 4: DEPT 90 NMR Spectrum of *N*-Fmoc-L-Phe-L-Ser-OMe (**69**) in DMSO-d_6

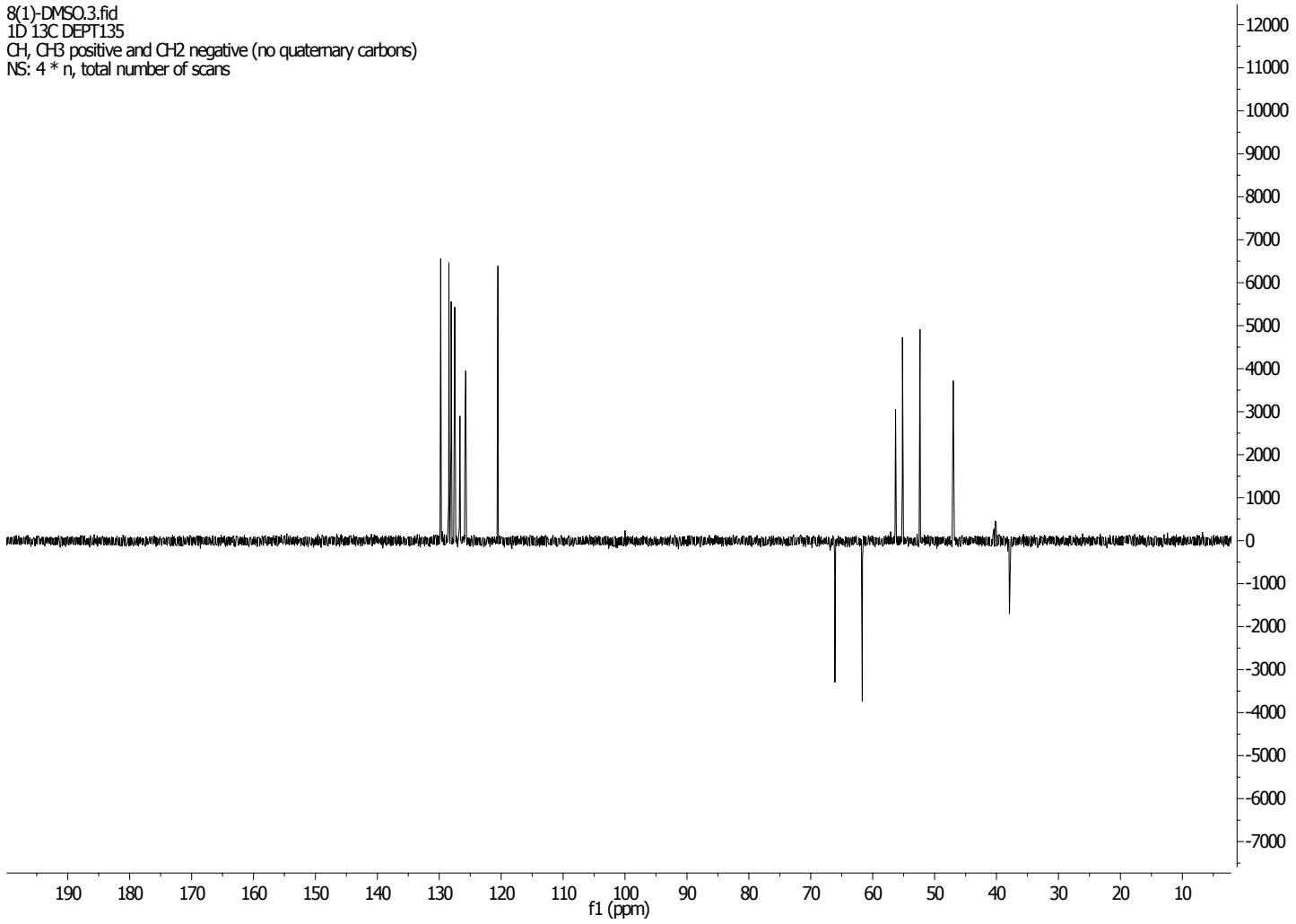

Appendix S 5: DEPT 90 NMR Spectrum of *N*-Fmoc-L-Phe-L-Ser-OMe (**69**) in DMSO-d_6

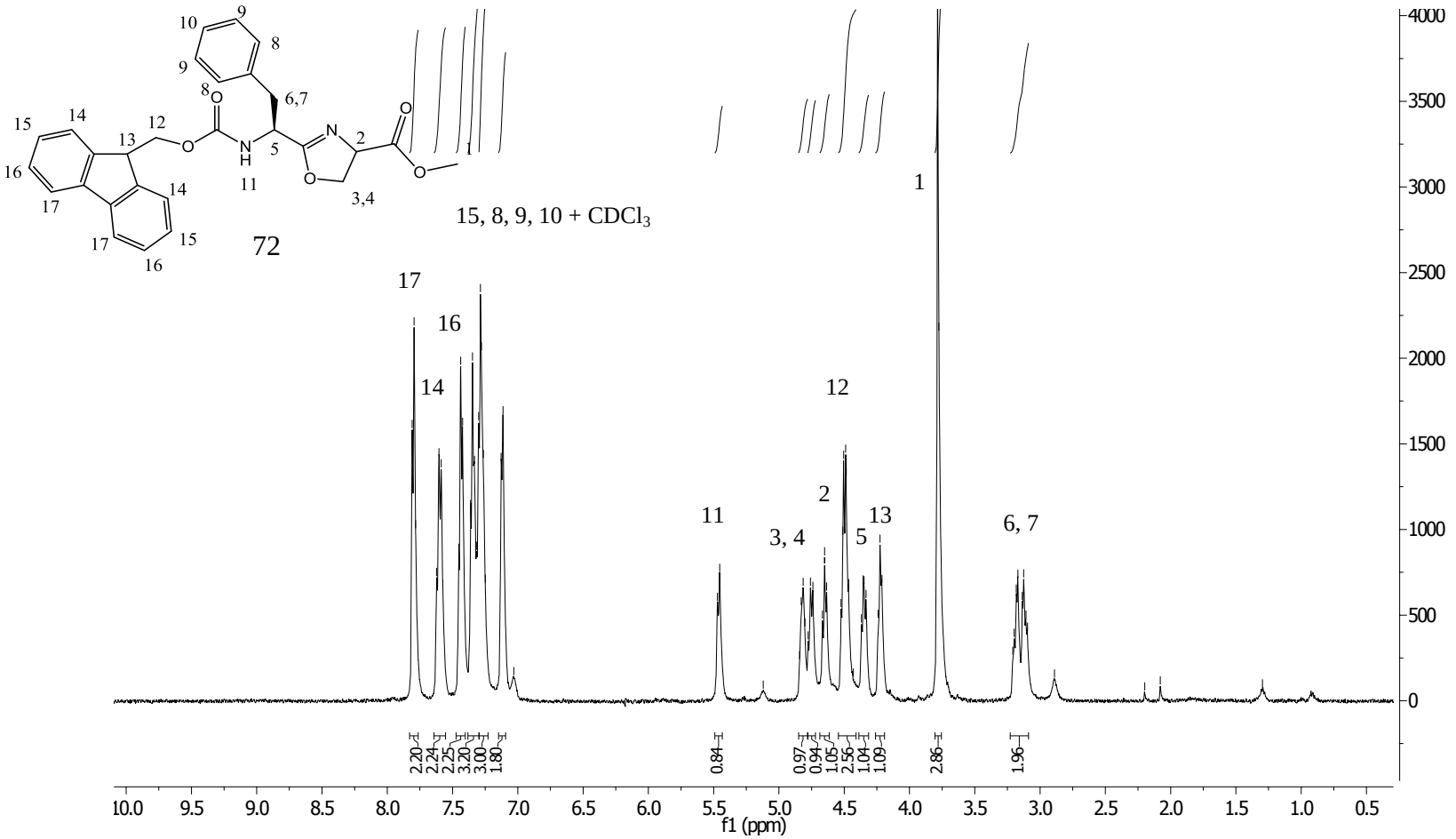

Appendix S 6: ^{1}H NMR Spectrum of *N*-Fmoc-L-Phe-L-Oxazoline-OMe (**72**) in $CDCl_3$

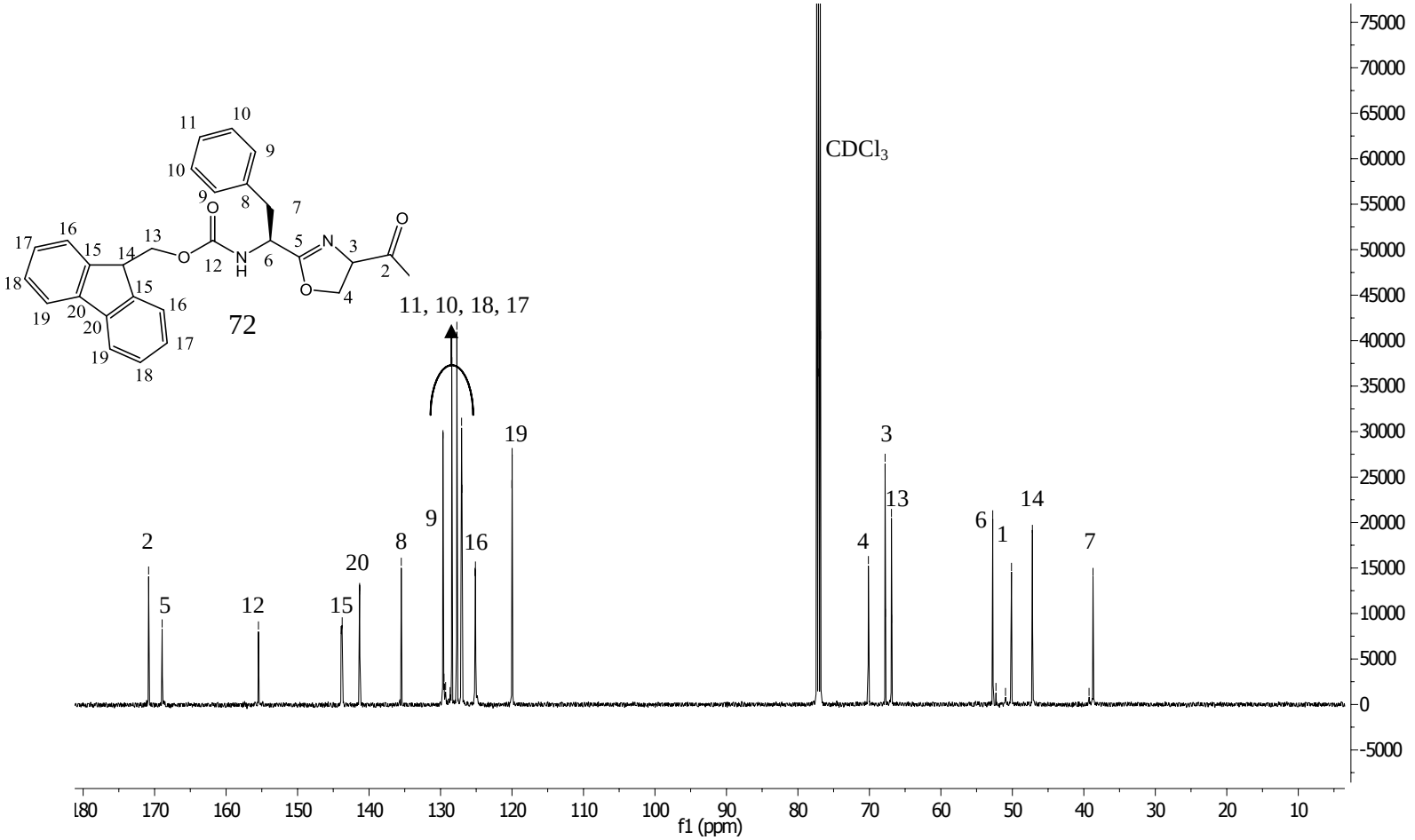

Appendix S 7: ^{13}C NMR Spectrum of *N*-Fmoc-L-Phe-L-Oxazoline-OMe (**72**) in $CDCl_3$

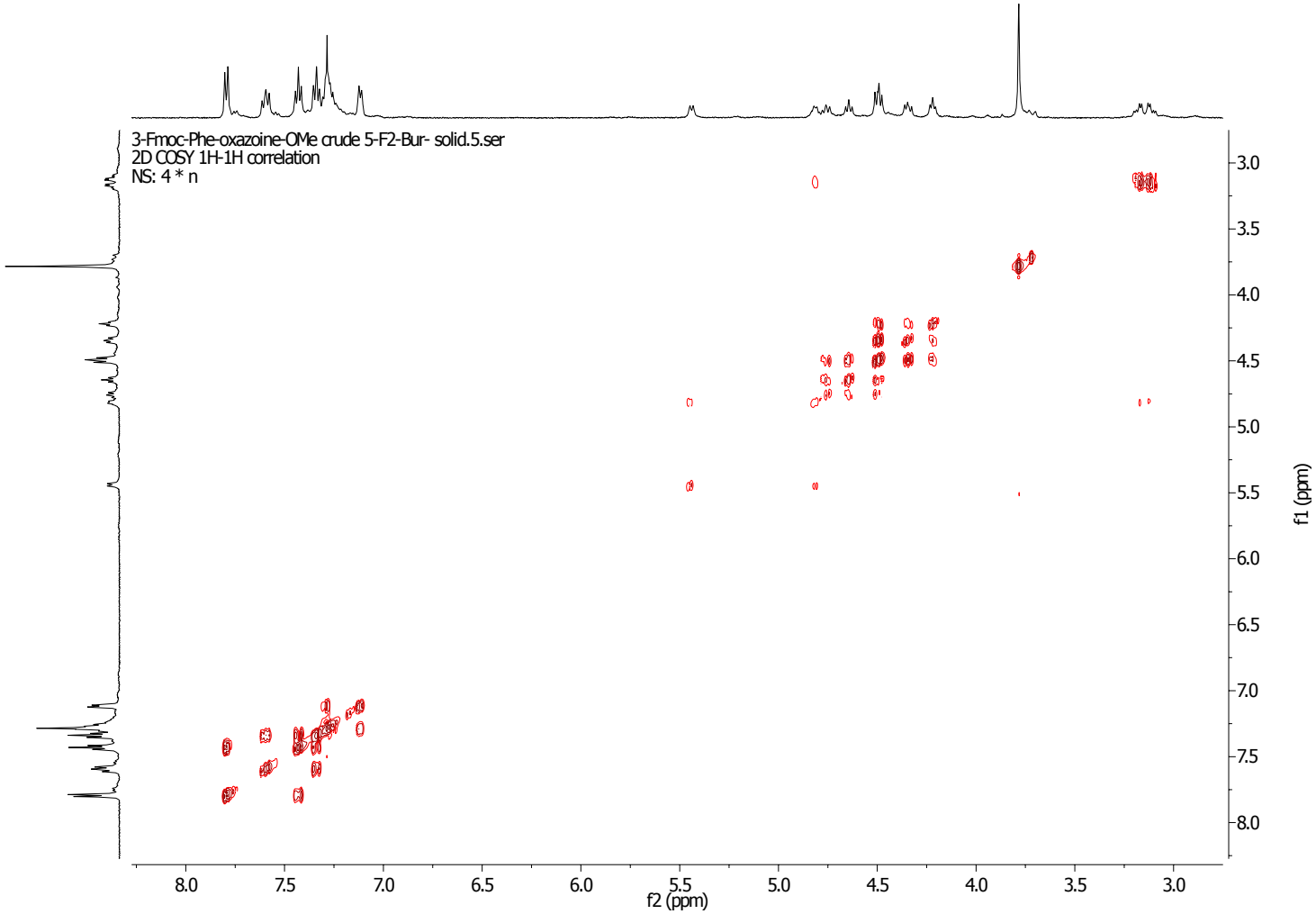

Appendix S 8: COSY NMR Spectrum of *N*-Fmoc-L-Phe-L-Oxazoline-OMe (**72**) in $CDCl_3$

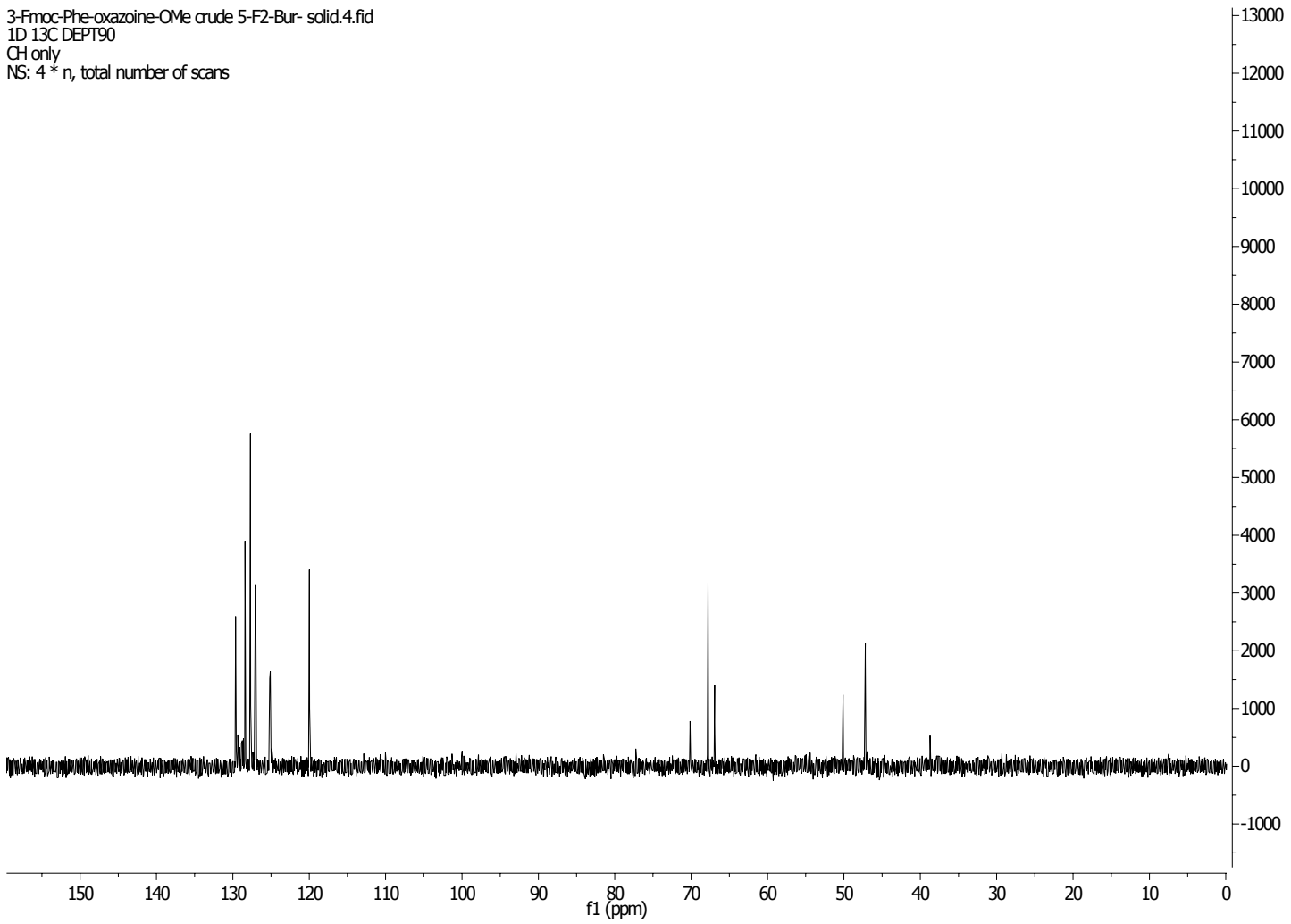

Appendix S 9: DEPT 90 NMR Spectrum of *N*-Fmoc-L-Phe-L-Oxazoline-OMe (**72**) in $CDCl_3$

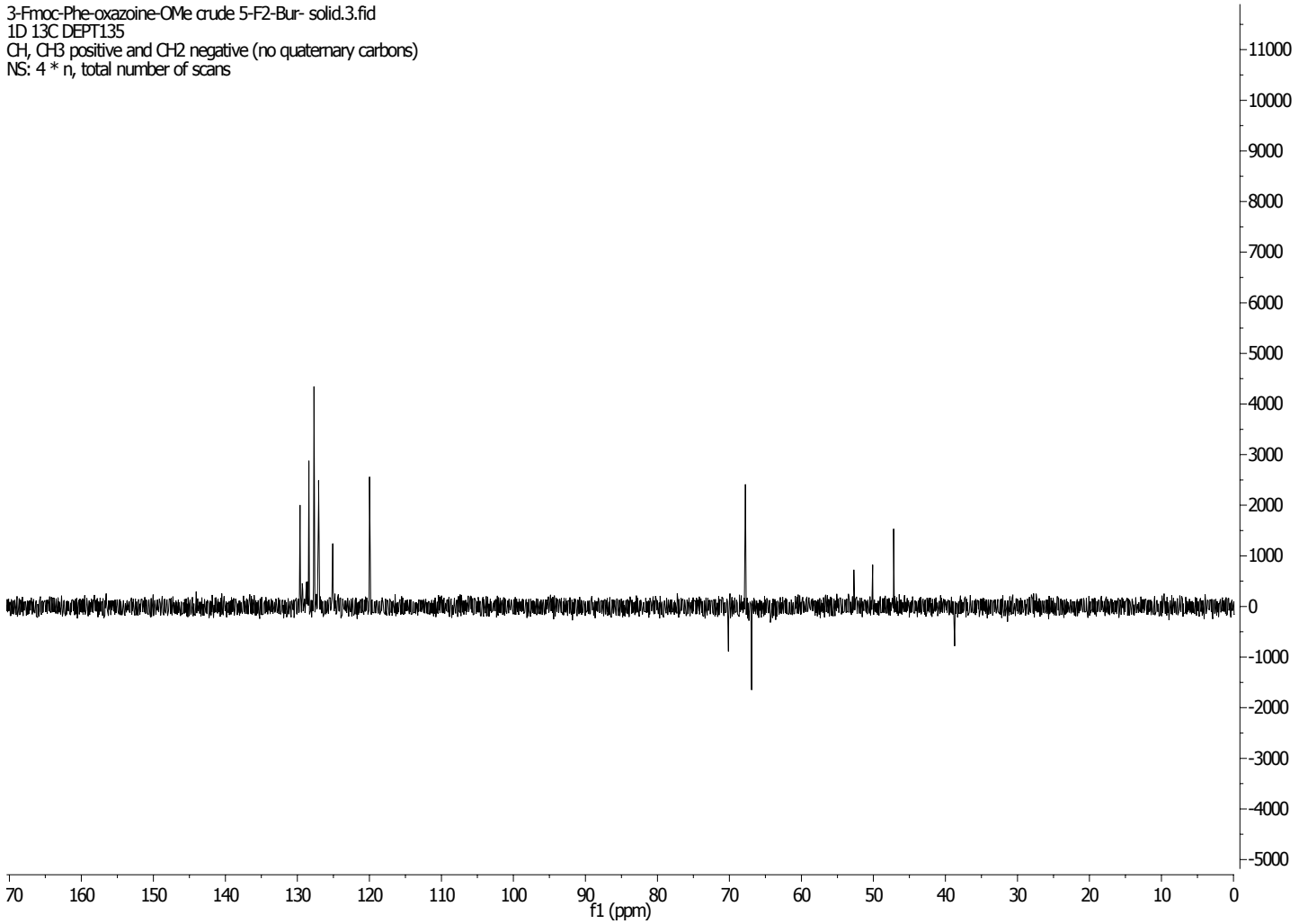

Appendix S 10: DEPT 135 NMR Spectrum of *N*-Fmoc-L-Phe-L-Oxazoline-OMe (**72**) in $CDCl_3$

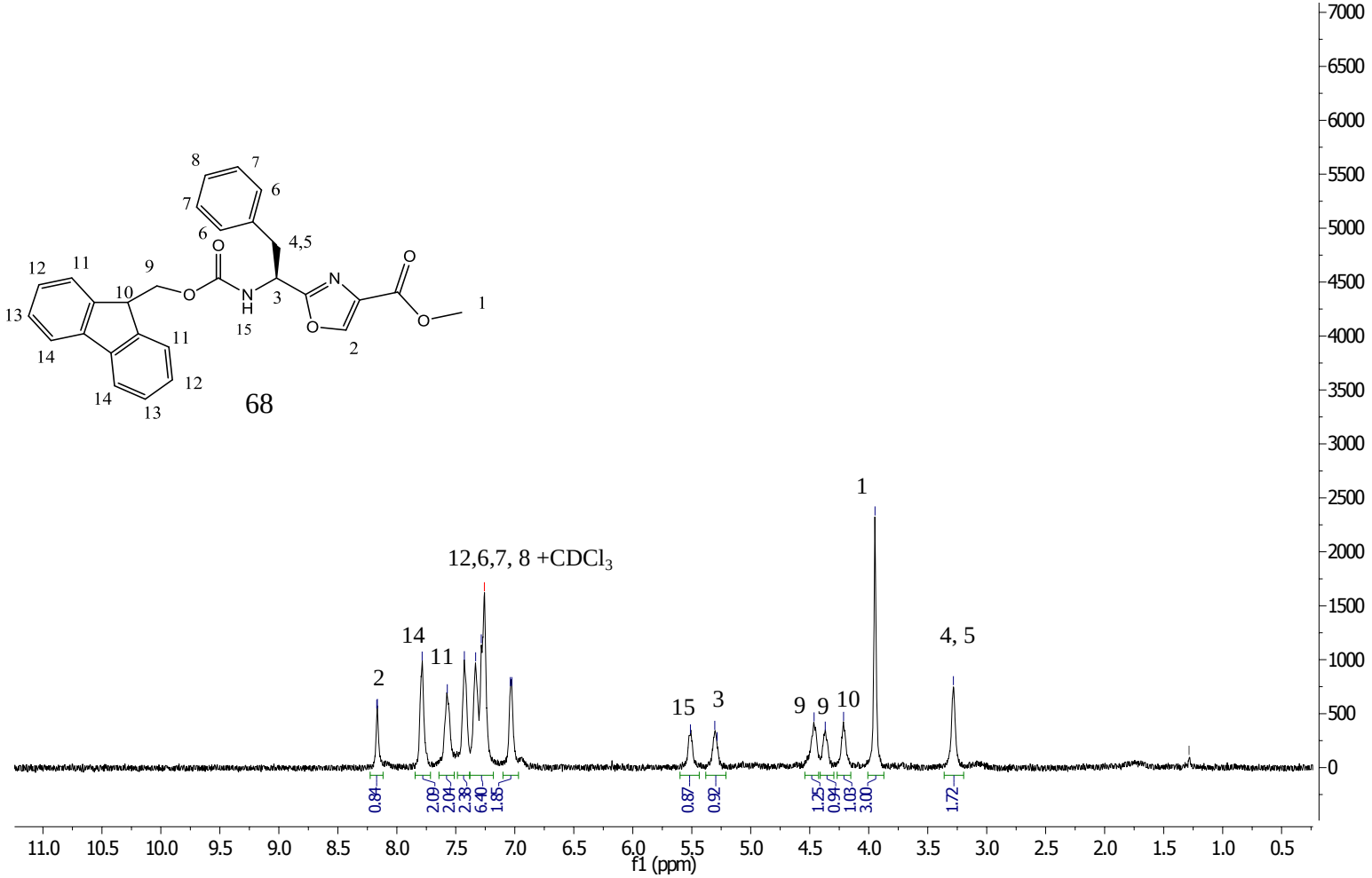

Appendix S 11: ^{1}H NMR Spectrum of *N*-Fmoc-L-Phe-L-Oxazole-OMe (**68**) in $CDCl_3$

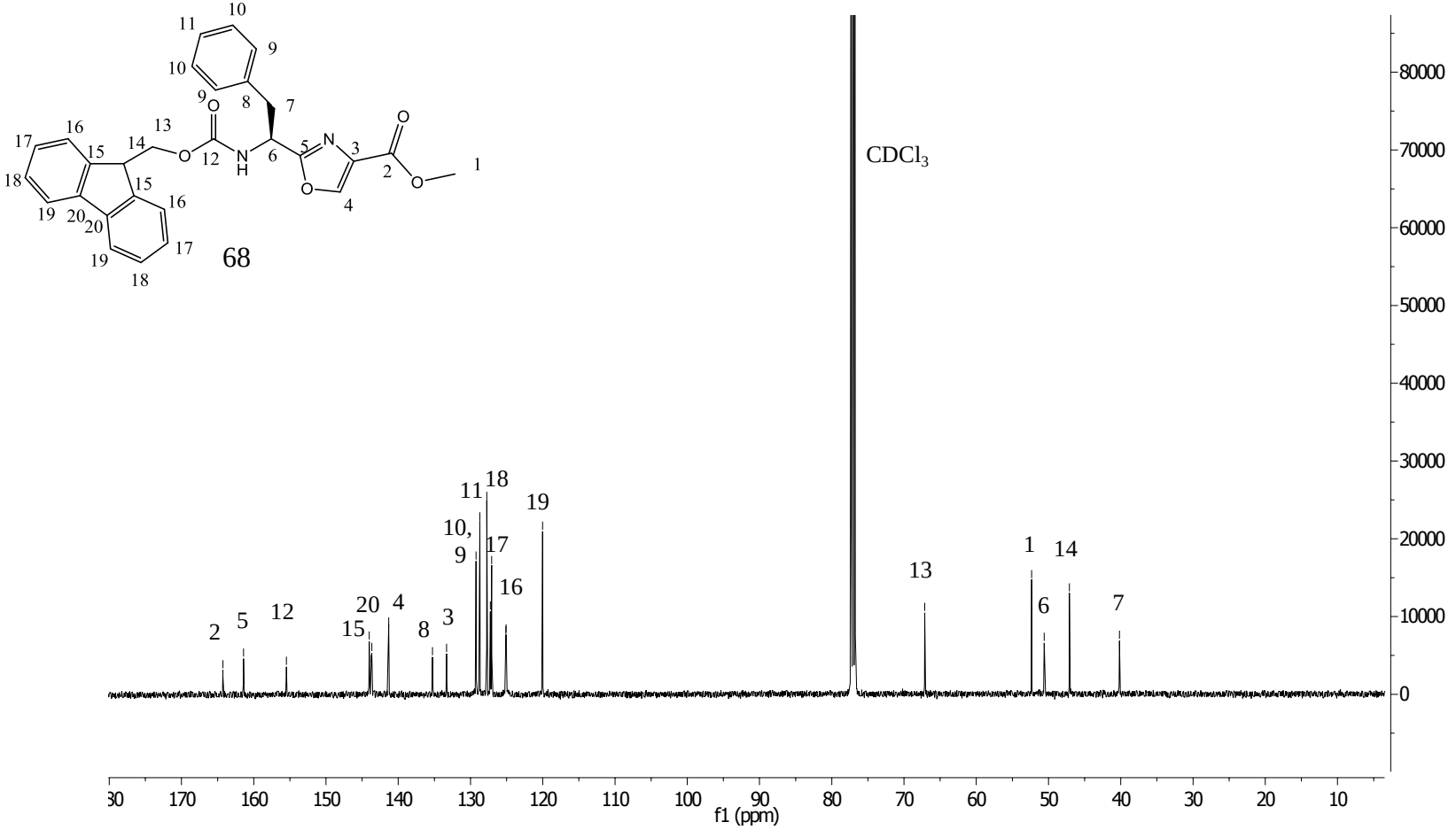

Appendix S 12: ^{13}C NMR Spectrum of *N*-Fmoc-L-Phe-L-Oxazole-OMe (**68**) in $CDCl_3$

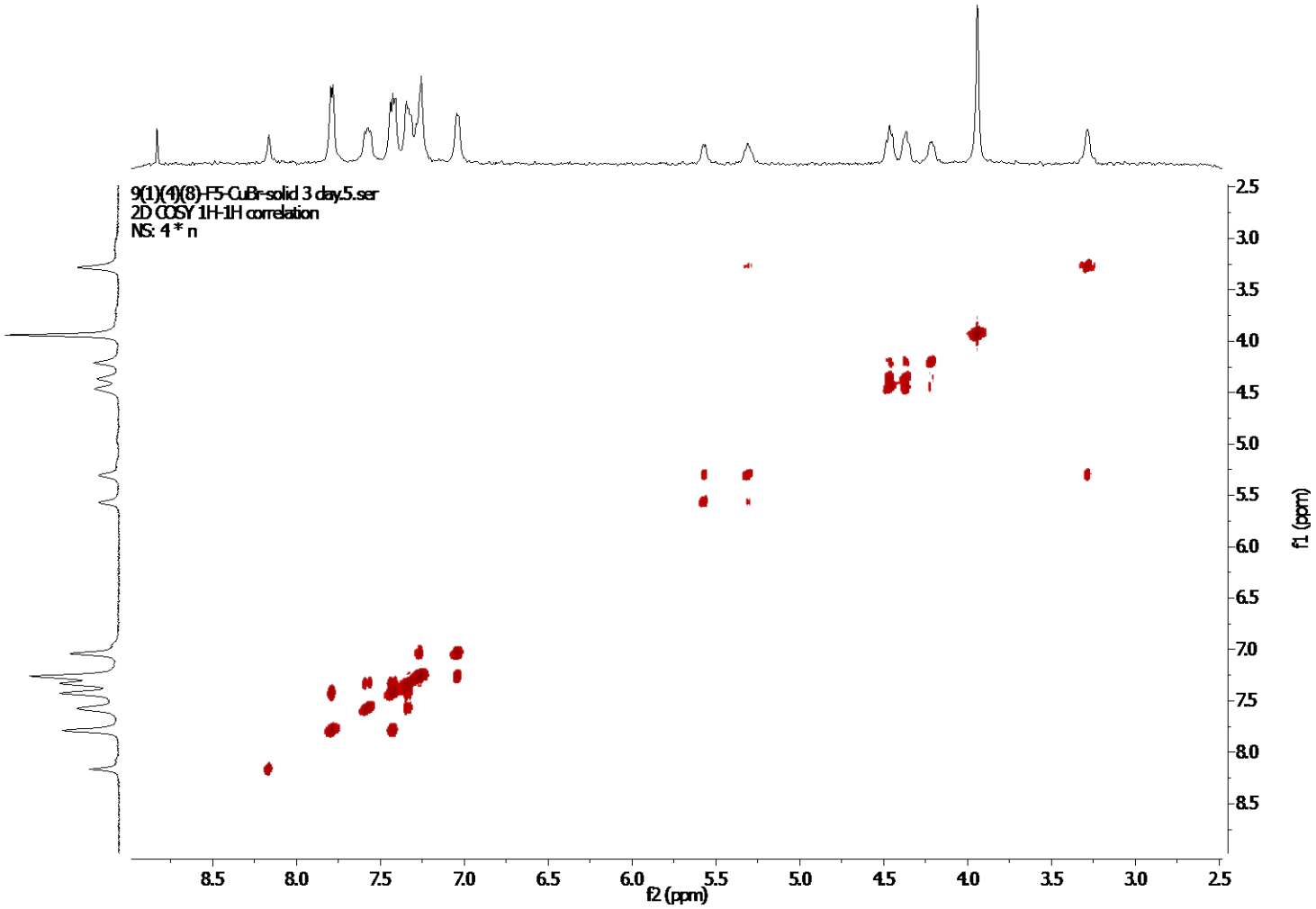

Appendix S 13: COSY NMR Spectrum of *N*-Fmoc-L-Phe-L-Oxazole-OMe (**68**) in $CDCl_3$

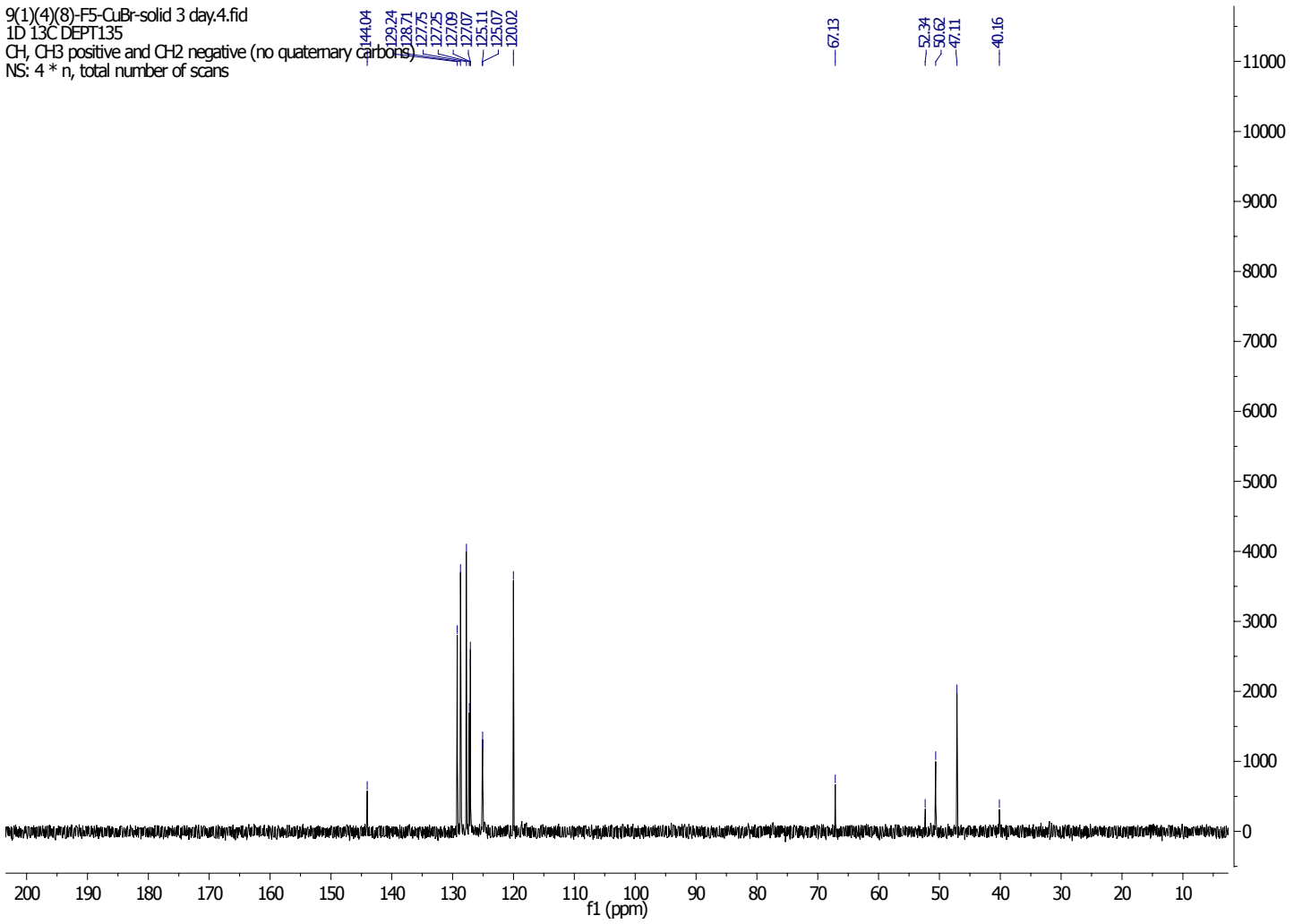

Appendix S 14: DEPT 90 NMR Spectrum of *N*-Fmoc-L-Phe-L-Oxazole-OMe (**68**) in $CDCl_3$

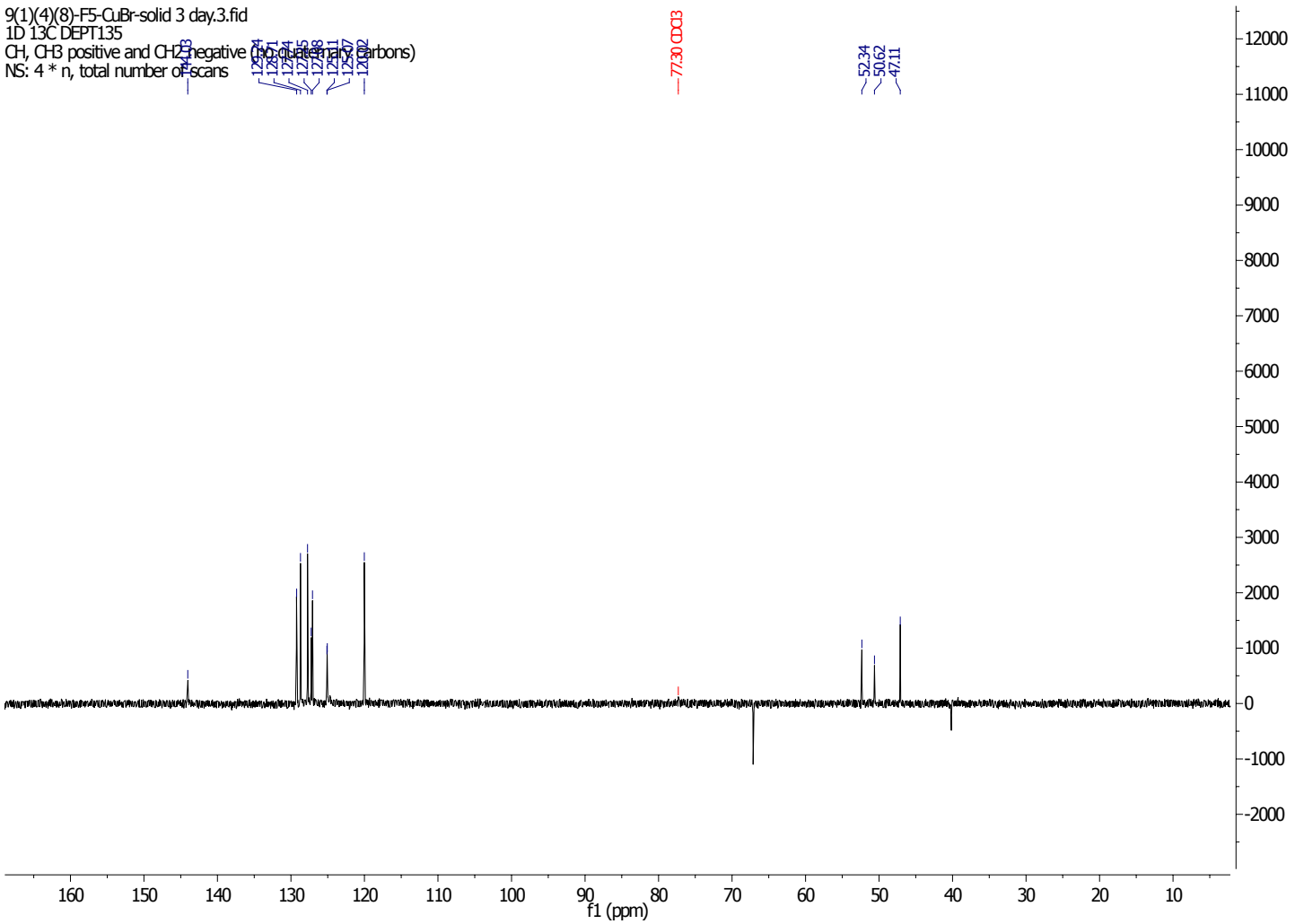

Appendix S 15: DEPT 135 NMR Spectrum of *N*-Fmoc-L-Phe-L-Oxazole-OMe (**68**) in $CDCl_3$

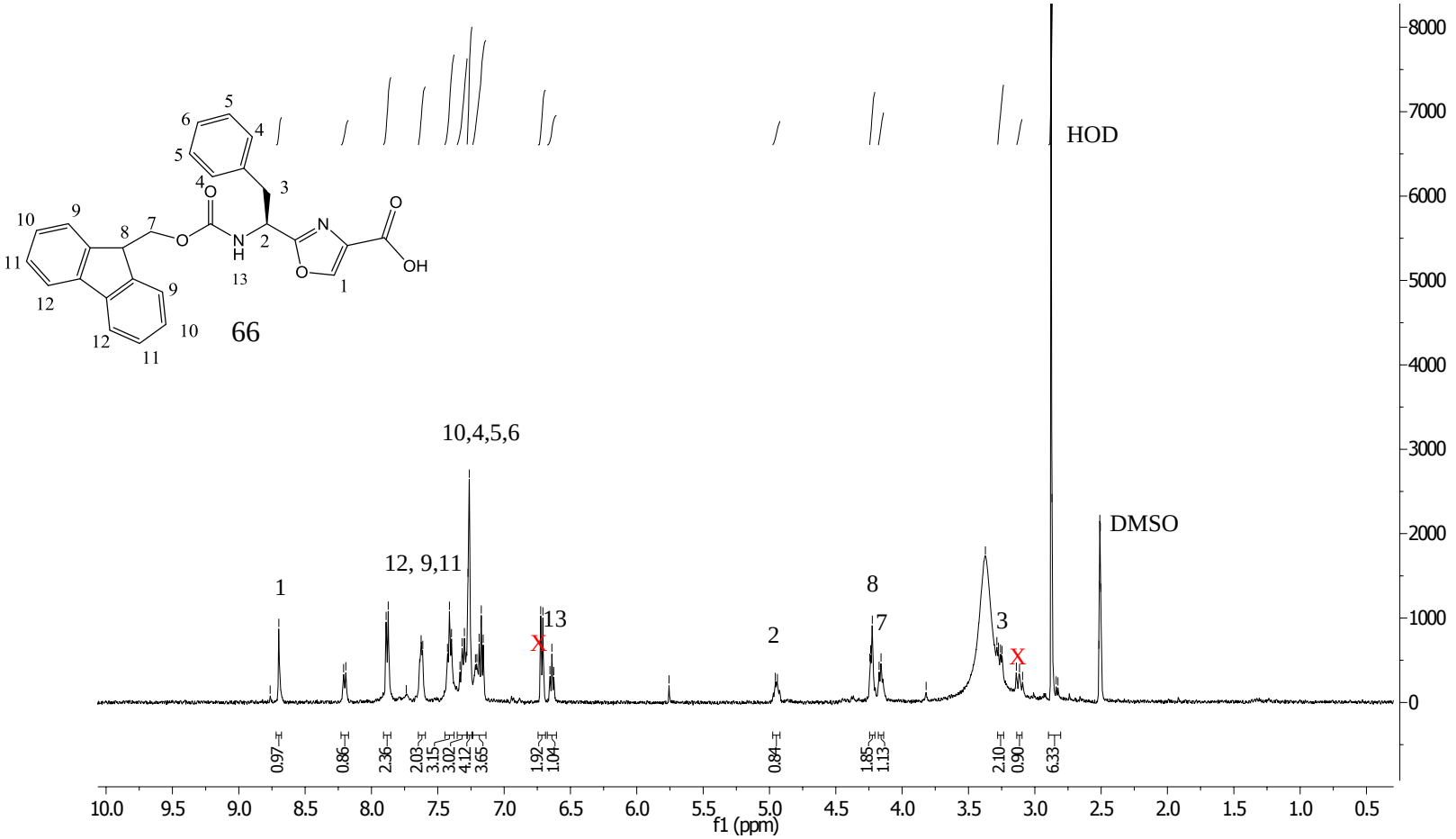

Appendix S 16: ^{1}H NMR Spectrum of *N*-Fmoc-D-Phe-Oxazole-OH (**66**) in DMSO-d_6

Signals marked with an X are due to dimethylaniline.

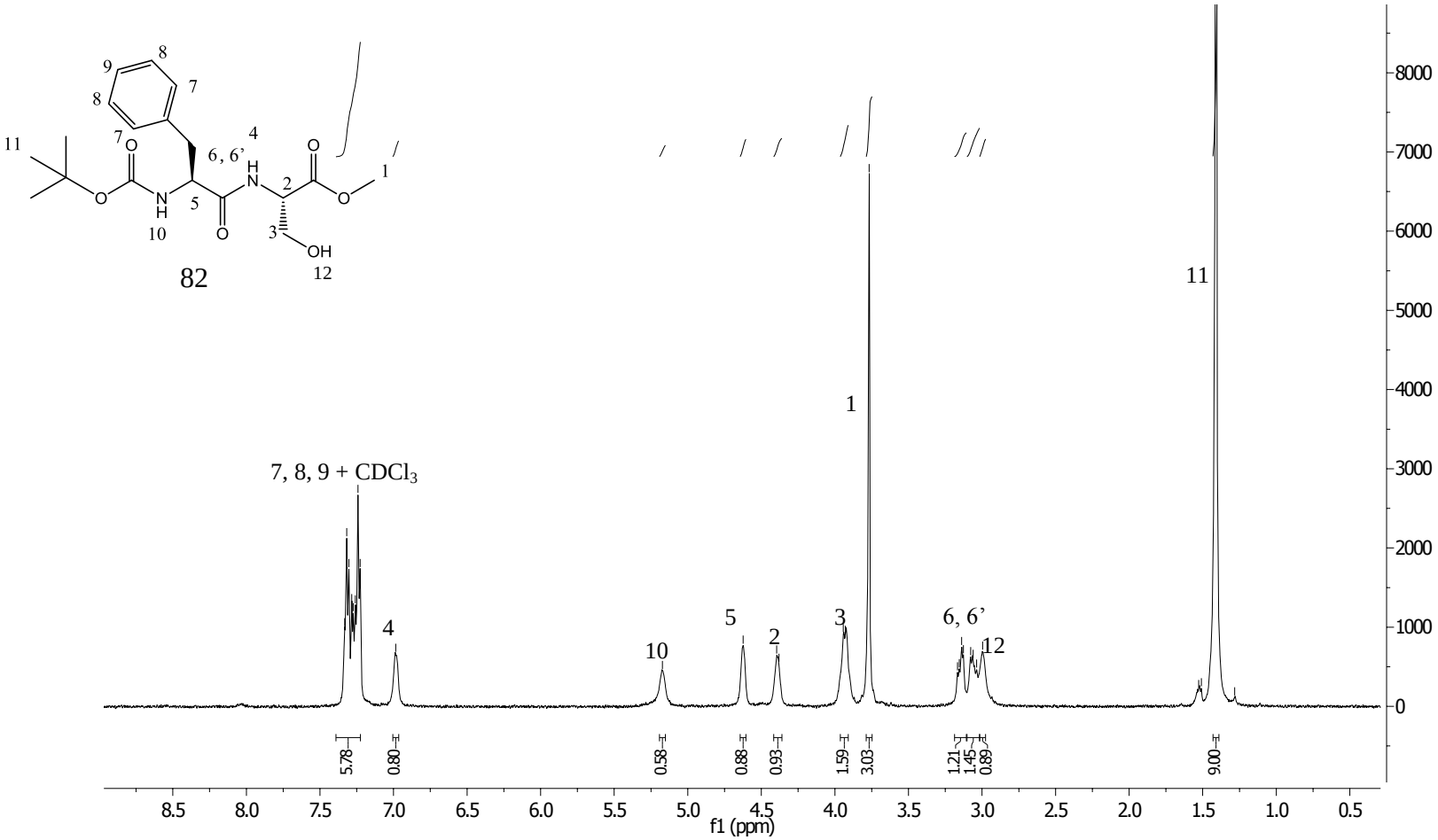

Appendix S 17: ^{1}H NMR Spectrum of *N*-Boc-L-Phe-L-Ser-OMe (**82**) in $CDCl_3$

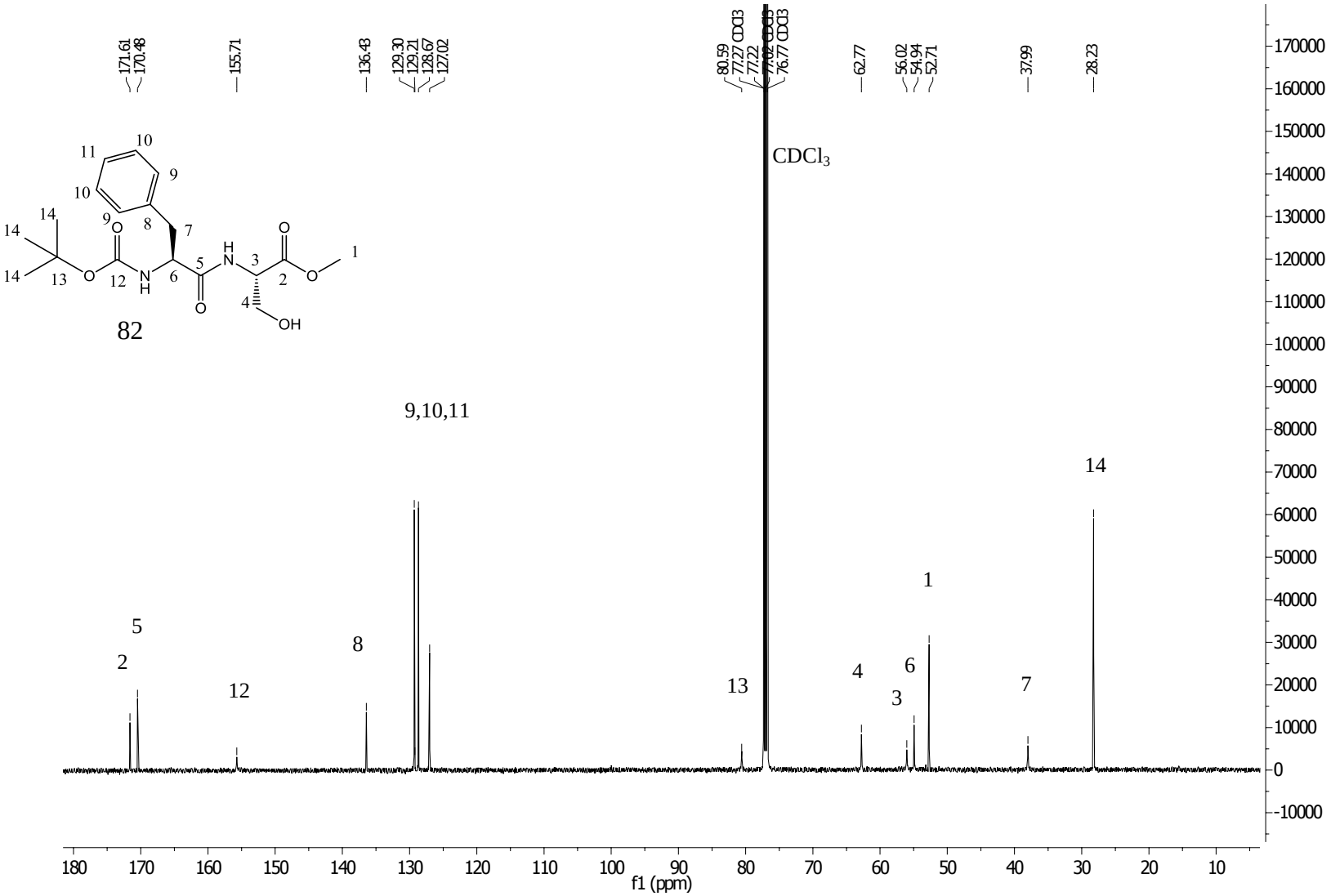

Appendix S 18: ^{13}C NMR Spectrum of *N*-Boc-L-Phe-L-Ser-OMe (**82**) in $CDCl_3$

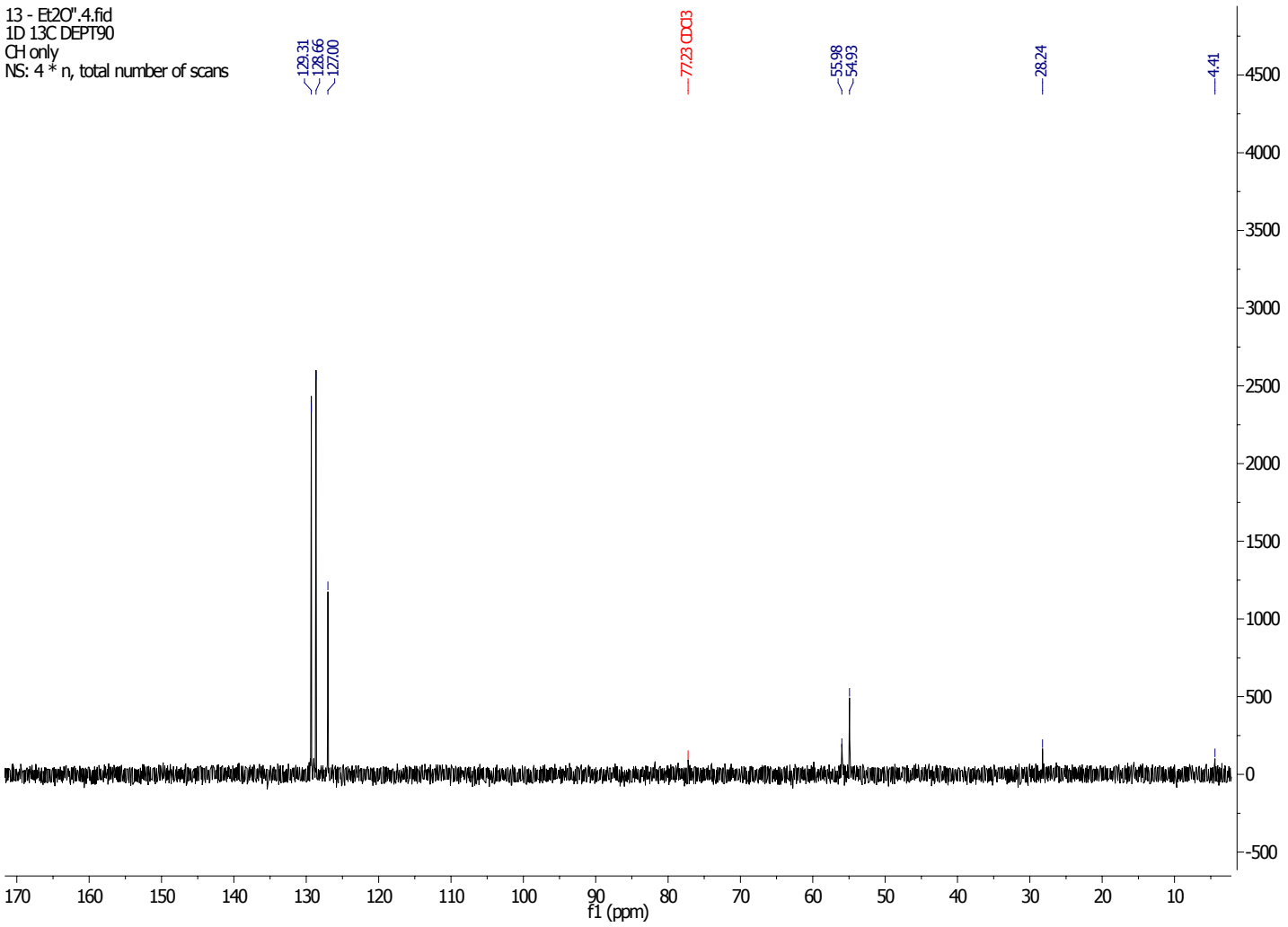

Appendix S 19: DEPT 90 NMR Spectrum of *N*-Boc-L-Phe-L-Ser-OMe (**82**) in $CDCl_3$

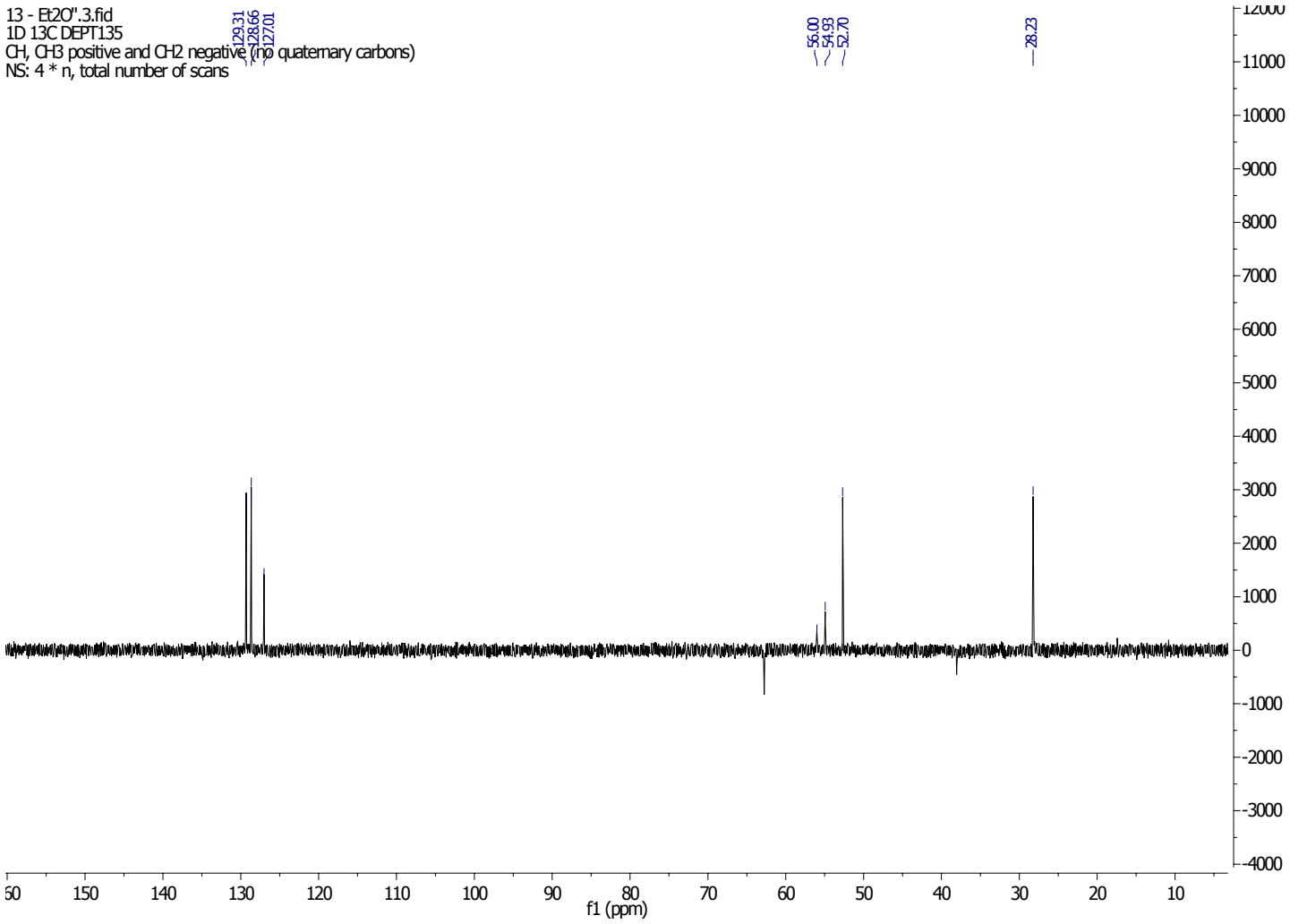

Appendix S 20: DEPT 135 NMR Spectrum of *N*-Boc-L-Phe-L-Ser-OMe (**82**) in $CDCl_3$

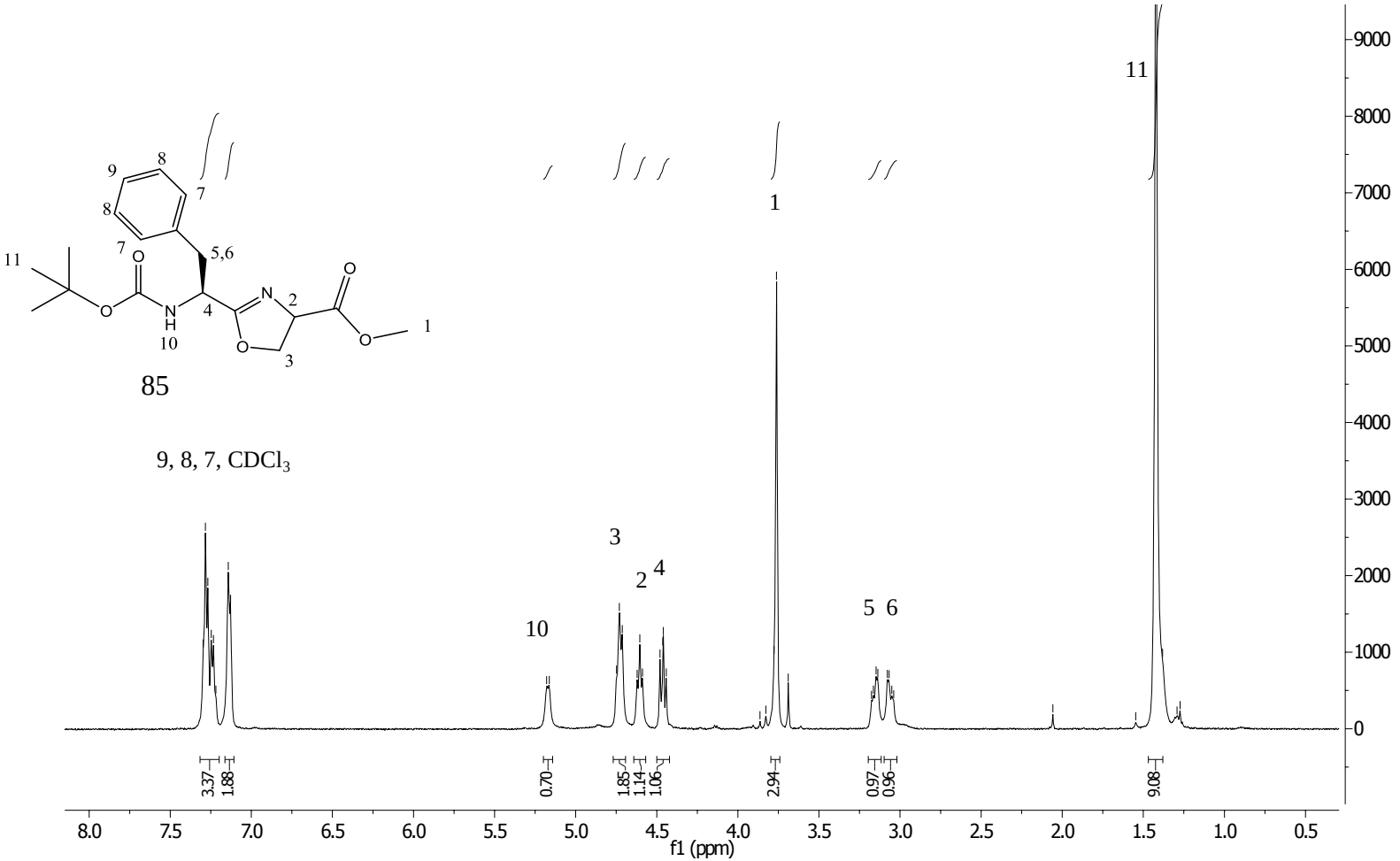

Appendix S 21: ^{1}H NMR Spectrum of *N*-Boc-L-Phe-Oxazoline-OMe (**85**) in $CDCl_3$

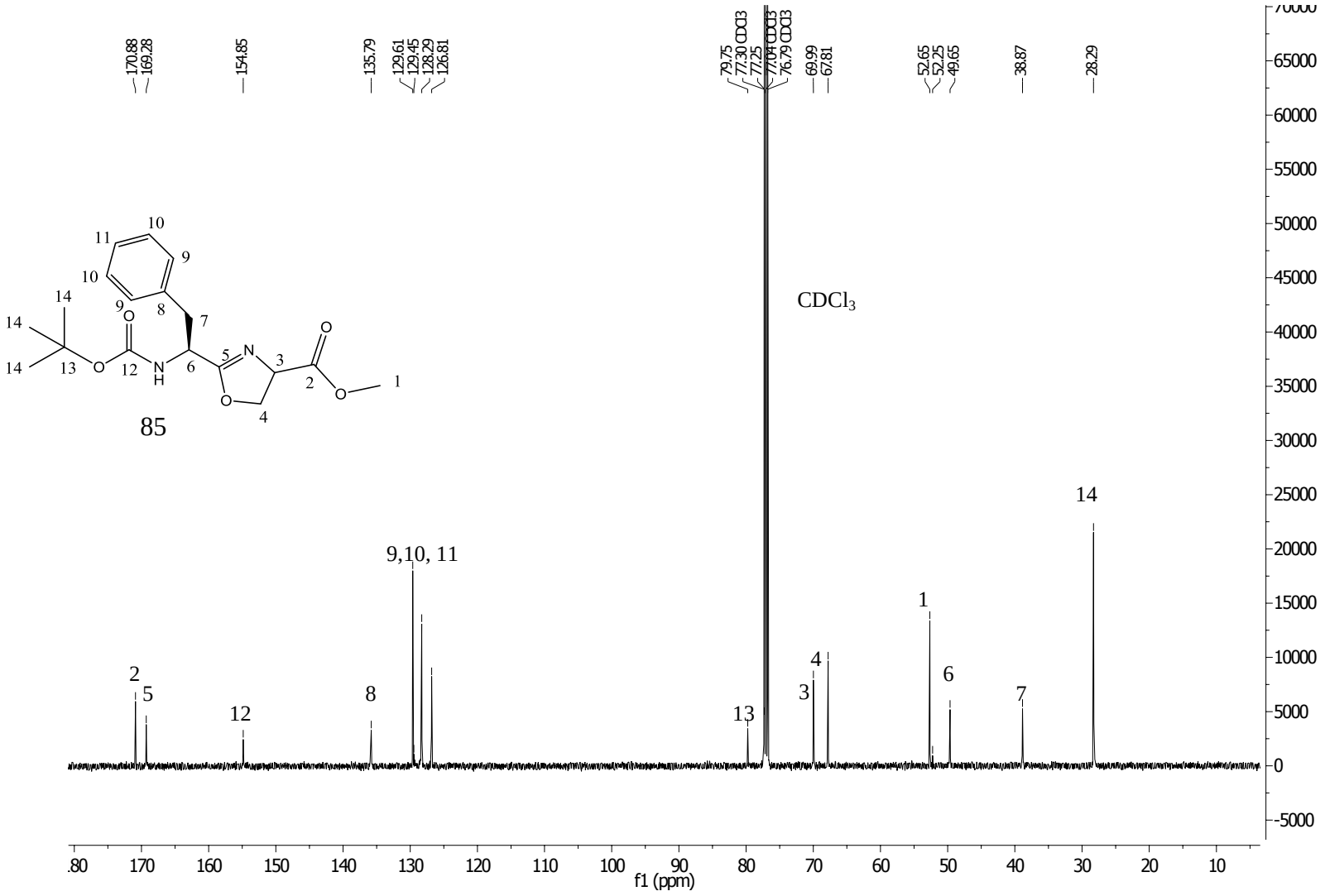

Appendix S 22: ^{13} C NMR Spectrum of *N*-Boc-L-Phe-Oxazoline-OMe (**85**) in $CDCl_3$

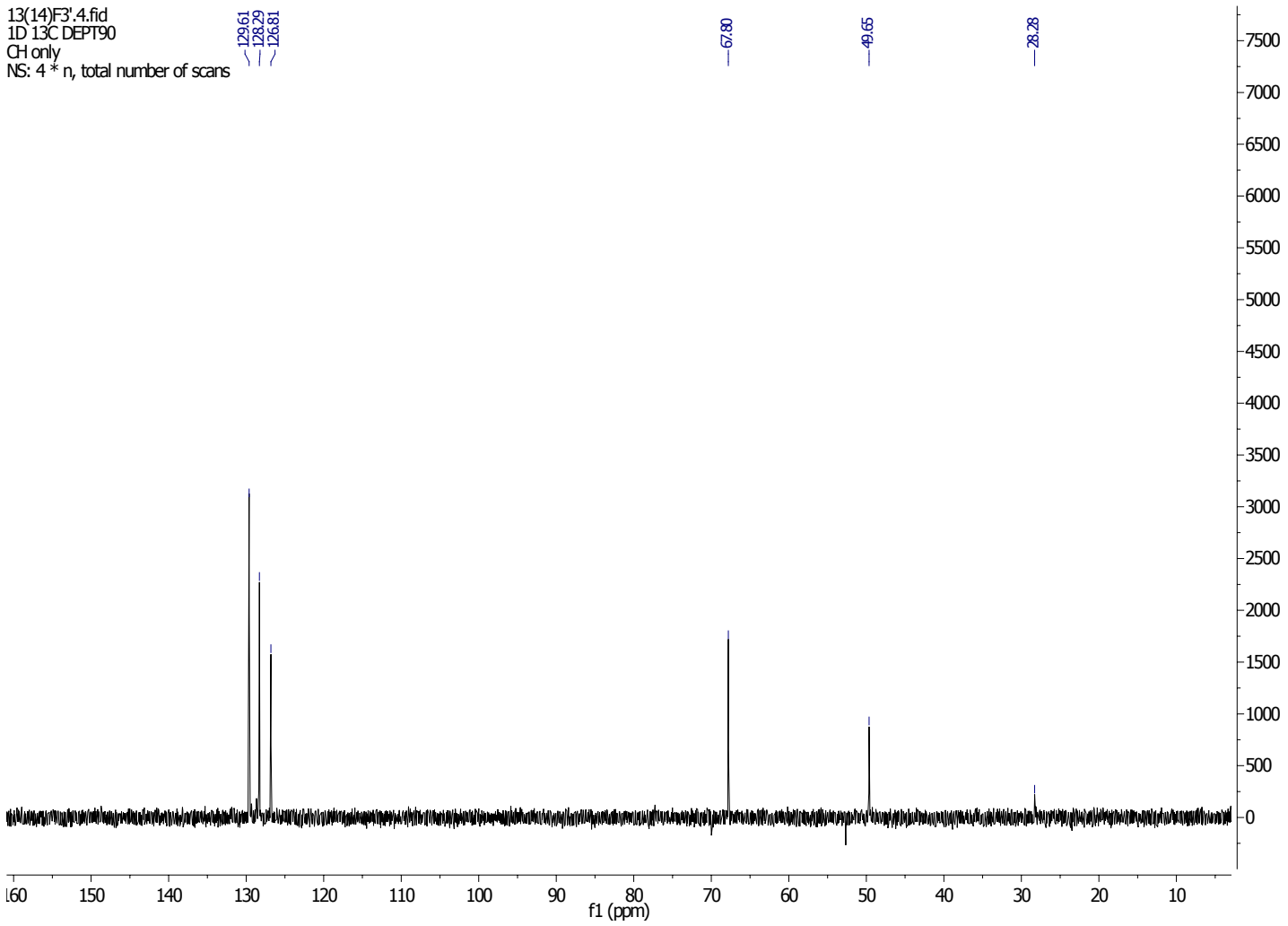

Appendix S 23: DEPT 90 NMR Spectrum of *N*-Boc-L-Phe-Oxazoline-OMe (**85**) in $CDCl_3$

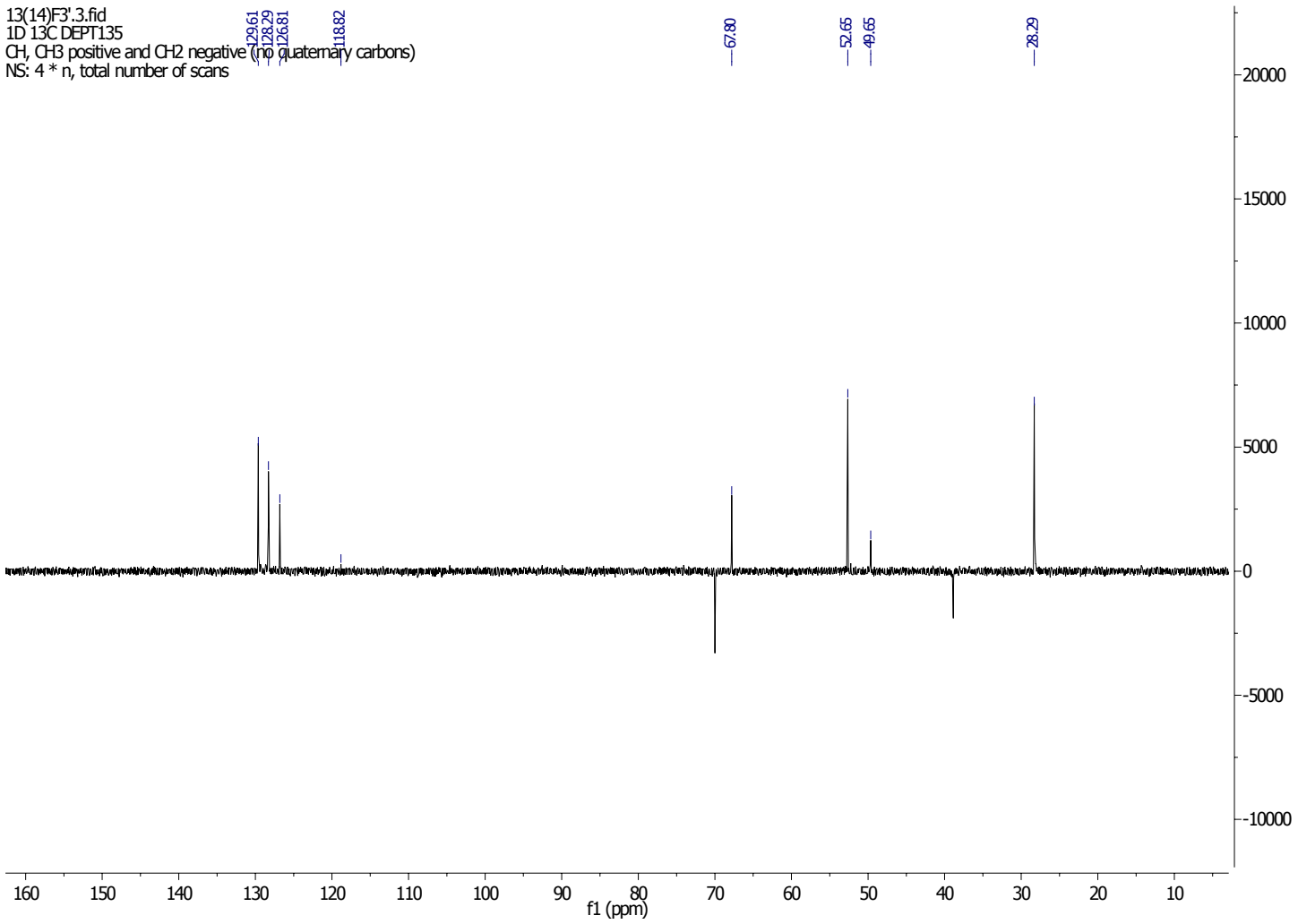

Appendix S 24: DEPT 135 NMR Spectrum of *N*-Boc-L-Phe-Oxazoline-OMe (**85**) in $CDCl_3$

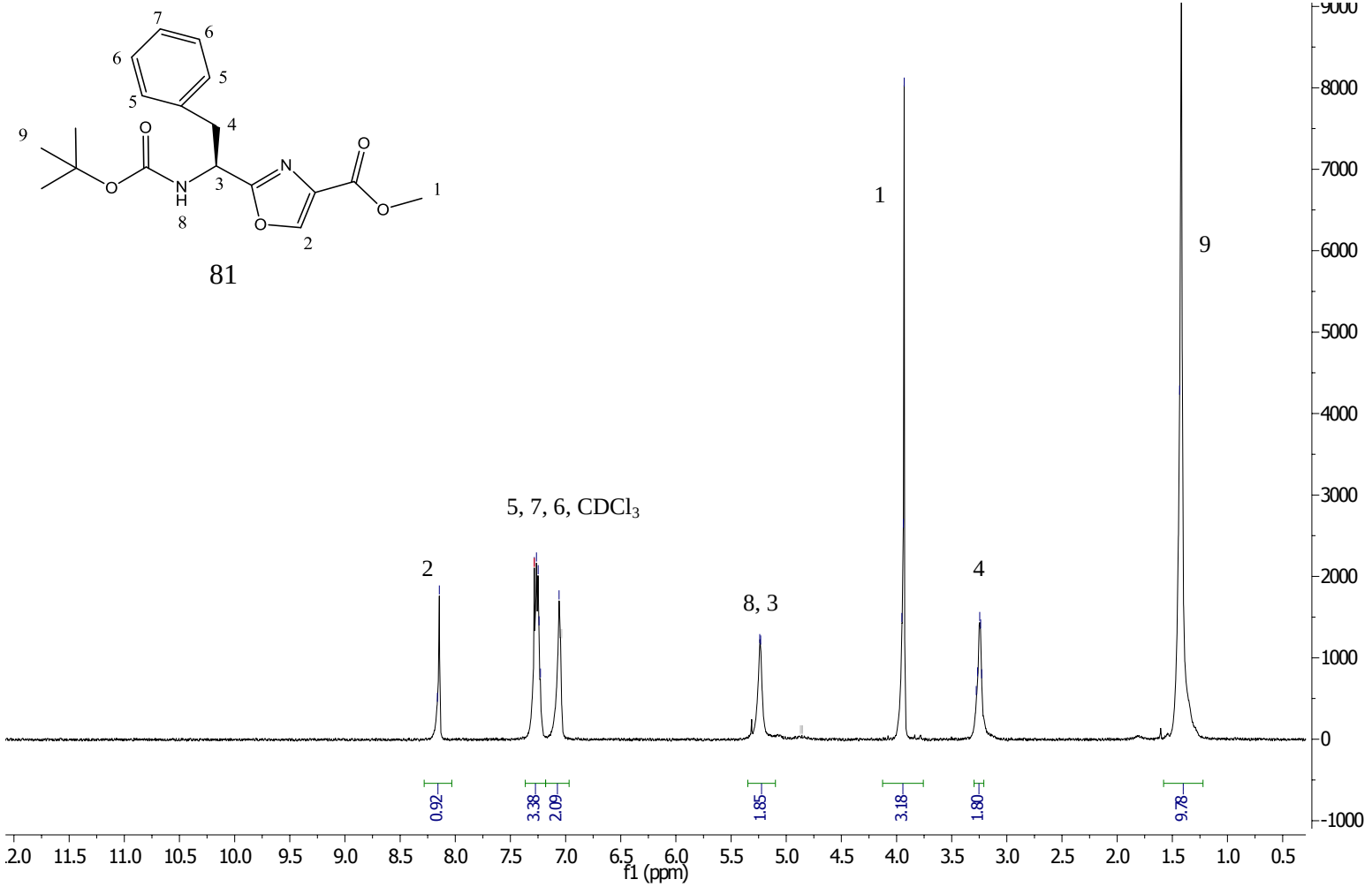

Appendix S 25: ^{1}H NMR Spectrum of *N*-Boc-L-Phe-Oxazole-OMe (**81**) in $CDCl_3$

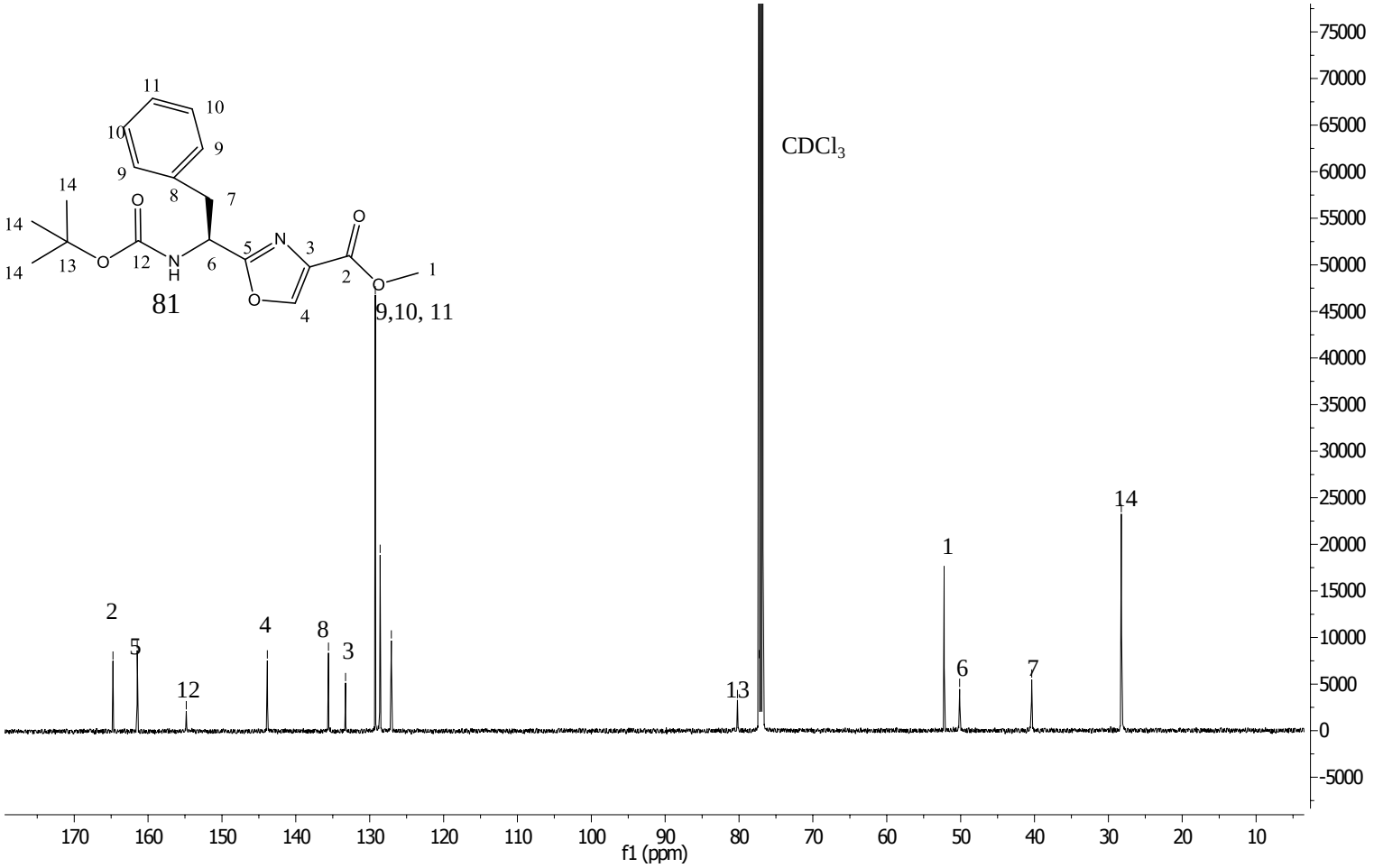

Appendix S 26: ^{13}C NMR Spectrum of *N*-Boc-L-Phe-Oxazole-OMe (**81**) in $CDCl_3$

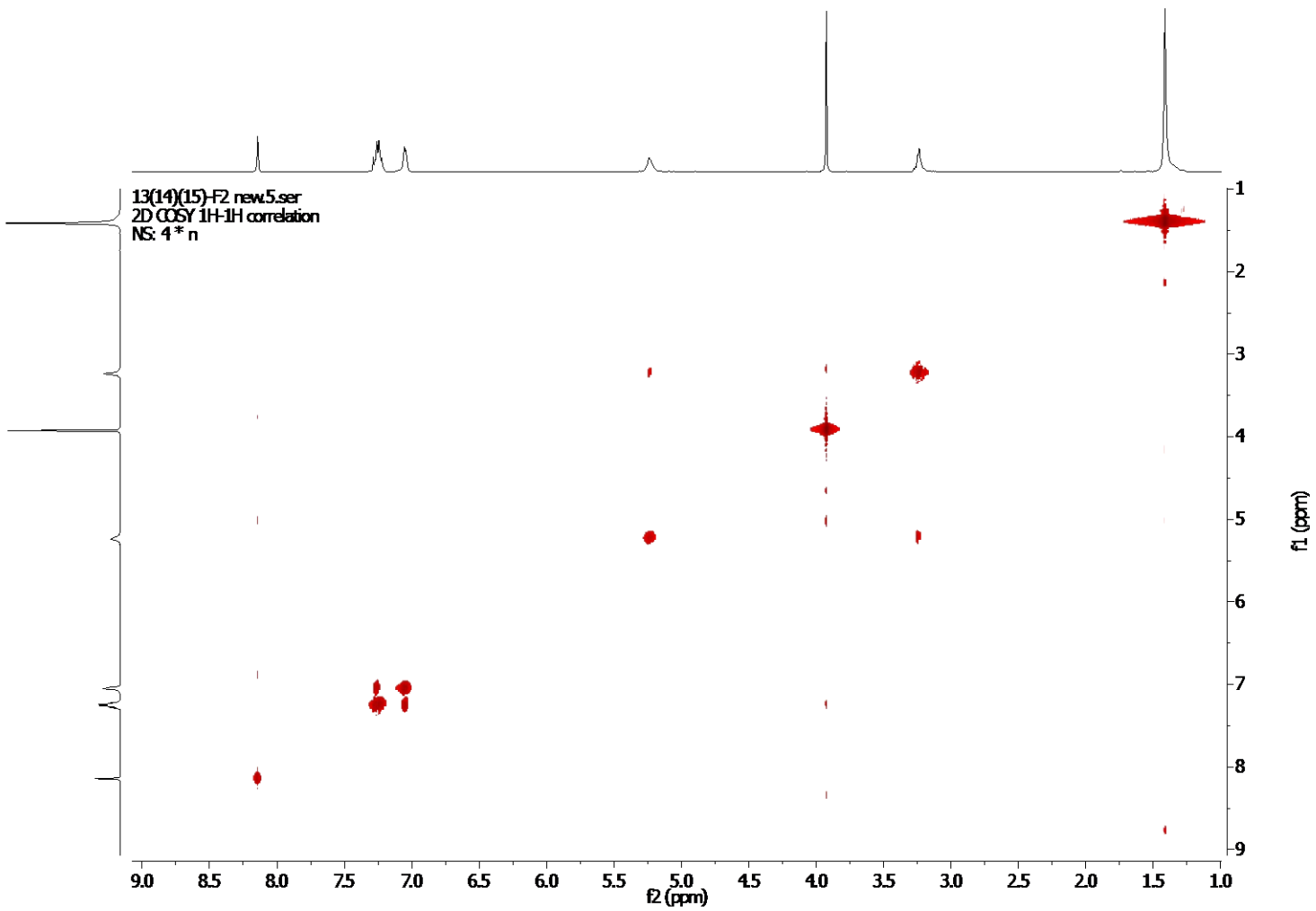

Appendix S 27: COSY NMR Spectrum of *N*-Boc-L-Phe-Oxazole-OMe (**81**) in $CDCl_3$

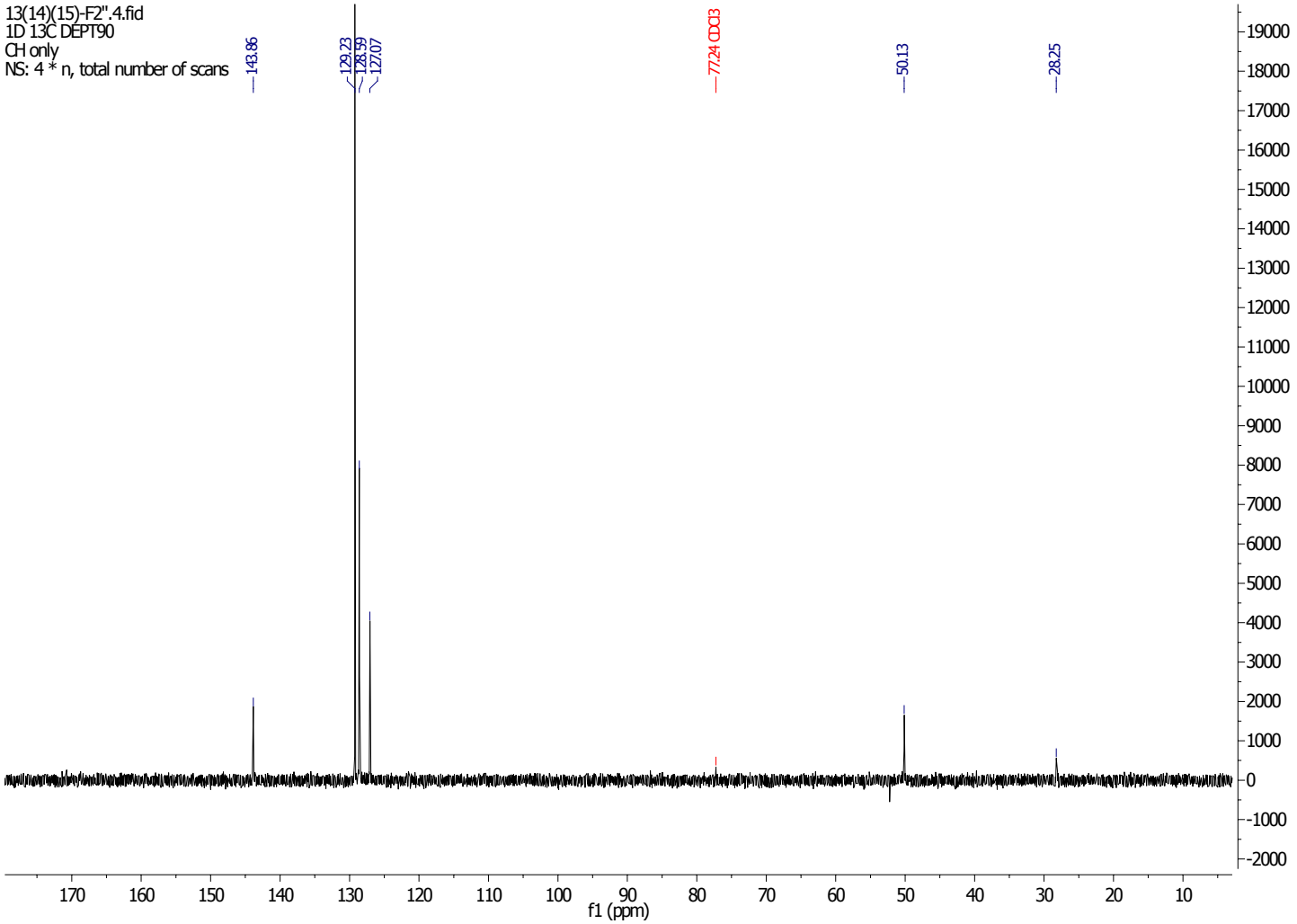

Appendix S 28: DEPT 90 NMR Spectrum of *N*-Boc-L-Phe-Oxazole-OMe (**81**) in $CDCl_3$

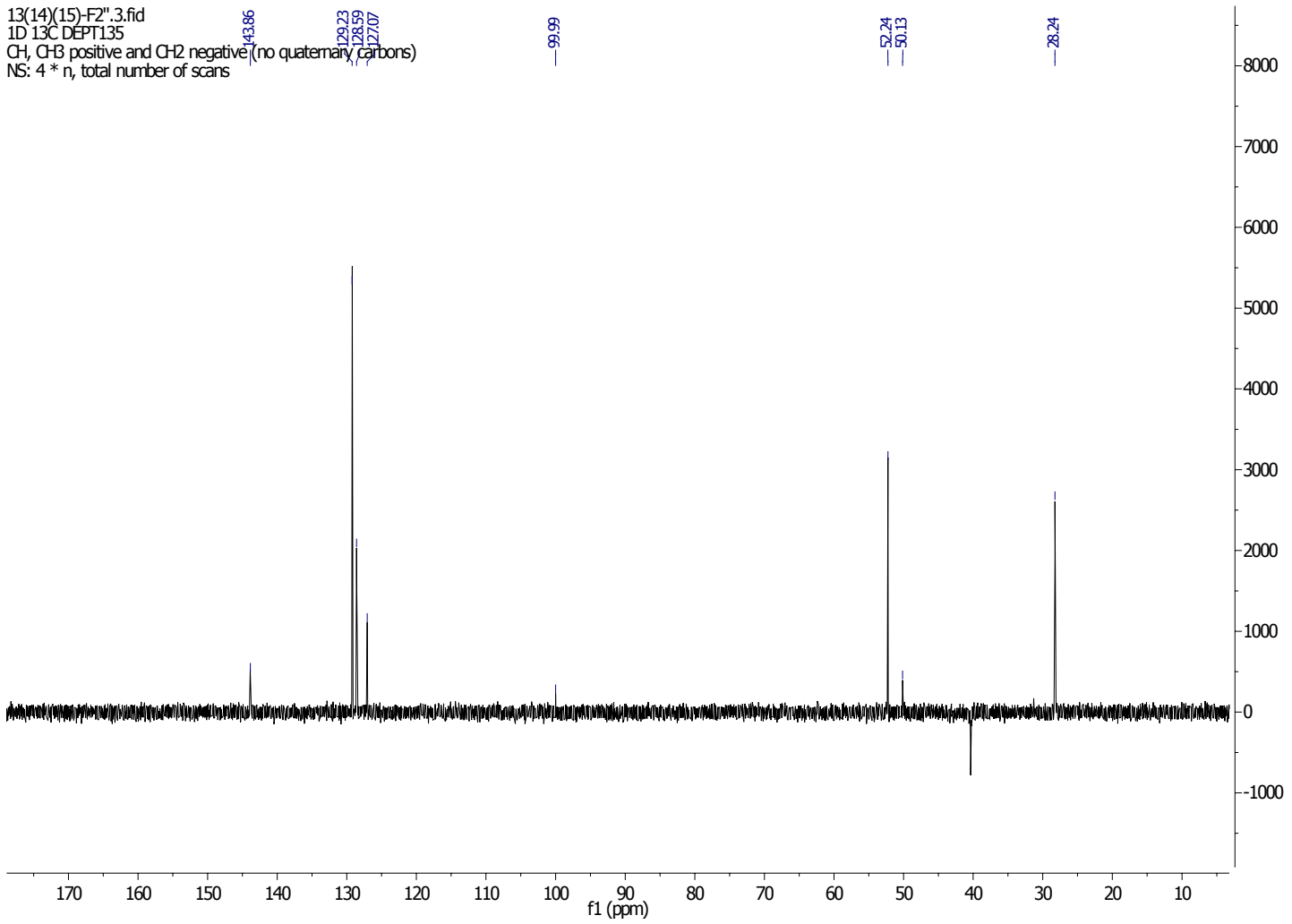

Appendix S 29: DEPT 135 NMR Spectrum of *N*-Boc-L-Phe-Oxazole-OMe (**81**) in $CDCl_3$

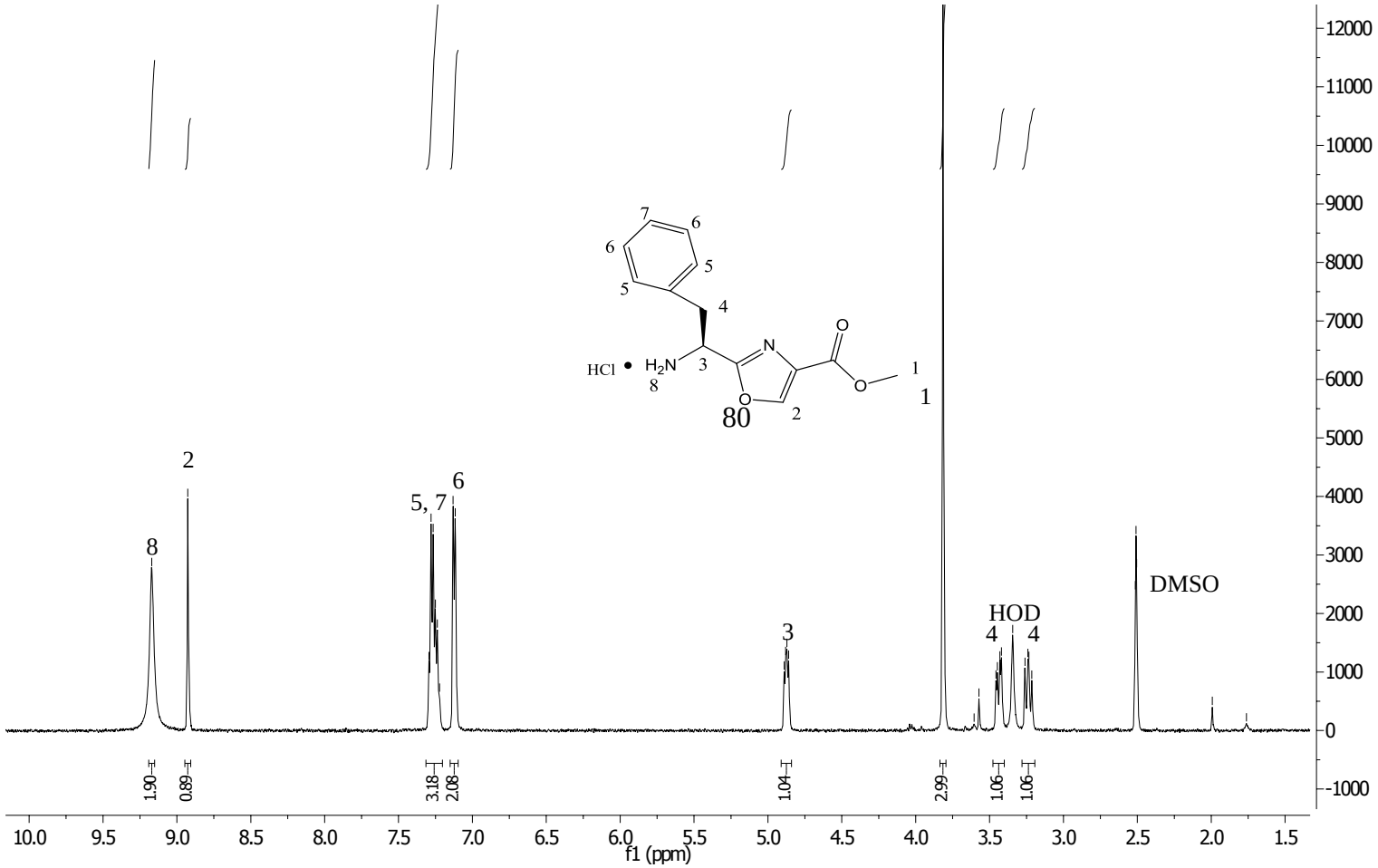

Appendix S 30: [1] H NMR Spectrum of HCl•H_2N-L-Phe-Oxazole-OMe (**80**) in DMSO-d_6

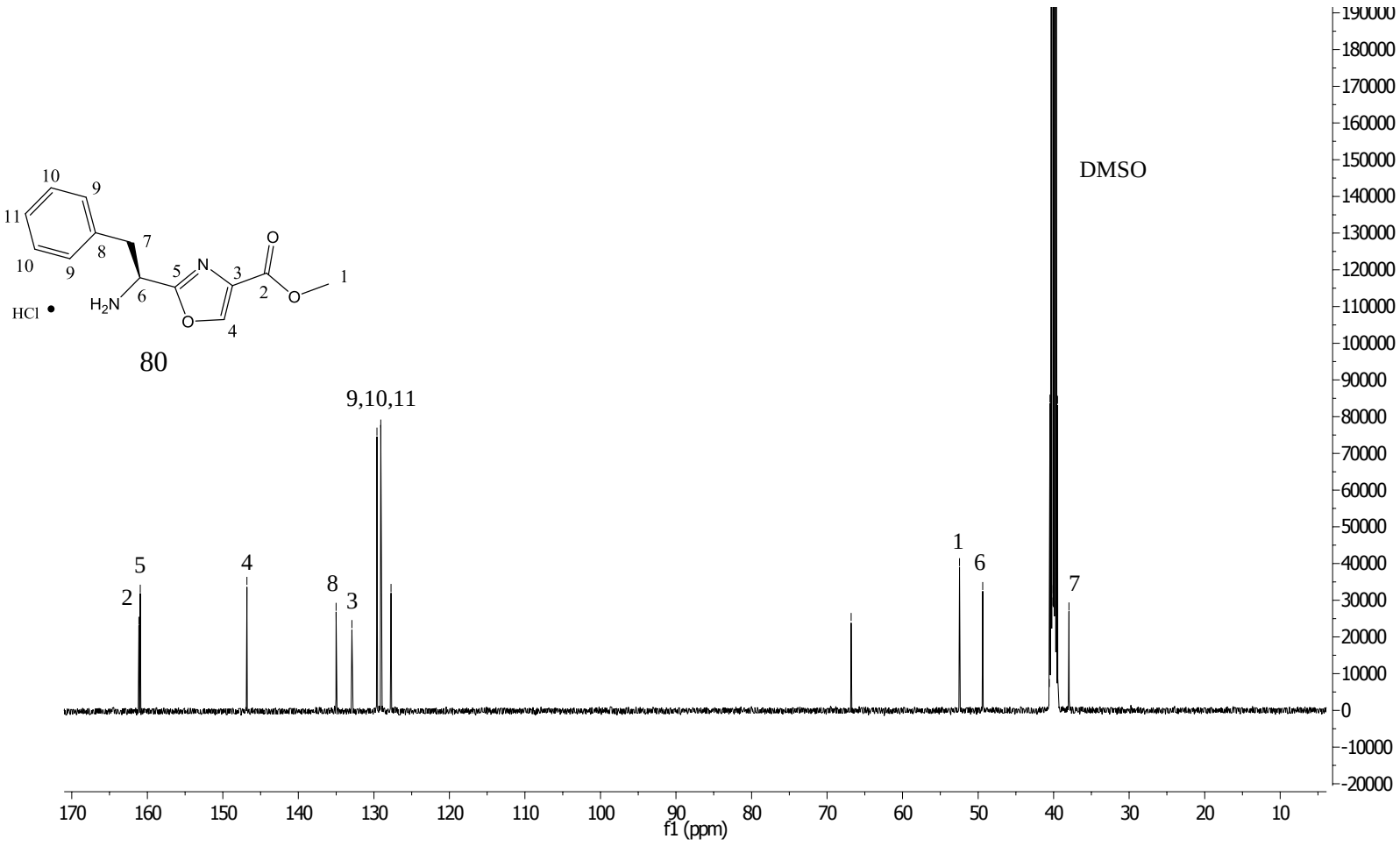

Appendix S 31: ^{13}C NMR Spectrum of HCl•H_2N-L-Phe-Oxazole-OMe (**80**) in DMSO-d_6

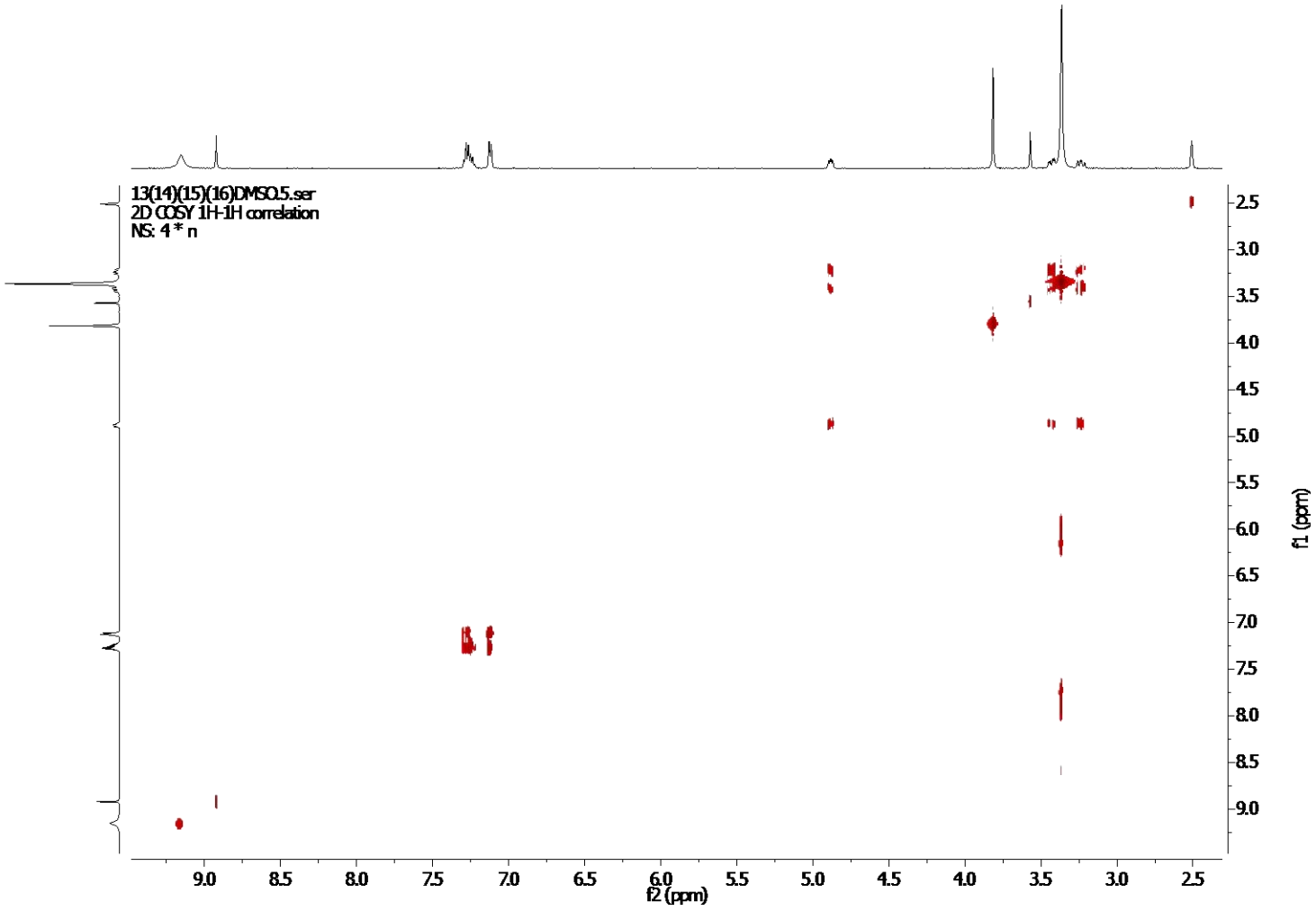

Appendix S 32: COSY NMR Spectrum of HCl•H_2N-L-Phe-Oxazole-OMe (**80**) in DMSO-d_6

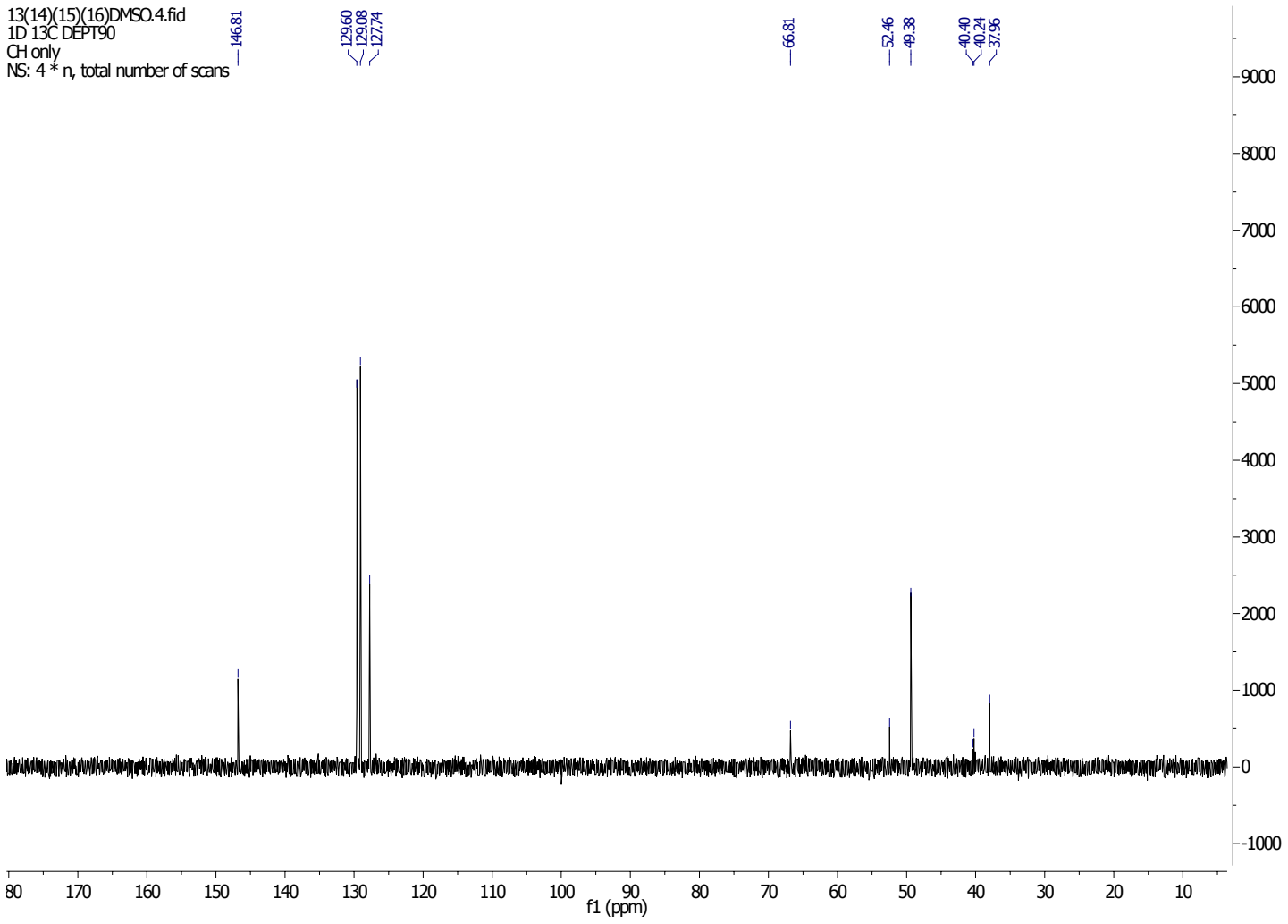

Appendix S 33: DEPT 90 NMR Spectrum of HCl•H_2N-L-Phe-Oxazole-OMe (**80**) in DMSO-d_6

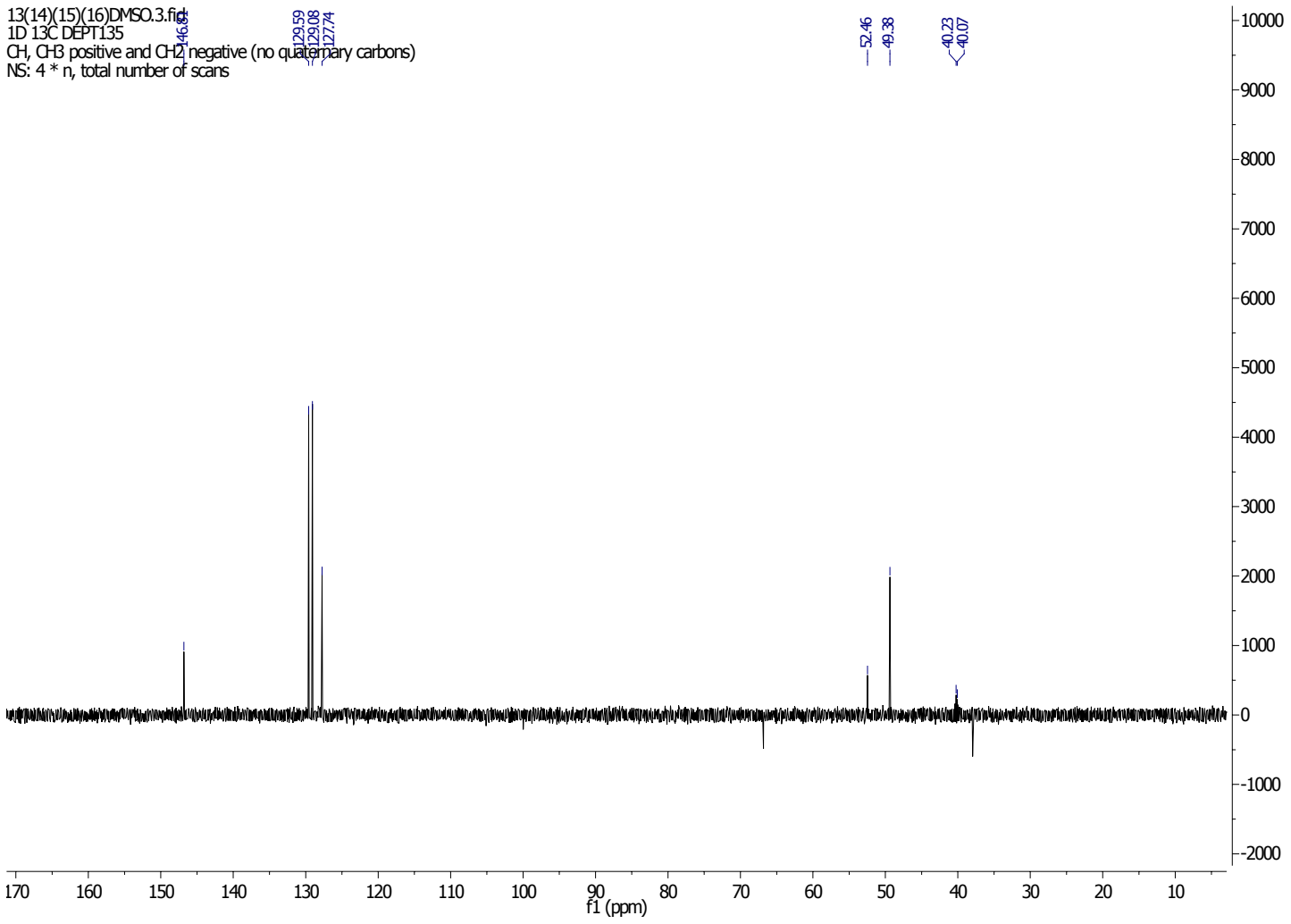

Appendix S 34: DEPT 135 NMR Spectrum of HCl•H_2N-L-Phe-Oxazole-OMe (**80**) in DMSO-d_6

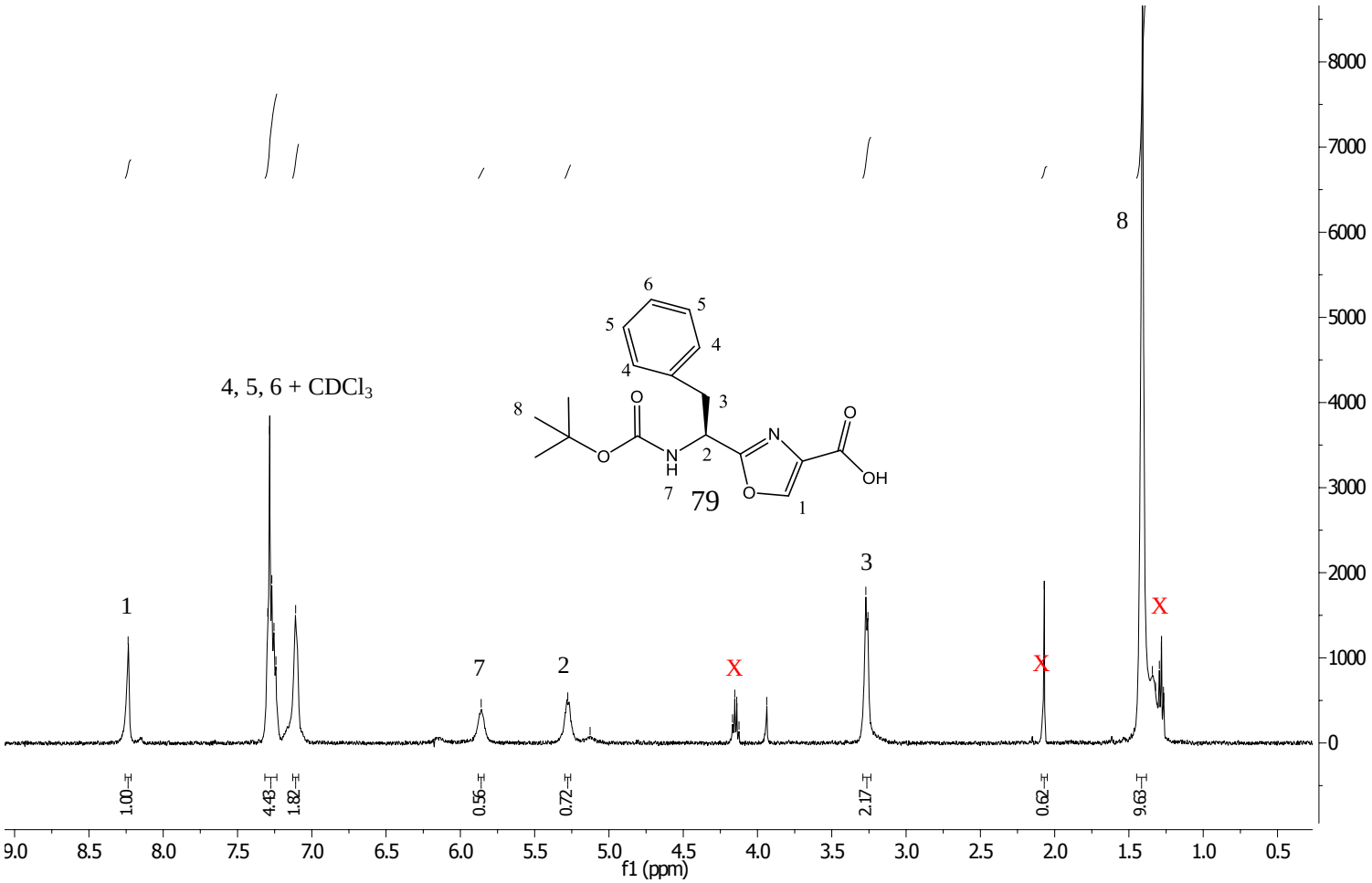

Appendix S 35: [1] H NMR Spectrum of *N*-Boc-Phe-Oxazole-OH (**79**) in $CDCl_3$

Signals marked with an X are due to ethyl acetate.

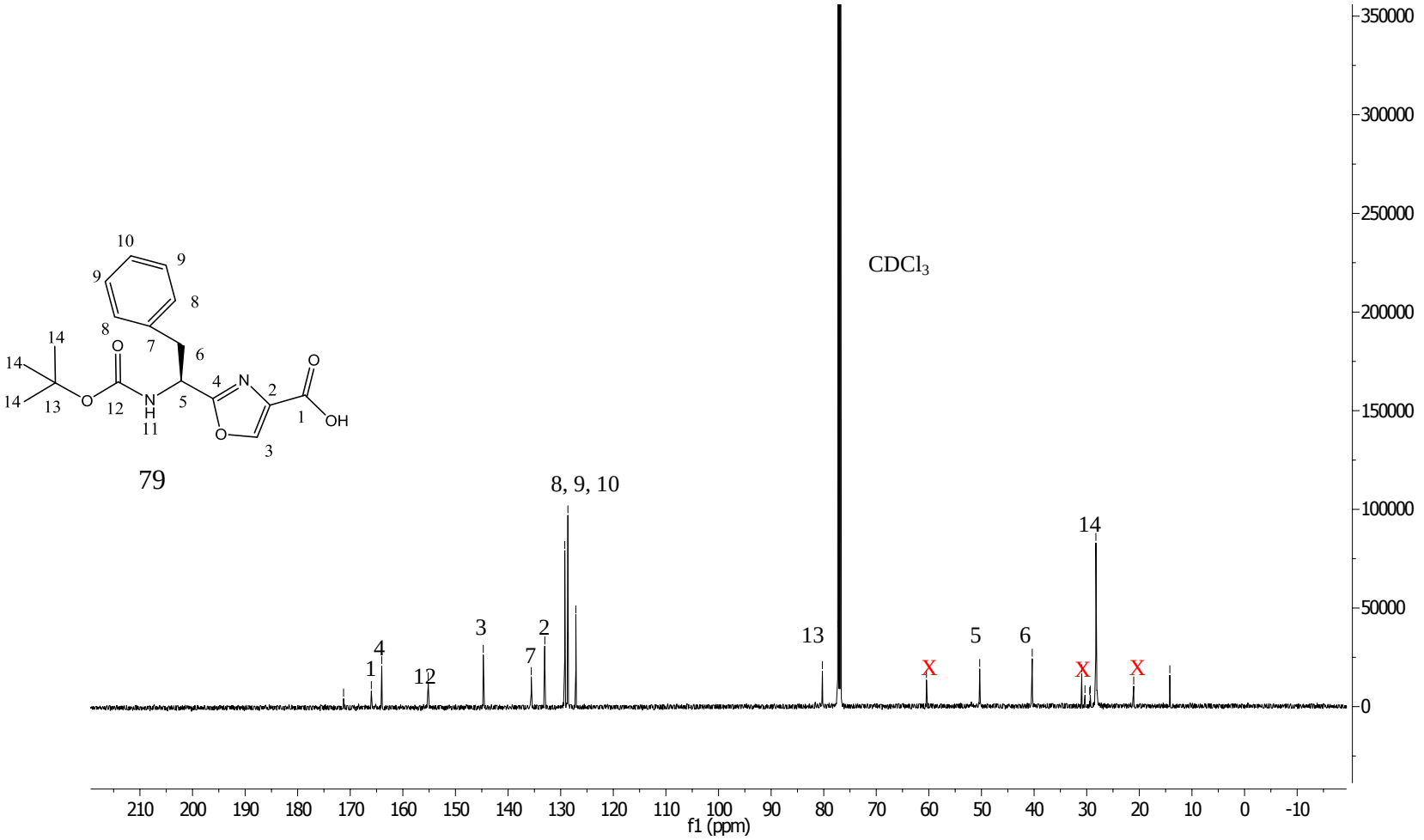

Appendix S 36: ^{13}C NMR Spectrum of *N*-Boc-Phe-Oxazole-OH (**79**) in $CDCl_3$

Signals marked with an X are due to ethyl acetate.

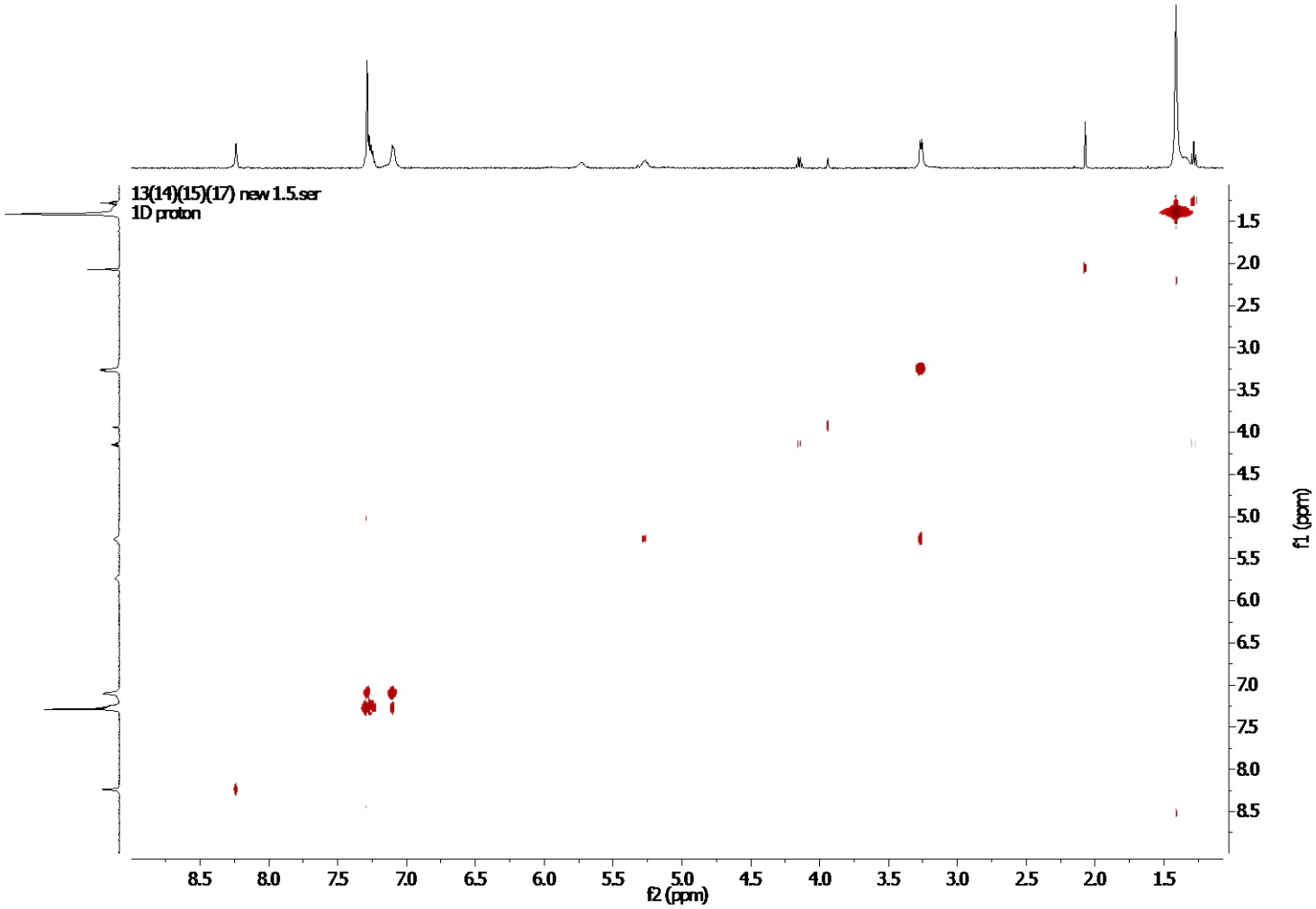

Appendix S 37: COSY NMR Spectrum of *N*-Boc-Phe-Oxazole-OH (**79**) in $CDCl_3$

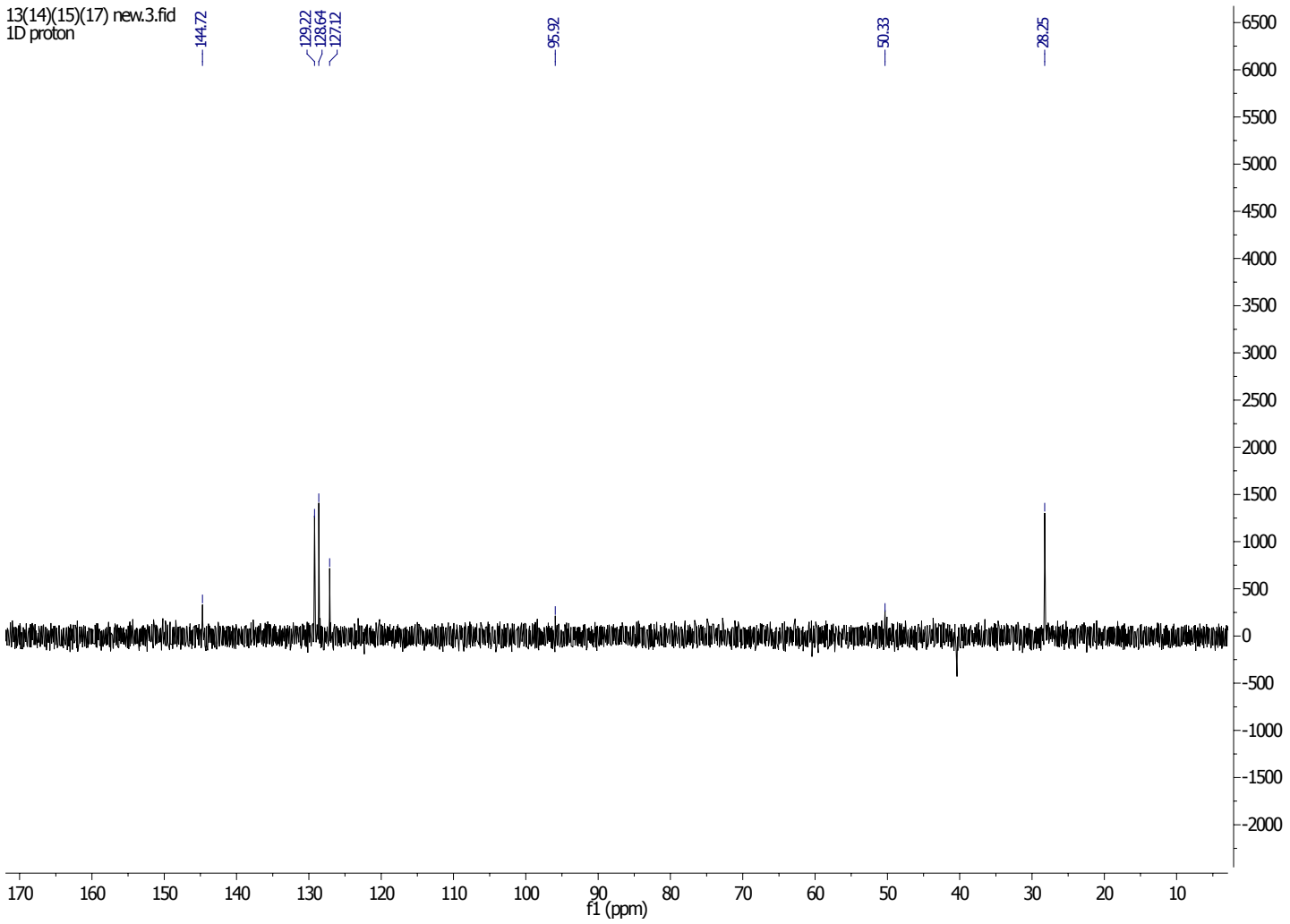

Appendix S 38: DEPT 90 NMR Spectrum of *N*-Boc-Phe-Oxazole-OH (**79**) in $CDCl_3$

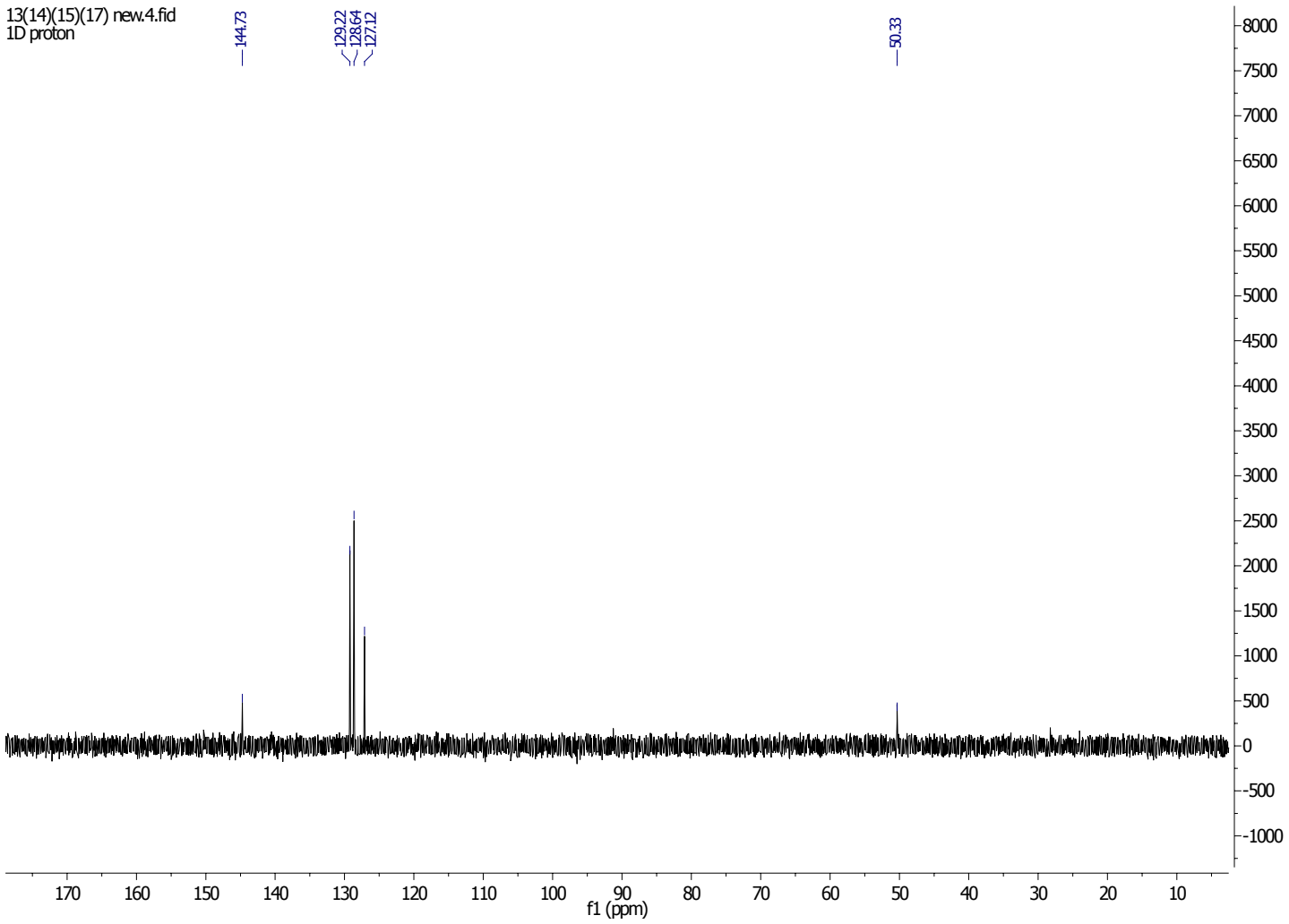

Appendix S 39: DEPT 135 NMR Spectrum of *N*-Boc-Phe-Oxazole-OH (**79**) in $CDCl_3$

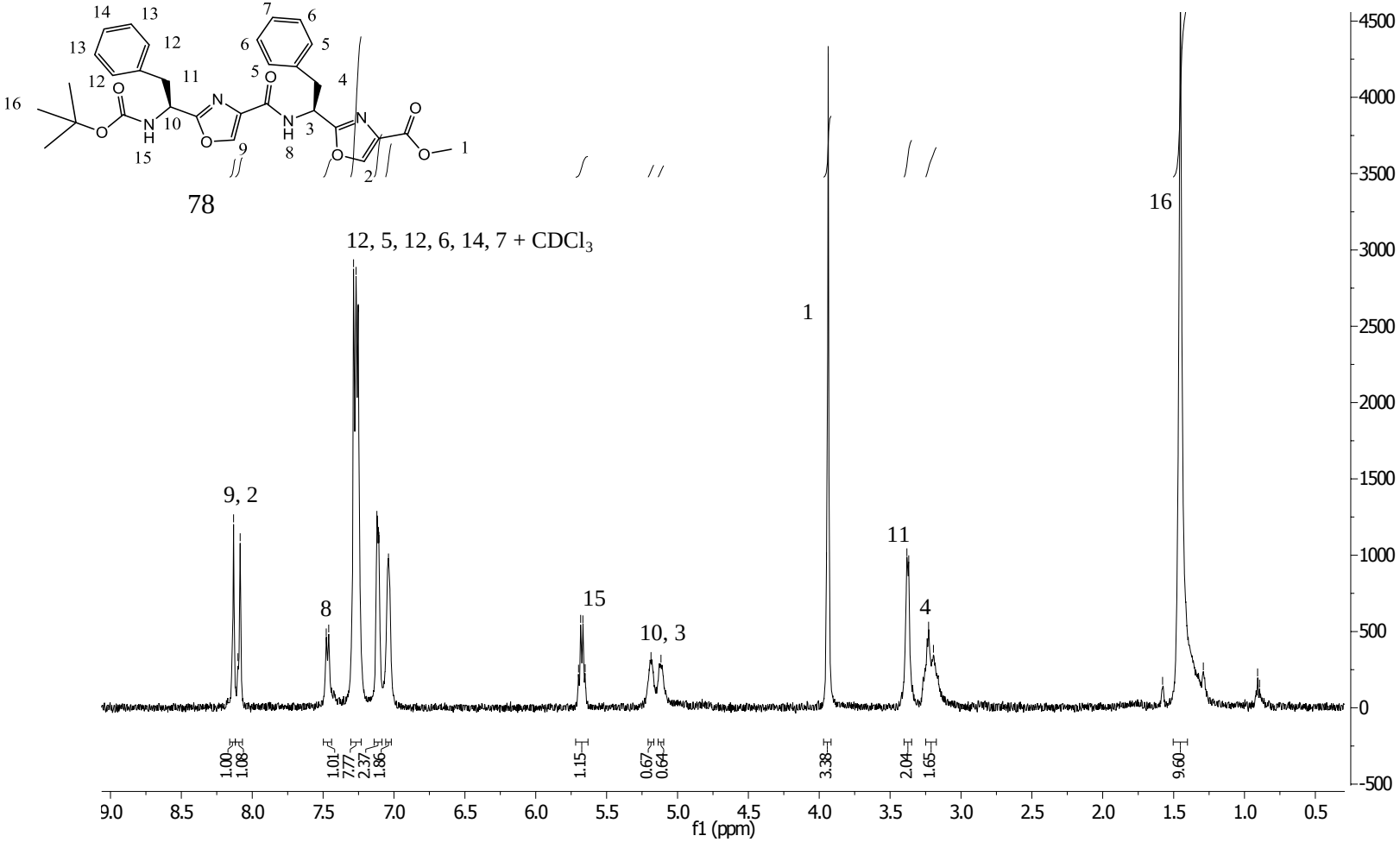

Appendix S 40: ^{1}H NMR Spectrum of *N*-Boc-L-Phe-L-Oxazole-L-Phe-Oxazole-OMe (**78**) in $CDCl_3$

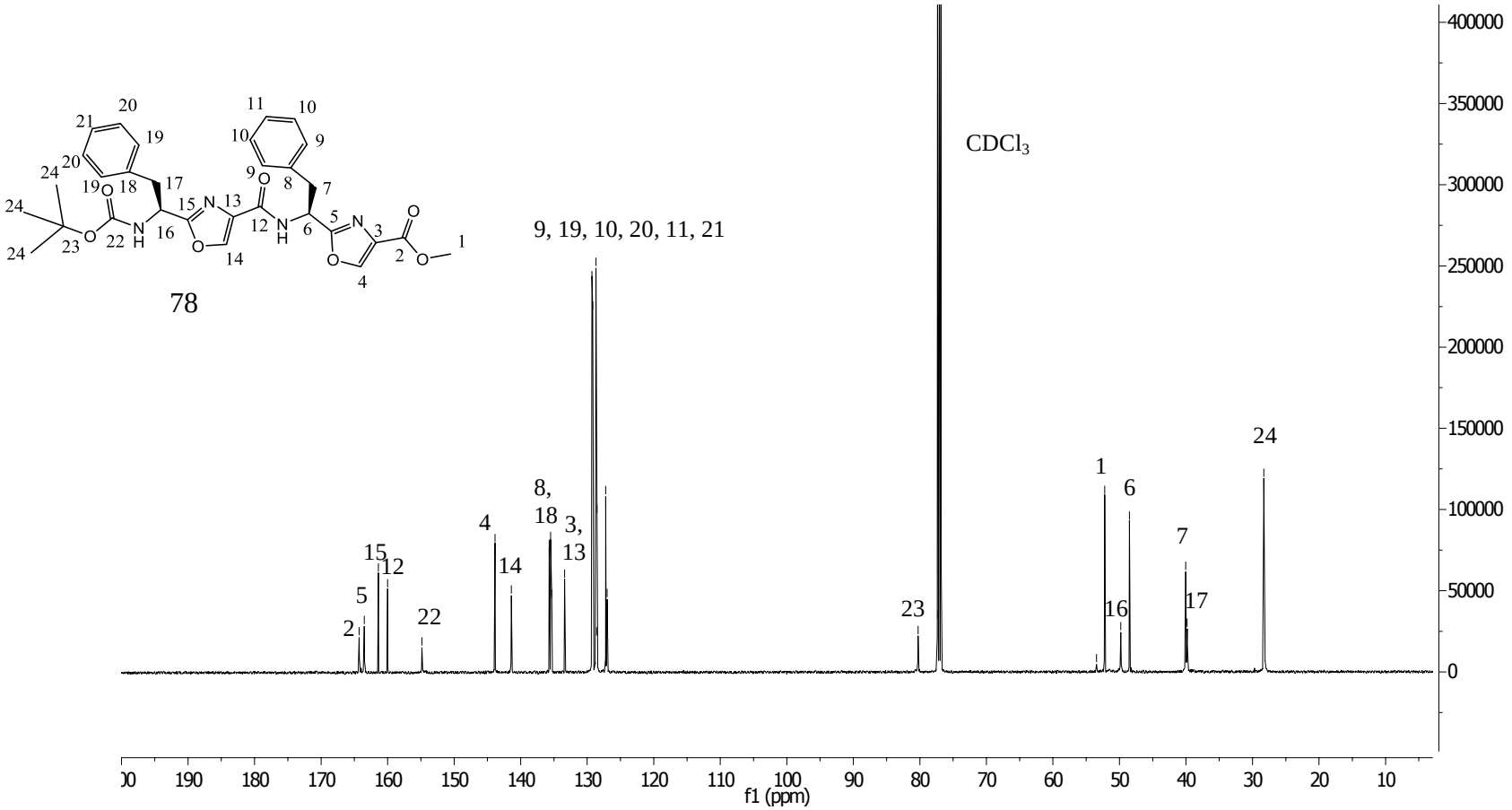

Appendix S 41: ^{13}C NMR Spectrum of *N*-Boc-L-Phe-L-Oxazole-L-Phe-Oxazole-OMe (**78**) in $CDCl_3$

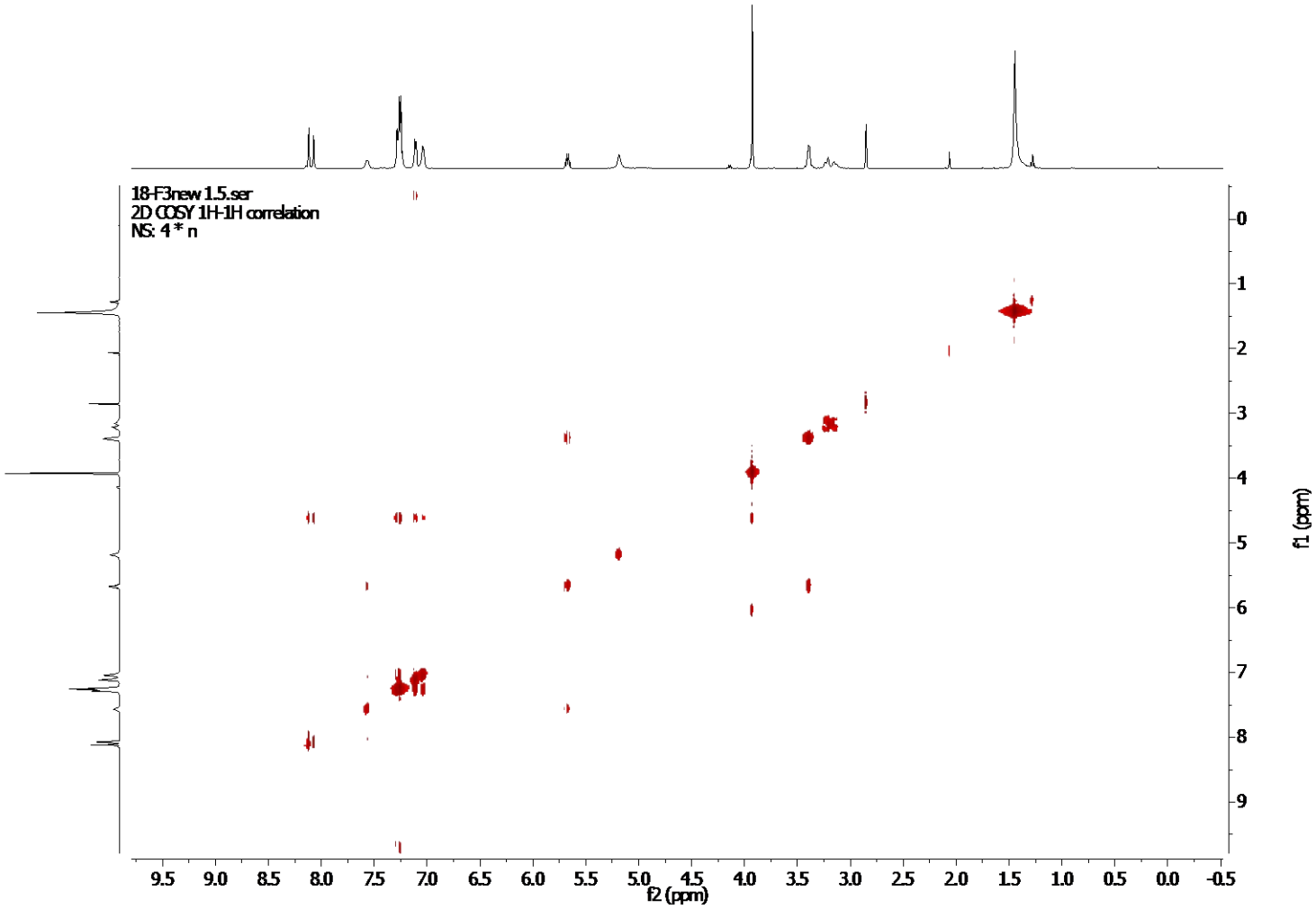

Appendix S 42: COSY NMR Spectrum of *N*-Boc-L-Phe-L-Oxazole-L-Phe-Oxazole-OMe (**78**) in $CDCl_3$

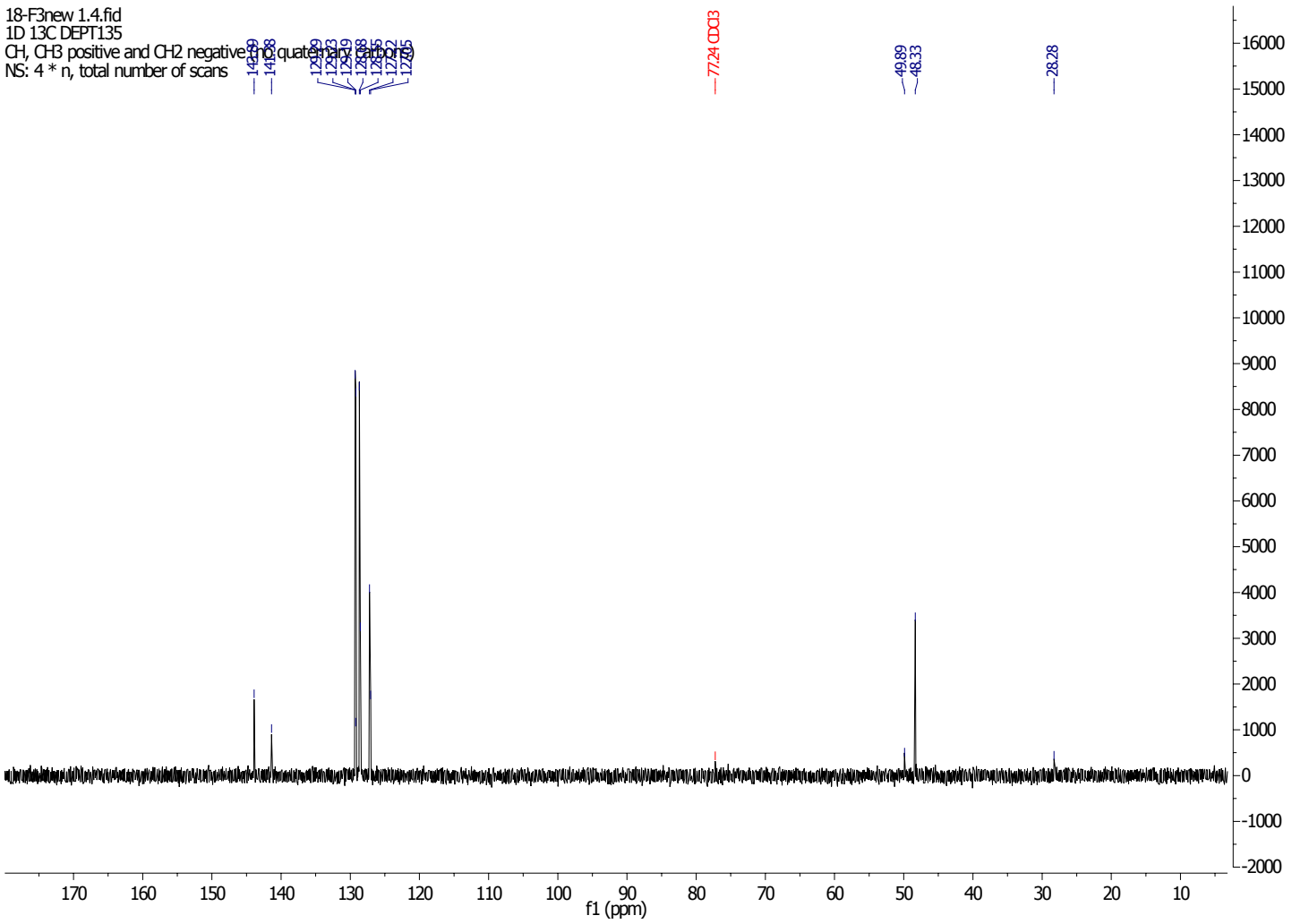

Appendix S 43: DEPT 90 NMR Spectrum of *N*-Boc-L-Phe-L-Oxazole-L-Phe-Oxazole-OMe (**78**) in $CDCl_3$

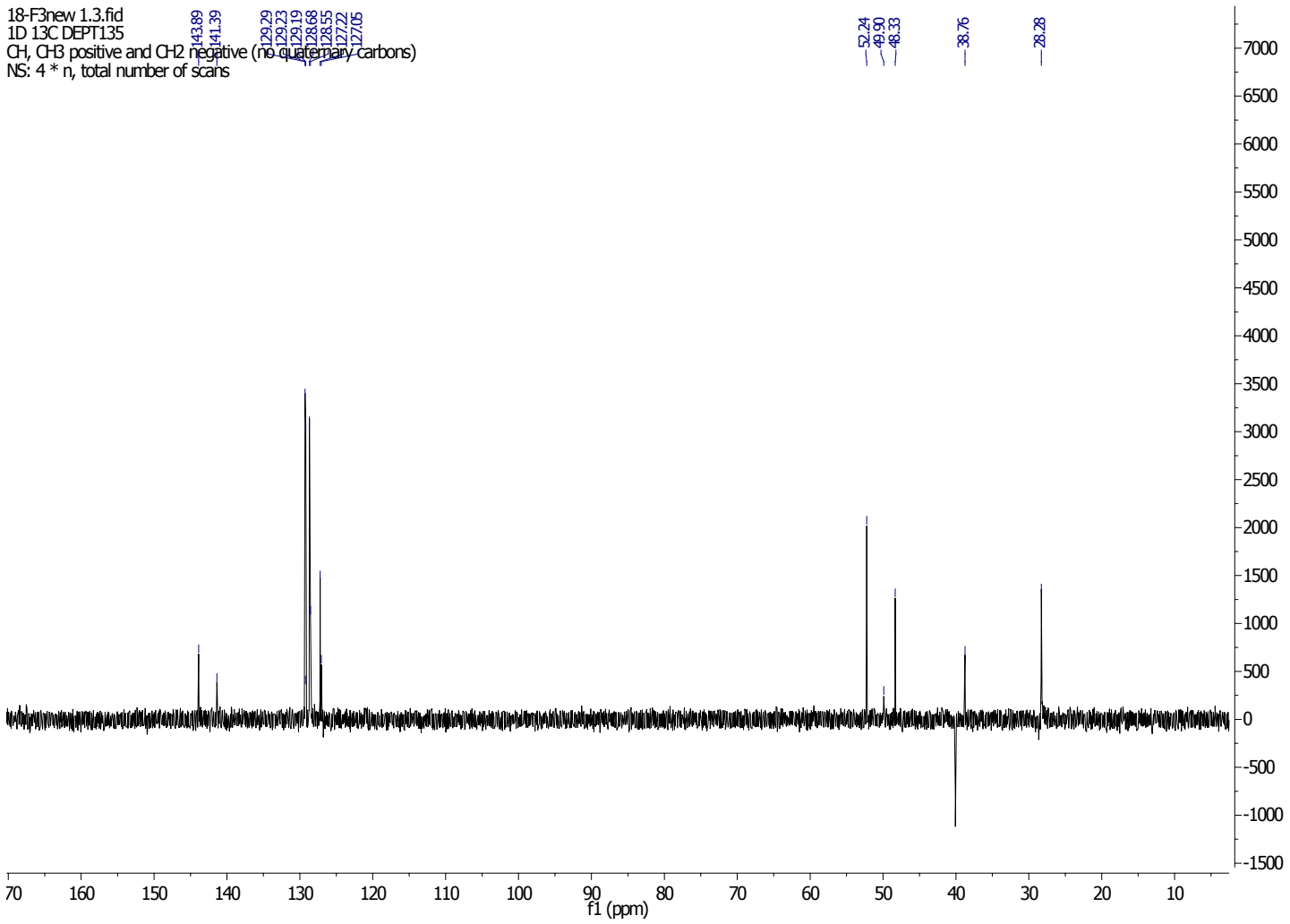

Appendix S 44: DEPT 135 NMR Spectrum of *N*-Boc-L-Phe-L-Oxazole-L-Phe-Oxazole-OMe (**78**) in $CDCl_3$

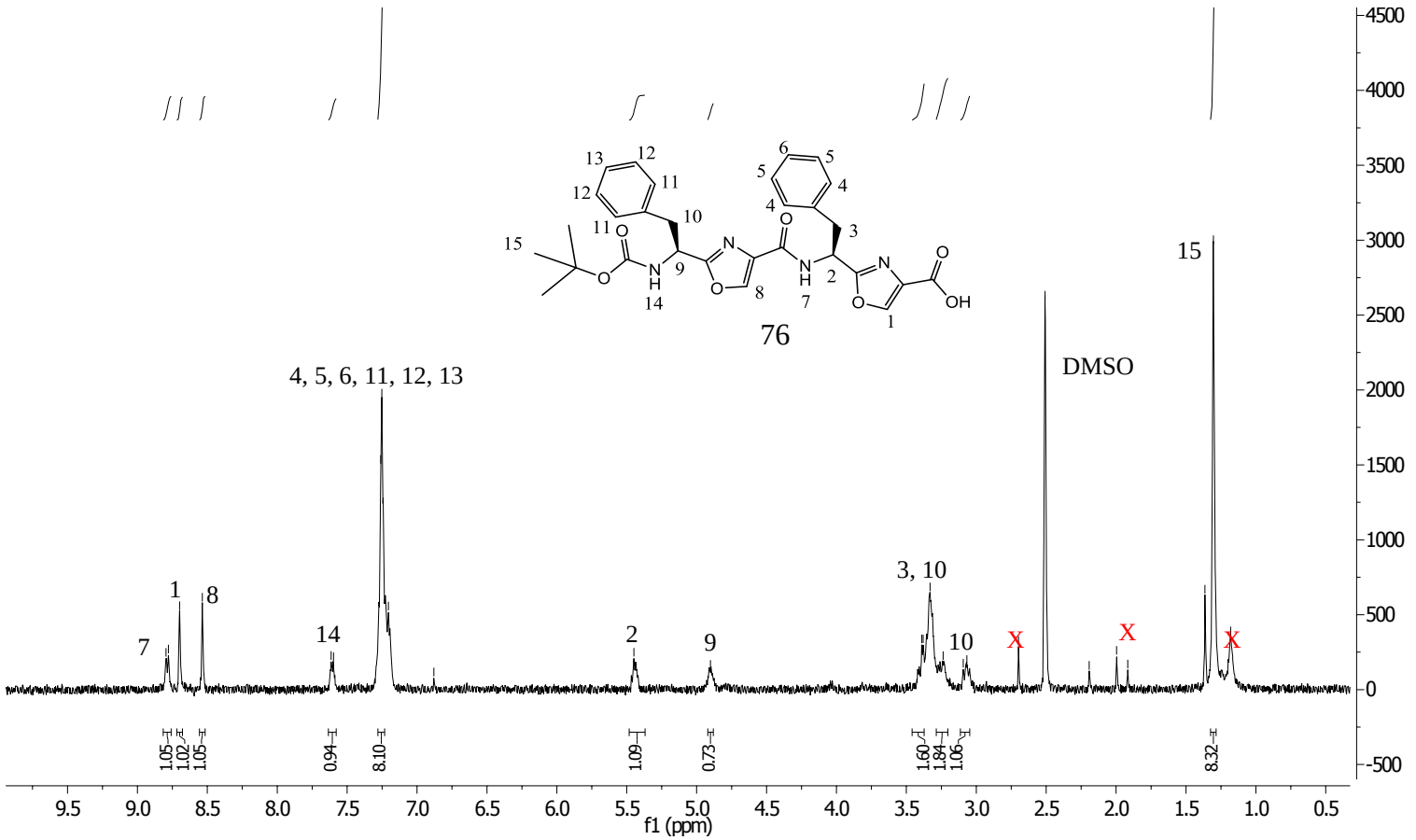

Appendix S 45: ^{1}H NMR Spectrum of *N*-Boc-L-Phe-Oxazole-L-Phe-Oxazole-Phe-OH (**76**) in DMSO-d_6

Signals marked with an X are due to ethyl acetate.

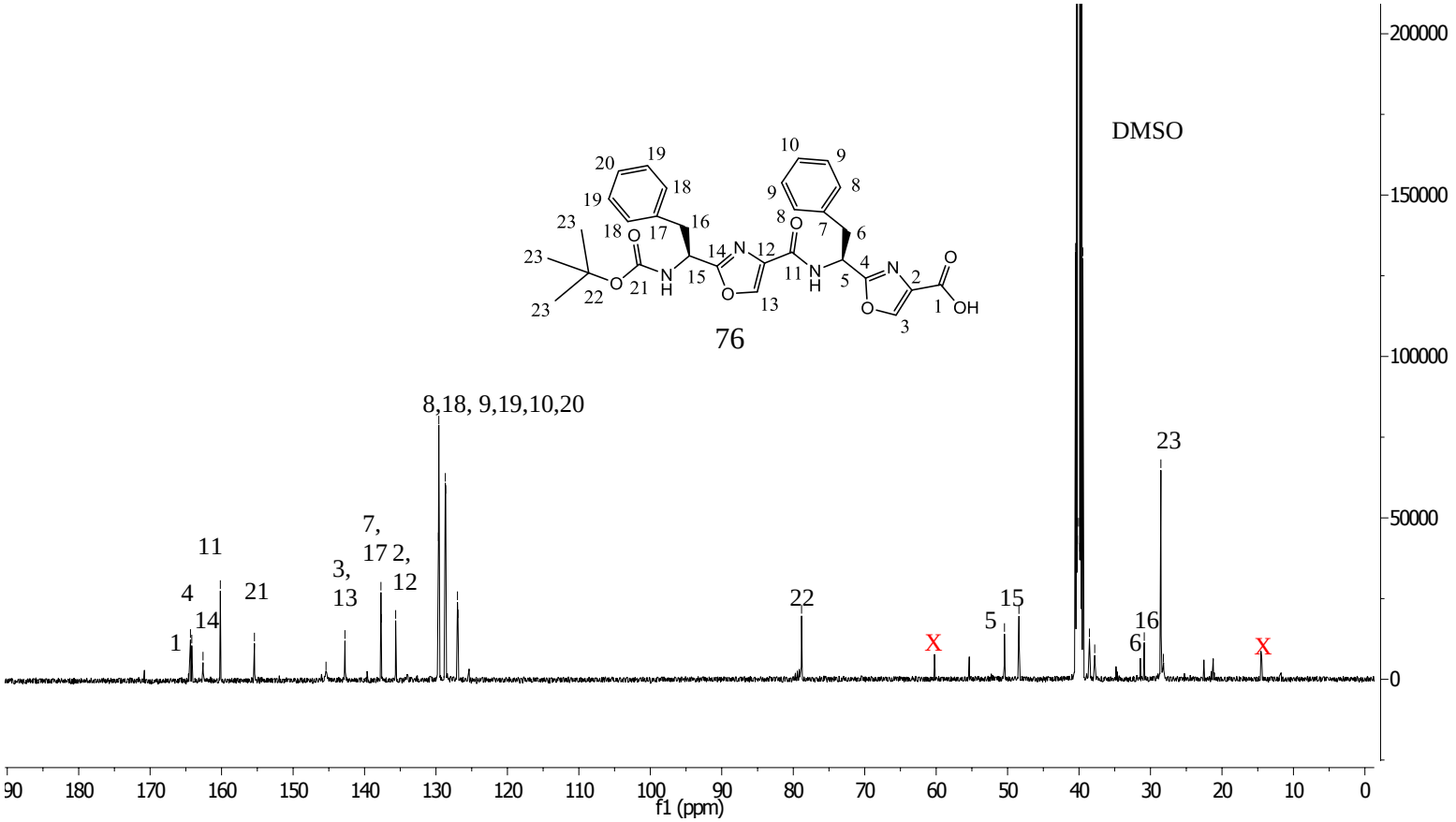

Appendix S 46: ^{13}C NMR Spectrum of *N*-Boc-L-Phe-Oxazole-L-Phe-Oxazole-Phe-OH (**76**) in DMSO-d_6

Signals marked with an X are due to ethyl acetate.

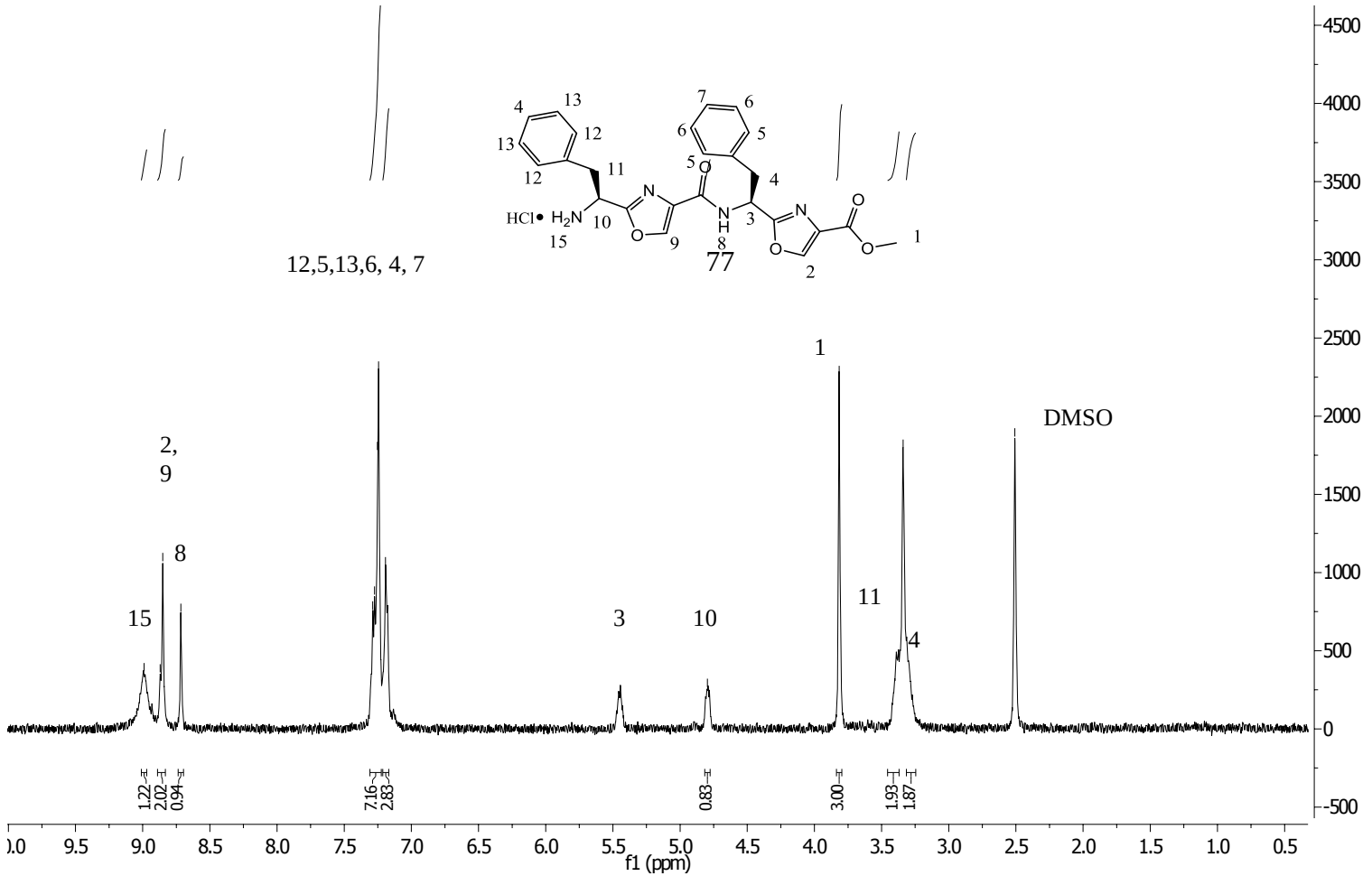

Appendix S 47: [1] H NMR Spectrum of HCl•NH_2-L-Phe-Oxazole-L-Phe-Oxazole-OMe (**77**) in DMSO-d_6

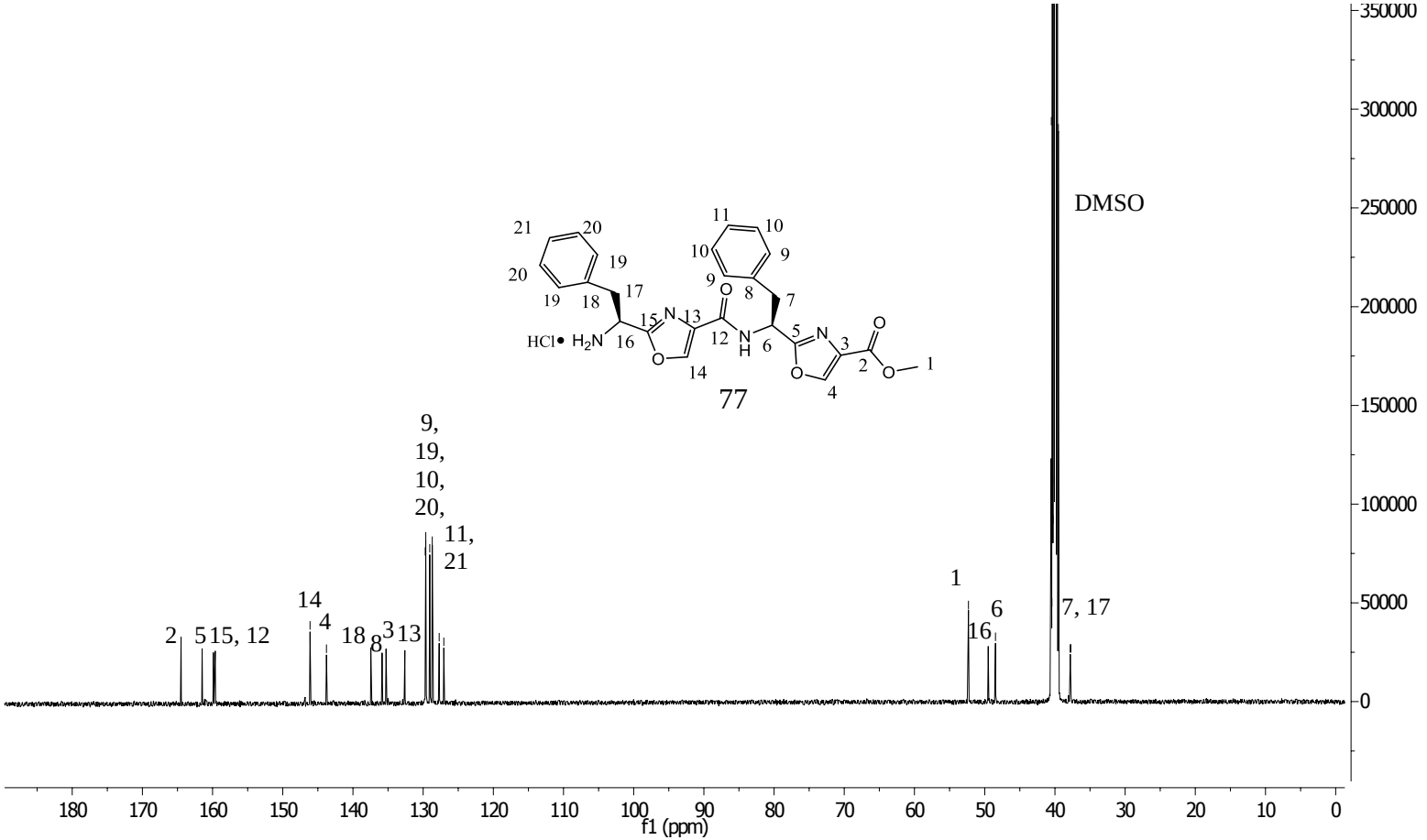

Appendix S 48: ^{13}C NMR Spectrum of HCl•NH_2-L-Phe-Oxazole-L-Phe-Oxazole-OMe (**77**) in DMSO-d_6

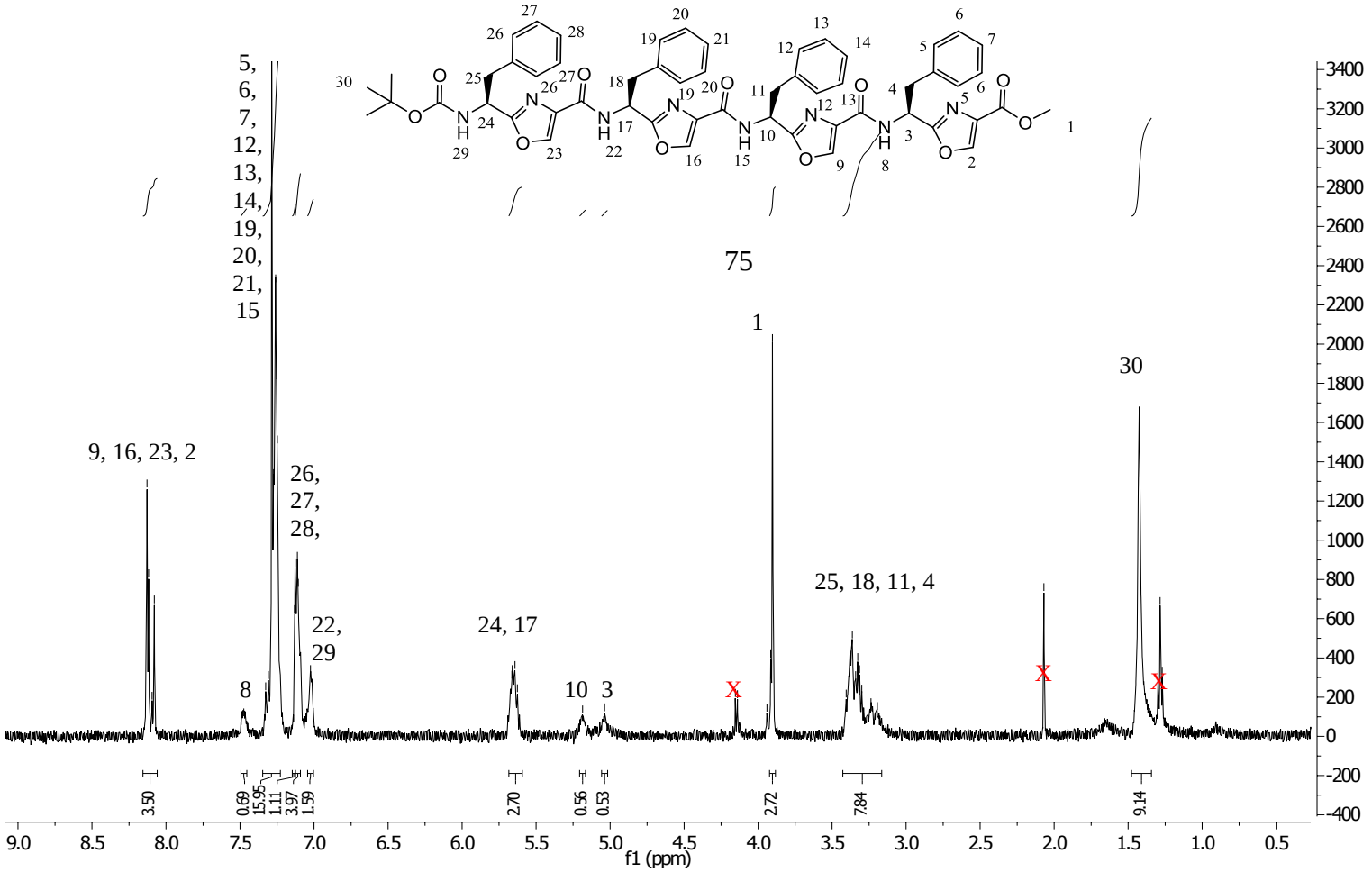

Appendix S 49: [1] H NMR Spectrum of *N*-Boc-L-Phe-Oxazole-L-Phe-Oxazole-L-Phe-Oxazole-L-Phe-Oxazole-OMe (**75**) in $CDCl_3$

Signals marked with an X are due to ethyl acetate.

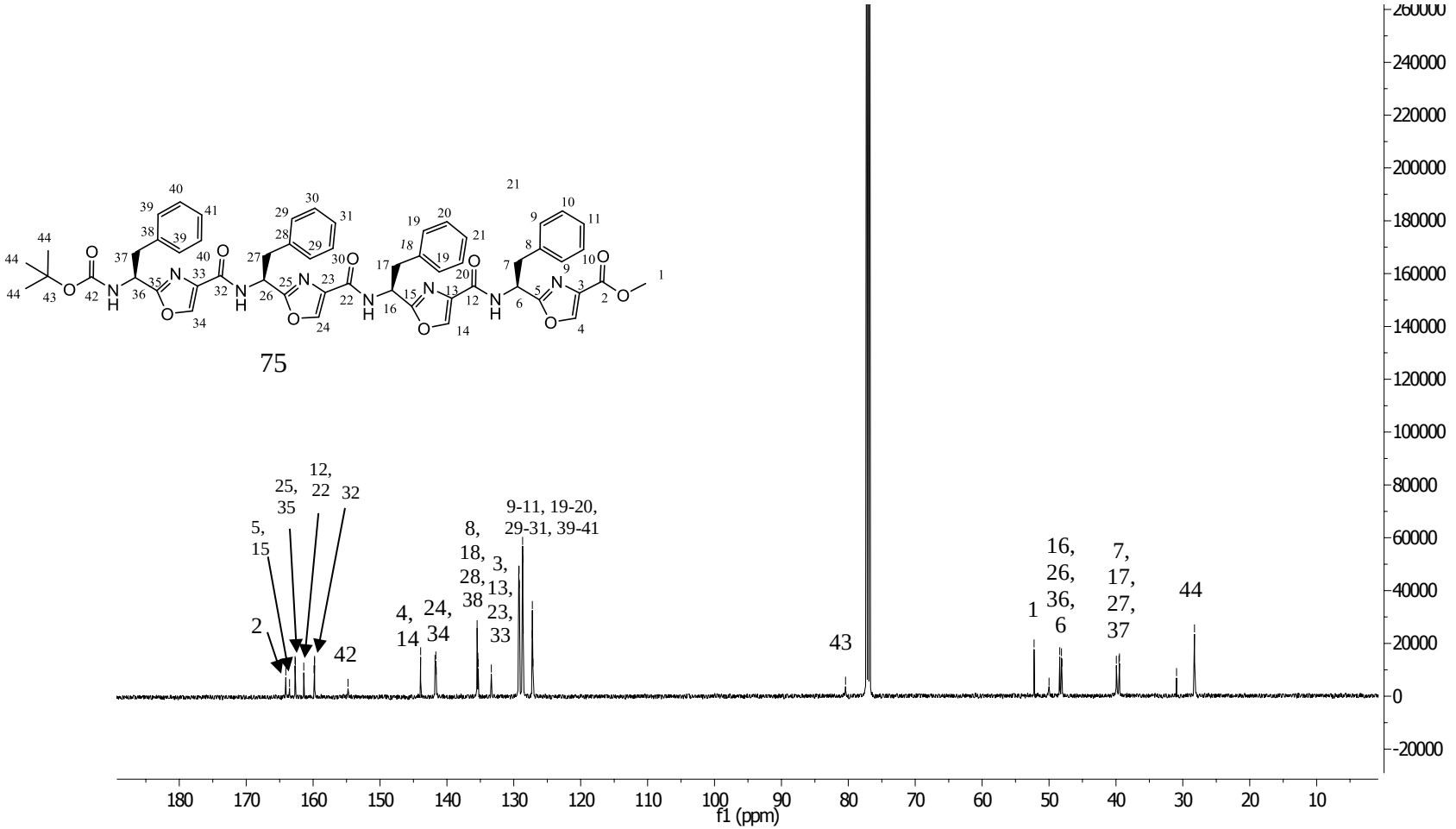

Appendix S 50: ^{13} C NMR Spectrum of *N*-Boc-L-Phe-Oxazole-L-Phe-Oxazole-L-Phe-Oxazole-L-Phe-Oxazole-OMe (**75**) in $CDCl_3$

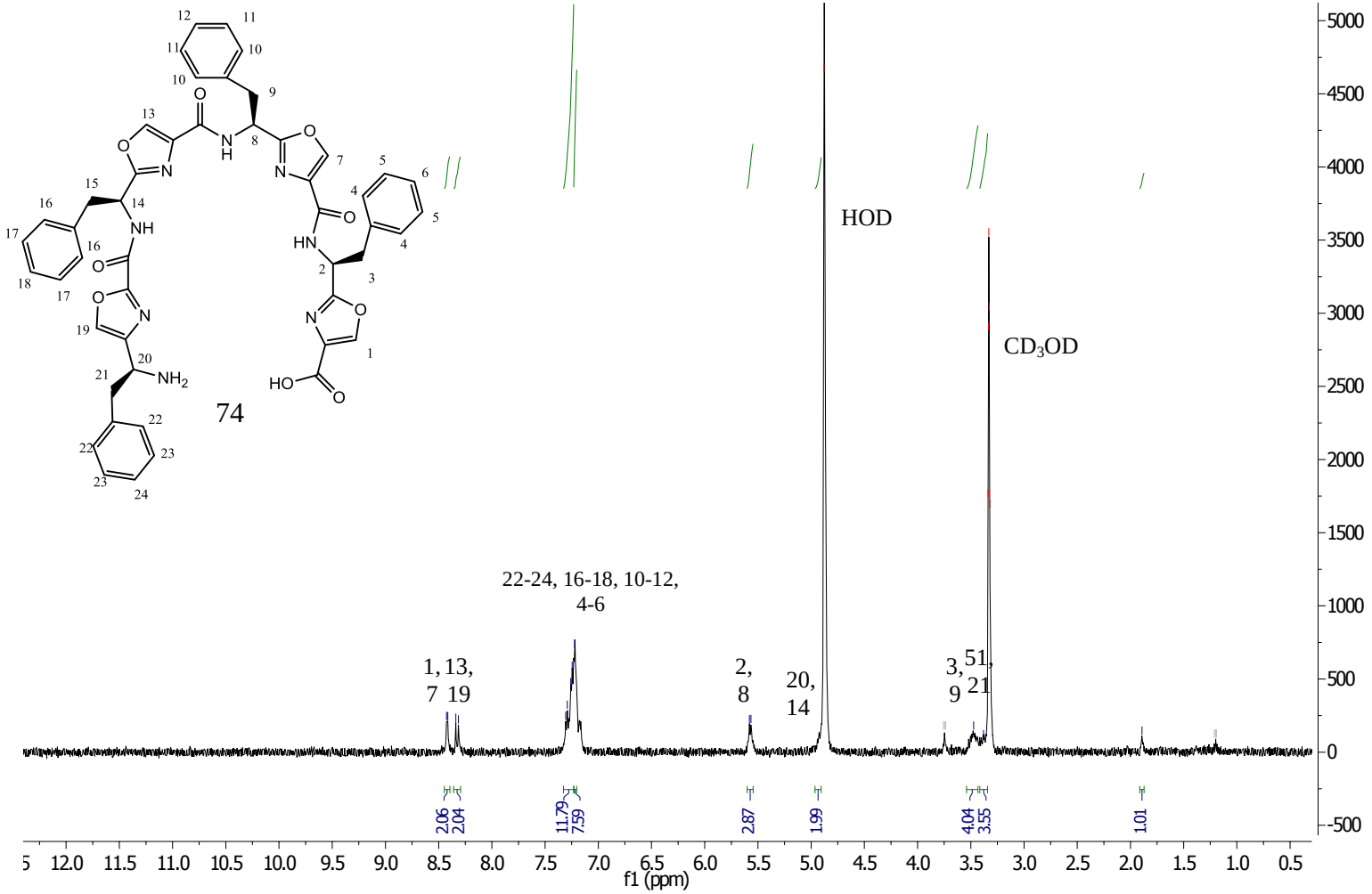

Appendix S 51: [1] H NMR Spectrum of HO-Oxazole-L-Phe-Oxazole-L-Phe-Oxazole-L-Phe Oxazole-L-Phe-NH_2 (**74**) in methanol-d_4

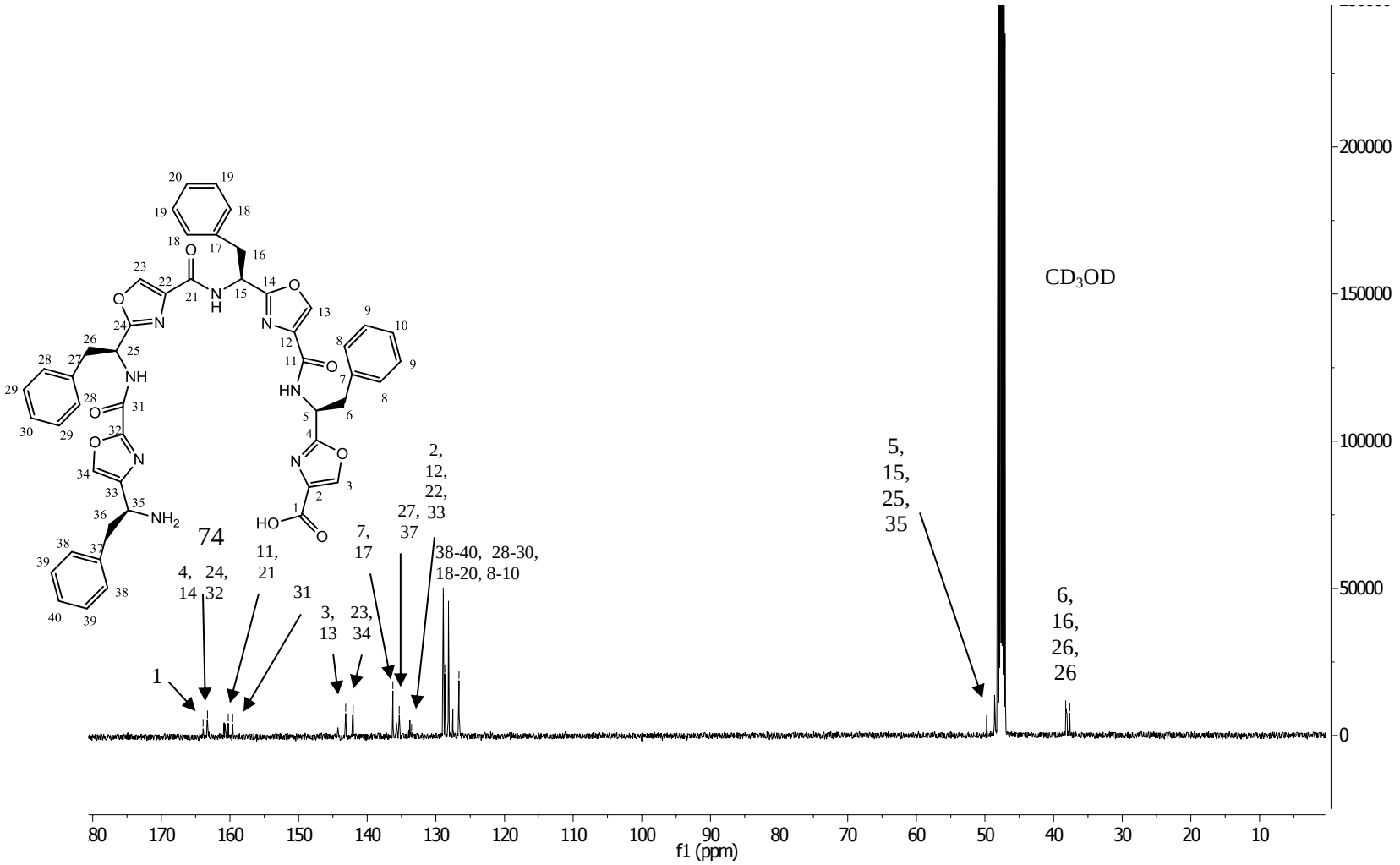

Appendix S 52: ^{13}C NMR Spectrum of HO-Oxazole-L-Phe-Oxazole-L-Phe-Oxazole-L-Phe Oxazole-L-Phe-NH_2 (**74**) in methanol-d_4

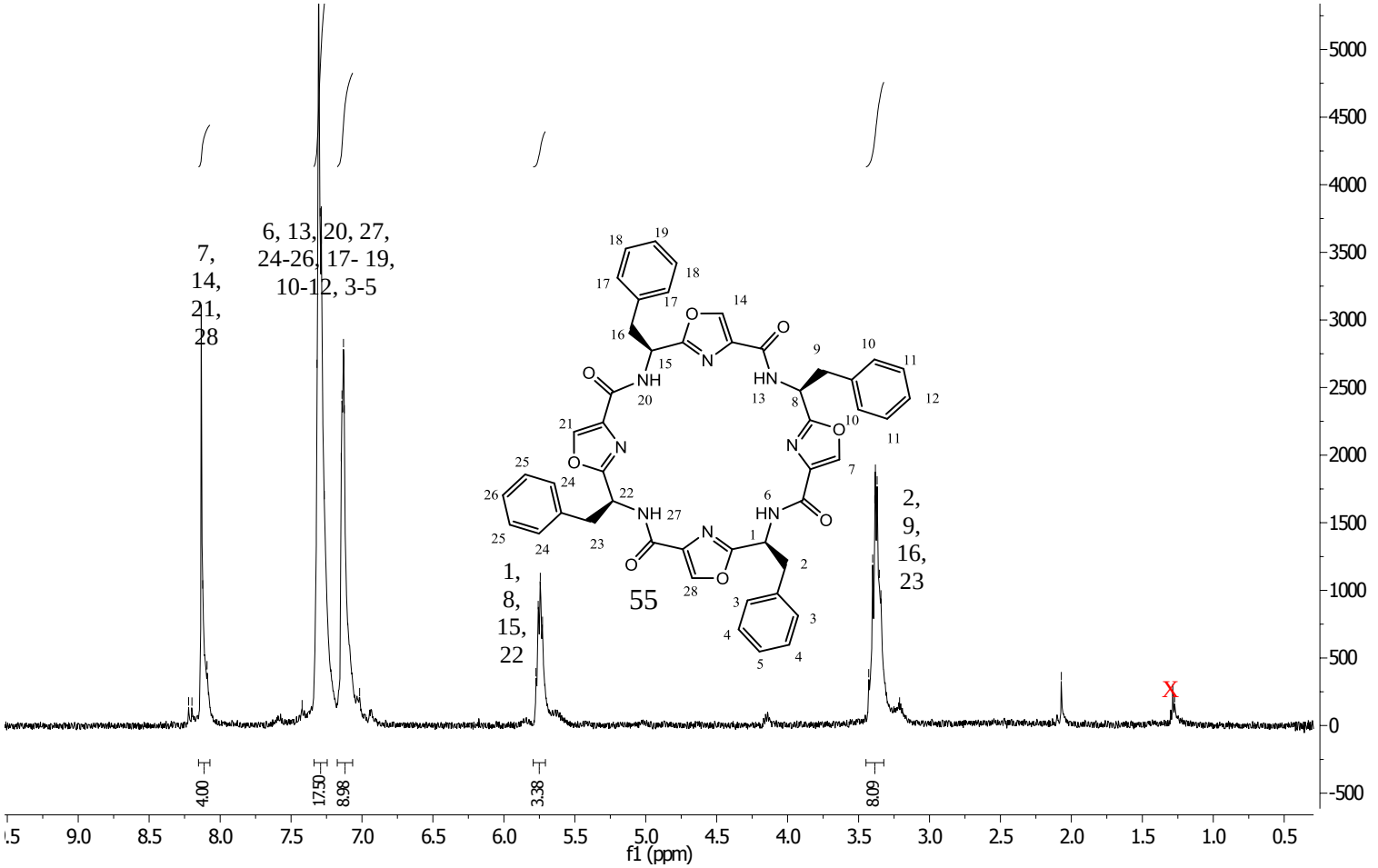

Appendix S 53: [1] H NMR Spectrum of Macrocycle Oxazole-L-Phe-Oxazole-L-Phe- Oxazole-L-Phe-Oxazole-L-Phe (**55**) in $CDCl_3$

Signals marked with an X are due to diethyl ether solvent

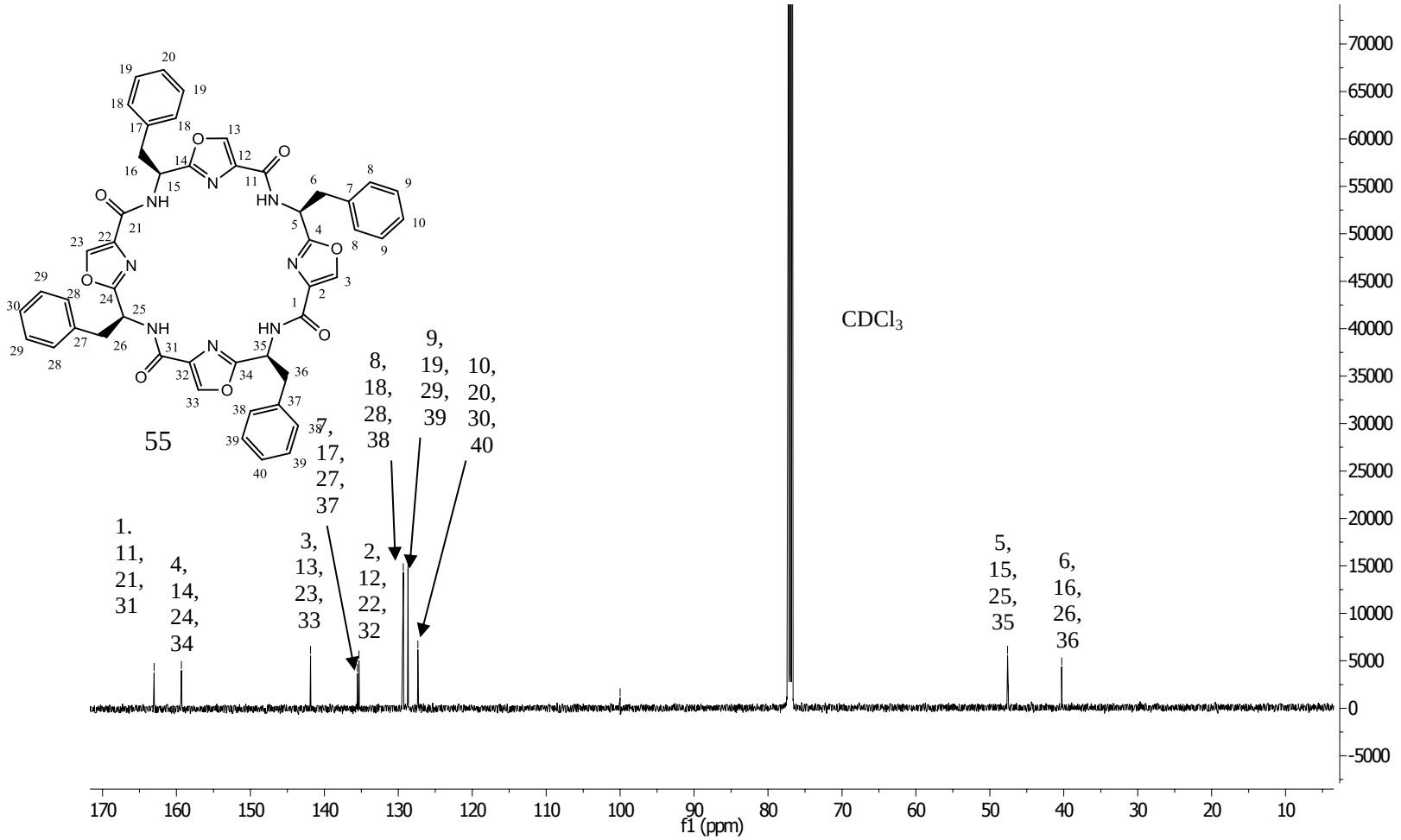

Appendix S 54: ^{13}C NMR Spectrum of Macrocycle Oxazole-L-Phe-Oxazole-L-Phe- Oxazole-L-Phe-Oxazole-L-Phe (**55**) in $CDCl_3$